MAWSON INSTITUTE

FOR

ANTARCTIC RESEARCH

UNIVERSITY OF ADELAIDE

POLAR SUBSTORM PHENOMENA

AT

MACQUARIE ISLAND

by

Frederick F.F. Yuan

B.Sc. (Hons.), M.Sc.

A Thesis presented for the

Degree of Doctor of Philosophy.

August 1970

I give consent to this copy of my thesis, when deposited in the University Library, being available for loan and photocopying.

Date 7.8.70 Signed

TABLE OF CONTENTS

SUMMARY

Equipment was designed and operated at the southern auroral zone station, Macquarie Island, in order to study fast time variations in the geomagnetic field, auroral luminosity and cosmic noise absorption. Additional data, including geomagnetic pulsations sonagrams, 30 MHz riometer records and all-sky photographs from Macquarie Island, as well as magnetograms from a number of auroral region stations, were also used in a study of polar substorm phenomena.

Some Pi geomagnetic pulsations events were recorded in digital form on 0.25 in. magnetic tape. These data were transcribed onto 0.5 in. tape to enable spectral analysis using a digital computer. Time-varying and time-averaged power spectra for the geomagnetic pulsations were produced by complex demodulation; it is believed that this is the first report of spectral analysis of Pi geomagnetic pulsations using this particular technique. Spectral analysis was carried out over the frequency bands 0.04 to 0.56 Hz, and 0.004 to 0.056 Hz. The latter includes the Pi 2 frequency band. Over the higher frequency band, Pi geomagnetic pulsations have the character of band-limited noise, seldom having any dominant frequency component. From the analysis of a limited amount of data, it was found that Pi geomagnetic pulsations at auroral zone stations which are equatorward of the auroral oval, were characterized by the presence of a dominant frequency component in the Pi 2 frequency band. Pi activity at stations inside the auroral oval, may be characterized by power spectra with many

peaks over the band 0.004 to 0.056 Hz.

A synoptic study of polar substorm phenomena was carried out in three local time sectors, the evening, midnight and morning sectors. It was found that Pi geomagnetic pulsations are a characteristic substorm phenomenon in each of those local time sectors. Typical time structuring and time relationships of Pi and auroral absorption events are discussed for each local time sector.

Two types of cosmic absorption absorption events occur in the evening sector. These were termed rapid evening absorption (REA) and gradual evening absorption (GEA). REA events are associated with the westward travelling surge in the auroral oval. GEA events are characterised by slow time variation and weak absorption, and appear to be an auroral zone phenomenon; they may be associated with asymmetric increases in the ring current, and occur over a substantial range of longitude in the evening sector during an early period of substorm activity.

The relationship of Pi geomagnetic pulsations and auroral absorption to the magnetospheric substorm is discussed. The typical development of the absorption region, during the expansive phase of the polar substorm, is also discussed.

STATEMENT OF AUTHENTICITY

This thesis contains no material which has been accepted for the award of any other degree or diploma in any University.

To the best of my knowledge and belief, the thesis contains no material previously published or written by another person, except when due reference is made in the text of the thesis.

(Frederick F.F. Yuan).

ACKNOWLEDGEMENTS

I am grateful to my supervisor, Dr. F. Jacka, for helpful discussions and criticisms. The assistance of D.F. Creighton, in the design and development of equipment, and of R.C. Schaeffer, in the development and operation of equipment, is gratefully acknowledged. I am also indebted to Mr. I. Caire of the Division of Computing Research, C.S.I.R.O., for his valued advice and assistance in computer programming.

I would like to thank the Antarctic Division of the Department of Supply, for logistic support for this project, which forms part of the programme of the Australian National Antarctic Research Expeditions. Construction of the equipment was financed in part by a grant from the Radio Research Board.

During my candidature, I was a holder of a Commonwealth Post-Graduate Award.

CHAPTER 1

INSTRUMENTATION FOR FAST TIME VARIATION STUDY AT MACQUARIE ISLAND

In the period January to March 1968, equipment was installed and operated at Macquarie Island to record ionospheric absorption of cosmic radio noise, auroral luminosity and geomagnetic field fluctuations. A block diagram of the data acquisition system is given in Figure 1-1. All instrumentation was designed so that time variations with frequencies from 0.005 Hz to greater than 1 Hz could be studied. All data was recorded on a six-channel chart recorder using a basic chart recording speed of 10 mm. per minute. On nights when auroral activity was observed, some data channels were recorded onto 0.25 in. magnetic tape using a digital data recording system designed to allow computer analysis of selected records to be carried out with a time resolution of one tenth of a second.

The Macquarie Island data acquisition system contains four subsystems, the geomagnetic pulsations detection system, three channel photometer, fast run riometer and digital data recording system, which will be described in the following sections.

1.1 Geomagnetic Pulsations Detection System

1.1.1 *Design and construction*

A solenoid wound onto a high permeability core has the inherent advantage of portability and consequent ease of installation. This basic

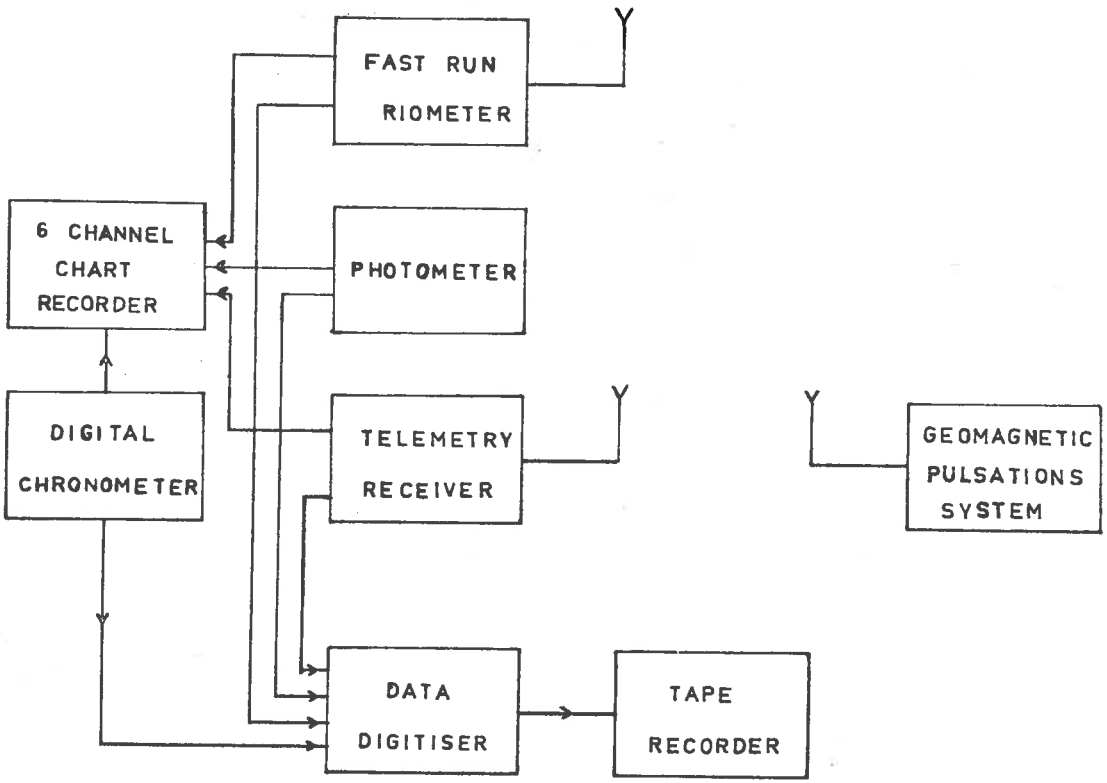

Fig. 1-1 Block diagram for data acquisition system.

configuration was chosen for the design of the geomagnetic pulsations sensor. Two design requirements for the sensor were:

1. The sensor should enable detection of small fluctuations in the geomagnetic field in the frequency range 0.005 to 5 Hz.

2. At the frequency of 1 Hz, a sinewave magnetic field fluctuation of 10^{-3} γ (peak to peak) should produce an output signal from the sensor of amplitude of approximately 1 x 10^{-6} volts (peak to peak) amplitude. (1γ is equal to 10^{-5} Oersted).

Mu - metal is a commonly used material for the cores of geomagnetic pulsations sensors. This particular material however, suffers from at least two disadvantages:

1. Permeability of mu - metal can be degraded appreciably by fluctuations in temperature and by mechanical vibration.

2. At the high frequency end of the geomagnetic pulsations spectrum (i.e. above 1 Hz) eddy current losses become significant and degrade the performance.

Ferrites, due to their high resistivity, do not give rise to significant eddy current losses at frequencies of the order of 1 Hz. It will be demonstrated by both calculation and experiment that a practical geomagnetic pulsations sensor meeting the abovementioned design requirements can be built.

1.1.2 *Sensitivity to magnetic pulsations of a solenoid with ferrite core*

The voltage induced in a solenoid by a magnetic field variation is proportional to the time rate of change of the flux of induction

through the windings of the solenoid. For a thin solenoid, the induced e.m.f. in the winding is given by

$$V = - N \frac{d\phi}{dt} \text{ volts} \qquad (1)$$

where ϕ is the magnetic induction flux. For a solenoid of uniform cross-sectional area A and N turns

$$V = - NA \frac{dB}{dt} \text{ volts}$$

$$= - NA \left(\frac{dB}{dH}\right)\left(\frac{dH}{dt}\right) \text{volts} \qquad (2)$$

For a low amplitude sinusoidal fluctuation in H, $\left(\frac{dB}{dH}\right)$ is the effective incremental permeability of the core.

For a coil wound around a core, the effective permeability will be less than the bulk permeability of the core material. As the core is magnetised, free magnetic poles will be induced on both ends, giving rise to a magnetic field opposing the magnetising field.

The apparent permeability μ' is given by

$$\mu' = \frac{B}{H} \qquad (3)$$

where H is the applied field. Bozorth and Chapin (1942) give a curve, reproduced in Figure 1-2, showing the relation between apparent permeability μ' and the bulk permeability μ for various values of a shape parameter m, the ratio of length to diameter, for cylinders. Although the core constructed using these calculations had a square cross-section, the calculations of Bozorth and Chapin will still provide a useful

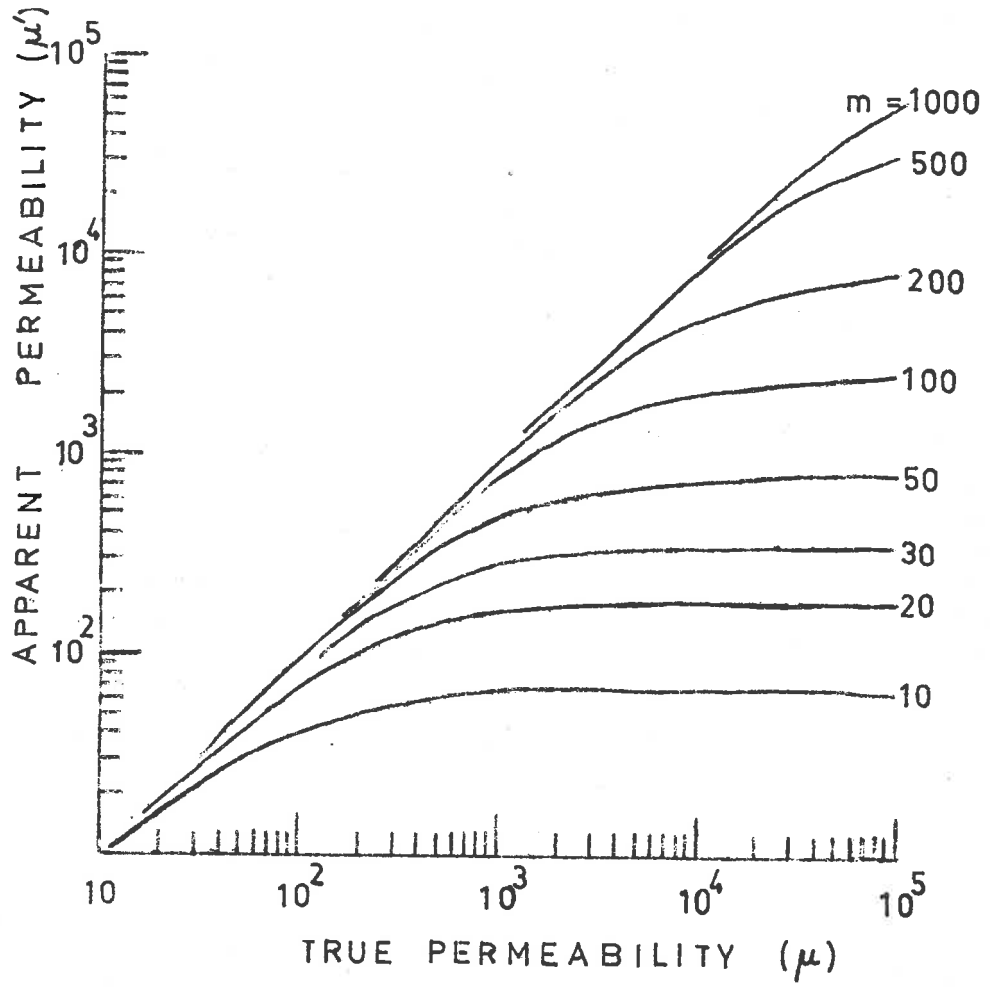

Fig. 1-2 Relation between apparent permeability μ' and bulk permeability μ of cylinders having a given ratio m of length to diameter. (After Bozorth et al, 1942).

approximation for the sensitivity of the solenoid to magnetic field fluctuations.

When the magnetising field undergoes a slow, alternating fluctuation between some values + Ho and - Ho, the flux density B will assume values following a curve similar to the one drawn in Figure 1-3. The curve P S_1 P' S_1 P is the hysteresis curve for the material. If the field H fluctuates about some mean level near H_1, the flux density will follow a minor hysteresis curve S_1 Q_1 S_2 Q_2 S_1. The slope of the line S_1 S_2 is the incremental permeability. For very small fluctuations in H, the incremental permeability is an estimate for the value of $(\frac{dB}{dH})$ at the appropriate point of the hysteresis curve.

If the steady state magnetising field H is much less than the saturation value, $(\frac{dB}{dH})$ varies only slowly with H and, to a good approximation, we can use Figure 1-2 to estimate the effect of the demagnetising field induced in a core of a given shape by a magnetising field. For a ferrite produced by Philips (Grade III C 2) the incremental permeability at 0.5 Oersted magnetising field strength is quoted as approximately 1000. For a core 54 in. long and 2 in. x 2 in. square cross section, the shape parameter m is approximately 27. Referring to Figure 1-2, an estimate of $(\frac{dB}{dH})$ for such a ferrite core, magnetised by the earth's magnetic field at the ground, would be approximately 250.

If we have a small sinusoidal fluctuation $\underset{\sim}{H}$ = H. sin ω t where Ho is amplitude, $\omega = 2\pi f$ where f is the frequency, equation (2) may be rewritten as

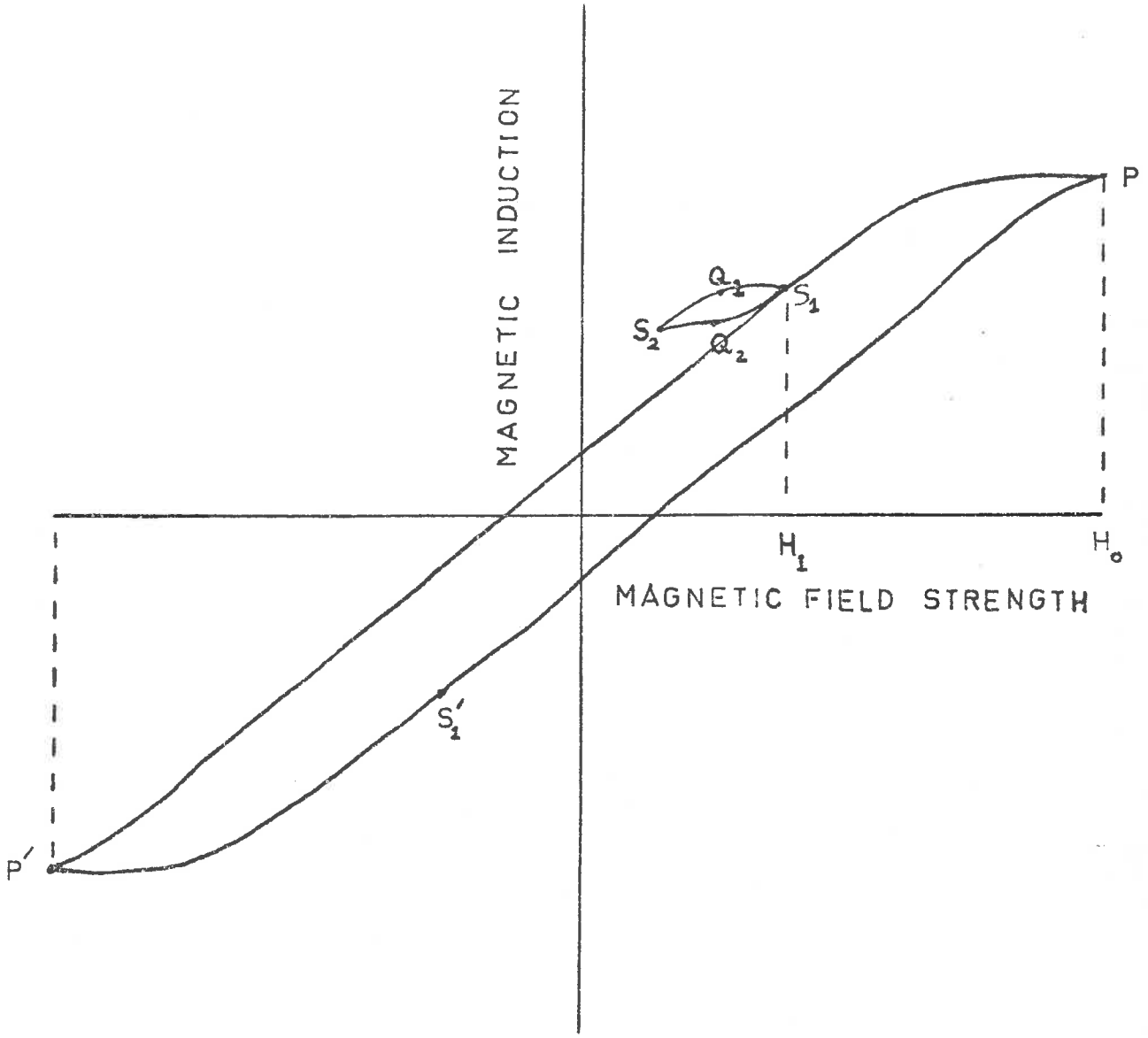

Fig. 1-3 Hysteresis curve for a ferrite material.

$$\underset{\sim}{v} = - NA \mu_{eff} \omega Ho \cos \omega t \qquad (2a)$$

We arrive at a simple formula for coil sensitivity K where

$$K = NA \mu_{eff} \omega \times 10^{-4} \text{ volts/Oersted} \qquad (4)$$

A is the cross-sectional area in square metres.

N is the number of turns.

μ_{eff} is the effective incremental permeability.

We can also define an effective area A_{eff} by the expression

$$A_{eff} = NA \mu_{eff} \qquad (5)$$

The effective area is the area of a single loop in vacuum which would have a sensitivity equal to K. In all this discussion, we are assuming that the direction of the magnetic field is parallel to the axis of the solenoid. It can be seen that the sensitivity K is proportional to frequency.

1.1.3 *Construction of the geomagnetic pulsations sensor*

Ferrite bars of dimensions 0.5 in. x 0.5 in. x 9.0 in. ground flat on all sides were cemented together using an epoxy casting resin to make up a core of dimensions 2 in. x 2 in. x 54 in. Specifications on the ferrite material used, Philips Ferroxcube, Grade III C2, are presented in Philips "Electronics Applications Bulletin" Vol. 13, pp 44-58 (1952).

A solenoid with winding thickness of two inches was wound in five sections. Each section consisted of 40,000 turns of 27 B&S copper wire

wound onto formers and encapsulated in epoxy resin. These coil sections were mounted onto a central fibreglass tube which provided a cavity for the core. The solenoid was finally coated with fibreglass and handles were mounted. Coil connections were wired to a socket mounted at one end of the assembly. Figure 1-4 is a photograph of the geomagnetic pulsations sensor. Its length is approximately five feet and the weight approximately 200 pounds.

Ignoring the thickness of the winding of the solenoid, the calculated effective area of the sensor is 1.3×10^5 m^2. Using this figure for the effective area, it is to be expected that a fluctuation in magnetic field strength of amplitude 1mγ (peak to peak) at 1 Hz frequency would produce an output signal of 0.8 μV (peak to peak) amplitude. The output resistance of the sensor at zero frequency is 1.3×10^4 ohms.

1.1.4 *Amplifier for geomagnetic pulsations sensor*

Two operational amplifiers in series provided the gain for the amplifier for signals from the geomagnetic pulsations sensor. The gain was controlled using a resistive negative feedback network and three amplifier sensitivities could be selected by shorting out resistors in the network by means of a rotary switch.

By using a metal oxide semiconductor field effect transistor in another feedback loop, a low frequency cut-off was introduced into the amplifier frequency response. At maximum gain, this feedback loop reduced the effects of voltage drifts at the input by a factor 10^3 over a time interval greater than 300 seconds. The amplifier was mounted in a heavy metal case and, because of the low frequency cut-off in the amplifier

Fig. 1-4 Geomagnetic pulsations sensor.

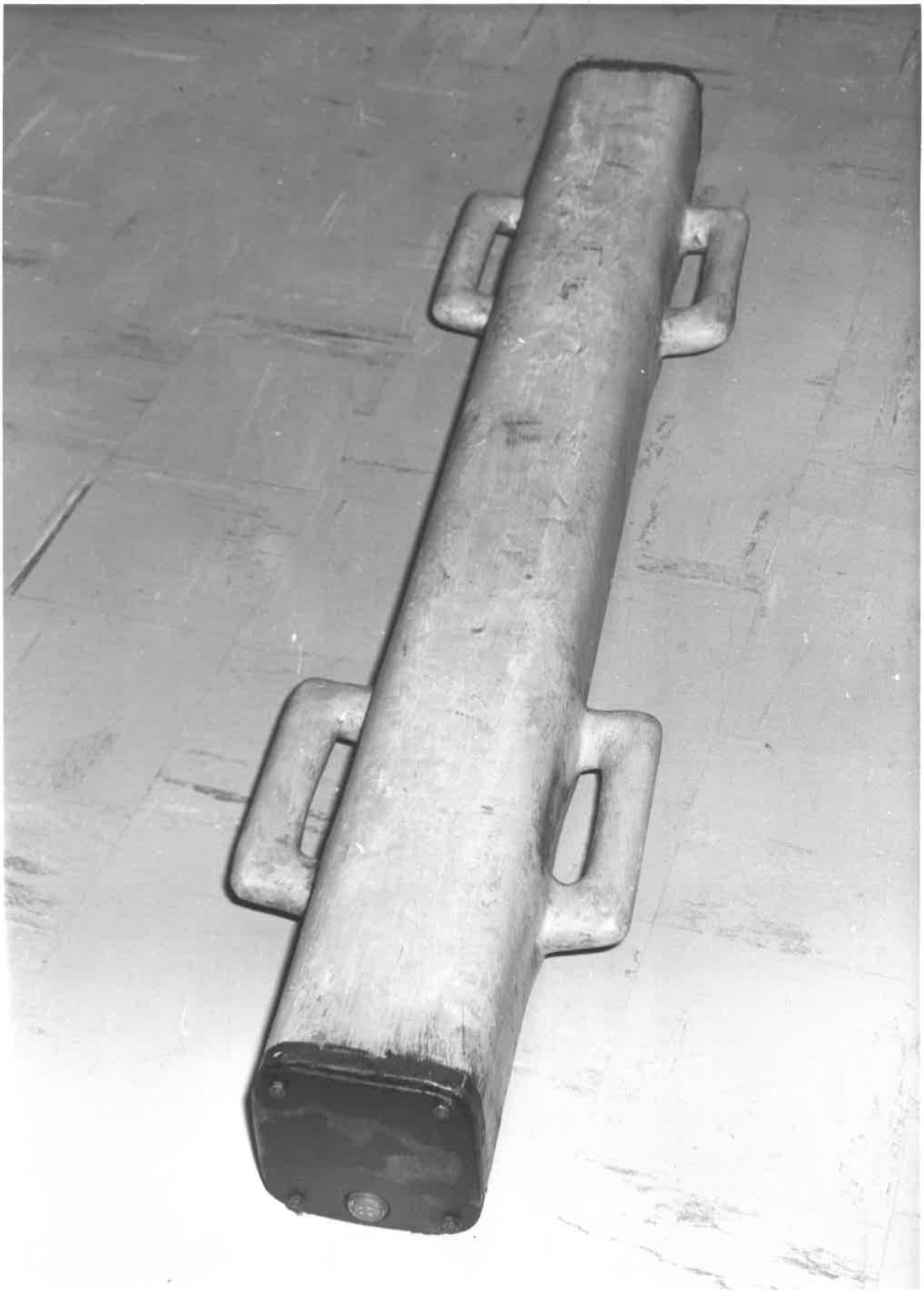

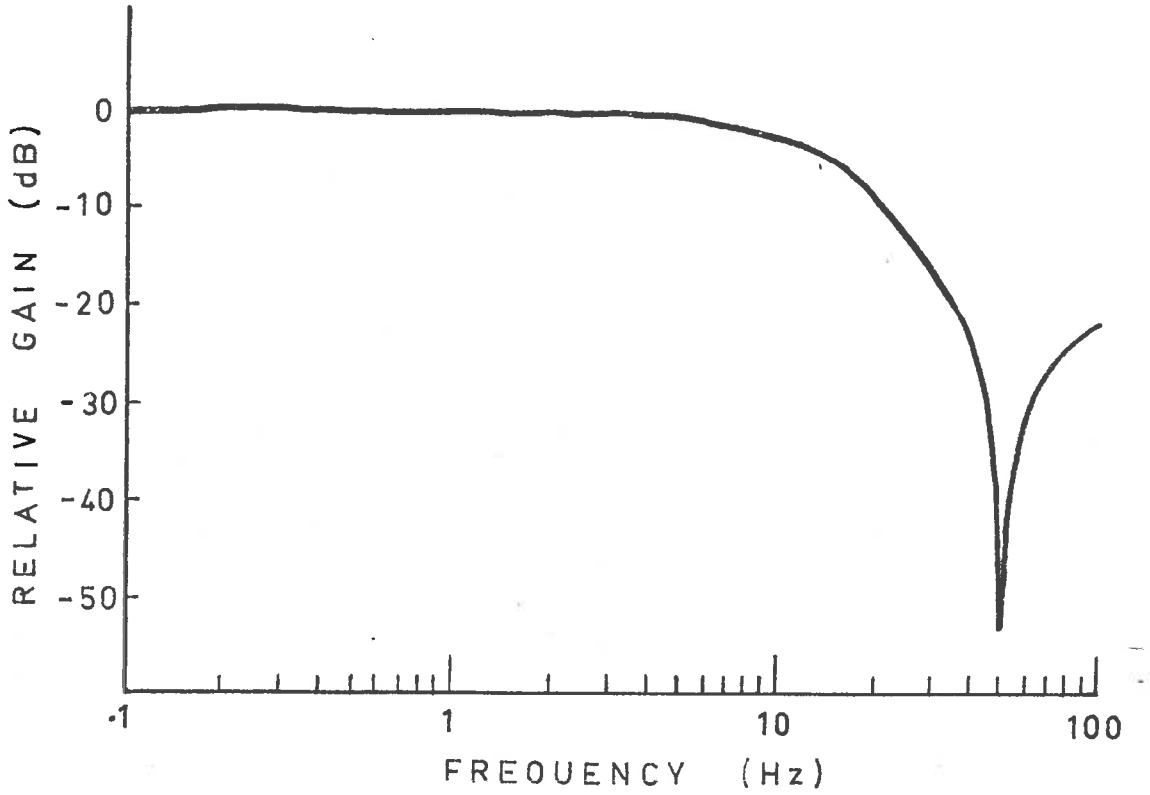

Fig. 1-5 Frequency response curve for geomagnetic pulsations amplifier.

frequency response, no problems due to thermal e.m.f's in the input circuitry were encountered.

A frequency response curve for the geomagnetic pulsations amplifier is given in Figure 1-5. The pronounced dip in response at 50 Hz is due to inclusion of a notch filter which attenuated signals due to the 50 Hz mains power source.

Input impedance for the amplifier was of the order of 10^{11} ohms and the noise had an amplitude of approximately 4 μV rms.

1.1.5 160 *MHz telemetry system*

The geomagnetic pulsations sensor and amplifier were sited at a location approximately one half a mile from the data recording site in order to reduce the effect of man-made interference. Sensor output was telemetered to the central base station by means of a 160 MHz radio link. Four rechargeable 6V. batteries provided power for the sensor amplifier and 160 MHz transmitter circuitry. Batteries had to be recharged once every two weeks.

The telemetry was developed around available sub-units. The receiver was a standard FM base station receiver, and the transmitter consisted of a commercial exciter-modulator with a low power final stage which delivered 80 mw. to the antenna. The output from the geomagnetic pulsations sensor amplifier was fed to a voltage to frequency converter, the output of which, in turn, was used to frequency modulate the 160 MHz carrier signal. The voltage to frequency converter produced pulses whose repetition rate was proportional to the input voltage.

Two outputs were provided by the 160 MHz receiver: a pulse output, which was fed to the digital data recording system, and an analogue output, whose amplitude was proportional to the pulse repetition rate.

A transmitter yagi antenna was mounted on a twenty foot aluminium pipe; it was found that, despite a fifty yard separation between antenna and the geomagnetic pulsations sensor, movements of the aerial, due to wind, produced significant output from the geomagnetic pulsations sensor. This was presumed to be caused by fields associated with currents induced in the moving metal structure. The original aerial was replaced by a folded dipole mounted on a wooden cross; this configuration proved satisfactory.

1.1.6 *Calibration of the geomagnetic pulsations sensor*

Calibration of the geomagnetic pulsations sensor was carried out by passing a known alternating current through an air-cored coil situated at a known distance from the sensor. The output of the pulsations sensor amplifier was then telemetered back to the recording site. Both the alternating current passing through the calibration coil and the output of the sensor amplifier were recorded on a multi-channel pen recorder. The calibration solenoid consisted of 1000 turns wound onto a ten cm. diameter former. The field produced by this coil was calculated using a dipole approximation which is valid if the distance between the calibration coil and the sensor is much greater than the radius of the calibration coil. The calibration coil had a 30 ohm impedance and was driven by a power amplifier which could pass a maximum of 1 amp. current through the

calibration coil. The power amplifier was driven by the output of a signal generator.

The field H at a point along the perpendicular to the axis of the calibration coil can be calculated using the expression:

$$H = \frac{\pi N\, i\, a^2}{10 r^3} \quad \text{Oersted} \qquad (6)$$

where i is the current passing through the coil in amperes

a is the radius in cm.

r is the distance in cm.

N is the number of turns.

Two calibration experiments were carried out: one at Mt. Torrens, South Australia, in November 1967 and one at Macquarie Island in March 1968. The sensitivity of the geomagnetic pulsations sensor - amplifier combination was calculated after allowing for the telemetry system bandwidth. From the Mt. Torrens experiment, a value of the sensor sensitivity of 0.5 μV/mγ at 1 Hz frequency was obtained. For the Macquarie Island calibration, two estimates of the coil sensitivity at 1 Hz were obtained i.e. 0.4 and 0.5 μV/mγ. The frequency response for the geomagnetic pulsations sensor obtained from the Macquarie Island calibration experiment is given in Figure 1-6. The gain of the sensor is plotted as gain in decibels relative to the gain at 1 Hz. From considerations on sensitivity outlined previously, the dependence of the solenoid sensitivity on frequency should give rise to a slope in the frequency response curve of 20 dB/decade. It can be seen that the experimental curve in Figure 1-6 has a slope near to the expected value.

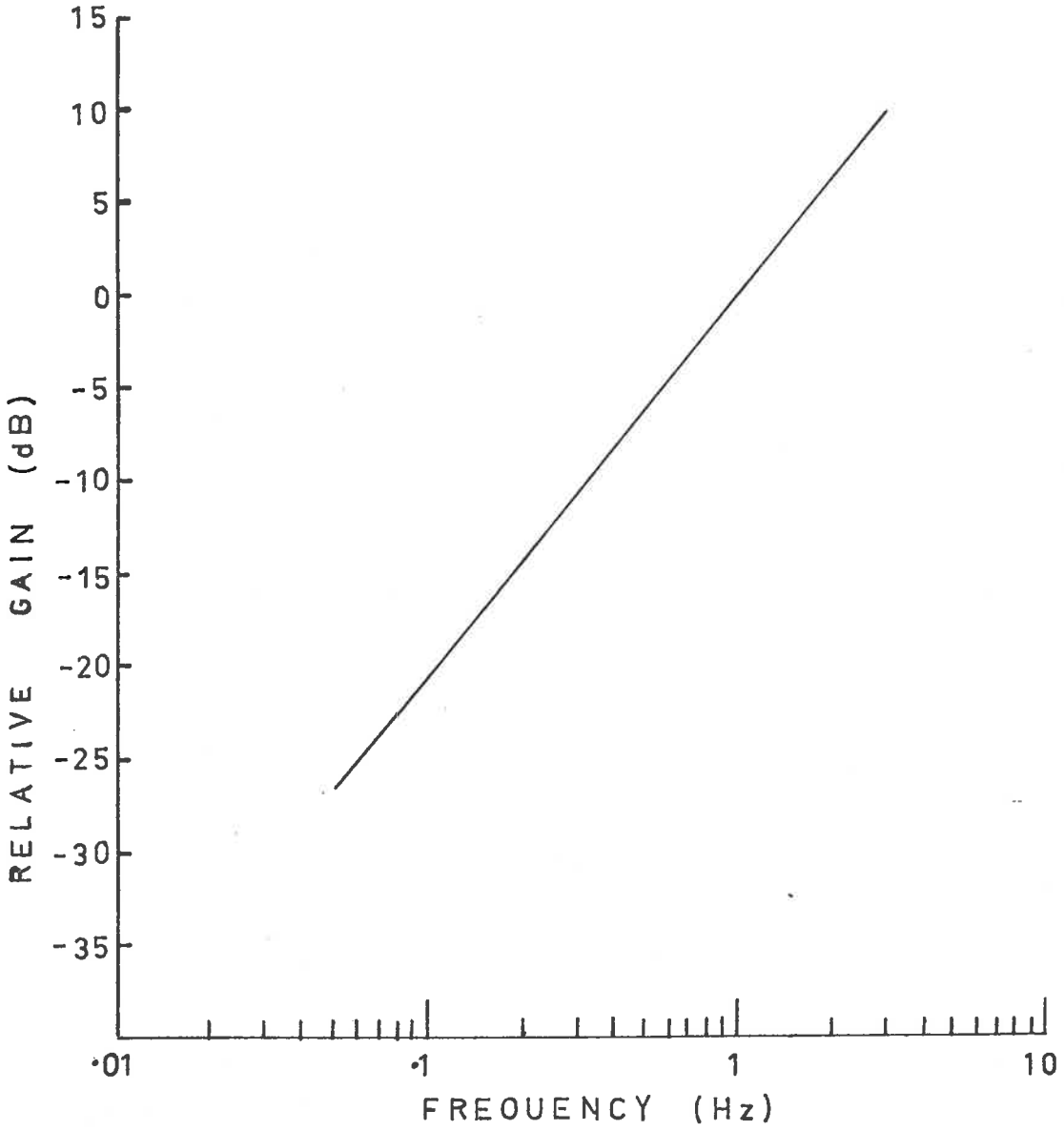

Fig. 1-6 Geomagnetic pulsations sensor frequency response.

The experimentally obtained values for solenoid sensitivity are of the same order of magnitude as the estimated value of 0.8 μV/mγ at a frequency of 1 Hz.

The geomagnetic pulsations sensor was aligned so that its axis was parallel to the local magnetic north-south direction, which is approximately along the L meridian (see Appendix A).

1.2 Three Channel Photometer

A photometer which enabled recording of auroral luminosity in three wavelengths 5577 Å, 6300 Å and 4278 Å was designed and constructed. In the 6300 Å and 5577 Å channels, the filter could be rocked through an angle of ten degrees. The 4278 Å channel had a fixed filter. By installing a heater-thermostat combination inside the photometer, the internal temperature was kept constant. Normal practice was to turn on the heater a few hours before nightly observations commenced to allow temperature stabilisation. The photometer was mounted on a steel base and could be rotated through 360° in azimuth angle and tilted from zero to 90° elevation angle. Each channel had a circular field of view with semi-angle equal to 2.5 degrees. A photograph of the photometer is given in Figure 1-7.

The photometer was sited on the isthmus at Macquarie Island behind a six-foot high wind fence which gave protection against the prevailing westerly winds.

The 5577 Å and 6300 Å channels were used by Mr. R.C. Schaeffer in a study of airglow at Macquarie Island. The present work made use of the 4278 Å channel with the instrument usually directed to the zenith. This

Fig. 1-7 Three channel photometer.

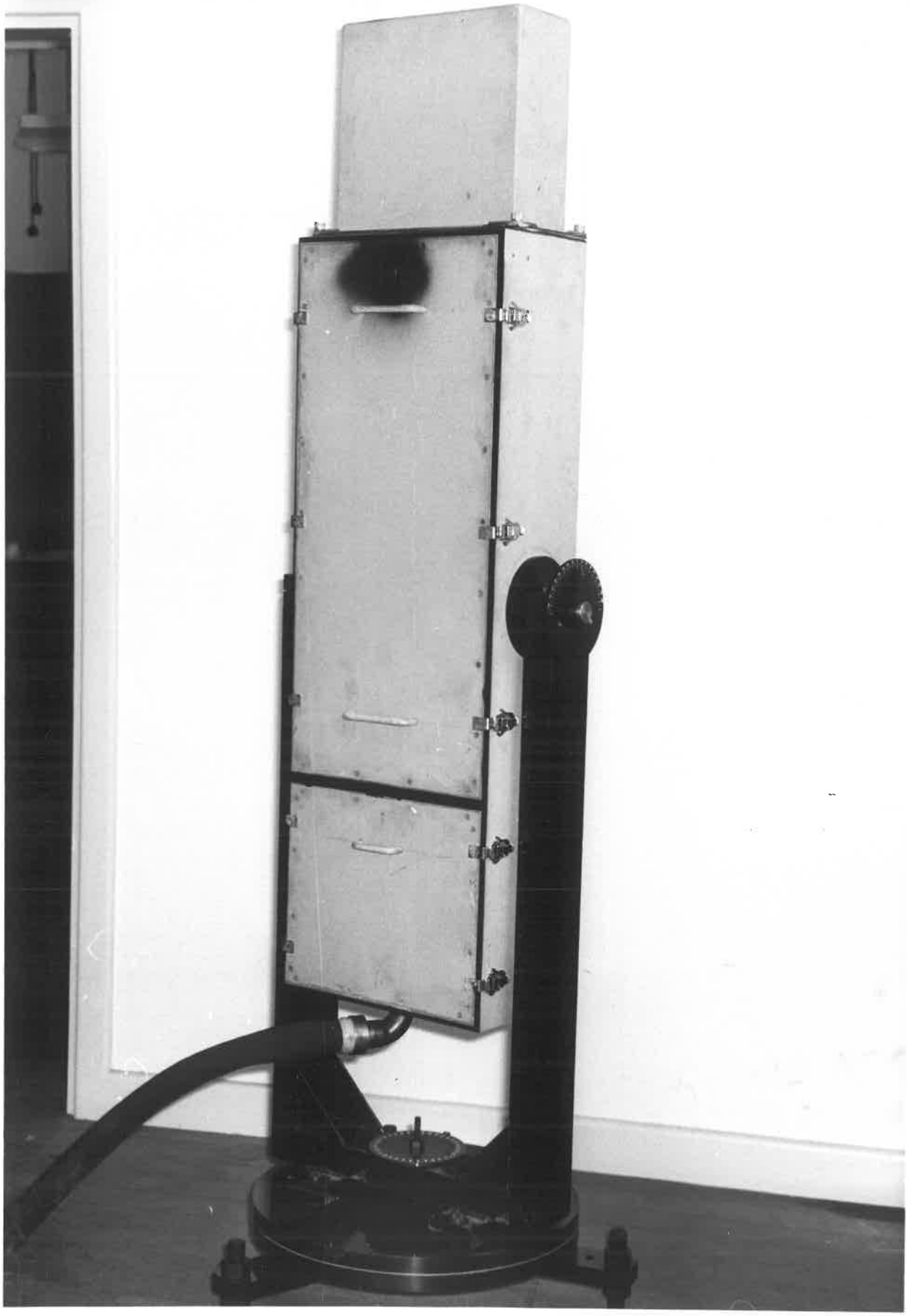

wavelength is emitted by N_2^+ ions. The intensity of the 4278 Å band is a direct measure of the total energy flux of incoming energetic electrons (Dalgarno, 1964). Roughly 35 eV of energy is required to produce one photon in the 4278 Å band. The spectral response for the 4278 Å filter for normal incidence light is illustrated in Figure 1-8.

Each photometer channel contained an E.M.I. 9558B photomultiplier as the photon detector. Outputs from the photomultiplier tubes were fed to current amplifiers. Five ranges of current sensitivity could be selected for each amplifier and three values of integration time constant could be selected for each of these ranges. Occasionally, a backing-off signal was introduced into the amplifier in the 4278 Å channel to enable high resolution study of time structuring of luminosity pulsations.

Relative calibration of photometer channels was maintained by use of a lamp source mounted at a fixed distance from the photometer and powered by a constant voltage supply.

1.3 Fast-run 30 MHz Riometer

A riometer (relative ionospheric opacity meter) which enable monitoring of rapid fluctuations in ionospheric absorption of galactic radio noise was constructed. As distinct from normal riometers which contain an automatic gain control loop, this riometer contained no such loop. The detector output of a modified Australian National Antarctic Research Expeditions riometer receiver was fed to operational amplifiers to provide both a fast response and slow response output. The slow response output was provided to allow comparison with normal riometer records. The

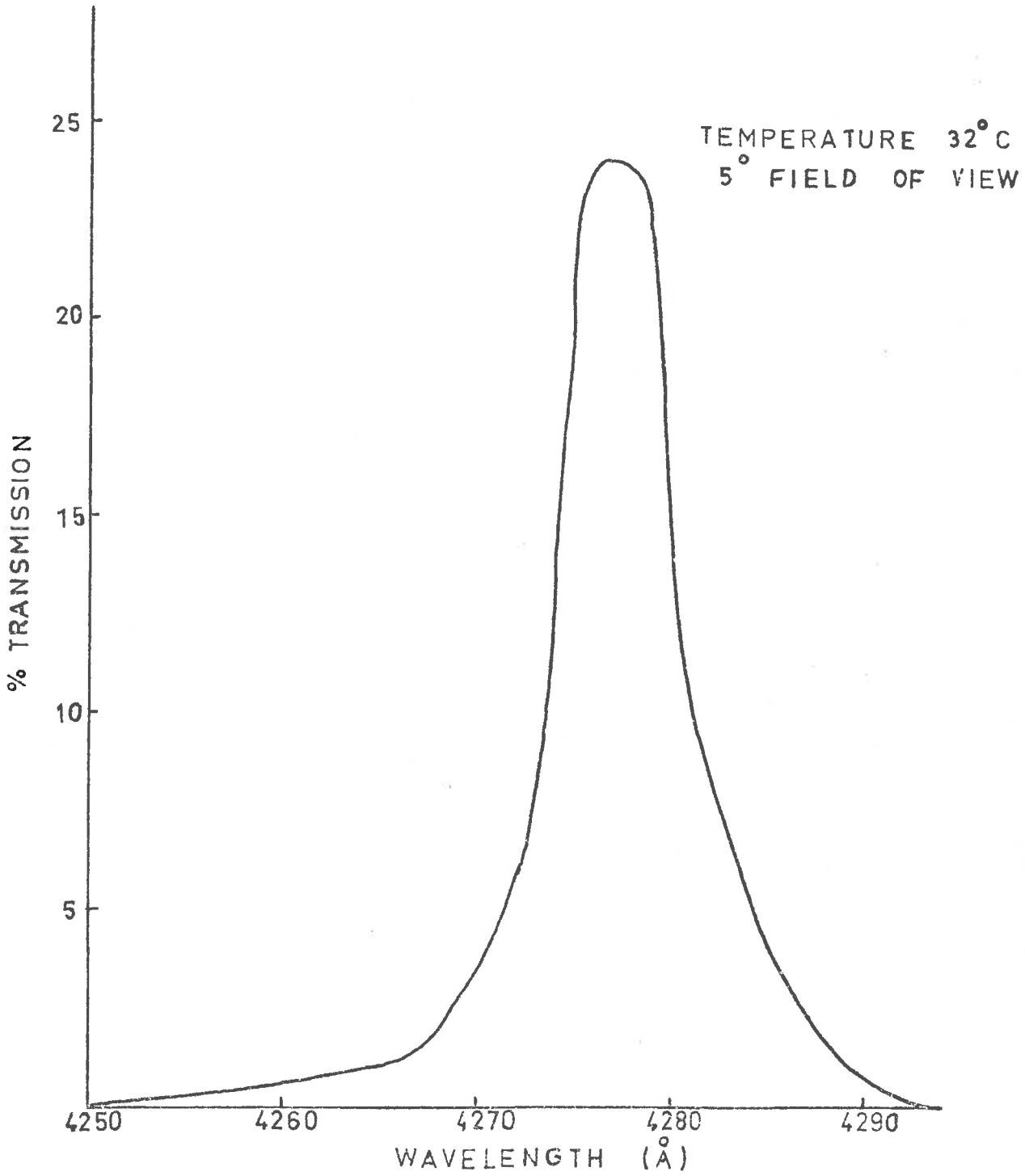

Fig. 1-8 4278 Å channel filter response curve for normal incidence light.

fast response output had a fixed low frequency 3dB point at 0.8 mHz. A high frequency 3dB point of 10 Hz, 2 Hz or 1 Hz and variable gain settings of X2, X5 and X10 relative to the slow response output could be selected from front panel switches. Tests with a sweep frequency oscillator showed that the riometer receiver bandwidth was approximately 85 KHz. The riometer aerial was a 3-element Yagi.

The riometer was frequently calibrated using a noise diode circuit and a relay was installed in the riometer receiver so that on the hour, the input to the riometer receiver was attenuated by a 3dB attenuator pad to give an hourly calibration.

During initial trials of the riometer, the receiver preamplifier was mounted in a weatherproof box near to the aerial site. It was found that this positioning of the preamplifier led to considerable fluctuation in gain which appeared to be due to temperature effects. Re-siting of the preamplifier inside the central base-station building led to a considerable improvement in performance. During periods when the station communications transmitter was operating, the inputs to the output operational amplifiers was shorted to earth; any data recordings made during these periods would have been useless due to transmitter interference.

1.4 Digital Data Recording System

A digital data recording system which uses a high quality domestic four-track tape recorder and 0.25 in. magnetic tape as the primary recording medium was designed and constructed to enable computer analysis of selected data records with a time resolution of one tenth of a second. The ideal

tape recorders for such a system are the instrumentation tape recorders which enable recording with low error rates and consequent ease of data retrieval and storage on computer tape files. Suitably chosen domestic tape recorders afford the advantage of robustness and ease of maintenance, important advantages for a project which must function in a remote location like Macquarie Island. Another advantage in the use of a domestic tape recorder is that capital outlay requirements are small, an advantage of no small importance in our considerations.

The data recording speed used was $1\frac{7}{8}$ inches per second. Adoption of a higher tape recording speed would have given the advantage of lower error rates, but this option conflicted with the requirement that data tapes should have a reasonable information packing density. The tape recorder chosen for the experiment was the Ampex 850 four-track recorder, which was found to have excellent characteristics in construction and ease of maintenance and in the frequency response of its electronics at $1\frac{7}{8}$ inches per second recording speed. The tape transport system was distinctive in that two capstans were used, one on each side of the read/record head. This feature reduced the drop-out rates obtained with commercial tapes. The magnetic tape which was found to give the best performance was a 3M tape (triple play, number 290). With this combination of recorder and tape, error rates of the order of one tape drop-out every five minutes were obtained. Up to thirteen hours of data could be stored on one 3600 foot, 7 inch reel of tape.

Experimental data from three separate experiments was converted into digital form and recorded, together with time and housekeeping informa-

tion, by a data digitiser designed and constructed for the purpose. Information was recorded in the form of a serial bit stream consisting of successive data frames, each data frame being composed of 320 bits. Timing for the digitiser came from a crystal controlled digital chronometer.

The basic data word length of 8 bits provided 7 bits for data plus one bit for parity. One data frame can be regarded as being composed of ten four-word blocks, or lines, which differ in the fourth word. The first three words of each data line correspond to experiment inputs and the fourth is the time and housekeeping word.

1.4.1 *Data digitiser*

Figure 1-9 is a block diagram of the data digitiser. The data digitiser features extensive use of Texas Instruments TTL Logic Integrated Circuits. Experimental inputs consist of two analogue inputs and one pulse counting input. The analogue signal inputs were wired to voltage to frequency converters, the outputs of which were fed to seven bit accumulator circuits. The pulse counting input was fed directly to the input of a seven bit accumulator circuit.

Control logic provided the control signals for a four line commutator which selects, in turn, one of four seven bit sources to be set into the data shift register. After seven bits of information have been set into the data shift register, seven successive clock pulses shift this information into the output flip-flop. Before the arrival of an eighth clock pulse, a parity computing flip-flop is gated to the output flip-flop. On the eighth clock pulse, the parity bit is shifted to the

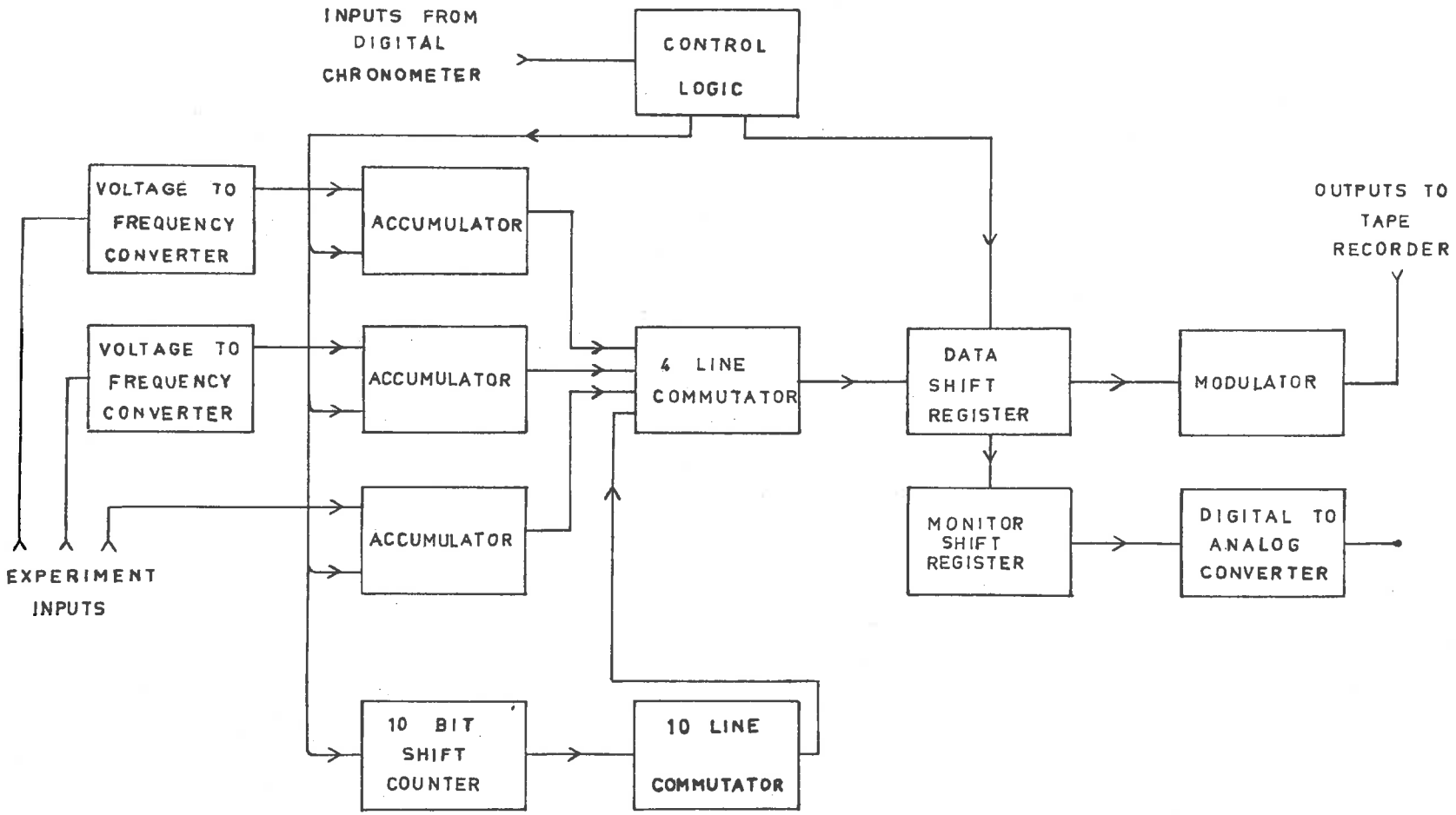

Fig. 1-9 Block diagram for data digitiser.

output of the data shift register. Before the next clock pulse arrives, the parity flip-flop is reset and another seven bits of information are set into the data shift register. Thus successive eight bit data words, always having an even number of zeros and ones, constitute the output.

While a seven bit source is being read into the data shift register, counting on that accumulator is inhibited. After information from a seven bit accumulator is read into the data shift register, the accumulator is reset. Each channel of information is sampled ten times per second.

One seven bit source is the output of a ten line sub-commutator which selects one of ten time and housekeeping information sources. Four time and housekeeping words are pre-wired. One of these data words is wired to provide the frame marker word which can be decoded and used for synchronizing purposes on replay. Five data words containing time information are provided by the chronometer. The digitiser is synchronized to the chronometer so that the time and housekeeping word containing the number of seconds is shifted into the data shift register at the start of each second. One time and housekeeping word can be set by means of thumbwheel switches mounted on the front panel. Circuitry is provided to prevent the setting of the frame marker word into the data shift register by means of the thumbwheel switches.

An eight bit shift register was connected to the output of the data shift register to allow display of eight bit words by means of lamps mounted on the front panel. The contents of the monitor shift register

are set into a buffer by read pulses which are selected through logic gates controlled by rotary switches mounted on the front panel. It is thus possible to display any particular experiment channel or time and housekeeping word on the display lamp array, enabling checks on performance of the digitiser.

The output of the data shift register was also used to amplitude modulate a 1.6 KHz tone which was recorded on one track of the tape recorder. Another modulated 1.6 KHz tone carrying a signal from the control logic was recorded on another tape track to provide reference pulses for synchronization on replay.

1.4.2 *Digital data transfer, decode and display circuitry*

A transfer unit was built to provide an interface with a data logger built by the Cosmic Ray Physics Group, University of Adelaide, to enable loading of data onto computer-compatible tape. By changing one card in the data digitiser and feeding in signals from the transfer unit, it was possible to decode and display any eight bit word of the bit stream recorded on a data tape. Data tapes were played back at the recording speed. The systems to be described in this section can easily be modified to accommodate playback speeds which are faster than the record speed, an option which provides the important advantages of faster transcription to 0.5 in. computer tape and lower wow and flutter in the tape transport system during replay of data tapes.

A block diagram of the transfer unit is given in Figure 1-10. The detectors included an input active filter with a Q of 5.3 and voltage gain

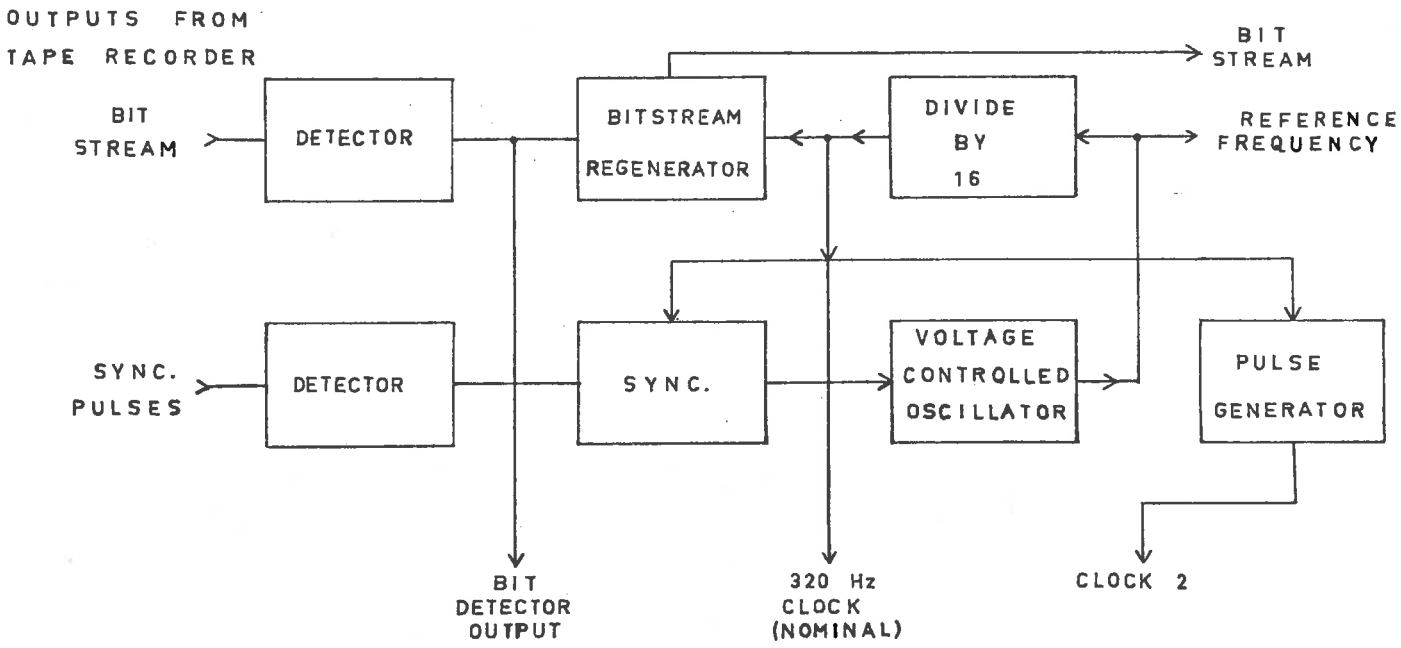

Fig. 1-10 Block diagram for transfer unit.

of 11 with centre frequency of 1.6 KHz. The resultant amplitude modulated 1.6 KHz tone was converted to a series of constant charge pulses which were fed to an integrator circuit, the output of which was limited and fed to a Schmitt trigger circuit, producing a sequence of pulses. Pulses from the bitstream channel were fed to the bitstream regenerator circuit.

Pulses from the synchronization channel were fed to a circuit which controlled a voltage-controlled oscillator circuit (V.C.O.) which provided a reference frequency with centre frequency sixteen times the nominal bit rate of 320 Hz. The centre frequency for the V.C.O. could be varied to allow the synchronizing circuit to lock onto data which had a basic bit rate differing from the nominal bit rate by up to $\pm$ 10 Hz. The V.C.O. output, which provided a reference frequency for the data logger, was divided by sixteen to provide the 320 Hz Clock (nominal) output, which was fed to the bitstream regenerator circuit, the output of which was also fed to the data logger.

A block diagram of the decode and display circuitry is given in Figure 1-11. Three control signals were provided by the transfer unit, namely:

(1) The bit detector output from the bitstream channel.

(2) The 320 Hz Clock (nominal) output which was synchronized to the synchronization channel on the data tapes.

(3) The Clock 2 output which was produced by a pulse generator circuit driven by the 320 Hz Clock (nominal) output.

The bit detector output for the bitstream channel was fed to an

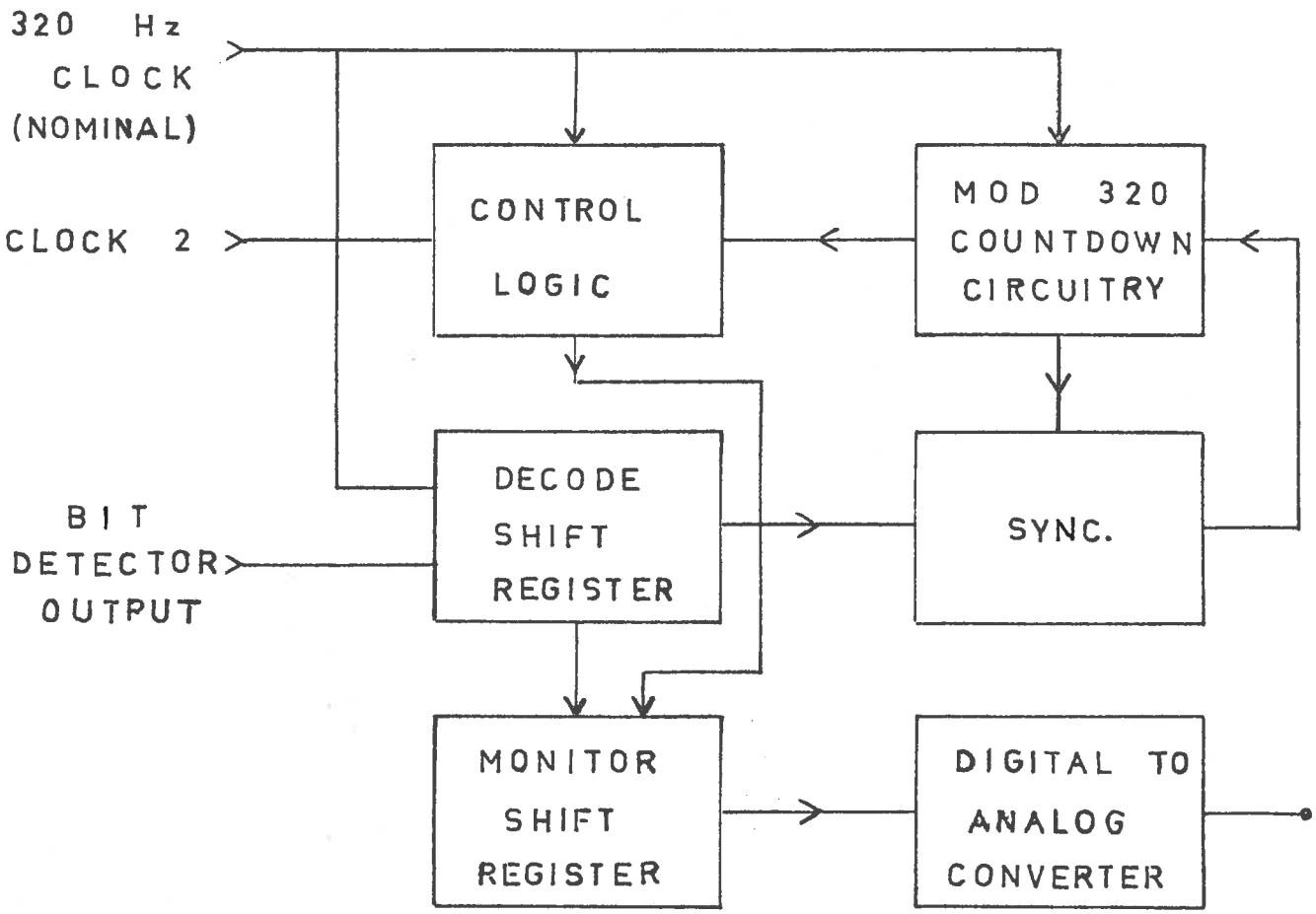

Fig. 1-11 Block diagram for decode and display circuitry.

eight bit shift register, called the decode shift register, one output of which was fed to the monitor shift register. The frame marker word was decoded from the decode shift register.

The sync. circuit (see Figure 1-11) inhibited counting in the modulo 320 countdown circuitry if, after four successive cycles of 320 clock pulses, there was no coincidence between the decode frame marker output (from the decode shift register) and the decode zero output (from the modulo 320 countdown circuitry) and allowed counting to restart when the next frame marker word was decoded from the decode shift register, thus ensuring correct timing in the display circuitry i.e. monitor shift register.

The input of a four bit accumulator was wired to a socket on the front panel of the digitiser and the four outputs were wired to display lamps. By counting the number of times counting in the modulo 320 countdown circuitry was inhibited during replay of a data tape, an estimate of the error rates due to failures in synchronizing could be obtained. A digital to analogue converter was wired to the monitor shift register so that any particular channel of information on the data tapes could be recorded on a chart recorder during replay.

CHAPTER 2

AURORAL ABSORPTION AND Pi GEOMAGNETIC PULSATIONS EVENTS AT MACQUARIE ISLAND

2.1 Introduction

Through the pioneering work of Shain (1951) and Little (1954), the use of the riometer in measuring cosmic radio noise absorption (abbreviation: CNA) in the ionosphere has become a routine procedure at stations in the auroral regions.

Absorption is usually defined as

$$A = 10 \log_{10} \left(\frac{I_Q}{I}\right)$$

where A is the absorption in decibels, I is cosmic noise power received in the aerial and I_Q is the quiet day value of cosmic noise power i.e. cosmic noise power received when there is no ionospheric disturbance.

Ansari (1964) asserts that in a typical night of absorption activity observed at College, Alaska, four distinct phases of aurorally associated absorption are noted, namely:

1. A prebreakup phase characterized by weak and slowly varying absorption.
2. A brief phase characterized by a sharp onset in absorption.
3. A phase characterized by recovery from the second phase associated with the post-breakup phase of the auroral display.

4. A phase characterized by a relatively slow rate of absorption increase which persists for a longer period of time, the slowly varying intense absorption phase (SVIA).

Ansari outlined his classification scheme before a model of the auroral substorm had been fully formulated. In this work, cosmic noise absorption and Pi geomagnetic pulsations activity will be examined in the various local time sectors at Macquarie Island with a particular emphasis on study of relationship to the auroral substorm.

2.2 Classification of Cosmic Noise Absorption Increases

In order to study the relationship between cosmic noise absorption and other phenomena, a classification scheme for absorption increases is introduced. This scheme simplifies description and does not require any initial assumptions concerning causation. Two classes of absorption increase, based on speed of increase, are proposed, namely rapid absorption increases (abbreviation RAI) and gradual absorption increases (abbreviation GAI). The RAI are defined as being significant increases in absorption where the time taken for the increase from one level to a new level of disturbance is less than, or equal to, five minutes. The GAI are those absorption increases where time taken for the increase from one level to a new level is greater than or equal to ten minutes.

Introduction of two subclasses of gradual absorption increase has been found to be of some utility. These subclasses of GAI are:

1. Gradual absorption onset (abbreviation GAO) which is gradual increase in absorption from the quiet day level to a disturbed level.

2. Gradual absorption enhancement (abbreviation GAE) which is any gradual absorption increase from one disturbed level to a new level of disturbance.

Any absorption increase which does not fall into either of the classes proposed above will be referred to simply as absorption onsets or enhancements. Examples of the various types of absorption increase, as proposed, will be given in §2.3.

2.3 Pi Geomagnetic Pulsations

Geomagnetic pulsations are divided into two main types: continuous pulsations having a regular nature (Pc) and irregular pulsations (Pi) (Jacobs et al 1964). The Pi and Pc classes are further subdivided according to the following scheme:

Type	Period Range (sec)
Pc 1	0.25 - 55
Pc 2	5 - 10
Pc 3	10 - 45
Pc 4	45 - 150
Pc 5	150 - 600
Pi 1	1 - 40
Pi 2	40 - 150

Jacobs and Sinno (1960) have shown that Pi 2 pulsations are associated with positive and negative bay disturbances in the auroral regions. Pi 2 pulsations have a diurnal occurrence maximum near geo-

magnetic midnight (Romaná and Cardús, 1962).

Pi 1 geomagnetic pulsations are commonly observed in the auroral zones, being closely associated with auroral, - ve bay activity and electron precipitation (Campbell and Matsushita, 1962; Troitskaya, 1961).

A very useful means of displaying the time structuring of geomagnetic pulsations is provided in the sonagram, which is a representation of the time varying power spectrum. The most obvious characteristic of Pi geomagnetic pulsations activity is its non-stationary character. Pi geomagnetic pulsations are observed, in the auroral zones, to occur in bursts which last for periods typically from one to three hours. As the level of planetary magnetic disturbance rises, Pi activity is observed for longer periods during the night hours; during highly disturbed periods, Pi activity commences in the early evening, continues through the night and morning, ending in the early afternoon.

During January to March 1968, geomagnetic pulsations were recorded at Macquaire Island by John Annextadt of the Geophysical Institute, College, Alaska. His data were recorded on a slow-speed tape recorder. These tapes were played back at speeds much faster than the record speed into a multi-channel spectrum analyser, the output from which was recorded onto 35 mm. photographic emulsion to provide a continuous record of frequency-time behaviour of geomagnetic pulsations activity. These sonagrams have been made available to the author for the present study.

A characteristic of the sonagrams of Pi geomagnetic pulsations at Macquarie Island is their noise-like character. Power is often distributed

over the frequency band 0.1 to 0.5 Hz. Changes in amplitude of Pi geomagnetic pulsations, as observed on amplitude - time records, are observed as changes in frequency content on sonagrams. For instance, during an increase in amplitude of Pi geomagnetic pulsations, the upper limit to the frequency band over which power is observed increases on sonagrams. Changes in frequency content observed on sonagrams will be referred to as Pi "features".

In order to facilitate the detailed study of Pi activity, a classification scheme for Pi features is introduced. Two classes of Pi features are distinguished, based on speed of change in frequency content viz. rapid and gradual Pi features.

Rapid Pi features are defined as those features characterized by appearance of power extending over a band of frequencies from 0.1 to 0.3 Hz within a time interval of less than or equal to five minutes. Three sub-classes of rapid Pi features are proposed:

(1) Rapid irregular pulsations onset (abbreviation R Pi O).

(2) Rapid irregular pulsations enhancement (abbreviation R Pi E).

(3) Rapid irregular pulsations burst (abbreviation R Pi B). This particular pulsations type has the appearance on the sonagram of a burst with duration of the order of 5 minutes, and is referred to by French and Russian workers as S.I.P. (Gendrin et al, 1968; Troitskaya, 1961).

Gradual Pi features are defined as those features characterized by a slow change in frequency content i.e. the change takes place over a time interval greater than or equal to ten minutes. Two subclasses of gradual

Pi features are distinguished:

(1) Gradual irregular pulsations onset (abbreviation G Pi O).

(2) Gradual irregular pulsations enhancement (abbreviation G Pi E).

Using this classification, sonagrams of geomagnetic pulsations (H component) at Macquarie Island, January to March 1968, were scaled by noting commencement times of distinctive features of the sonagrams together with the classification. If there was doubt as to whether a Pi feature fell into either the rapid or gradual classes, it was noted as a Pi onset or enhancement (abbreviations Pi O and Pi E respectively).

In Figure 2-1, examples of some of the proposed classes of absorption increases and Pi features are illustrated using records obtained for the night of 17 February 1968 at Macquarie Island.

From the normal run magnetometer record included in Figure 2-1, it can be seen that there are two periods of negative bay activity, one starting at 0900 U.T. and the other starting around 1100 U.T. Similarity in time structuring in magnetometer H component, geomagnetic pulsations sonagram and cosmic noise absorption record are evident. Examples of rapid absorption increases can be seen starting at approximately 1150, 1200 and 1420 U.T. The first RAI can be associated with a rapid irregular pulsations onset (R Pi O). The last two can be associated with rapid irregular pulsations enhancements (R Pi E). At about 1315 U.T., a GAI commenced which can be associated with a gradual irregular pulsations enhancement (G Pi E).

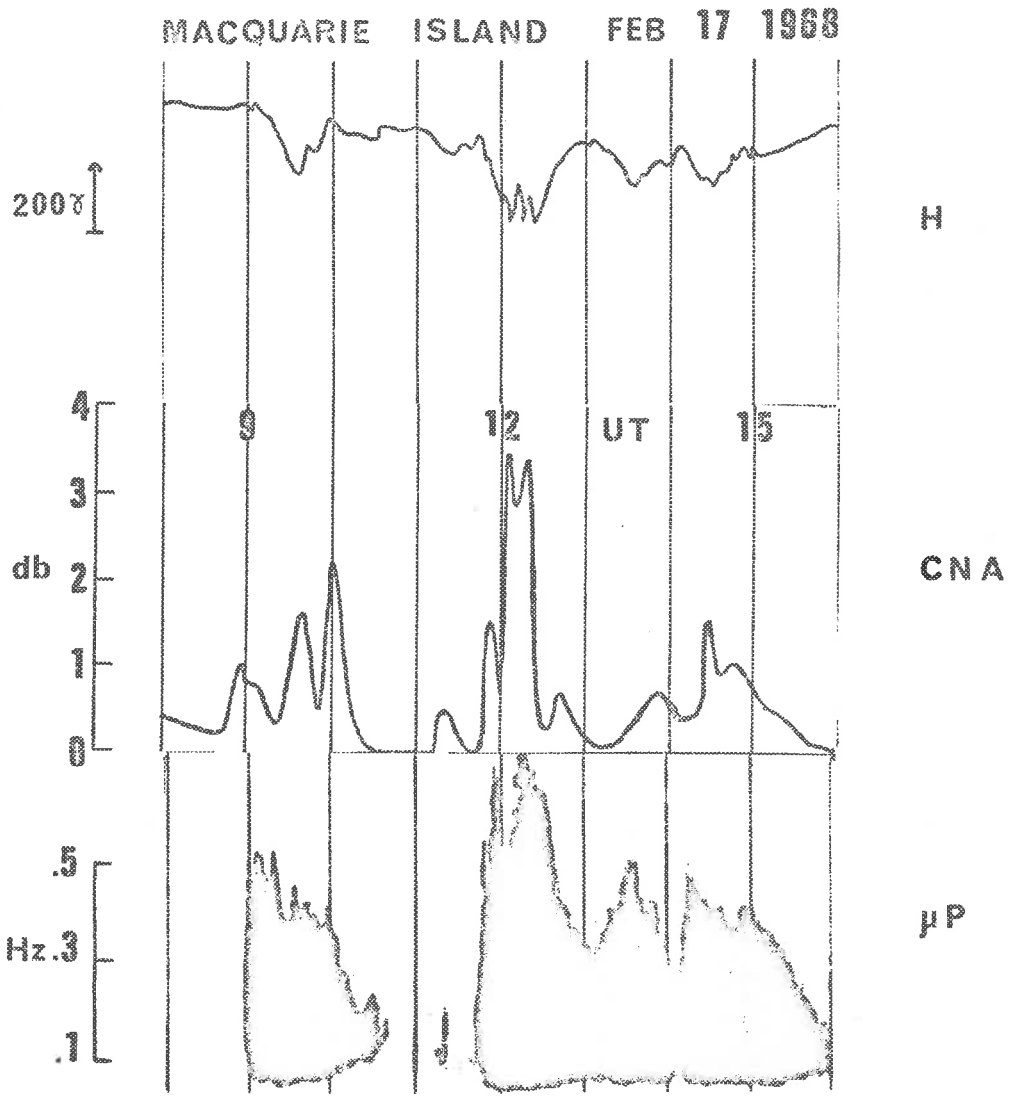

Fig. 2-1 Magnetometer, normal 30 MHz riometer and geomagnetic pulsations sonagraph records for Macquarie Island for the period 0800 to 1600 U.T. on 17 February 1968.

2.4 Rapid Absorption Increases

Statistical studies of cosmic noise absorption by many workers (for example: Holt et al (1961) using data from Norwegian riometer networks, Driatskiy (1966) using Soviet Arctic riometer data, Basler (1963) using Alaskan riometer data, and Hartz et al (1963) from a Canadian riometer network) have shown that absorption of the type generally known as "auroral absorption" is characterized by a maximum in the late morning hours and a secondary maximum in the late evening to midnight hours. A minimum in absorption is found in the afternoon hours.

It has been found that the latitudinal variation of auroral absorption shows a maximum near geomagnetic latitudes of 65°, close to the latitude of maximum auroral occurrence frequency. Basler (1963), Hartz et al (1963) and Driatskiy (1966) find that the latitude of the absorption maximum is from 1 to 5 degrees equatorward of the visual aurora maximum. Driatskiy (1966) gives evidence that during the decreasing phase of the solar activity cycle, the auroral absorption maximum moves poleward in a manner analogous to the movement of the visual aurora maximum, (Davies, 1950).

The distinctive feature of auroral absorption in the midnight sector is the occurrence of rapid absorption increases.

In Figure 2-2(a), the occurrence frequency of strong RAI for the period 5 January to 22 March 1968 is shown in histogram form. Numbers of RAI, with relative absorption value greater than 1dB, recorded in given one hour U.T. intervals are tabulated. Relative absorption A_r for the

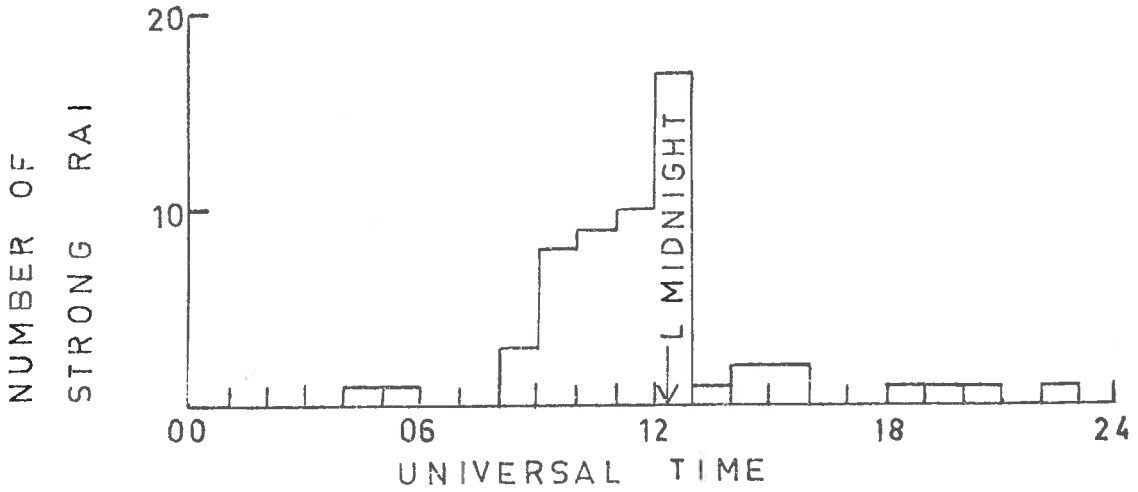

Fig. 2-2(a) Diurnal variation of occurrence of strong rapid absorption increases at Macquarie Island, January to March 1968.

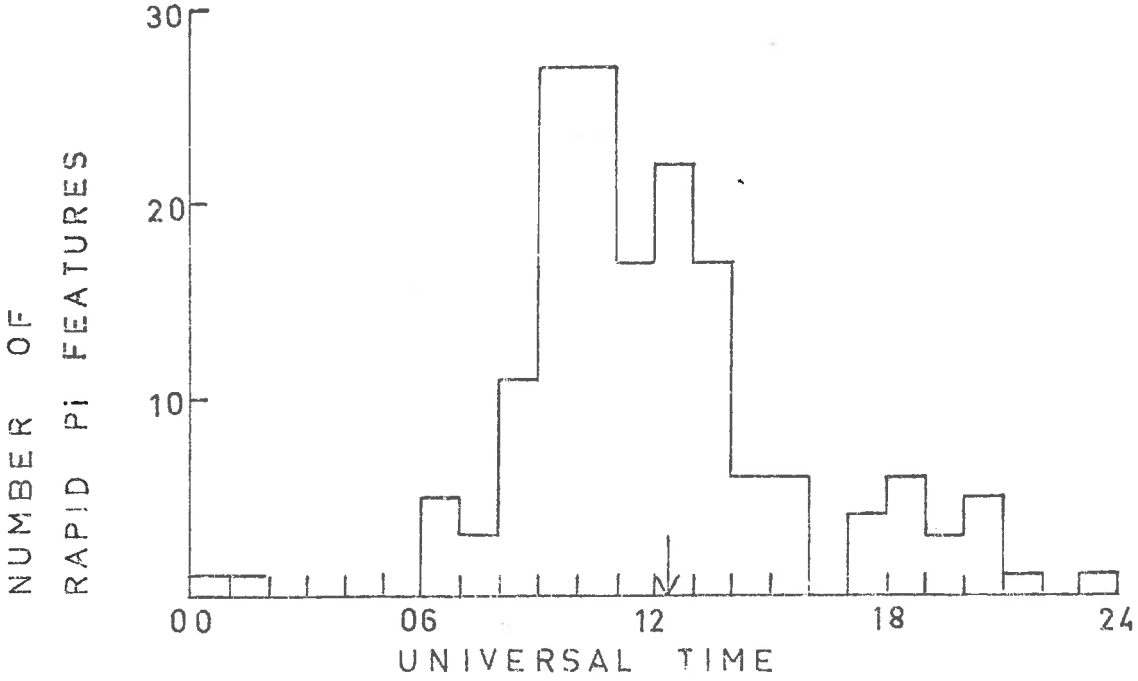

Fig. 2-2(b) Diurnal variation of occurrence of rapid Pi features at Macquarie Island, January to March 1968.

absorption increase is defined by:

$$A_r = 10 \log_{10} \frac{I_{PR}}{I_M}$$

where I_{PR} is the cosmic noise power at the start of the absorption increase and I_M is the cosmic noise power at the maximum level of disturbance for the absorption increase.

Using a geomagnetic co-ordinate system proposed by Kilfoyle and Jacka (1968), geomagnetic midnight at Macquarie Island is approximately 1220 U.T. It can be seen that most strong RAI were recorded near geomagnetic midnight i.e. 44 out of a total of 58 were recorded in the time interval 0900 - 1259 U.T. This result is in agreement with the result of a similar study of diurnal variation of occurrence frequency of type F events carried out by Berkey and Parthasarathy (1964) using Alaskan riometer data. These events begin with a feature similar to what the author calls RAI. This applies also to the events called SAI by Ansari (1964) and SIA by Bather and Jacka (1966).

The occurrence of strong RAI was correlated with the occurrence of rapid Pi features. In Figure 2-2(b) a histogram is given showing the number of rapid Pi features i.e. onsets, bursts or enhancements, recorded in one hour U.T. intervals for the period 5 January to 22 March 1968. It can be seen that both rapid Pi features and strong RAI have diurnal occurrence frequency maxima near midnight. Of the 39 strong RAI recorded in the hours 0900 - 1400 U.T., 29 could be associated with a rapid Pi feature. An absorption increase and Pi feature were regarded as being related if they occurred in the same ten minute interval. Heacock (1967a) has also

demonstrated a close relationship between type F absorption events and Pi events having rapid onsets.

2.5 A Class of Auroral Absorption Events at Macquarie Island

In discussion of Pi or absorption activity, the term "event" is introduced. An event is defined as a period of activity preceded and followed by quiet periods.

A class of slowly varying absorption events (abbreviation SVA) is now defined as that class of events which do not contain any rapid absorption increases and in which the rise-time of the absorption onset is greater than or equal to ten minutes.

In Figure 2-3, examples of SVA events for the records for 8 February 1968, together with magnetograms and geomagnetic pulsations sonagrams, are given. It can be seen that there are three separate SVA events, starting at approximately 1414, 1840 and 2140 U.T. respectively and that each SVA event is accompanied by a negative bay in the H component magnetogram. The typical relationship between SVA events and Pi activity can be seen, i.e. each SVA event occurs during a Pi event. During January to March 1968, days during which more than one SVA event was recorded in the morning to noon hours were not rare.

In Figure 2-4, a histogram is given showing the number of SVA events where the time of maximum absorption occurred in a given two-hour U.T. interval and where the maximum absorption was greater than 1 dB. It can be seen that there is an occurrence maximum around 1700 U.T. (near to mid-morning at Macquarie Island).

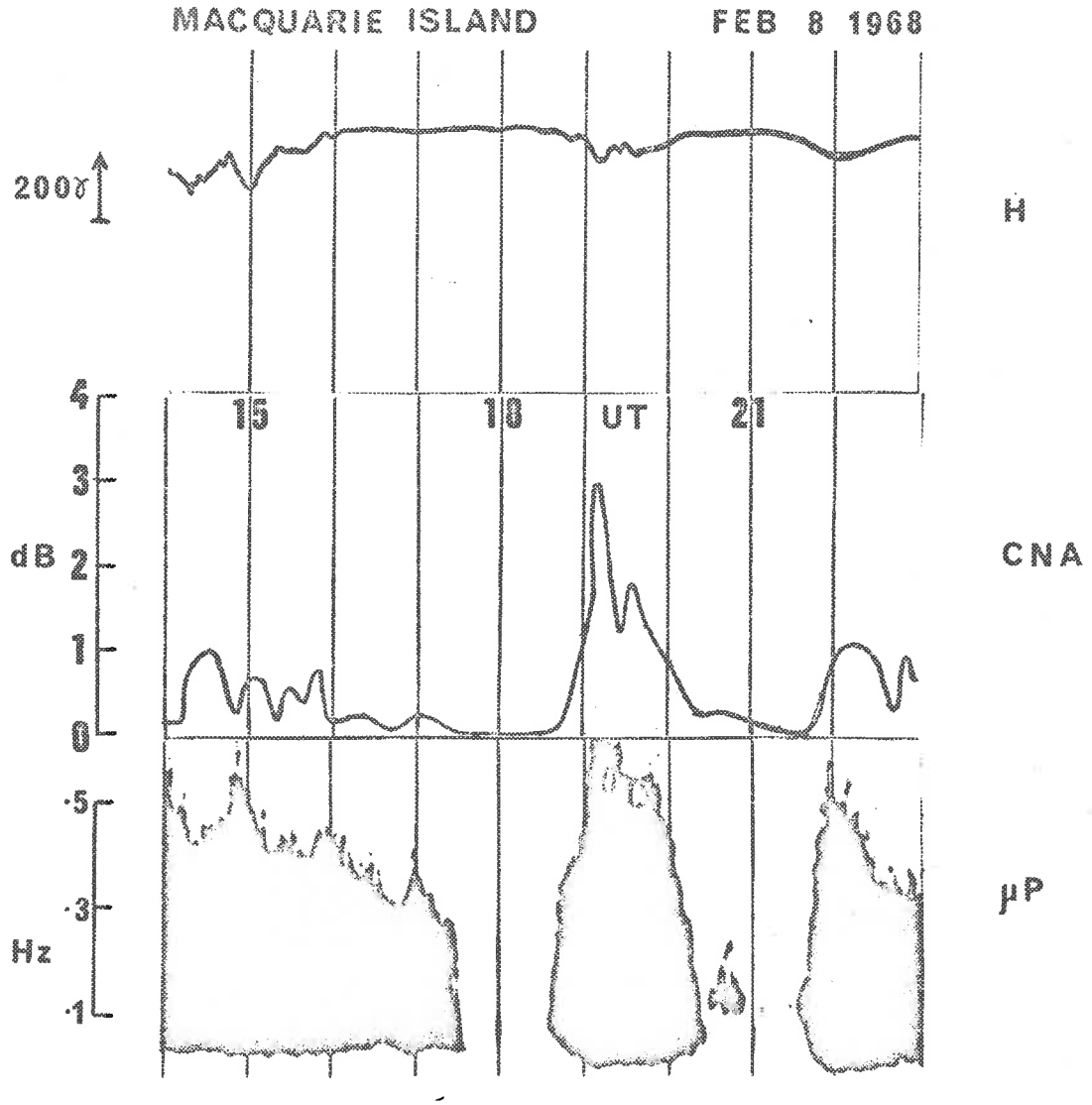

Fig. 2-3 Magnetometer, cosmic noise absorption and geomagnetic pulsations sonagraph records for Macquarie Island for the period 1400 to 2300 U.T. on 8 February 1968.

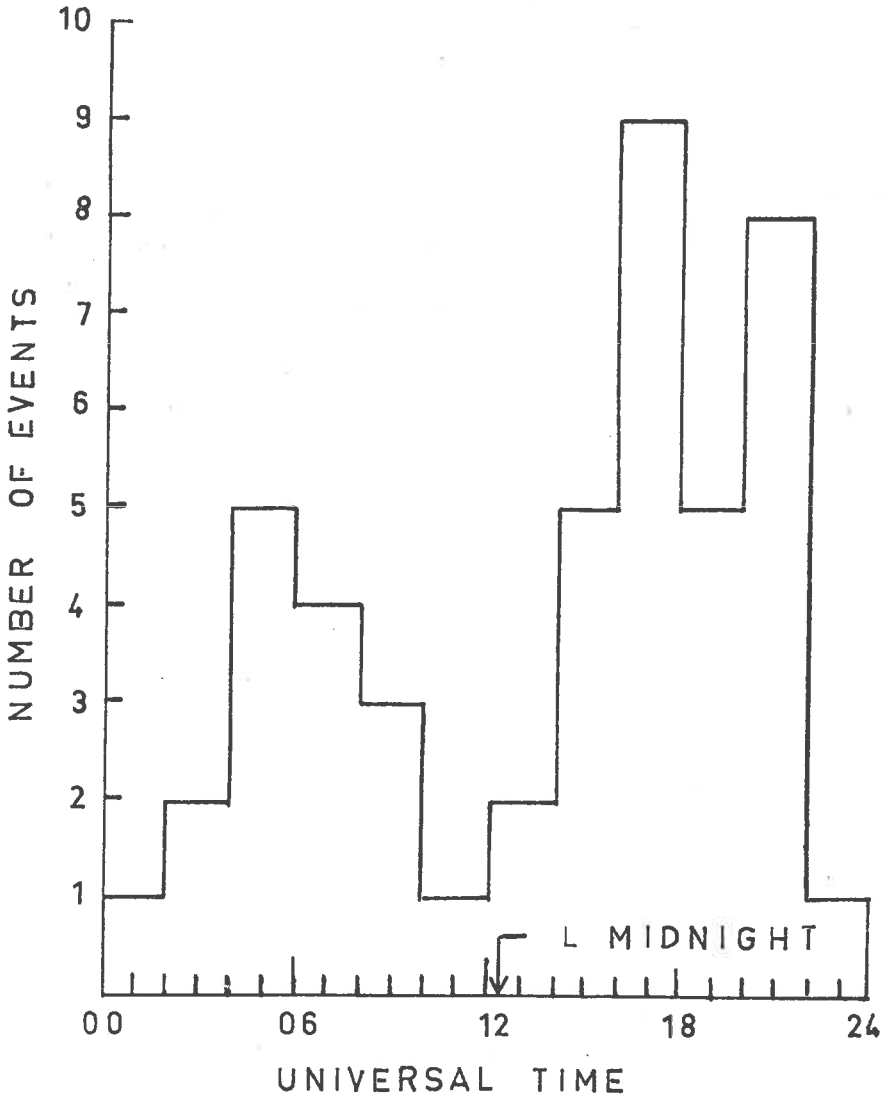

Fig. 2-4 Occurrence of SVA maxima (peak absorption > 1 dB) in given two hour U.T. intervals at Macquarie Island, January to March 1968.

It is believed that the class of SVA events defined here is the same class of events reported by many workers including Ansari (1963) and (1965), Brown (1964) and Ortner and Riedler (1964).

The relationship between SVA events with peak absorption greater than 1 dB (strong SVA) and Pi activity has a marked dependence on local time at Macquarie Island. Of 11 strong events which started in the hours 0200 to 0900 U.T. (afternoon to evening), 6 events could not be related to Pi activity, as there was no Pi activity in a three-hour period centred around the absorption onset time. Every one of the 26 SVA events which started in the hours 1400 to 2400 U.T. (the morning to noon hours) was accompanied by Pi activity.

2.6 Rapidly Varying Morning Absorption Events

Some absorption events recorded at Macquarie Island in the morning to noon hours were distinctive in that they contained rapid and irregular, intense absorption increases. This particular type of absorption event was not common but at least four were recorded during the period January to March 1968, and occurred during periods of moderately high planetary magnetic disturbance (Kp > 3 +). It is proposed that this type of absorption event be considered as a separate class termed "rapidly varying morning absorption events" (abbreviated RVMA).

In Figure 2-5 an example of a RVMA event from the records for 10 February 1968 is given, together with Macquarie Island magnetometer (H component) record and geomagnetic pulsations sonagram. It can be seen that rapidly varying absorption begins after 1700 U.T. accompanied by a large

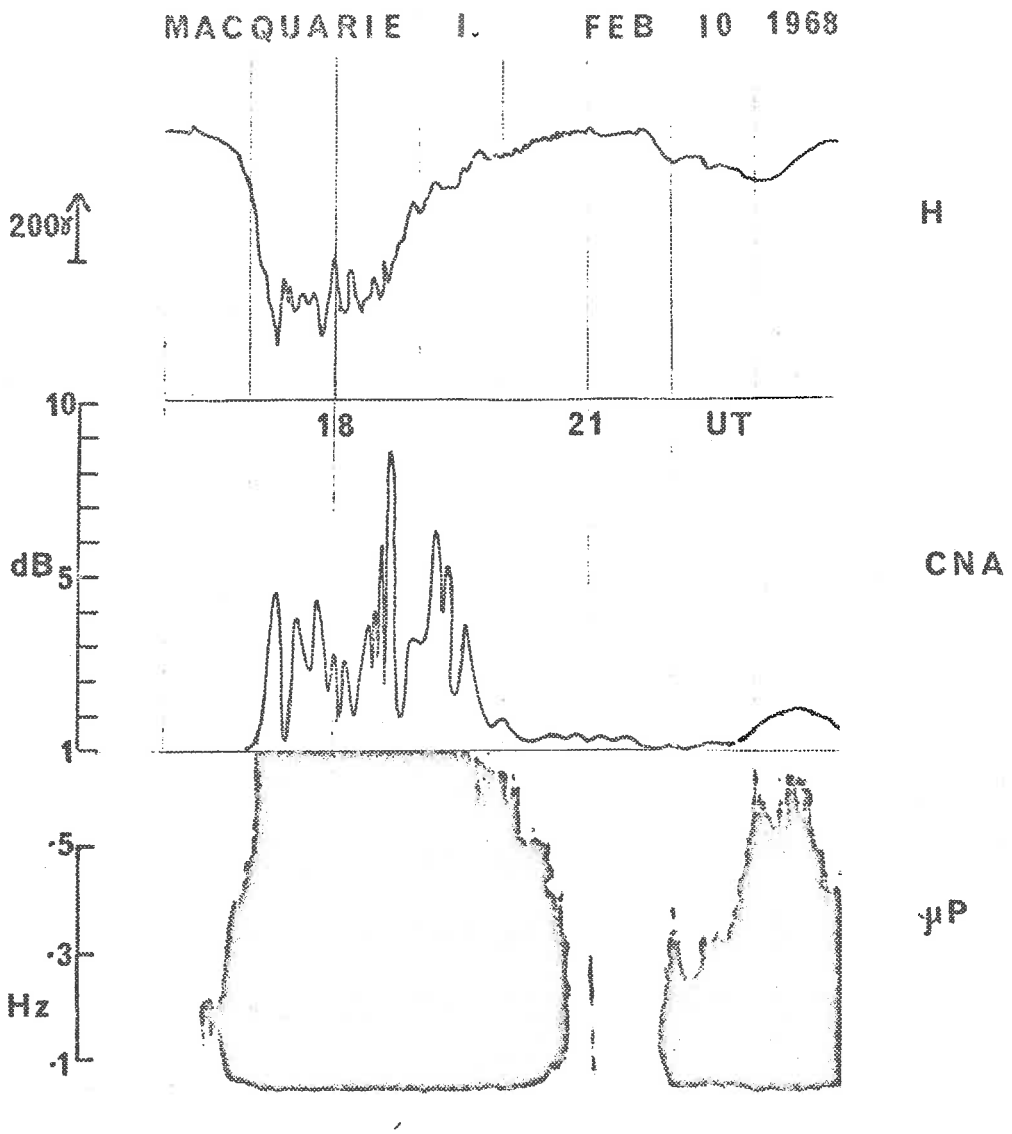

Fig. 2-5 Magnetometer, cosmic noise absorption and geomagnetic pulsations sonagraph records for Macquarie Island for the period 1600 to 2400 U.T. on 10 February 1968.

negative bay in H (650 γ) and an intense Pi event. By 2140 U.T., absorption has returned to quiet day values. Around this time the geomagnetic field is quiet and Pi activity has ceased.

At about 2145 U.T., it can be seen that Pi activity commences again, accompanied by decrease in magnetic H component. Slowly varying absorption commences after 2220 U.T., near geomagnetic noon at Macquarie Island.

2.7 Pi Activity during Cosmic Noise Absorption Events at Macquarie Island

In general, the occurrence of cosmic noise absorption was closely related to occurrence of Pi geomagnetic pulsations at Macquarie Island. Diurnal variation of Pi activity was examined in terms of the percentage of time Pi activity was observed in each hour (U.T.). Results are shown in Figure 2-6. It can be seen that for approximately half the total observing time, Pi activity was recorded at Macquarie Island. A histogram showing percentage of total observing time that detectable cosmic noise absorption was noted in a given 1 hour U.T. interval is given for comparison. The two histograms have similar features i.e. a diurnal minimum in the afternoon hours at about 0600 U.T. and a diurnal maximum in the morning hours.

In Table 2-1, the numbers of times both CNA and Pi activity were noted in the same 1 hour (U.T.) interval are tabulated. The expected numbers assuming that Pi and absorption activity are unrelated phenomena were calculated using the formula given by Jánossy (1950).

$$N_{(calc)} = N_1 e^{-N_1 t} + N_2 e^{-N_2 t} - (N_1 + N_2) e^{-(N_1 + N_2)t}$$

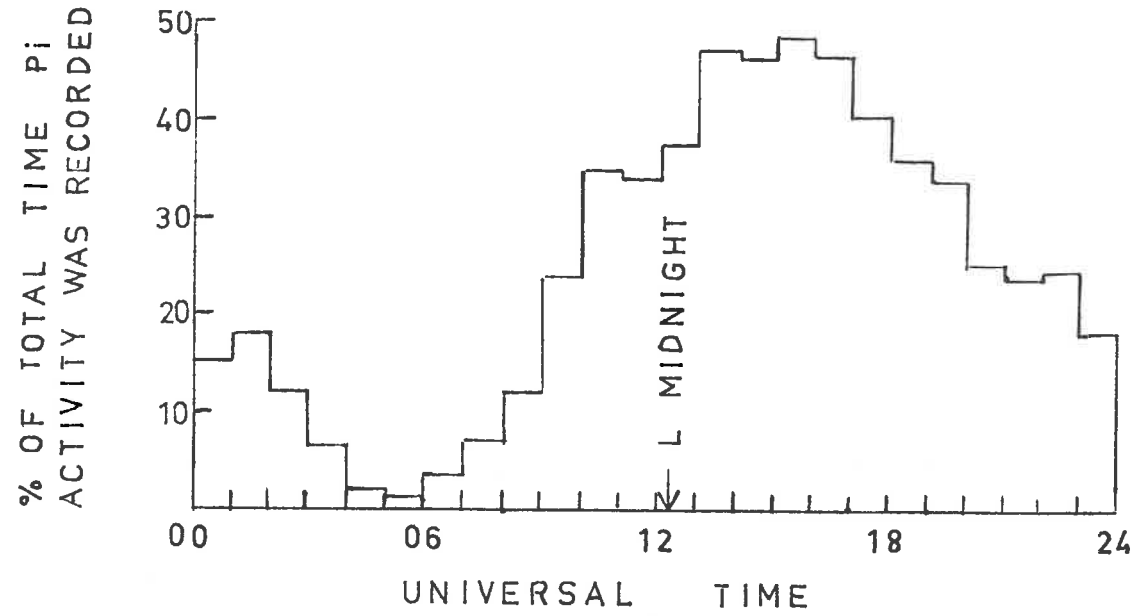

Fig. 2-6(a) Percentage of total time for each hour U.T. interval that Pi activity was recorded at Macquarie Island, January to March 1968.

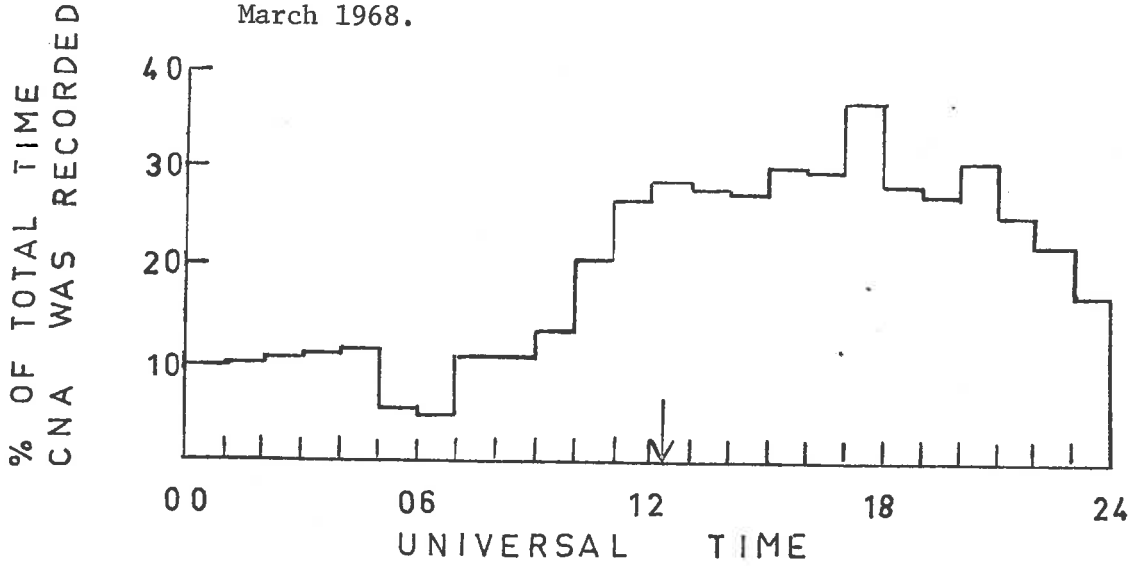

Fig. 2-6(b) Percentage of total time for each hour U.T. interval that detectable cosmic noise absorption was recorded at Macquarie Island, January to March 1968.

TABLE 2-1

1 hour (U.T.) Time Interval	No. of times Pi activity is recorded	No. of times absorption is recorded	No. of times both types of activity are recorded N(obs)	Expected number, assuming random coincidence N(calc)
00 - 0059	19	11	5	4
01 - 0159	17	10	5	3
02 - 0259	12	11	4	3
03 - 0359	9	13	5	2
04 - 0459	4	13	1	1
05 - 0559	1	6	0	0
06 - 0659	4	5	0	0
07 - 0759	8	15	3	2
08 - 0859	17	14	7	5
09 - 0959	25	16	15	7
10 - 1059	33	25	22	12
11 - 1159	37	24	21	13
12 - 1259	39	27	24	14
13 - 1359	45	28	27	16
14 - 1459	41	26	23	15
15 - 1559	43	30	29	18
16 - 1659	43	30	25	17
17 - 1759	39	33	29	17
18 - 1859	34	29	24	14
19 - 1959	33	27	24	13
20 - 2059	28	27	20	12
21 - 2159	24	29	20	11
22 - 2259	23	22	17	9
23 - 2359	17	17	10	5

where $N_{(calc)}$ is the expected frequency of occurrence of the event that both Pi and absorption activity are recorded in the same time interval t assuming random coincidence, N_1 is the frequency of occurrence of the event that Pi activity is recorded in the interval t, and N_2 is the corresponding occurrence frequency for absorption. The parameter t was set to one hour.

From Table 2-1 we can see that the total number of times that Pi activity and absorption activity were noted in the same 1 hour (U.T.) time interval considerably exceeds the expected number, assuming random coincidance, for the hours from 0900 to 2300 U.T. (late evening, midnight and morning to noon hours) at Macquarie Island for the period 5 January to 22 March 1968.

CHAPTER 3

DIGITAL SONAGRAMS OF Pi GEOMAGNETIC PULSATIONS

3.1 Data Processing

Selected data, recorded on 0.25 in. magnetic tape at Macquarie Island, were transcribed onto 0.5 in. computer tape using the digital data replay system described in Chapter 1. The basic aim of all computer processing of these 0.5 in. tape records, prior to loading onto masterfile tapes, was to preserve continuity of data records, to minimise loss of data and to avoid introduction of spurious data values into data files.

During the process of creating files of information, which could be readily manipulated in the memory of a digital computer, data was lost by:

(i) drop-outs during recording or replay of 0.25 in. data tapes due to dust or imperfections in tape coating and

(ii) inconstancy in tape speeds during recording or replay of 0.25 in. data tapes which led to occasional loss of synchronizing information during transcription of 0.25 in. data tapes to 0.5 in. computer tapes using the data logger referred to in Chapter 1.

The loss of synchronizing information during transcription of data tapes will be referred to as "sync. loss".

Data was recorded on 0.25 in. tape in the form of a serial bit stream, composed of successive data frames. Each data frame comprised

320 bits. When data was transcribed onto 0.25 in. tape, four successive data frames were written onto the 0.5 in. tape as one 380 character record. Each standard length record contained 1280 bits of information which were easily decoded using a digital computer. Whenever sync. loss occurred during transcription of 0.25 in. data tapes, odd length records were written onto the 0.5 in. tape. These odd length records were normally greater than 380 characters.

A computer program was written which enabled decoding of data logger tapes using a CDC 3200 computer at the C.S.I.R.O. Computing Research Section, Adelaide. Data tapes, with uniformity in record lengths, were produced by this program for processing which was carried out using a more powerful machine, the CDC 6400 computer at the University of Adelaide Computing Centre. Inspection of the information content of sequences of records on data logger tapes showed that most of the data in complete and partial data frames stored in odd length records could be extracted using algorithms involving the manipulation of sequences of bits which had lengths of the order of thousands of bits. The processing program contained two loops:

(i) a main processing loop in which standard length records were decoded. Parity of the forty data words in each data frame were checked. If all data parity values were correct, data was transferred to an output tape and the next record processed.

(ii) a subsidiary processing loop in which information was extracted from odd length records using bit-manipulation routines.

For a data logger tape of sufficiently good quality, most processing was carried out in the main processing loop. If a record was found where the length was non-standard or one or more data word parity values was incorrect, such records and all following records were processed in the subsidiary processing loop until a standard length record, with no data word parity errors, was encountered.

The serial bitstream contained in odd-length records was stored in an array of computer memory words (which will be referred to as the "bitstore"). Correct data lines and frames were extracted from the bitstore and written onto the output tape using two algorithms.

In one algorithm, which was used to extract data lines, use was made of the way time and housekeeping information was stored in every data frame. The first word of a data line, which consisted of four data words, contained time and housekeeping information and will be referred to as a "THK word". Given the ten THK words decoded from one data frame, it was possible to predict exactly what time and housekeeping information should have been contained in the next data frame. The bitstore was scanned for 72-bit strings containing three valid THK words which had correct inter-relationships and where all eight-bit word parities were correct. When such 72-bit strings were found, data lines could be extracted and written onto the output tape.

The other algorithm, which was used to extract complete data frames from the bitstore, involved scanning the bitstore for bit-strings having a length 320 bits, where all 8-bit word parities were correct and where the first and seventh THK words were also correct. The 2nd, 3rd,

4th, 5th and 6th THK words of a data frame contained time and index word information and were variable from one data frame to the next. It was found that if only the first THK word was checked, it was possible to extract spurious data frames. By checking one additional THK word, this problem of introduction of spurious data values was eliminated.

Data tapes produced using the CDC 3200 computer were checked using test programs on the CDC 6400 computer. By checking time information in successive data frames, it was found that the effect of sync. loss in breaking of continuity of the data record during transcription of data could be counteracted in a satisfactory manner using the primary processing program on the CDC 3200 computer. Linear interpolations provided substitutes for missing data values.

In Figure 3-1a data section which was automatically digitised using the digital data recording system is reproduced. The lower trace in Figure 3-1 is the same data section digitised manually from chart records. This diagram was produced using a Calcomp X-Y plotter. Data for the bottom trace was punched onto 80-column cards. Data for the top trace was taken from a data tape produced from a masterfile data tape.

3.2 Digital Filtering using Z Transform Techniques

For a continuous function f(t) of time t, we can define the time series $f^*(t)$ resulting from sampling the function f(t) with sampling interval T, the first sample being taken at time t=o by the expression:

$$f^*(t) = \sum_{n=0}^{\infty} f(t)\ \delta(t-nT) \qquad (1)$$

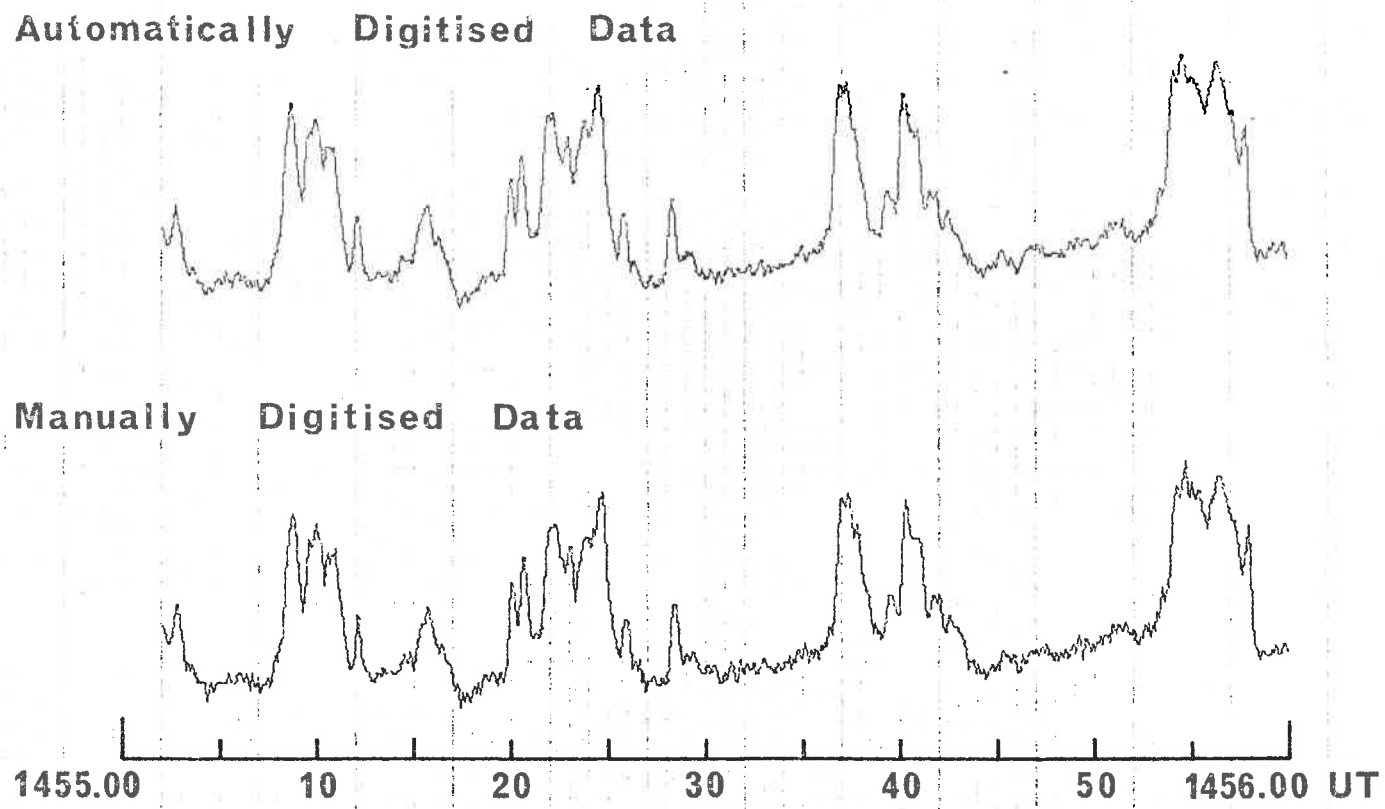

Fig. 3-1 A data section digitised manually and also automatically.

$\delta(t)$ is the delta-function and n is an integer.

The z transform F(z) of the time series f*(t) is defined by the following equation:

$$F(z) = \sum_{n=0}^{\infty} f(nT)\, z^{-n} \qquad (2)$$

The variable z is complex, being related to the Laplace transform variable s by

$$z = e^{Ts} \qquad (3)$$

It can be seen that the z transform of a time series delayed by i sampling intervals is given by the z transform of the original time series multiplied by z^{-i}.

3.2.1 *Linear difference equations*

Input-output relationships for a digital filter may be conveniently formulated using linear difference equations, i.e. where x*(t) and y*(t) are the input and output time series respectively, then the value of y*(t) at time t=nT may be expressed as

$$y(nT) = \sum_{i=0}^{r} A_i\, x(nT-iT) - \sum_{i=1}^{m} B_i\, y(nT-iT) \qquad (4)$$

where A_i and B_i are constants. m is the order of the linear difference equation.

If X(z) and Y(z) are the z transforms of x*(t) and y*(t) respectively, the transfer function H(z) of the digital filter is defined by

$$Y(z) = H(z)\, X(z) \qquad (5)$$

From (4), the following relationship may be derived (c.f. Rader and Gold, 1967).

$$H(z) = \frac{\sum_{i=0}^{r} A_i z^{-i}}{1 - \sum_{i=1}^{p} B_i z^{-i}} \qquad (6)$$

Response of the digital filter to sinusoidal inputs can be found by letting $x(nT) = e^{j\omega nT}$. The frequency response function $F(\omega)$ is given by:

$$F(\omega) = H(e^{j\omega T}) \qquad (7)$$

If $F(\omega) = |H| e^{j\theta(\omega)}$, then $|H|$ is the amplitude response as a function of ω, and $\theta(\omega)$ is the phase response function.

3.2.2 *Digital simulation of continuous filters*

In one technique of digital simulation of a continuous filter, the digital filter transfer function $H(z)$ is the z transform of the time series which is the sampled version of the impulse response of the continuous filter.

The transfer function $H(z)$ may be derived using a correspondence pointed out by Rader and Gold (1967).

If the continuous filter has a transfer function $G(s)$ of the form

$$G(s) = \sum_{i=1}^{p} \frac{A_i}{s + s_i} \qquad (8)$$

then the digital filter will have the transfer function $H(z)$ of the form

$$H(z) = \sum_{i=1}^{m} \frac{A_i}{1-e^{-s_i T} z^{-1}} \qquad (9)$$

One disadvantage of this technique is that the frequency responses of the continuous filter and its digital simulation may not be identical over the frequency range from zero to $\omega_s/2$ due to aliasing effects. (ω_s is the sampling frequency). Aliasing effects will occur if $|G(s)| \neq 0$ for $\omega > \omega_s/2$ (c.f. Golden and Kaiser, 1964).

Golden and Kaiser (1964) have put forward a digital simulation technique in which the transfer function H(z) is derived from the continuous system transfer function G(s) by using the algebraic substitution

$$s = \frac{2}{T} \frac{(1 - z^{-1})}{(1 + z^{-1})} \qquad (10)$$

In this technique, a new variable $s_1 = \sigma_1 + j\omega_1$ is defined by using a mapping transformation

$$s = \frac{2}{T} \tan^{-1} \left(\frac{s_1 T}{2}\right) \qquad (11)$$

z is set equal to $e^{s_1 T}$. This transformation, termed the bilinear z transformation, maps the whole of the left half of the s-plane into the unit circle in the z-plane and the whole of the right half of the s-plane is mapped into all of the z-plane which is exterior to the unit circle. In particular, the positive half of the $j\omega$ axis in the s-plane is mapped into the top half of the unit circle in the z-plane. Thus the frequency characteristics of the digital filter are identical to those of the

continuous filter except for a nonlinear warping of the frequency scale (Golden and Kaiser, 1964).

By using the bilinear z transformation, filters of varied character i.e. low-pass, high-pass and band-pass, may be simulated, even when cut-off frequencies are close to frequencies near half the sampling frequency. Transfer functions for continuous high-pass and band-pass filters may be derived from the transfer function of a low-pass filter using suitable mapping transformations of the s-plane (see Storer, 1957).

3.3 Computation of Time-Varying Power Spectra

The time-varying power spectrum for any signal can be estimated by means of the process of feeding of this signal to an array of band-pass filters and of detecting the output of each filter using a square law detector. The filters used are tuned with overlapping frequency responses so that frequency content across some pre-determined frequency band can be measured with a resolution determined by the bandwidths of the filters. Any representation of the detected output of each filter from such an array of filters which allows examination of frequency content as a function of time is a sonagram. Sonagrams produced by computation of time-varying power spectra using a digital computer will be referred to as digital sonagrams.

Significant advantages are gained through the use of digital computers in the production of sonagrams. Components for analogue filters with cut-off frequencies in the range .005 to 5 Hz are usually bulky. No such disadvantage is encountered when filtering is performed using a

digital computer. Problems encountered due to temperature sensitivity of analogue filters can be avoided using digital filtering. If automatic digitisation is used, frequency stability is determined primarily by the accuracy and stability of timing equipment used.

The impulse response function of a band-pass filter tuned to frequency ω_o and with width $\Delta\omega$ tends, as $\Delta\omega$ decreases to resemble a function proportional to the damped sinusoid function $e^{-\frac{t}{\Delta T}} \sin \omega_o t$, where t is time and ΔT is proportional to $1/\Delta\omega$. This property of band-pass filters illustrates an uncertainty principle in spectral analysis. Frequency resolution can be gained only at the expense of time resolution and vice versa. If power spectra are estimated using a set of constant bandwidth filters, the frequency resolution $\Delta\omega$ and time resolution ΔT are related by an expression

$$\Delta\omega . \Delta T = K \tag{12}$$

where K is a constant.

3.3.1 *Smoothing and resampling of data prior to spectral analysis*

It is pointed out that every data value obtained using the data digitiser, described in Chapter 1, was estimated by taking a sum over a time interval of duration of one-tenth of a second. This sampling procedure results in data smoothing. The smoothing effect may be described qualitatively by defining a power transfer function $F(\omega)$ where

$$F(\omega) = \frac{P_s(\omega)}{P_u(\omega)} \tag{13}$$

where $P_s(\omega)$ is the time-averaged power spectrum for the smoothed data and

$P_u(\omega)$ is the time-averaged power spectrum for the unsmoothed data. $P_u(\omega)$ and $P_s(\omega)$ are computed for the same period of time.

In particular, for the case when smoothing is accomplished by taking sums over a constant time interval of duration T, the power transfer function is given by the following expression:

$$F(\omega) = \frac{\sin^2 (\frac{\omega T}{2})}{(\frac{\omega T}{2})^2} \tag{14}$$

A curve giving values for $F(\omega)$ in the range of frequencies 0 to 5 Hz for T = 0.1 seconds is given in Figure 3-2.

In computing digital sonagrams, data sampled at a standard sampling frequency often must be resampled at lower sampling frequencies to minimise the computation time required for analysis. The standard procedure to protect against aliasing errors introduced by resampling is to smooth data points before resampling (Blackman and Tukey, 1958). The following simple scheme was used for data smoothing. Given a data time series f*(t), sampled using a constant sampling interval T, a smoothed version f'(t) was computed using the formula

$$f'(nT) = \frac{1}{2m+1} \sum_{i=-m}^{i=m} f(nT - iT) \tag{15}$$

where f(nT) is the value of f*(t) at time t=nT and m is an integer. The smoothed time series f'(t) was resampled by taking every m^{th} value i.e., the new sampling interval was equal to mT.

The power transfer function $F'(\omega)$ for the smoothing operation

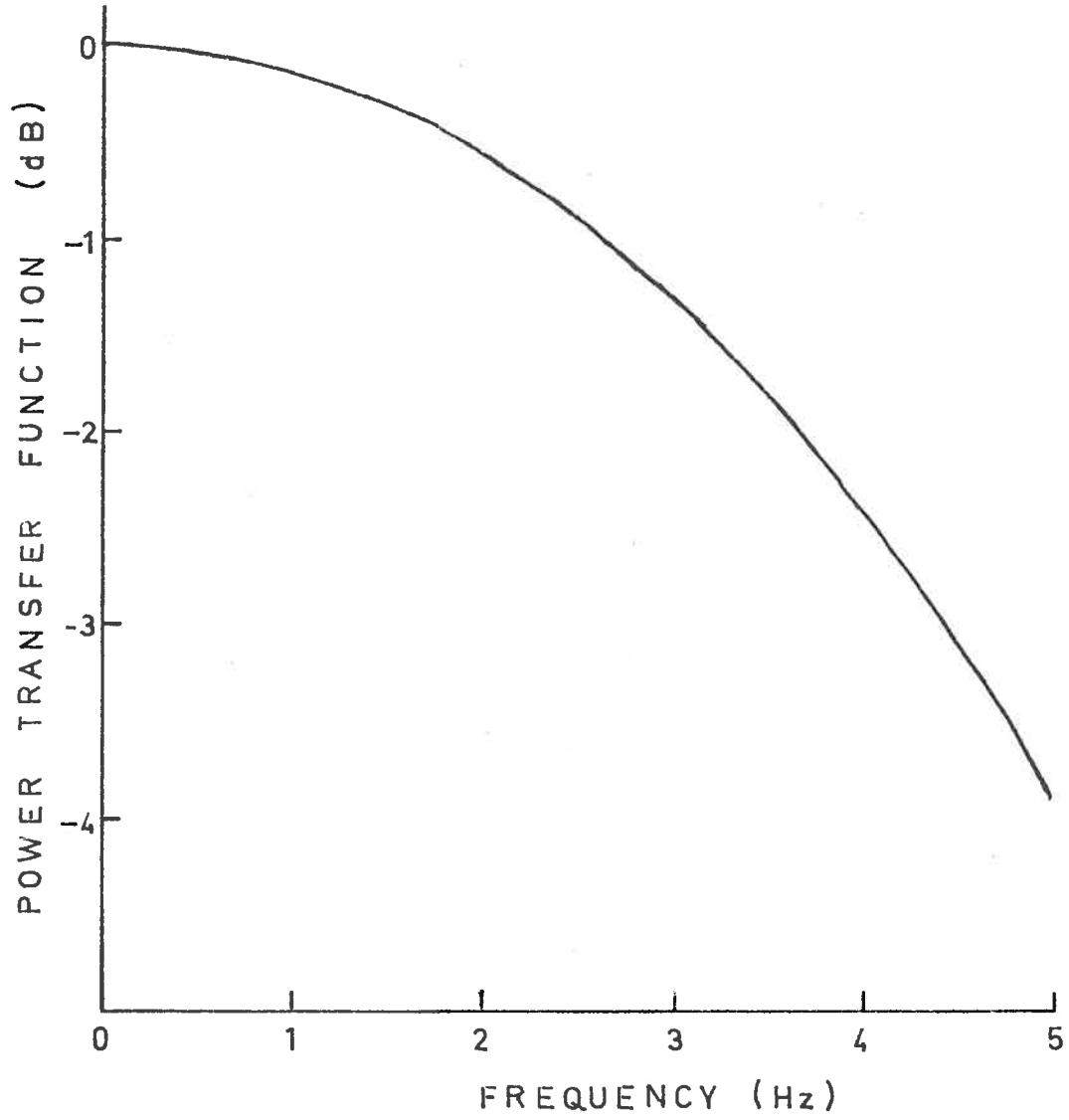

Fig. 3-2 Power transfer function for smoothing effect introduced by summing over an interval of one tenth of a second.

formulated in equation (14) is given by the following equation (Blackman and Tukey, 1958).

$$F'(\omega) = \left[\frac{\sin\left(\frac{k\omega T}{2}\right)}{k \sin\left(\frac{\omega T}{2}\right)}\right]^2 \qquad (15)$$

where $k = 2m + 1$. In Figure 3-3, a curve giving the value of $F'(\omega)$ over the frequency range 0.04 to 0.56 Hz is given for $m = 5$.

3.3.2 *Algorithm used for computation of time-varying power spectra*

Arrays of contiguous, constant bandwidth band-pass filters were used to produce digital sonagrams. Band-pass filtering was simulated using complex demodulation, which is particularly suitable for this type of spectral analysis (see Bingham et al, 1967 for a review of complex demodulation techniques).

Essentially, complex demodulation of a function of time f(t) is equivalent to the analogue process of heterodyning of a signal using a sine-wave generator. The complex demodulate of a function f(t) at frequency ω is equal to $f(t)e^{j\omega t}$. The process of forming the complex demodulate of a function f(t) at frequency ω_o and then filtering the complex demodulate with a low-pass filter with 3 dB cut-off frequency $\Delta\omega$, where $\Delta\omega < \omega_o$, is equivalent to the process of filtering the function f(t) with a band-pass filter with centre frequency ω_o, a frequency response symmetrical about the centre frequency and 3 dB cut-off frequencies at $\omega_o + \Delta\omega$ and $\omega_o - \Delta\omega$.

The basic procedure used to produce digital sonagrams will now be

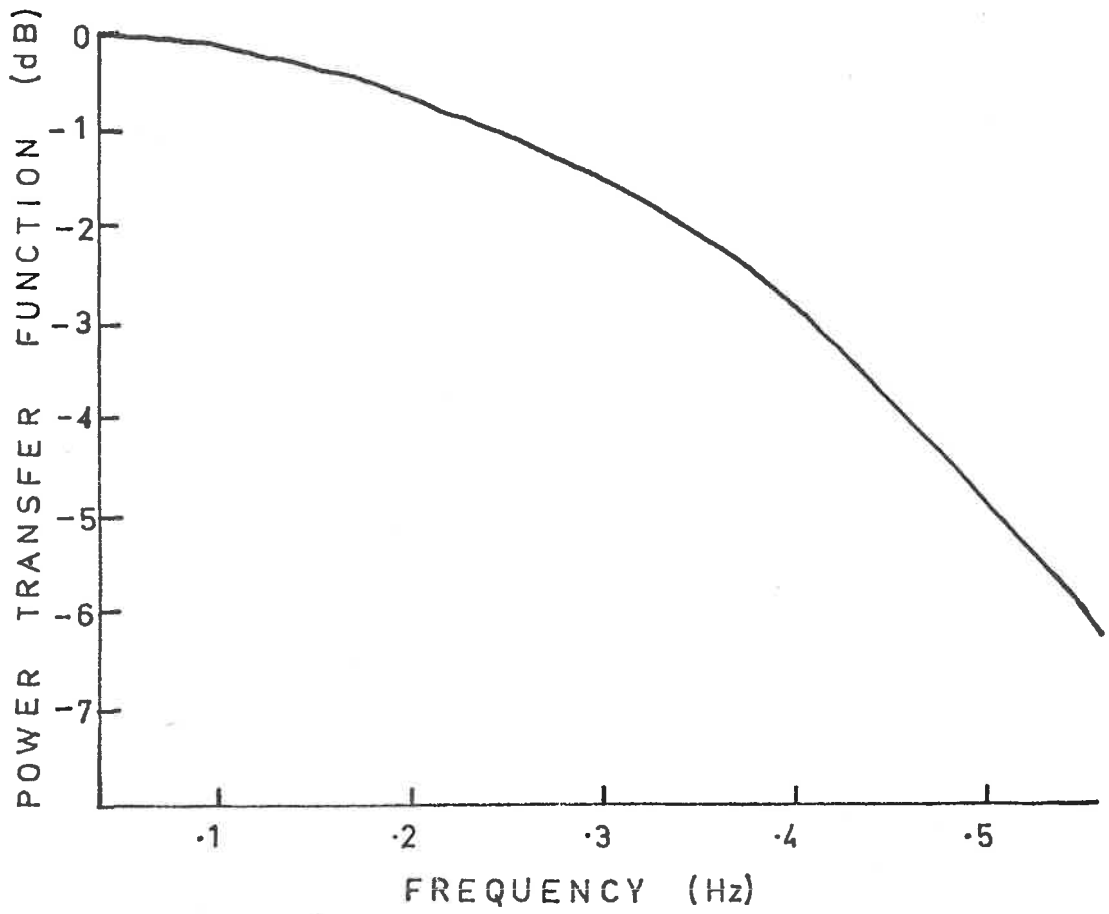

Fig. 3-3 Power transfer function for smoothing, performed by using an 11-point moving average. Sampling interval for raw data was 0.1 seconds.

outlined. A program was written to enable selection of data sections from masterfile tapes. Each data section was written onto magnetic tape as one file of information in blocked form. This data tape production program provided the option of smoothing and resampling of data prior to spectral analysis. One digital sonagram was produced for each file of information on the data tape. As spectral analysis was performed without the use of transformation from the time domain to the frequency domain, the digital sonagram program could easily be organised so that continuous sonagram records could be produced from a data file containing any number of blocks.

The first computational procedure carried out in the digital sonagram program was high-pass filtering of data to remove the zero-frequency component. The high-pass filter was simulated using procedures discussed in §3.2.

Complex demodulates for a specified number of frequency channels were then computed. Given the high-pass filtered time series $f^*(t)$, which has a value $f(nT)$ at time $t = nT$, the complex demodulate, $F_\omega(t)$, of $f^*(t)$ at frequency ω is given by

$$F_\omega(nT) = f(nT)\, e^{j\omega nT} \qquad (17)$$

Cosine and sine values were computed efficiently using recursion equations (c.f. R.D. Kelly et al).

Band-pass filtering for the frequency channel with centre frequency ω was simulated by low-pass filtering the complex demodulate $F_\omega(t)$. If

we formulate the low-pass filtering operation by using a low-pass filter operator S, then the smoothed demodulate $F'_\omega(t)$ resulting from the low-pass filtering of the complex demodulate $F_\omega(t)$ is given by

$$F'_\omega(nT) = S[f(nT)\sin \omega nT] + jS[f(nT)\cos \omega nT]$$

$$= R(\omega, nT) + jI(\omega, nT) \qquad (18)$$

An instantaneous power $P'(\omega,t)$ at frequency ω and time $t = nT$ was defined as

$$P'(\omega, nT) = R^2(\omega, nT) + I^2(\omega, nT) \qquad (19)$$

The time-varying power spectrum $P(\omega, t)$ was obtained through smoothing the function $P'(\omega, t)$ using a simple moving average i.e.

$$P(\omega, nT) = \frac{1}{2m+1} \sum_{i=-m}^{i=m} P'(\omega, nT - iT) \qquad (20)$$

for m an integer. Usually m was taken as the integer nearest to $\Pi/(\Delta\omega T)$, where T is the sampling interval and $\Delta\omega$ is the frequency separation between centre frequencies of adjacent frequency channels.

As the time-varying power spectrum results from a smoothing operation, it may be adequately represented by sampling the function $P(\omega,t)$, with a sampling interval mT. The value of $P(\omega,t)$ was calculated only at every mth data point for display purposes. This process of sampling the time-varying power spectrum to achieve computational economies is similar to a process referred to by Blackman and Tukey (1958) as "decimation".

To allow examination of average frequency characteristics over

some interval of time, it is convenient to compute time-averaged power spectra. From the function $P(\omega,t)$, time-averaged power spectra $P_{AV}(\omega)$ for a time interval $t = i\ m\ T$ to $t = j\ m\ T$ were estimated using the following formula:

$$P_{AV}(\omega) = Ko \sum_{r=i}^{r=j-1} P(\omega,\ r\ m\ T) \qquad (21)$$

The normalisation constant Ko was chosen so that $P_{AV}(\omega_o)$ was equal to unity, ω_o being the lowest centre-frequency in the array of band-pass filters used to compute the time-varying power spectrum function.

3.3.3 *Graphic representation of time-varying power spectra*

A digital sonagram is a three-dimensional representation, showing power as a function of frequency and time, and may be in the form of a contour map. Shaded contour map representations were produced using the line-printer facilities at the Adelaide University Computing Centre by selective over-printing of line-printer characters. This technique has been used by McPherron (1968) in production of digital sonagrams. Six levels of shading were available, the lightest shade being produced using the blank character. Standard spacing between contour levels was 3 dB. Examples of this type of sonagram representation will be given in the next section.

3.4 Digital Sonagrams of Pi Geomagnetic Pulsations

Digital sonagrams of Pi geomagnetic pulsations, recording during the midnight and morning hours, were produced for eight nights when auroral activity was observed at Macquarie Island. It is believed that

this is the first report of computation of digital sonagrams of geomagnetic pulsations using the complex demodulation technique. A total of 35 hours of data was processed. Pi activity was recorded for approximately 97% of that total time.

Examples of digital sonagrams of Pi geomagnetic pulsations are given in Figures 3-4 and 3-5. In each of these diagrams, two sonagrams are given. The top one is the digital sonagram, while the bottom one in each diagram is an "analogue sonagram" produced at College, Alaska from Macquarie Island tape records. In the digital sonagrams, the lowest frequency is .04 Hz. In the analogue sonagrams, the lowest frequency is approximately .005 Hz. Comparing the digital and analogue sonagrams over the frequency range 0.1 to 0.6 Hz, it can be seen that there is a very good correspondence between Pi features evident in each of the two types.

All digital sonagrams of Pi geomagnetic pulsations were found to have the characteristic evident in Figures 3-4 and 3-5 i.e. power was concentrated at low frequencies and generally decreased as frequency increased. The wideband character of Pi geomagnetic pulsations is also evident, in contrast to that of sinusoidal pulsations, where power is concentrated over a narrow frequency band. This wideband character of Pi geomagnetic pulsations is also evident in analogue sonagrams of pulsations recorded at College (c.f. Heacock, 1967a).

Although the persistent tendency for power to decrease with increasing frequency is evident in the digital sonagrams shown in Figures 3-4 and 3-5, this characteristic is more easily seen when time-averaged

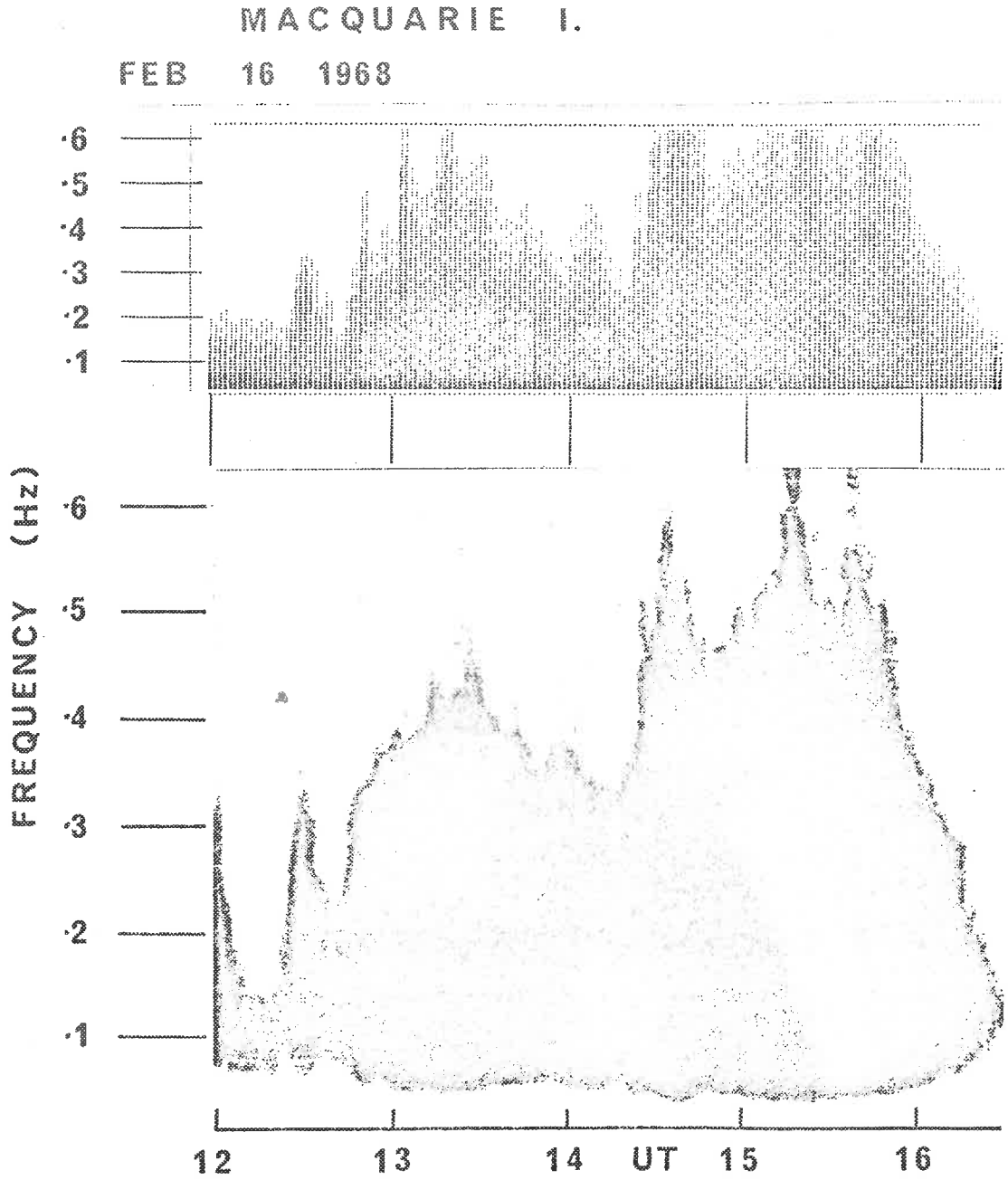

Fig. 3-4 Digital and analogue sonagrams of Pi geomagnetic pulsations recorded at Macquarie Island for the period 1200 - 1620 U.T. on 16 February 1968. The feature on the analogue sonagram at 1200 U.T. is a time mark.

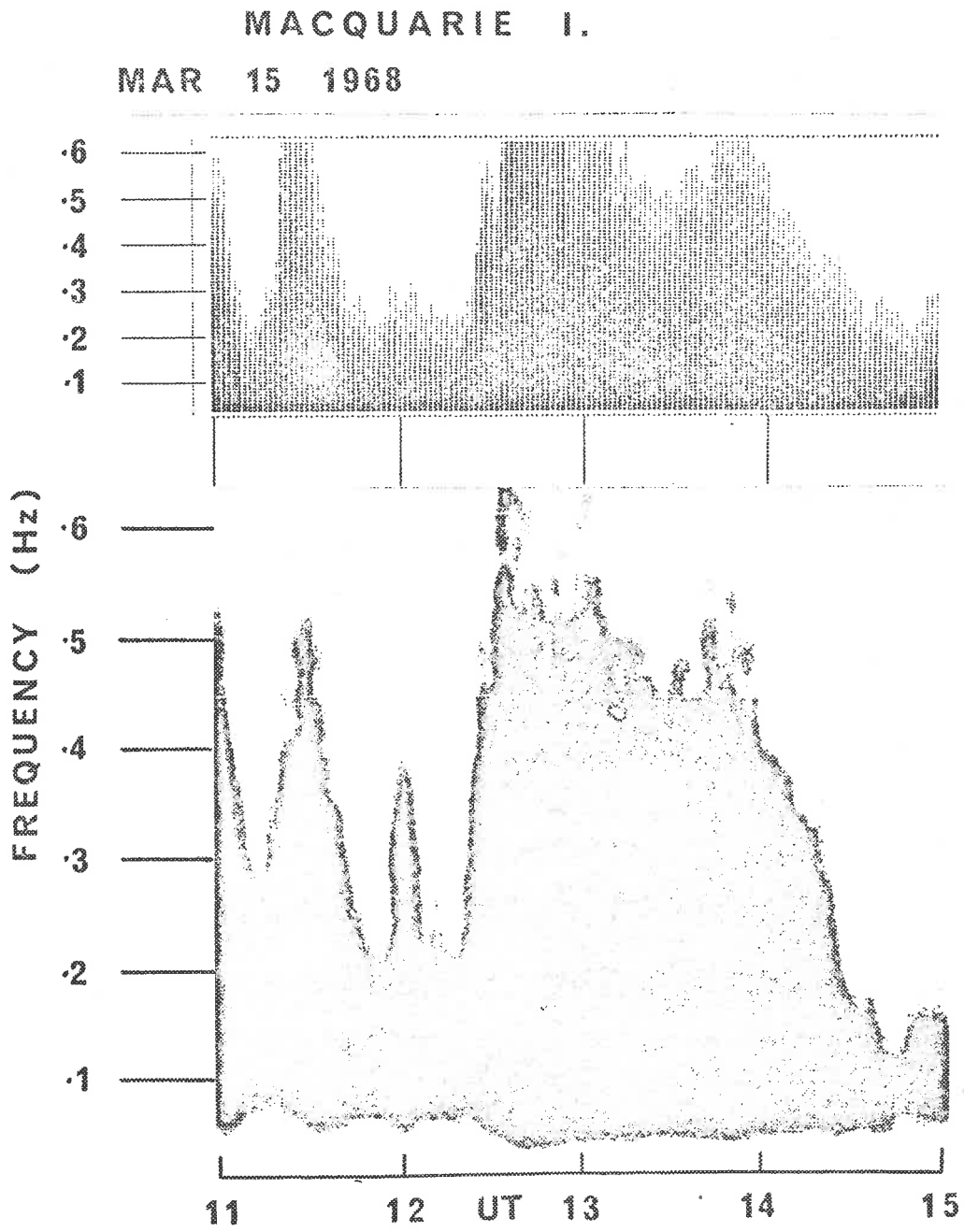

Fig. 3-5 Digital and analogue sonagrams of Pi geomagnetic pulsations recorded at Macquarie Island for the period 1100 - 1500 U.T. on 15 March 1968. The feature on the analogue sonagram at 1200 U.T. is a time mark.

power spectra are examined. Time averaged power spectra which have been obtained from consecutive one hour time intervals of digital sonagram data already illustrated, are given in Figures 3-6 and 3-7. All of these spectra show a decrease in power with increasing frequency. Typically, the power at 0.5 Hz is about 20 dB less than the power at 0.1 Hz. It is pointed out that the digital sonagrams, given in Figures 3-4 and 3-5, resulted from processing of smoothed and resampled data. The original data, sampled with a sampling interval of 0.1 sec, was resampled with a sampling interval of 0.5 sec. The power transfer function for the smoothing which was also introduced is given in Figure 3-3. It can be seen that this smoothing would result in a decrease in power levels at 0.5 Hz of about 5 dB relative to the power levels at 0.1 Hz in the digital sonagram. Referring to Figure 3-2, it can be seen that the smoothing effect due to the particular sampling procedure used to obtain the raw data for processing (discussed in §3.3.1) would not give rise to a difference in relative power of more than 0.1 dB, over the frequency band 0.1 to 0.5 Hz in the digital sonagram. Thus it is concluded that the decrease in power over the frequency band 0.1 to 0.5 Hz which is observed in digital sonagrams of Pi geomagnetic pulsations, is a real effect.

3.5 Discussion

Many workers, including Troitskaya (1961), Campbell and Rees (1961) and Victor (1965) have pointed out that geomagnetic pulsations which were associated with optical aurora and were recorded in the auroral regions, have typical pulsation periods from a few seconds to a few tens of seconds.

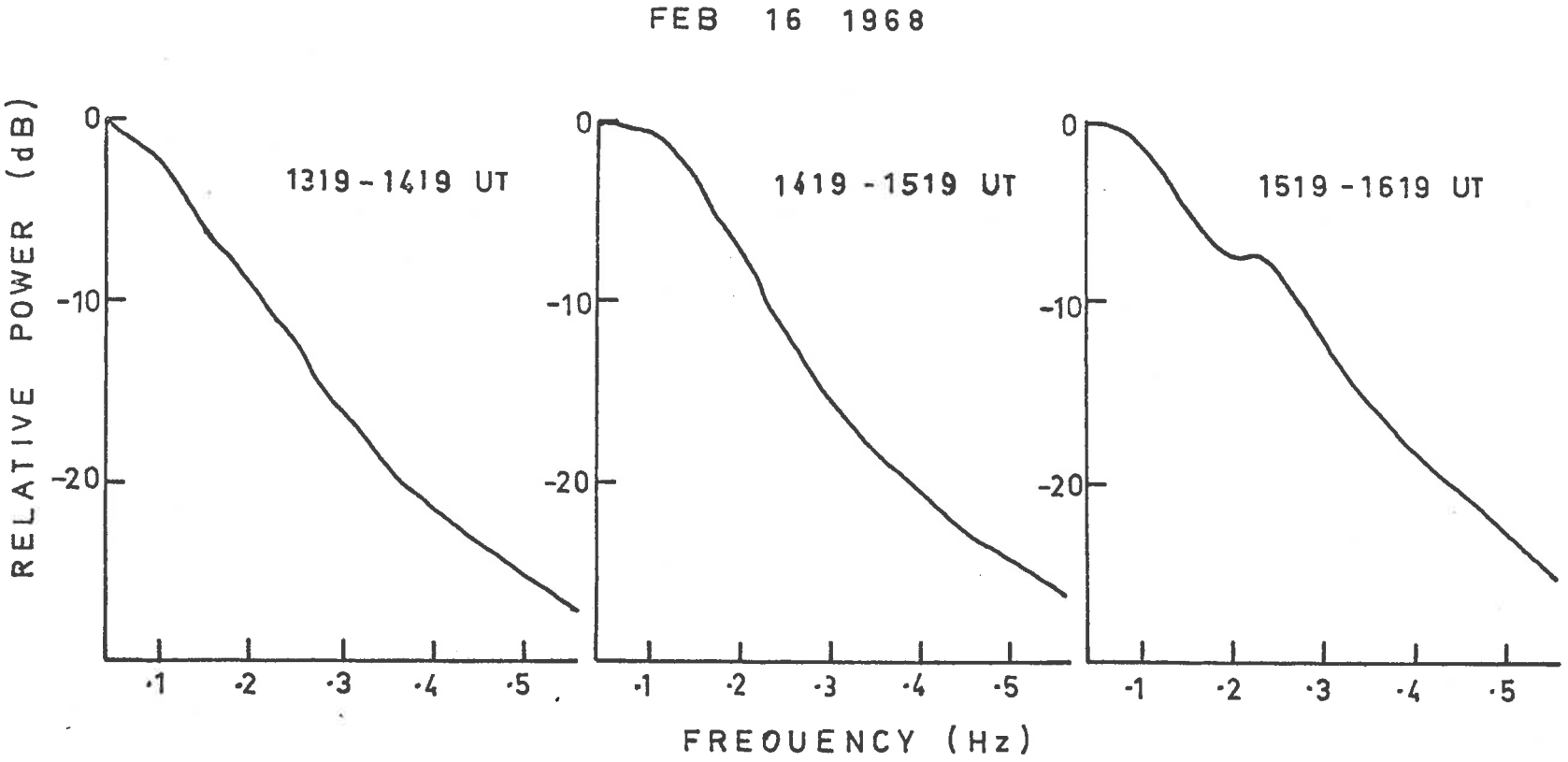

Fig. 3-6 Time-averaged power spectra for Pi geomagnetic pulsations recorded at Macquarie Island on 16 February 1968.

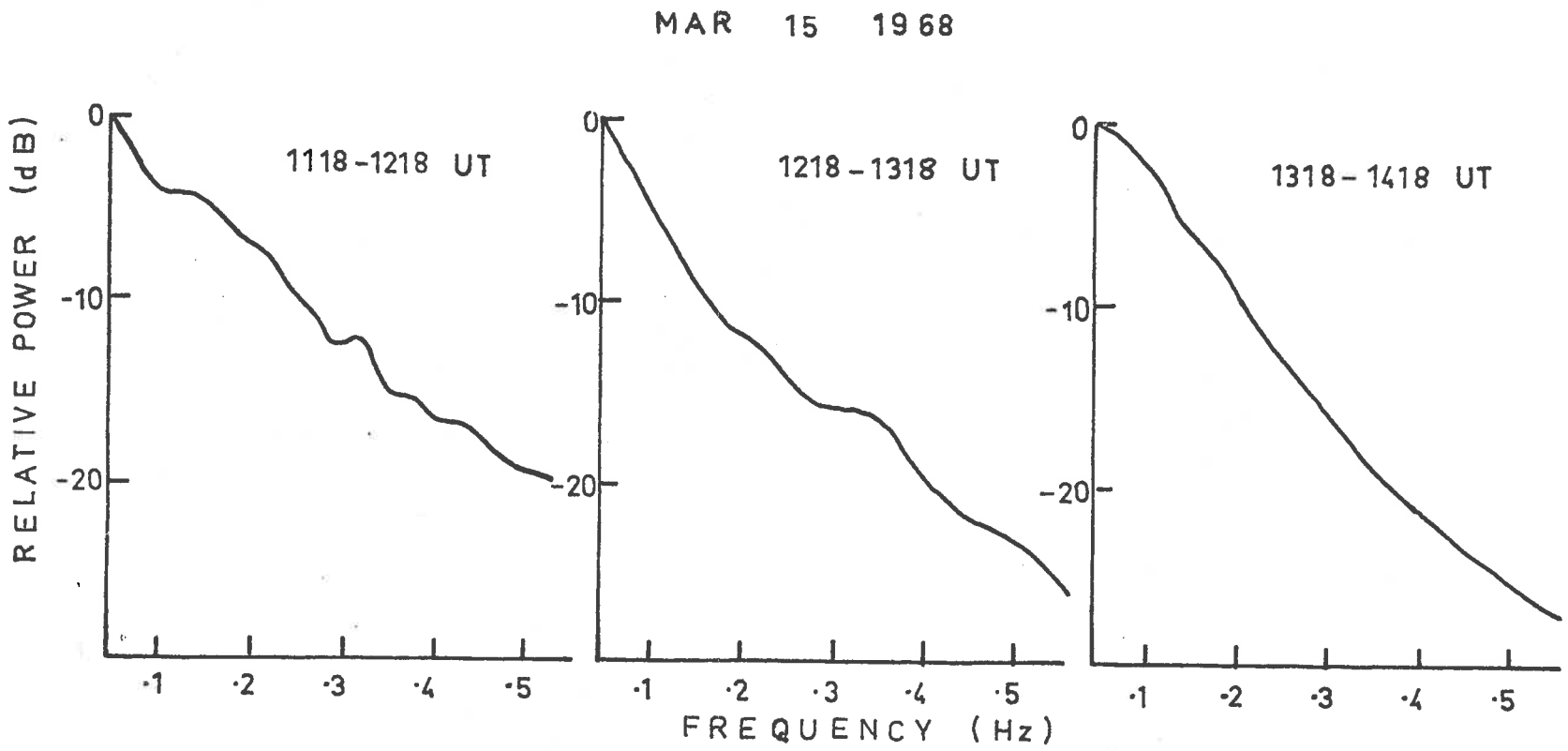

Fig. 3-7 Time-averaged power spectra for Pi geomagnetic pulsations recorded at Macquarie Island on 15 March 1968.

However, there is no general agreement amongst these authors concerning the character of these geomagnetic pulsations. Troitskaya (1961) reports that irregular geomagnetic pulsations in the period range 1 to 15 seconds, which are recorded mainly in the polar regions, are closely associated with aurora. Campbell and Rees (1961) describe the geomagnetic pulsations which accompanied auroral luminosity pulsations at College, as being quasi-periodic. Victor (1965) describes the geomagnetic pulsations, observed to accompany auroral luminosity pulsations at Byrd, Antarctica, as being regular pulsations. None of these workers computed time-varying or time-averaged power spectra for the geomagnetic pulsations which they recorded. Because of this, their descriptions of geomagnetic pulsations characteristics are regarded by the author as being highly subjective. However, all of the abovementioned workers report that usually, geomagnetic pulsations observed during aurora consisted of a superimposition of pulsations with different periods. These pulsations are probably Pi geomagnetic pulsations which are not characterized by the persistant occurrence of sinusoidal pulsation; over the frequency band 0.1 to 0.5 Hz, Pi geomagnetic pulsations have the character of band-limited noise so that the shortest pulsation periods readily observed on chart records are typically of the order of a few seconds.

CHAPTER 4

THE POLAR SUBSTORM IN THE EVENING SECTOR

4.1 The Polar Substorm

The geomagnetic field is considerably deformed in its interaction with the solar wind, being confined to a comet-shaped region called the magnetosphere (see Figure 4-1). Geomagnetic field lines in the outer magnetosphere are stretched by the solar wind to form a tail. The inner magnetosphere is characteristically populated by trapped charged particles. The boundary of this inner zone or trapping region, when projected onto the polar cap, approximately delineates the auroral oval (Feldstein 1966, Akasofu 1966a). There is characteristically a continuous influx of particles into the ionosphere in the region of the auroral oval. Exterior to the trapping region is the outer magnetosphere characterised by highly variable particle populations. (c.f. Vernov et al 1969).

The level of geomagnetic disturbances is controlled by the sun through the solar wind. The magnetic planetary index K_p is correlated with solar wind velocity, tending toward higher values as solar wind velocity increases (Snyder et al 1963). During a solar flare, a plasma cloud may be ejected from the sun which, in its interaction with the magnetosphere, initiates a disturbance lasting several days, the magnetospheric storm, which is manifested as a world-wide magnetic storm. A magnetospheric storm is characterized by the frequent occurrence of the magnetospheric substorm which has typical durations of from one to three hours and shows distinct

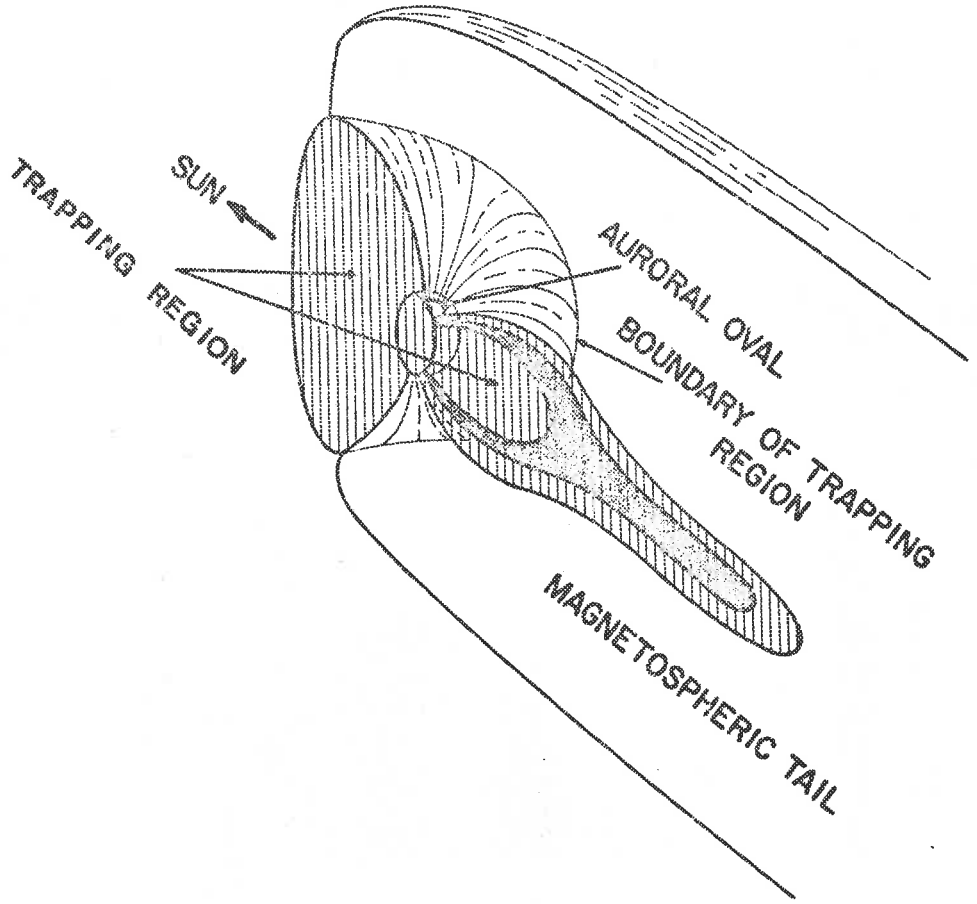

Fig. 4-1 Noon to midnight cross-section of the magnetosphere showing its structure and relation to the auroral oval. The auroral oval delineates the projection of the boundary between the trapping region and the outer magnetosphere onto the polar atmosphere (after Akasofu, 1968a).

growth and decay phases of activity.

Magnetospheric substorms are manifested in many ways. At high latitudes, particularly on the night side of the earth, strong ionospheric absorption of cosmic radio noise and geomagnetic pulsations are observed. Currents forming the auroral electrojet are strongly enhanced and magnetic disturbance is observed on the surface of the earth. Auroral activity undergoes considerable enhancement. The many different types of activity, observed at high latitudes, associated with the magnetospheric substorm constitute a disturbance which is known as the polar substorm. The manifestation of the polar substorm in activation of auroral is referred to as the auroral substorm. The associated magnetic disturbance is referred to as the polar magnetic substorm.

In this work, cosmic noise absorption and geomagnetic pulsations activity at Macquarie Island, in the southern auroral zone, will be related to the polar substorm phenomenon by studying activity during individual substorms.

4.1.1 *The auroral substorm*

The expansive phase of the auroral substorm begins with the brightening of a quiet arc in the auroral oval (Akasofu 1964). In the midnight sector of the auroral oval, arcs brighten and fold, taking part in a poleward expansion of aurora which results in the formation of an auroral "bulge". The shaded regions in Figure 4-2 indicate the extent of the bulge region.

In the evening sector, the leading edge of the expanding bulge folds

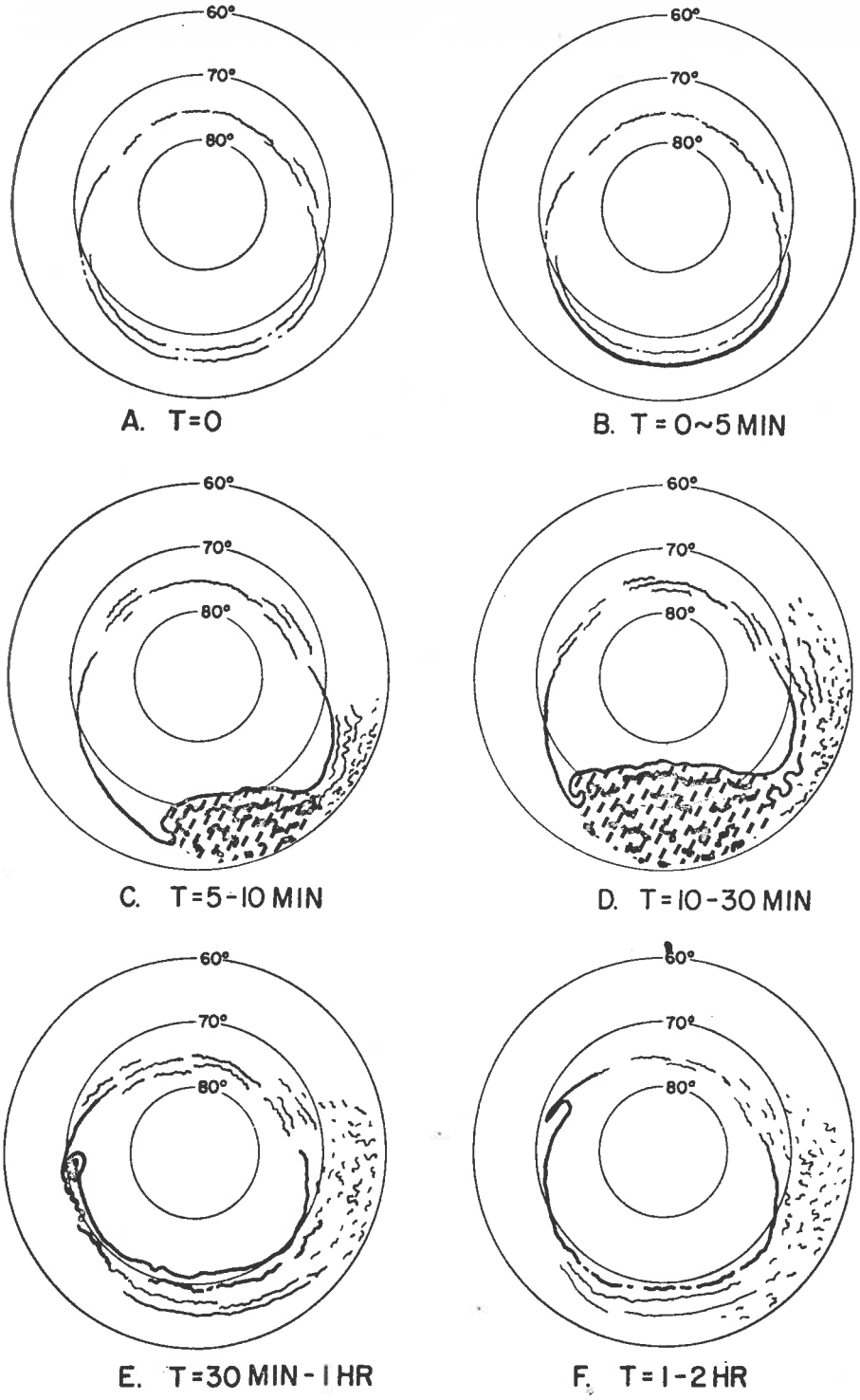

Fig. 4-2 Schematic diagram showing the typical development of the auroral substorm (after Akasofu, 1968a). The shaded region in C and D is referred to as the "auroral bulge".

and propagates westward along the auroral oval. This feature of the auroral substorm is referred to as the westward travelling surge (c.f. Akasofu et al, 1965c).

As the bulge expands, arcs inside the bulge region break up into patches and irregular arc fragments which drift eastwards with speeds of the order of a few hundreds of metres per second. In addition to this eastward movement, there is an equatorward movement of irregular bands and patches (c.f. Akasofu et al, 1969, pp 174). Break-up of arcs begins near the equatorward edge of the auroral oval in the midnight sector and spreads rapidly both poleward and eastward (c.f. Akasofu, 1968a).

In the morning sector, if a station is located poleward of the auroral oval before substorm onset, the expansion of the bulge may be observed. Bright auroral forms will usually move eastward over such a station. Within the oval, irregular eastward-drifting bands will be observed. Near the equatorward edge of the auroral oval, arcs break up into patches which drift eastward. Break up of arcs in the morning sector may begin from 10 to 30 minutes after substorm onset and is preceded by equatorward movement of the arcs (Akasofu et al, 1966b).

The recovery phase of the substorm begins after the expansion of the bulge ceases. During this phase, the size of the bulge region decreases. Contraction of the bulge region sometimes does not begin until 10 to 30 minutes after the bulge front reaches its most poleward point (c.f. Akasofu, 1964). During the recovery phase, the westward travelling surge degenerates as it propagates along the auroral oval, forming sometimes a loop or group of loops (c.f. Akasofu et al 1965b). These westward drifting loops may

travel a few thousand kilometres with little distortion.

During the contraction of the bulge, formerly bright arcs become faint and move equatorward. Arcs may reform and move equatorward. The westward movement of auroras also gradually ceases. If another polar substorm does not interrupt the recovery phase, the auroral oval eventually returns to a quiet pre-substorm condition.

4.2 A Pattern of Polar Magnetic Substorm Activity in the Evening Sector

Normal magnetometer records for the northern hemisphere stations Barrow and Meanook, together with the corresponding records for Macquarie Island for January to March 1968, were examined for recurring patterns of magnetic activity while Barrow and Macquarie Island were in the evening sector. This study is dependent upon the assumption that polar substorm activity in magnetically conjugate regions will be similar. Wescott and Mather (1965) have shown that Macquarie Island is conjugate to a region centred upon Kotzebue, Alaska from comparison of magnetograms of Alaskan and Siberian stations with Macquarie Island records. Leinbach and Basler (1963) have demonstrated conjugacy of Macquarie Island to Kotzebue through comparison of riometer records. By use of airborne instrumentation in simultaneous flights in both northern and southern hemispheres in March of 1967 and 1968, Belon et al (1969) have demonstrated conjugacy of visual auroral activity for the Macquarie Island and Alaskan auroral regions.

Akasofu et al (1965a) have suggested that after onset of a polar substorm, intense negative bays occur in the midnight sector and that the

negative bay region expands along the auroral oval in the evening sector. Akasofu et al (1965a) suggest that this westward expansion of the negative bay region is closely related to the westward travelling surge which propagates along the auroral oval in the evening sector after onset of the polar substorm.

For the time interval 0600 to 1000 U.T., Meanook is in the midnight sector and is normally close to the equatorward boundary of the auroral oval (c.f. Appendix A). Macquarie Island and Barrow have approximately the same geomagnetic L longitude; Barrow has a geomagnetic L latitude approximately 5 degrees higher than the corresponding latitude for Macquarie Island. For the time interval 0600 - 1000 U.T., Barrow will normally be in the auroral oval, whereas Macquarie Island will normally be several hundred kilometres equatorward of the auroral oval.

Study of the Meanook, Barrow and Macquarie Island magnetometer records showed that, commonly, at approximately the same time that a negative bay began at Meanook, a positive bay began at Macquarie Island and a slow decrease in magnetic H component began at Barrow. Some time later, a more rapid decrease in H began at Barrow. Also at some time after substorm onset, a negative indentation in the positive bay at Macquarie Island occurred. The latter features of magnetic activity at Barrow and Macquarie usually occurred at the same time and were attributed to the transit of a westward travelling surge through the Macquarie Island - Barrow longitude.

The particular pattern of simultaneous magnetic activity at Meanook, Barrow and Macquarie Island described will be illustrated using records

obtained on 3 March 1968. This example is of particular importance as a successful constant local time flight was made, starting from Churchill, Canada at 0521 U.T. and arriving at the Macquarie Island - Barrow longitude around 0900 U.T., by the NASA Airborne Auroral Expedition (Akasofu, 1968b). The flight was planned so that the instrumented aeroplane stayed in the late evening sector of the auroral oval on its journey from Churchill to Ft. Yukon, Alaska.

At 0700 U.T., the aeroplane was near the longitude of Meanook. From the Meanook magnetogram (Figure 4-3), we can estimate that a polar substorm began around 0710 U.T., in agreement with Akasofu's estimate. The all-sky photographs on board the aeroplane show that at 0710 U.T. aurorae to the east of the plane suddenly became bright and that at around 0713 U.T., a westward travelling surge caught up with the plane. Akasofu points out that the surge was seen to the north of Bettles, Alaska at 0735 U.T. As the travel time between the location of the plane at 0713 U.T. and Bettles was 22 minutes, the speed of the surge was of the order of 1.3 Km/sec. (Akasofu, 1968b).

From Figure 4-3, it can be seen that a slow decrease in H at Barrow and a slow increase in H at Macquarie Island began at about the same time that a negative bay began at Meanook. At 0740 U.T., a sharp dip in H began at Barrow, simultaneous with negative indentation in the positive bay at Macquarie Island, which can be associated with the arrival of a westward travelling surge at the Macquarie Island-Barrow longitude. As the substorm began at 0710 U.T., an estimate of 30 minutes can be obtained for the travel time of the westward travelling surge between Meanook and Barrow. As the

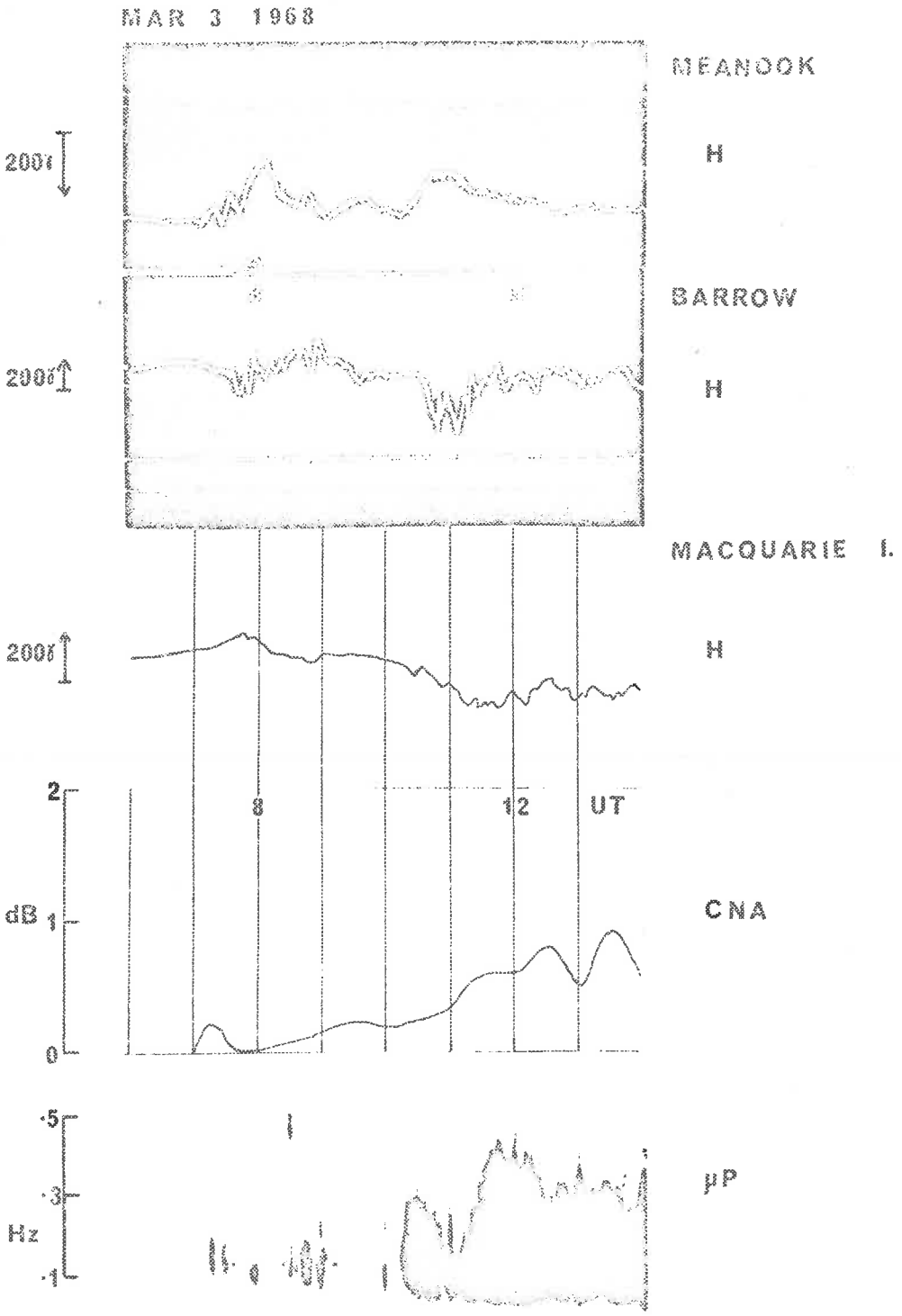

Fig. 4-3 Magnetometer records from Meanook, Barrow and Macquarie Island; cosmic noise absorption record and geomagnetic pulsations sonagram for Macquarie Island for the period 0600 to 1400 U.T. on 3 March 1968.

distance between Meanook and Barrow is approximately 2750 Km, we can estimate the speed of the westward travelling surge as 1.5 Km/sec., close to Akasofu's figure.

From records of January to March 1968, eight examples of substorms were found where magnetic activity at Meanook, Macquarie Island and Barrow followed a similar pattern to that described above. Dates, estimated substorm onset times and estimated times that a westward travelling surge reached the Macquarie Island - Barrow longitude are given in Table 4-1 for the eight substorms.

TABLE 4-1

Date (1968)	Substorm Onset Time Estimate (U.T.)	Estimated Time Surge Crosses Barrow Longitude (U.T.)	ΔT (min.)
6 Jan	0340	0915	35
17 Jan	0730	0812	42
20 Jan	0940	1012	32
21 Jan	0830	0930	60
8 Feb	0835	0940	65
20 Feb	0630	0725	55
3 Mar	0710	0740	30
16 Mar	0705	0750	45

Estimated substorm onset time was taken to be the commencement time

for the negative bay at Meanook. The time that a westward travelling surge reached the Macquarie Island - Barrow longitude was taken to be the time of the maximum deflection in H for the first fast change in H at Barrow after substorm onset. For the substorms in Table 4-1, a mean travel time for westward travelling surges between Meanook and Barrow of approximately 46 minutes was obtained. This travel time corresponds to a speed of approximately 1 Km/sec. Akasofu et al (1965c), from a sample of 72 well defined surges found that the most common speed of westward travelling surges is of the order of 500 to 800 m/sec., although some surges had estimated speeds greater than 1 Km/sec.

Averages of the H component for a two hour interval centred around estimated substorm onset time were computed for the eight substorms listed in Table 4-1 to illustrate the average magnetic activity as a function of time relative to substorm onset time for each of the stations Meanook, Barrow and Macquarie Island. From the results, shown in Figure 4-4, it can be seen that before substorm onset, weak fluctuations in H were usually observed at Meanook, Barrow and Macquarie Island. At substorm onset time, a strong decrease in H began at Meanook which was usually accompanied by onset of a negative bay at Barrow and onset of a positive bay at Macquarie Island.

Another example of polar substorm activity from records for 16 March 1963 is illustrated in Figure 4-5. The estimated substorm onset time, the time of onset of the negative bay at Meanook, was approximately 0705 U.T. A sharp dip in H at Barrow, together with negative indentation in the positive bay at Macquarie Island, occurring at about 0745 U.T., can be

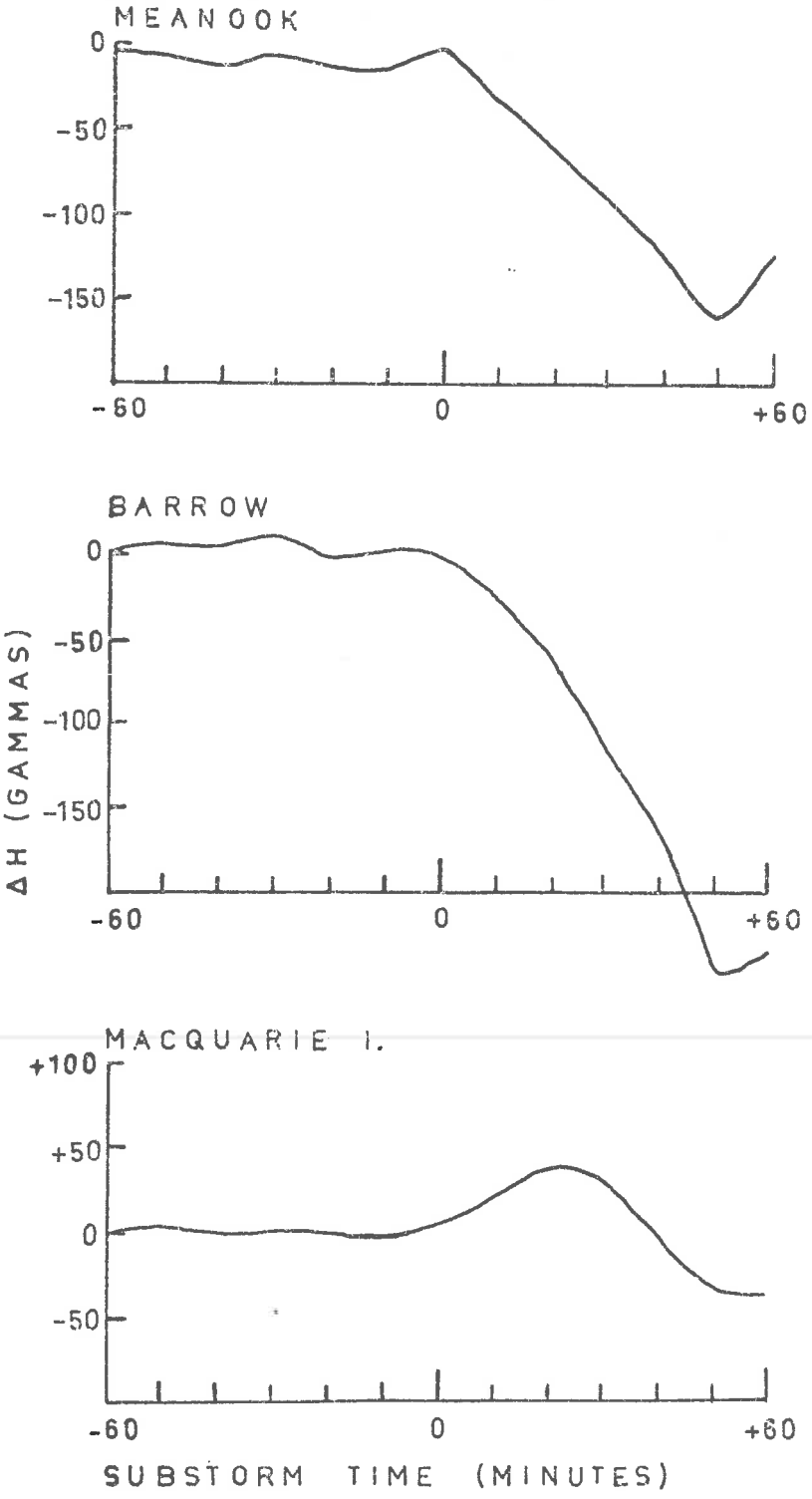

Fig. 4-4 Magnetic (H) fluctuations at Meanook, Barrow and Macquarie Island averaged over the eight polar substorms discussed in §4.2.

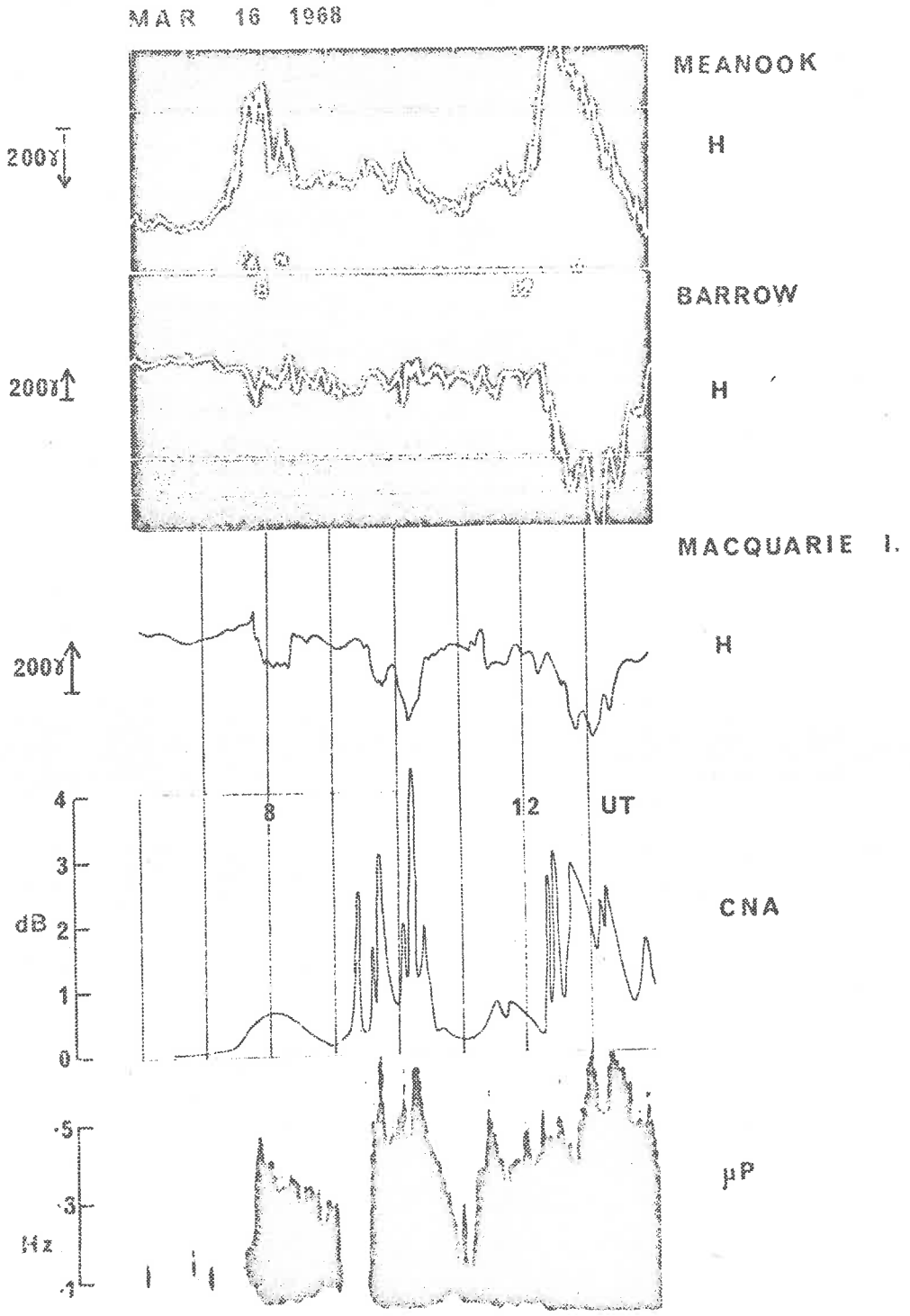

Fig. 4-5 Magnetometer records from Meanook, Barrow and Macquarie Island; cosmic noise absorption record and geomagnetic pulsations sonagram for Macquarie Island, for the period 0600 - 1400 U.T. on 16 March 1968.

attributed to the approach of a westward travelling surge toward the Macquarie Island - Barrow longitude.

In any study of substorm activity, the location of the auroral oval must be considered. The size of the auroral oval is variable, being dependent upon the level of planetary magnetic disturbance (Feldstein and Starkov, 1967). Furthermore, the location of any station in relation to the auroral oval is dependent on local time.

Akasofu and Meng (1967a) have shown that in the evening sector, during polar substorms, positive bays are observed in a region equatorward of the auroral oval, and that negative bays are observed in the auroral oval. The pattern of magnetic activity for Barrow and Macquarie Island discussed in this section is consistent with location of Barrow in the auroral oval and location of Macquarie Island several hundred kilometres equatorward of the auroral oval.

It is suggested that polar substorm activity at a station in the evening sector consists of two distinct phases. The initial phase begins at polar substorm onset time. The second phase of activity, which may be termed the surge transit phase, is associated with the approaching westward travelling surge as it travels along the auroral oval.

For the sample of substorms discussed in this section, it is suggested that during the initial phase, slow decrease in magnetic H component begins at auroral oval stations, e.g. Barrow, and positive bays begin at stations in a region equatorward of the auroral oval, e.g. Macquarie Island. During the surge transit phase, fast negative changes

in H are observed at auroral oval stations and negative indentation in positive bays are recorded at stations in a region equatorward of the auroral oval.

4.3 Cosmic Noise Absorption in the Evening Sector during Polar Substorms

During the initial phase of the polar substorm, cosmic noise absorption was commonly recorded at Macquarie Island. Absorption commenced within ten minutes of substorm onset time (estimated from Meanook magnetometer records) in five of the eight substorms discussed in §4.2. These absorption events were characterized by lack of fast time variation and typical values for peak absorption were of the order of a few tenths of a decibel. These events occurred during positive bays, with a distinct onset, at Macquarie Island.

Occasionally, a CNA event or enhancement could be associated with the surge transit phase of substorm activity at Macquarie Island. This type of absorption increase was recorded during three of the substorms discussed in §4.2. Every example of this type of absorption increase was associated with a distinct negative change in H at Macquarie Island.

The cosmic noise absorption record and geomagnetic pulsations sonagram, together with magnetometer records for Meanook, Barrow and Macquarie Island for 21 January 1968 are given in Figure 4-6. At approximately 0830 U.T., the estimated substorm onset time, a negative bay commenced at Meanook. Slow decrease in H began at Barrow and an increase in H began at Macquarie Island within ten minutes of that time. It can

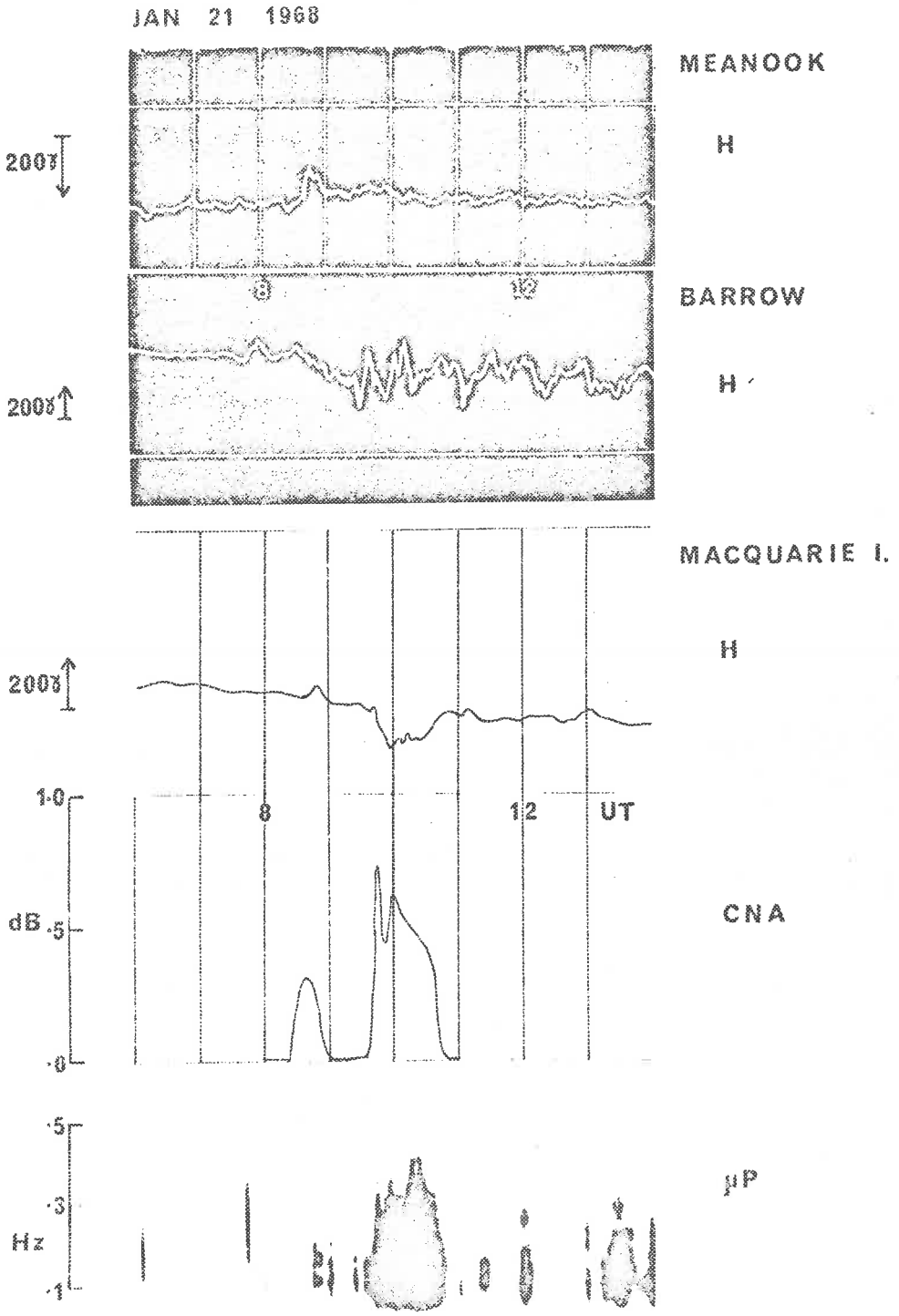

Fig. 4-6 Magnetometer records from Meanook, Barrow and Macquarie Island; cosmic noise absorption record and geomagnetic pulsations sonagram for Macquarie Island for the period 0600 to 1400 U.T. on 21 January 1968.

be seen that a weak absorption event began at Macquarie Island near to estimated substorm onset time.

At about 0930 U.T., a fast negative change in H was recorded at Barrow and a decrease in H began at Macquarie Island. These changes are attributed to the approach of a westward travelling surge toward the Macquarie Island - Barrow longitude. It can be seen that during the surge transit phase of the substorm, a CNA event was recorded at Macquarie Island.

During the polar substorm commencing at approximately 0705 U.T. on 16 March 1968 (see Figure 4-5) it can be seen that a CNA event, which commenced at approximately 0730 U.T., can be associated with the approach of a westward travelling surge toward the Macquarie Island - Barrow longitude.

Another example of absorption recorded in the evening sector is given for 20 January 1968. At 0940 U.T., the estimated substorm onset time, a negative bay commenced at Meanook (see Figure 4-7). By that time, a slow decrease in H had already begun at Barrow. A distinct increase in H occurred at Macquarie Island near to substorm onset time. At approximately 1000 U.T., fast negative changes in H were recorded at both Barrow and Macquarie Island which were attributed to the arrival of a westward travelling surge at the Macquarie Island - Barrow longitude. It can be seen from Figure 4-7 that cosmic noise absorption commenced at Macquarie Island at the estimated substorm onset time 0940 U.T. Despite a break in the riometer record, due to an automatic calibration sequence, it is apparent that an absorption enhancement (starting near 1000 U.T.) was recorded which can be associated with the surge transit phase of the

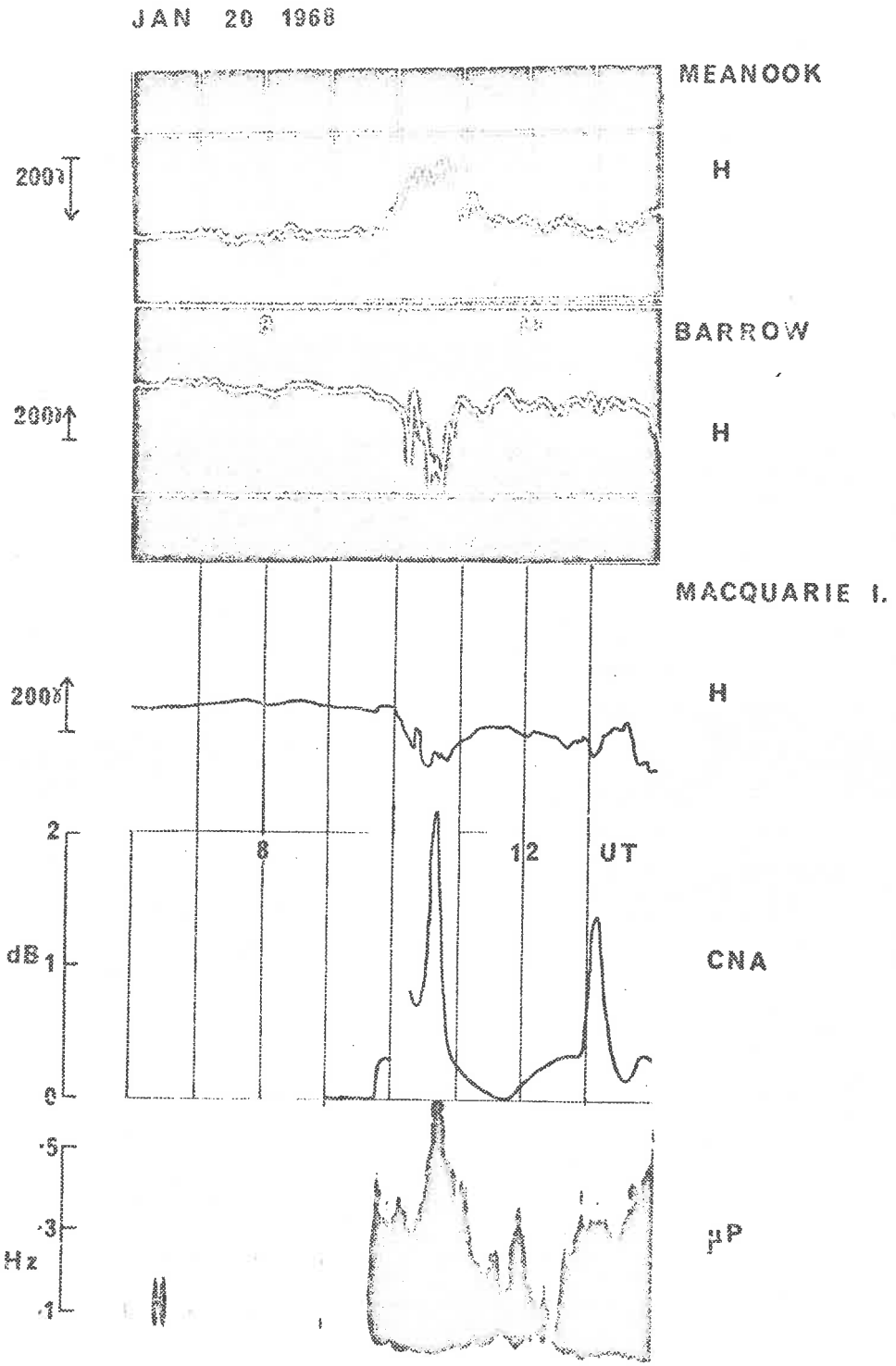

Fig. 4-7 Magnetometer records from Meanook, Barrow and Macquarie Island; cosmic noise absorption record and geomagnetic pulsations sonagram from Macquarie Island for the period 0600 to 1400 U.T. on 20 January 1968.

substorm.

4.4 Pi Geomagnetic Pulsations Recorded in the Evening Sector during Polar Substorms

Jacobs and Sinno (1960) have reported the existence of two types of Pi 2 events. One type was associated with negative bays, having a latitudinal variation which had a sharp maximum in the auroral zone. The other type was associated with positive bays and had a latitudinal variation with a broad maximum at sub-auroral latitudes, near 50° geomagnetic latitude. As positive bay activity is characteristic of the afternoon to evening hours, the second type of Pi 2 activity may be characteristic in the evening sector during polar substorms.

McPherron et al (1968) have reported the observation of a type of geomagnetic pulsations recorded at Flin Flon (an auroral zone station in Canada) while a polar substorm was in progress several hours to the east of that station. This pulsations type, referred to by McPherron et al as "premidnight pulsations", was distinguished by noise - like character. Thus they belong to the Pi class of geomagnetic pulsations. These pulsations had a spectral characteristic where signal amplitude decreased as frequency increased.

Pi activity was recorded at Macquarie Island during polar substorms while that station was in the evening sector. Pi geomagnetic pulsations were observed to commence within ten minutes of substorm onset time (estimated from Meanook magnetometer record) for six out of the eight substorms discussed in §4.2. Enhancements or onsets in Pi activity which could be associated with the surge transit phase of substorms were also

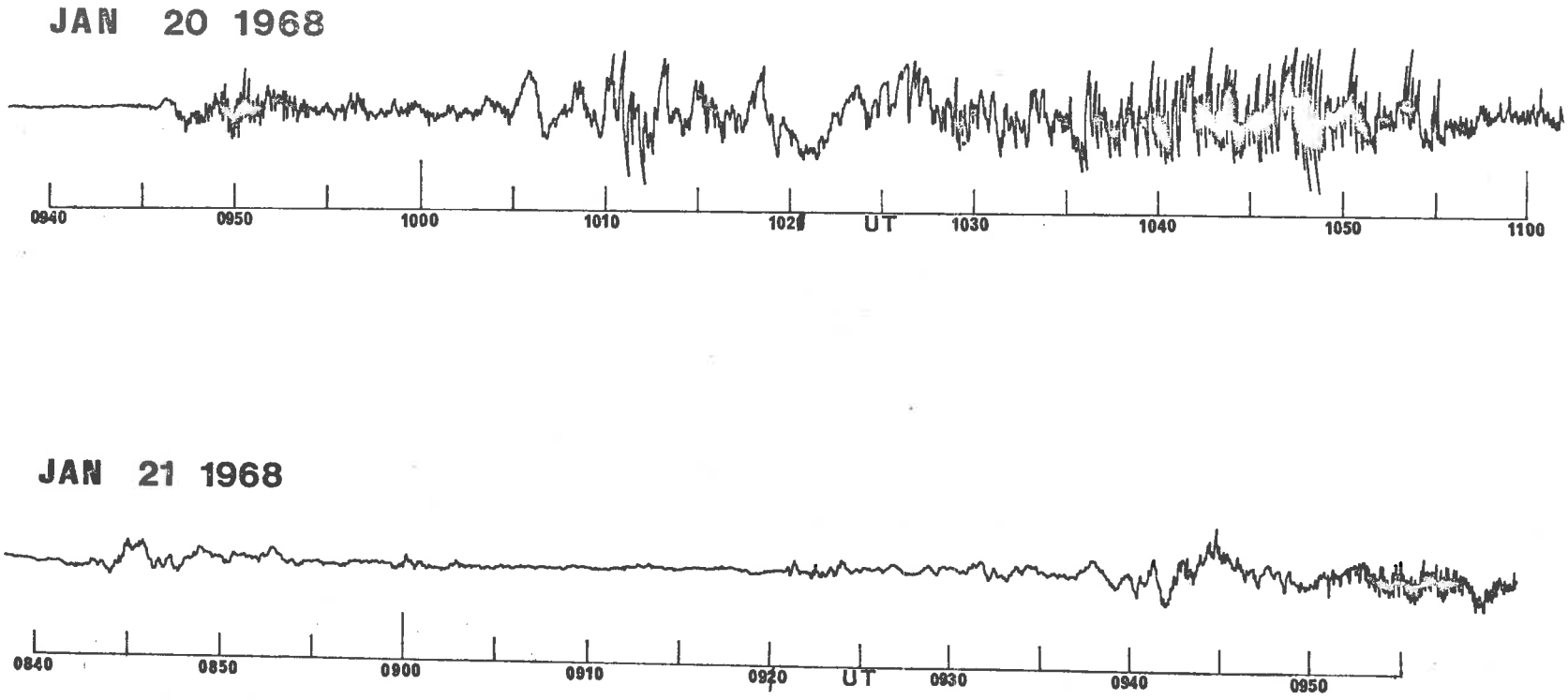

Fig. 4-8 Pi geomagnetic pulsations recorded at Macquarie Island on 20 January 1968 and 21 January 1968.

commonly recorded.

Two examples of Pi activity recorded at Macquarie Island during polar substorms are given in Figure 4-8. These examples are for substorms which were discussed in detail in §4.3. For the first trace, taken on 20 January 1968, estimated polar substorm onset time is 0940 U.T. Pi activity, including some weak Pi 1 pulsations, commenced at 0945 U.T. at Macquarie Island. The enhancement in Pi activity which started at 1005 U.T. can be associated with the surge transit phase of the substorm.

For the second trace, taken on 21 January 1968, estimated substorm onset time is 0830 U.T. Pi activity commenced at Macquarie at about 0840 U.T. By 0910 U.T. no disturbance in the magnetic field could be detected. The onset to Pi activity which commenced at about 0920 U.T. can be associated with the surge transit phase of the substorm.

4.5 Occurrence of IPDP Geomagnetic Pulsations during Polar Substorms

Heacock (1967b) has reported that at College, Alaska, an auroral zone station, a particular geomagnetic pulsations type, characterized by rise in mid-frequencies over a period of one hour, is commonly observed in the evening hours. This geomagnetic pulsations type, named as IPDP by Troitskaya (1961), was associated with positive bay activity by Heacock. McPherron et al (1968) have suggested that IPDP pulsations will be observed in the evening sector during polar substorms but have not given an example of such activity. Akasofu (1968a) has also suggested that IPDP may be recorded during polar substorms. Recently Fukunishi (1969) has demonstrated

that IPDP recorded in the evening sector can be related directly to the onset of polar substorms by showing that IPDP were always preceded by fast onset of a negative bay in the midnight sector. The delay times between onset of IPDP in the evening sector and onset of polar magnetic substorms, which ranged from a few minutes to an hour, were found to be inversely proportional to the time rate of change of the midfrequencies of the IPDP. Fukunishi argues that this particular characteristic indicates that IPDP may be produced through a westward drift of protons in the magnetosphere after an initial injection on the night side, together with a proton cyclotron resonance interaction which would produce hydromagnetic waves with rising midfrequencies which would be observed at the ground as IPDP.

Study of geomagnetic pulsations activity in the evening sector at Macquarie Island shows that IPDP are not recorded at Macquarie Island during all polar substorms. They were not observed on sonagrams or amplitude-time records of geomagnetic pulsations for any of the eight substorms discussed in §4.2.

A striking example of IPDP was found from records for 14 March 1968 (see Figure 4-9). At about 0910 U.T., a negative bay commenced at Meanook, probably due to onset of a polar substorm. No distinctive magnetic activity was observed at Barrow from 0900 to 1000 U.T. Weak fluctuations in H were observed at Macquarie Island during that period. After 1000 U.T., an IPDP event began at Macquarie Island and was accompanied by a cosmic noise absorption event. Negative changes in H were recorded at Barrow and Macquarie Island at about 1015 U.T. Thus the IPDP could be associated with the transit of a westward travelling surge through the Macquarie Island -

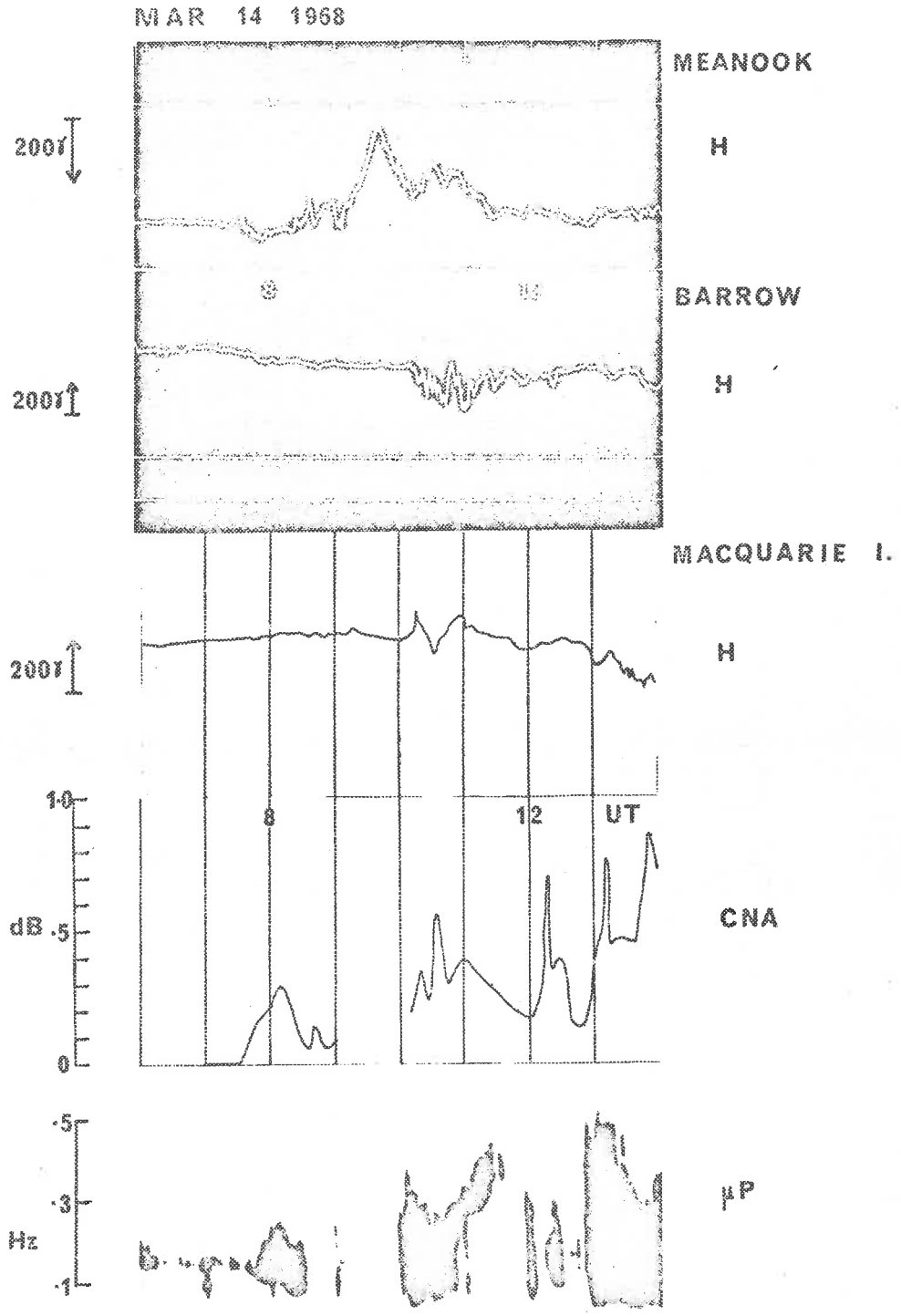

Fig. 4-9 Magnetometer records from Meanook, Barrow and Macquarie Island; cosmic noise absorption record and geomagnetic pulsations sonagram for Macquarie Island for the period 0600 to 1400 U.T. on 14 March 1968.

Barrow longitude.

It is clear that more investigations of IPDP are needed to clarify the relationship between them and the polar substorm. IPDP may not occur during all substorms; their occurrence during polar substorms may, for example, be dependent upon the level of planetary magnetic disturbance. Possibly, there may be a large range of amplitudes of IPDP events; thus the weaker events might not be readily observed on sonagrams.

Gendrin and Lacourly (1963) report that IPDP are observed over a range of L values from L = 5 to L = 8. Knaflich and Kenney (1967), from a dispersion analysis of IPDP events, suggest that IPDP may be generated in a region of L values between about 6 and 13. Possibly, they may always be generated during polar substorms. Should they be generated at fairly high L values e.g. L = 8, these pulsations could often be severely attenuated as they propagate toward stations with lower L values. Such attenuation might be severe enough to prevent detection of IPDP on sonagrams from stations near L = 6.

4.6 Evening Polar Substorm Activity during Moderately Disturbed Periods

All sky camera films from four Alaskan stations, Bettles, Ft. Yukon, College and Eagle, for some evenings during February 1968, were examined for examples of auroral substorm activity during moderately disturbed periods (i.e. Kp > 3- for at least two consecutive 3 hour intervals). The stations Bettles, College and Eagle lie in a region approximately conjugate to Macquarie Island. Geomagnetic L co-ordinates for the Alaskan all sky

camera stations and Macquarie Island are given in Table 4-2.

TABLE 4-2

Station	L - Latitude	L - Longitude
Macquarie Island	-64.2°	175.9°
College	64.8°	190.1°
Ft. Yukon	67.0°	190.6°
Eagle	66.0°	195.7°
Bettles	66.0°	185.1°

On 10 February 1968, a polar substorm began around 0820 U.T., as indicated by rapid onset of a negative bay at Meanook at that time (see Figure 4-10). Slow decrease in magnetic H component was evident on both the Barrow and Macquarie Island magnetometer records by 0830 U.T. At approximately 0910 U.T., rapid negative changes in H began at both Barrow and Macquarie Island. It is suggested that the latter changes were due to an approaching westward travelling surge.

All sky camera records from College and Fort Yukon (Figure 4-11) show auroral activity consistent with the suggested description of polar substorm activity. At 0822 U.T., it was noticed that an arc in the southern sky at College began to brighten and move poleward. At 0853 U.T., this arc was near geographic zenith at College. At 0905 U.T. the display brightened up considerably. From 0908 to 0912 U.T. a surge passed over the northern field of view of College. A rapid westward movement of the

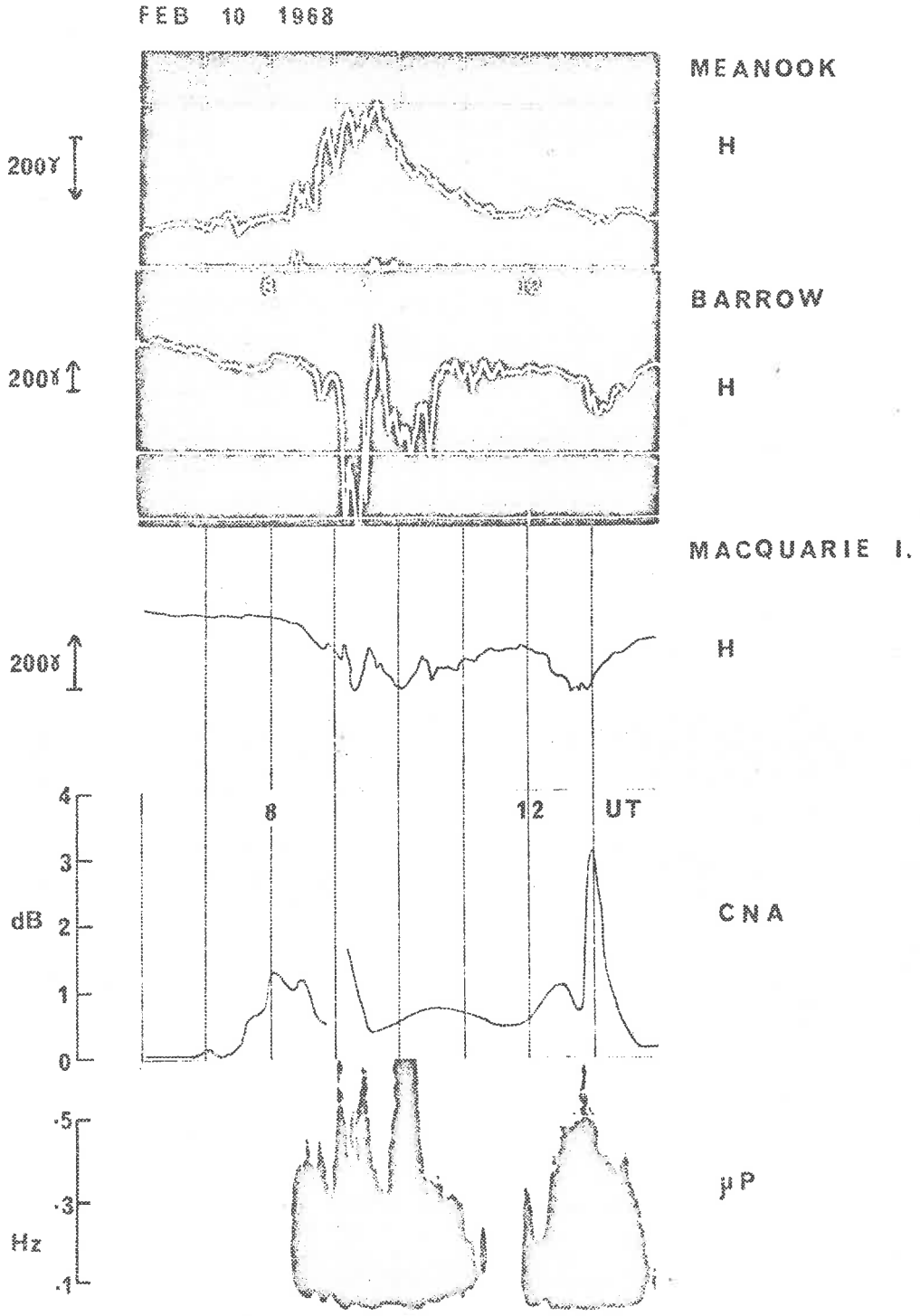

Fig. 4-10 Magnetometer records from Meanook, Barrow and Macquarie Island; cosmic noise absorption record and geomagnetic pulsations sonagram for Macquarie Island for the period 0600 to 1400 U.T. on 10 February 1968.

Fig. 4-11 All-sky photographs from College and Ft. Yukon recorded on 10 February 1968.

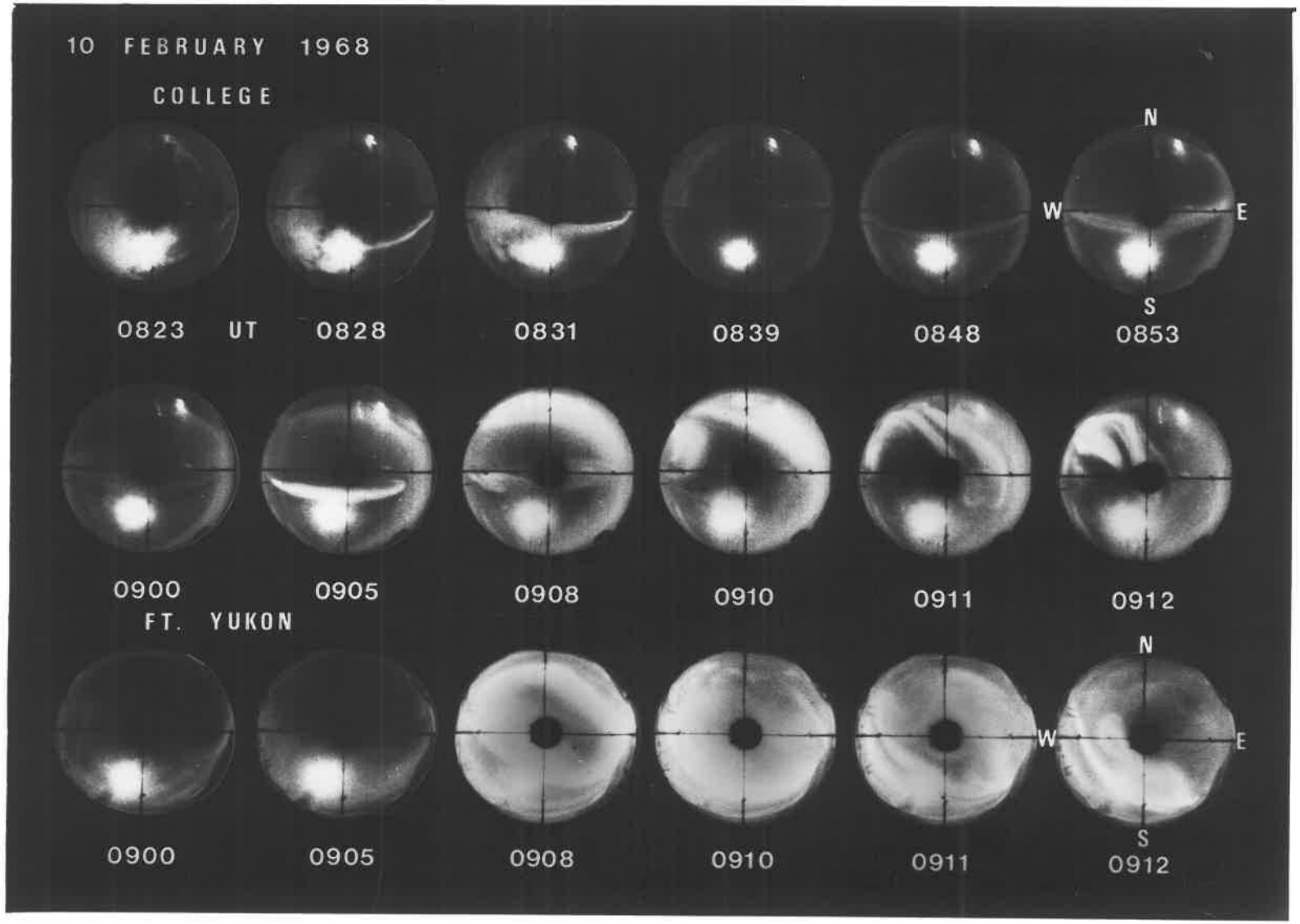
10 FEBRUARY 1968
COLLEGE
N
W
E
S
0823 UT
0828
0831
0839
0848
0853
0900
0905
0908
0910
0911
0912
FT. YUKON
N
W
E
S
0900
0905
0908
0910
0911
0912

surge is evident in Figure 4-11. For the time interval 0900 to 0912 U.T., all sky photographs for both College and Ft. Yukon provide more visual details of westward travelling surge activity.

In Figure 4-10, it can be seen that during the initial phase of the polar substorm at Macquarie Island, gradual enhancements in cosmic noise absorption were recorded. The geomagnetic pulsations sonagram (Figure 4-10) shows that the transit of the surge through the Macquarie Island - Barrow longitude was accompanied by rapid Pi bursts. An increase in cosmic noise absorption was also recorded.

Four examples of substorms were found in the period January to March 1968, where slow negative decrease in magnetic H component began at both Macquarie Island and Barrow at estimated substorm onset time while those stations were in the evening sector. All examples of this type of activity occurred on evenings preceding nights when high levels of magnetic and ionospheric disturbance were observed. As the level of planetary magnetic disturbance increases, the auroral oval expands (Feldstein and Starkov, 1967) and active auroral displays are seen at auroral zone stations in the evening hours (Akasofu and Meng, 1967b). It is suggested that the polar substorm illustrated in Figure 4-10 for 10 February 1968 is an example of this type of activity. (For the periods 0900 - 1200 and 1200 - 1500 U.T. on 10 February 1968, Kp values were 3+ and 3o respectively).

On 17 February 1968, a negative bay commenced at approximately 0850 U.T. at Meanook (Figure 4-12), marking onset of a polar substorm. After 0900 U.T., negative bays are evident on both the Barrow and Macquarie Island magnetometer records. At approximately 0920 U.T., fast negative changes in H began

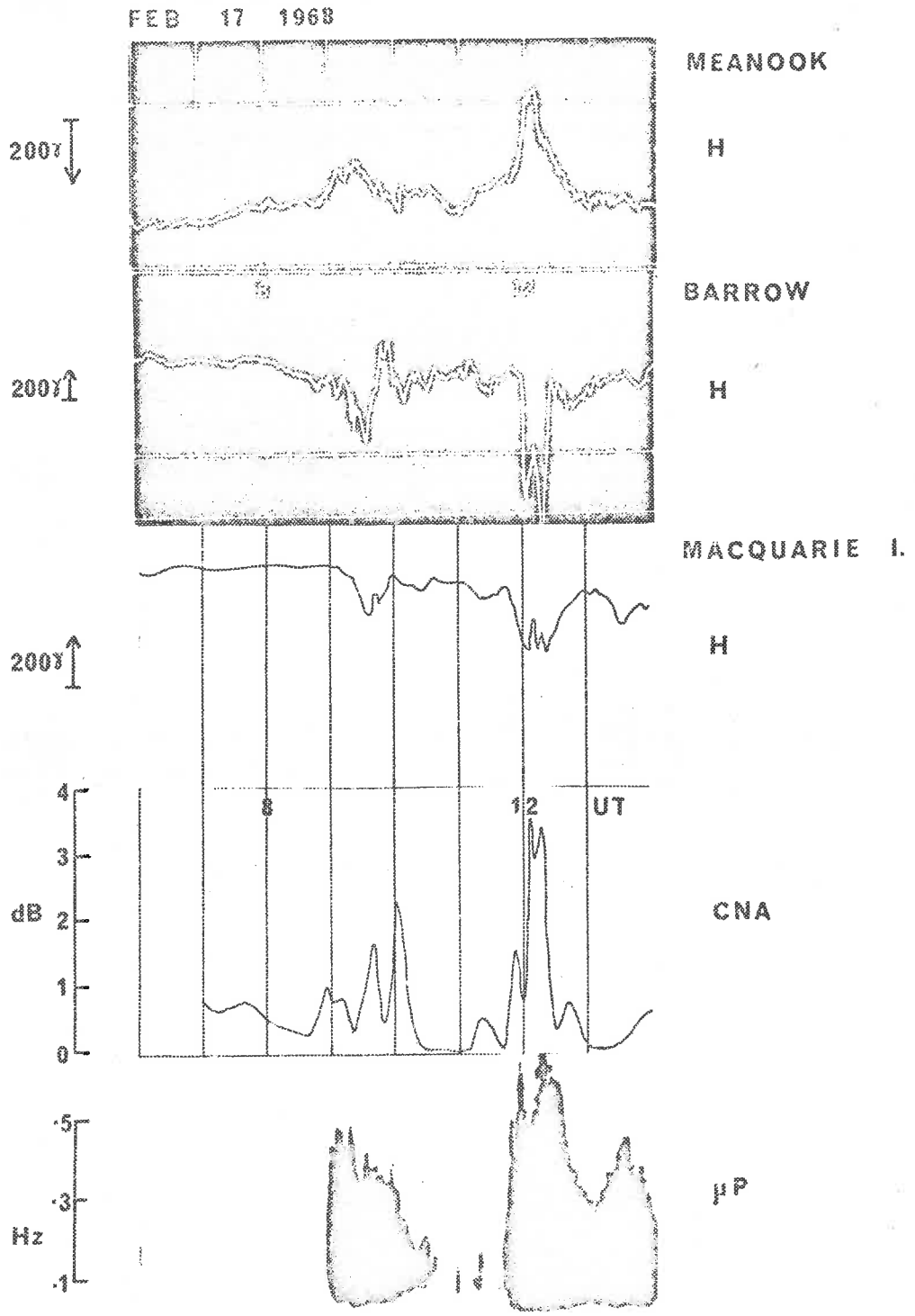

Fig. 4-12 Magnetometer records from Meancok, Barrow and Macquarie Island; cosmic noise absorption record and geomagnetic pulsations sonagram for Macquarie Island for the period 0600 to 1400 U.T. on 17 February 1968.

at both Barrow and Macquarie Island. From the all sky photographs (Figure 4-13), it can be seen that an arc initially in the southern sky of Eagle brightened and moved poleward. At 0905 U.T., a brightening of aurorae was observed at Bettles when the sky over Bettles was covered with bright auroral forms. It is suggested that the brightening of aurorae, over Bettles, evident at 0917 U.T., was due to the approach of a westward travelling surge.

During the initial phase of the substorm at Macquarie Island, a gradual absorption enhancement (see Figure 4-12) was recorded at that station. It can also be seen that during the surge transit phase, a strong absorption enhancement was recorded at Macquarie Island.

From the amplitude - time records of Pi activity for the evenings of 10 and 17 February (see Figure 4-14), it can be seen that certain features of Pi activity, recorded at Macquarie Island, can be correlated with particular features of auroral substorm activity as observed at the Alaskan all sky camera stations. For both substorms Pi 2, with Pi 1 superimposed, commenced near substorm onset time. At the times when a surge was approaching the Alaskan stations, (0902 U.T. on February 10 and 0918 U.T. on February 17), rapid Pi bursts were recorded at Macquarie Island. Akasofu (1968a) has suggested that the westward travelling surge may be associated with Pi bursts. These records indicate the correctness of that suggestion.

The two polar substorms discussed in this section show an interesting characteristic, namely a brightening of arcs in the evening sector which started near polar substorm onset time. This initial brightening of arcs may be explained by assuming that at substorm onset time, precipitation

Fig. 4-13 All-sky photographs from Eagle and Bettles recorded on 17 February 1968.

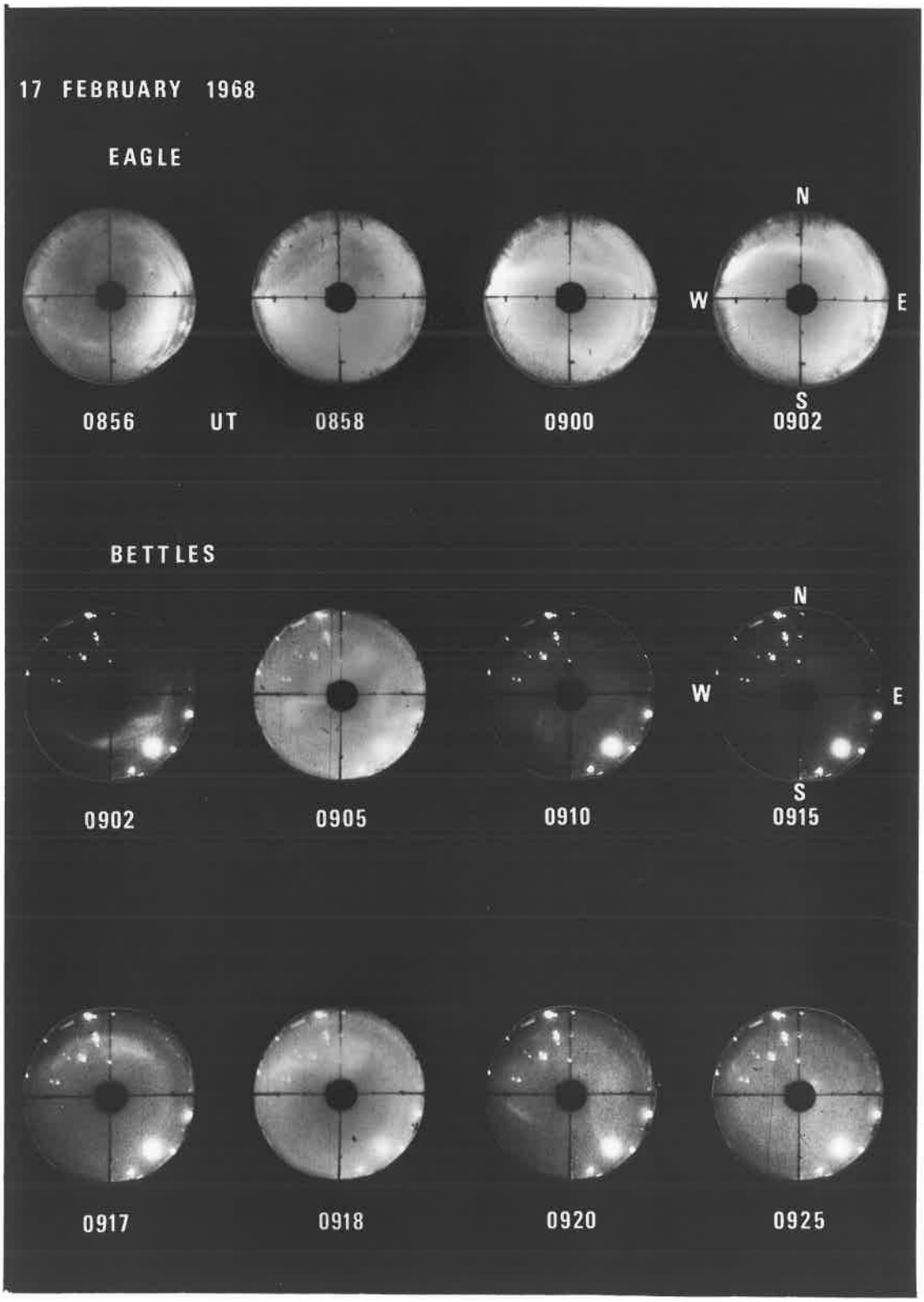
17 FEBRUARY 1968
EAGLE
N
W
E
S
0856 UT
0858
0900
0902
BETTLES
N
W
E
S
0902
0905
0910
0915
0917
0918
0920
0925

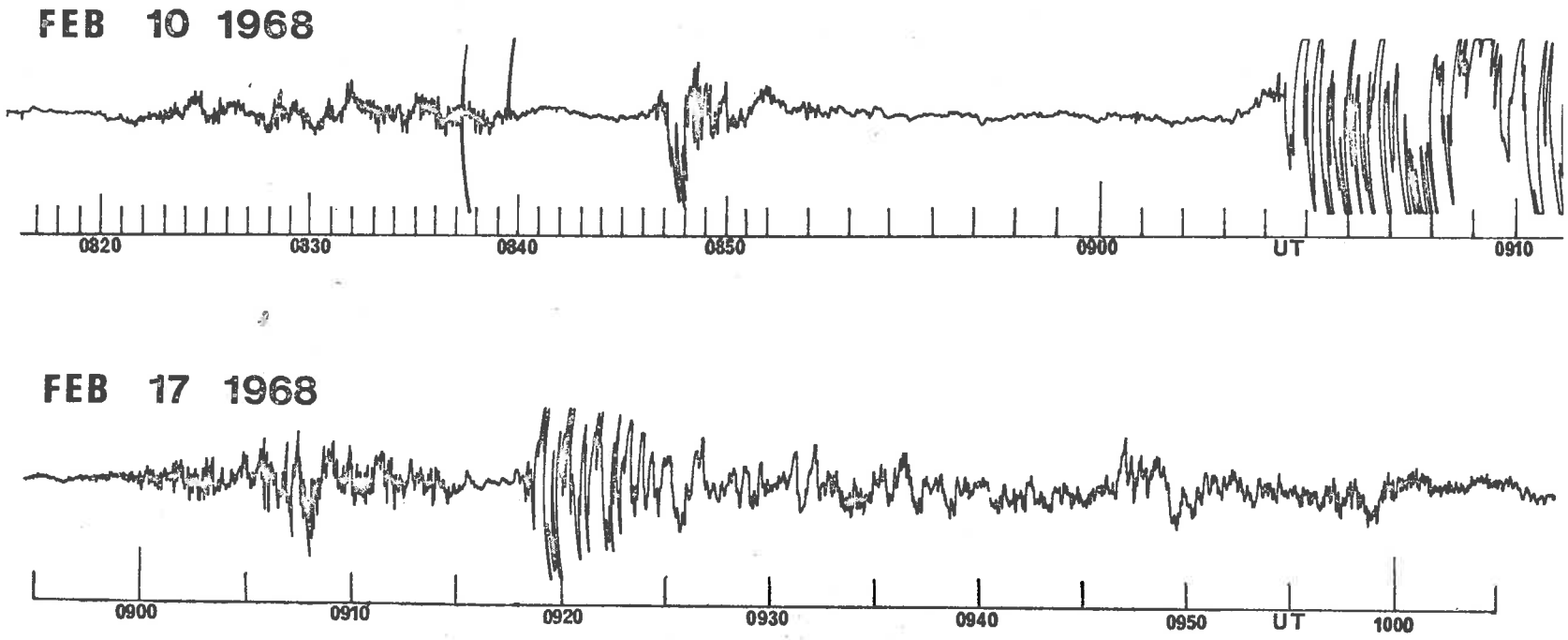

Fig. 4-14 Pi geomagnetic pulsations recorded at Macquarie Island on 10 February 1968 and 17 February 1968.

began over quite a wide segment of the auroral oval. During both substorms GAE were recorded before effects attributed to an approaching westward travelling surge were detected at Macquarie Island, i.e. these GAE were recorded during the initial phase of substorm activity at that station.

4.7 Two Types of Evening Absorption Events Occurring during Polar Substorms

Ansari (1964) in his description of a typical night of aurorally associated CNA activity at College, Alaska, refers to a pre-breakup phase of activity where absorption varies slowly with time, the peak absorption seldom exceeding 1-2 dB at 36 MHz. It is suggested that this pre-breakup activity may, on some evenings, be due to onset of a polar substorm or to the approach of a westward travelling surge while College is in the evening sector.

In §4.3 it was demonstrated that while Macquarie Island was in the evening sector, slowly varying absorption often commenced during the initial phase of polar substorms. Also, enhancements in absorption at Macquarie Island could be associated with transit of a westward travelling surge through the longitude of that station. This pattern of absorption activity may be typical for the situation when Macquarie Island is equatorward of the auroral oval during the evening hours (see §4.2). It is proposed that absorption events, which start with a gradual onset and which are recorded during the initial phase of polar substorm activity at an evening sector station, should be referred to as "gradual evening absorption events" (abbreviation GEA events).

Akasofu (1968a) has shown that absorption events with rapid onsets are observed at evening sector stations when a westward travelling surge passes over. It is proposed that this type of absorption event should be referred to as "rapid evening absorption events" (abbreviation REA events). It is suggested that the GEA and REA events are two distinct types of absorption events which may be due to different magnetospheric processes.

An example of each of the two types of evening absorption events can be seen in Figure 4-15, where riometer records from Ft. Yukon and College for the period 0800 - 1000 U.T. on 13 February 1958 are given. An REA event commenced at approximately 0838 U.T. at Ft. Yukon. This event was probably accompanied by passage of a westward travelling surge over that station; a surge reached Wrangel Island, which is about 1 hour in longitude west of Ft. Yukon, around 0840 U.T. (c.f. Akasofu et al, 1969, pp.60). A GEA event started at College at about 0815 U.T., some time before onset of strong absorption at Ft. Yukon.

Another example of a GEA event can be seen in Figure 4-16, where riometer records for Ft. Yukon and College for the period 0600 to 0800 U.T., on 12 February 1958, are given. A strong absorption event accompanying passage of a surge over Ft. Yukon (c.f. Akasofu et al, 1969, pp.26) commenced at about 0655 U.T. at that station. A GEA event was recorded at College, commencing at about 0630 U.T.

It can be seen in both the examples given in Figures 4-15 and 4-16, that a GEA event commenced at the lower latitude station, College, before onset of strong absorption at the higher latitude station, Ft. Yukon. Thus these two examples indicate that GEA events may be observed mainly in a

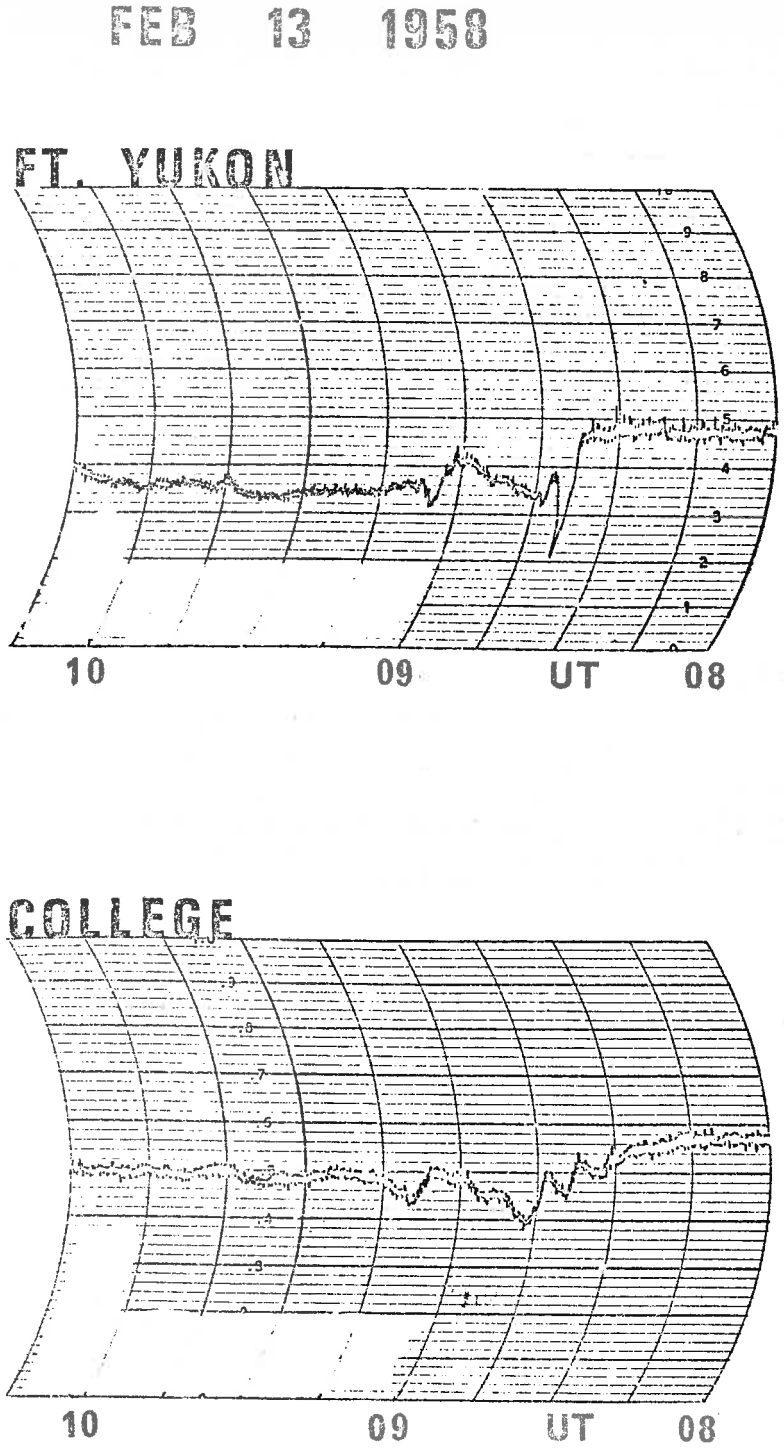

Fig. 4-15 Riometer records from Ft. Yukon and College for the period 0800 to 1000 U.T. on 13 February 1958 (after Akasofu et al, 1969). A GEA event started at College at about 0815 U.T.; a REA event started at Ft. Yukon at about 0838 U.T.

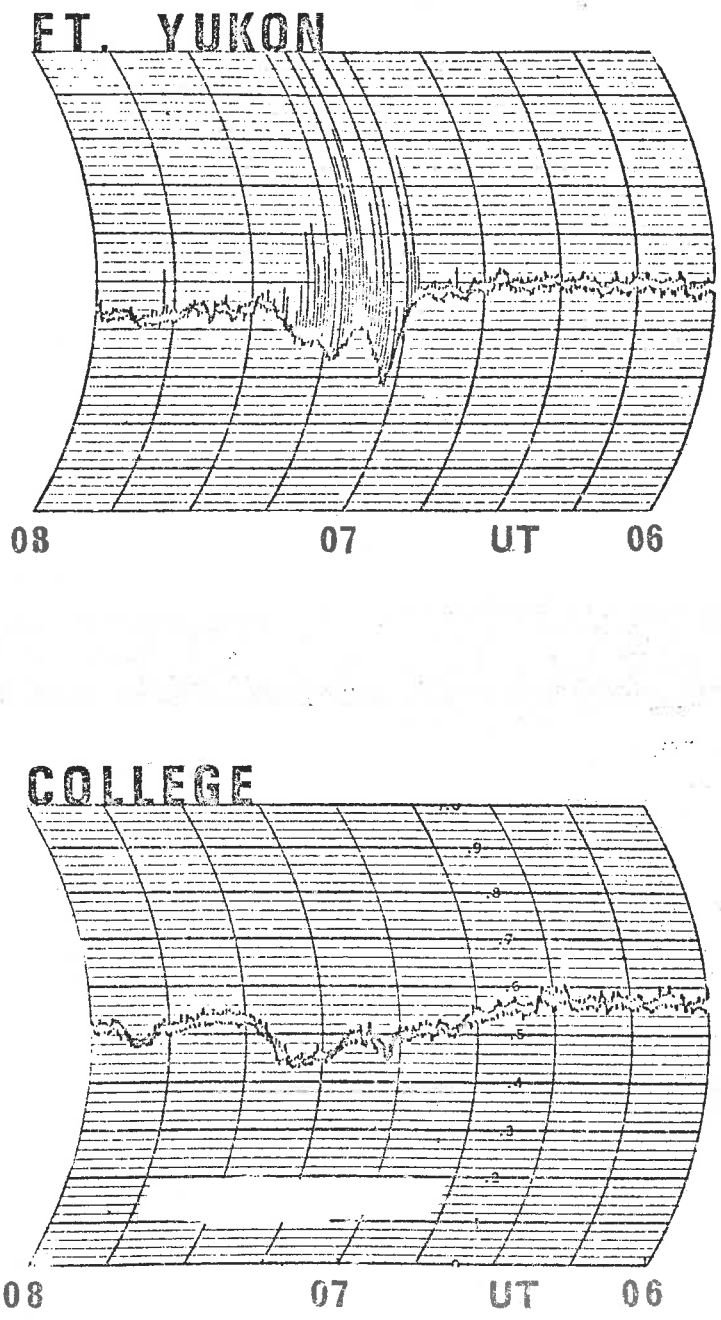

Fig. 4-16 Riometer records for Ft. Yukon and College for the period 0600 to 0800 U.T., 12 February 1958 (after Akasofu et al, 1969). The strong absorption recorded at Ft. Yukon accompanied transit of a surge over that station; a GEA event started at College at approximately 0630 U.T.

region equatorward of the auroral oval. It is expected that REA events, which are associated with the westward travelling surge, should be observed mainly within the auroral oval.

4.7.1 *Discussion*

From studies of auroral absorption using simultaneous measurements of λ 5577Å luminosity and absorption, Ansari (1964), Rather and Jacka (1966) and Berkey (1968) conclude that the class of rapid onset absorption events, which includes REA events, are caused by precipitation of electrons with soft energy spectra. Ansari (1964) finds that these events can be accounted for by assuming that they are due to enhancements in flux of electrons in the energy range 10 to 20 keV. Rather and Jacka (1966) found that if the electron spectra varied as $e^{-E/\beta}$, where E is the electron energy in keV, then values of β (the e - folding energy) in the range from 5 to 24 keV are needed to explain events of the REA type. Johansen (1965) at Tromso, has studied electron energy spectra using a 27.6 MHz riometer and λ 5577Å photometer. However, as his study was restricted only to cases when aurora covered most of the sky uniformly and because individual electron precipitation events were not studied, Johansen's results are of little use for the study of electron precipitation in the evening sector during polar substorms.

Barcus and Rosenberg (1966) have reported the observation of impulsive bursts and pre-breakup evening events characterised by relatively hard electron energy spectra i.e. e-folding energies were typically of the order of 30 to 50 keV. Akasofu (1968a) suggests that this particular type

of event may be associated with the eastward drift of electrons around the globe, beginning in the midnight sector and giving rise to absorption events which could be observed in the auroral zone in the afternoon and early evening hours. Such electron precipitation events may be similar to a type, mentioned in Chapter 2, which were recorded at Macquarie Island in the afternoon and evening hours and which were not accompanied by any Pi geomagnetic pulsations activity. Barcus and Rosenberg (1966) also reported observation of sudden-onset breakup events recorded in the evening and night-time, which were characterised by relatively soft energy spectra; the evening events were probably similar to RRA events. Bewersdorff et al (1967b) have studied electron energy spectra using balloon-borne instruments; however, they studied the average diurnal variation of the energy spectrum at Kiruna and very few observations were taken in the evening sector. More studies of electron precipitation in the evening sector using balloon-borne instruments, in conjunction with the study of riometer records, are needed.

At present, nothing is known concerning the type and typical energy spectra of the particles which give rise to GEA events. A further discussion of GEA events will be given in Chapter 7.

Note added in proofs - Driatskiy (1968) (in "Diurnal Pattern of Auroral absorption in the auroral zone" *Geomagnetism and Aeronomy* Vol. 8, pp. 33 - 38) has found that, in the auroral zone, auroral absorption events often accompany positive bays during the evening hours. These events are characterised by weak absorption values i.e. 0.2 - 0.5 dB (c.f. Feldstein, 1969); these may be GEA events.

CHAPTER 5

THE MIDNIGHT SECTOR

5.1 Pi Geomagnetic Pulsations and Cosmic Noise Absorption in the Midnight Sector of the Auroral Zone

In the midnight sector, the dominant feature of the polar substorm is the poleward expansion of auroral arcs, initially in the auroral oval, giving rise to formation of an auroral bulge. Intense negative bays with fast onsets in magnetic H component are observed in the region traversed by the bulge front (Akasofu et al, 1966a).

The onset of a polar substorm, which is referred to commonly as the "break-up" in the midnight sector, is often accompanied by rapid onset of Pi geomagnetic pulsations and cosmic noise absorption events, associated with impulsive electron precipitation (c.f. Heacock, 1967a and McPherron et al, 1968). It should be remembered that sometimes, during the recovery phase of an auroral substorm, another auroral substorm may commence; onset of the latter substorm would usually be associated with formation of an auroral bulge, together with observation of enhancements in Pi and CNA activity in the midnight sector of the auroral oval.

An example of onset of polar substorm activity, after a quiet period, is illustrated in Figure 5-1.

Near midnight, L time, an intense X-ray burst was recorded on instrumentation on board a balloon floating near College, Alaska. The onset

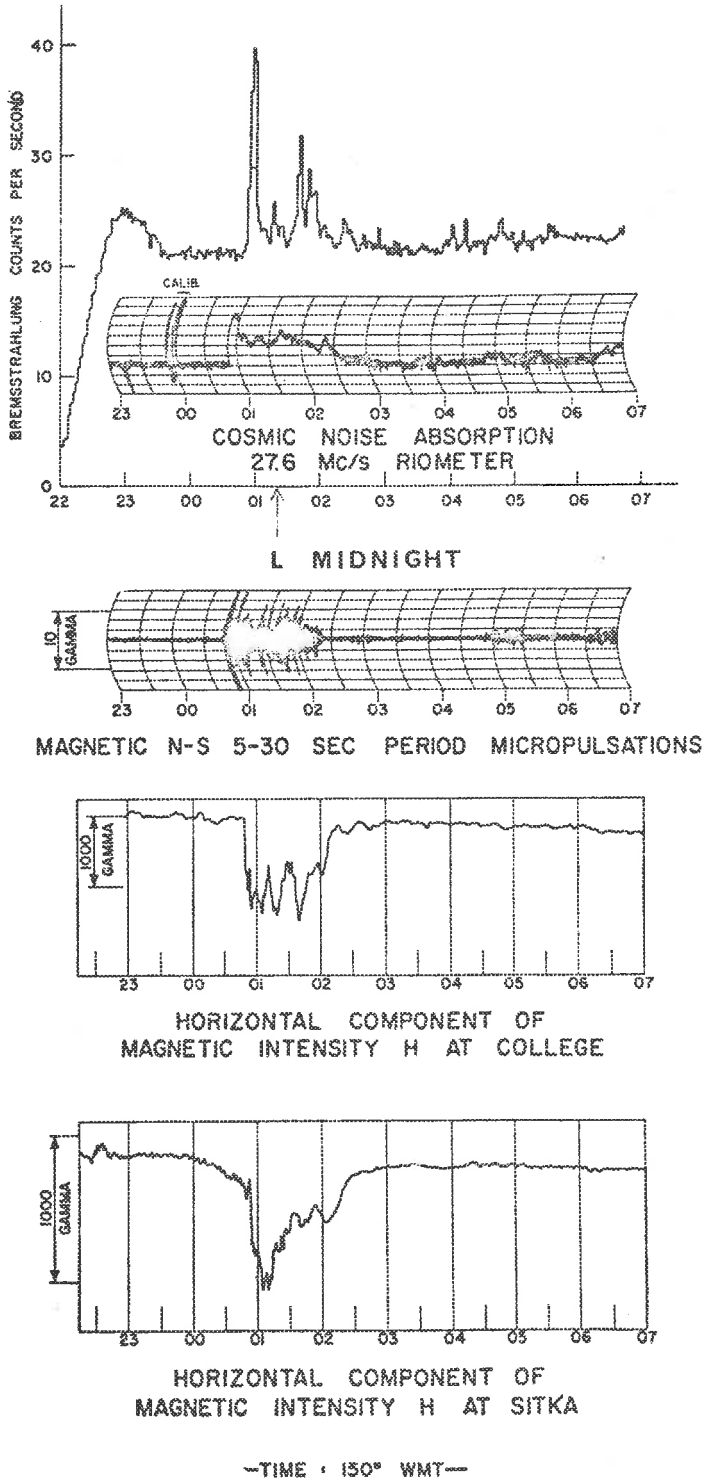

Fig. 5-1 Pi event and associated bremsstrahlung and riometer absorption recorded at College, Alaska on 28 June 1960; magnetometer records for College and Sitka are also given (after Campbell and Matsushita, 1962).

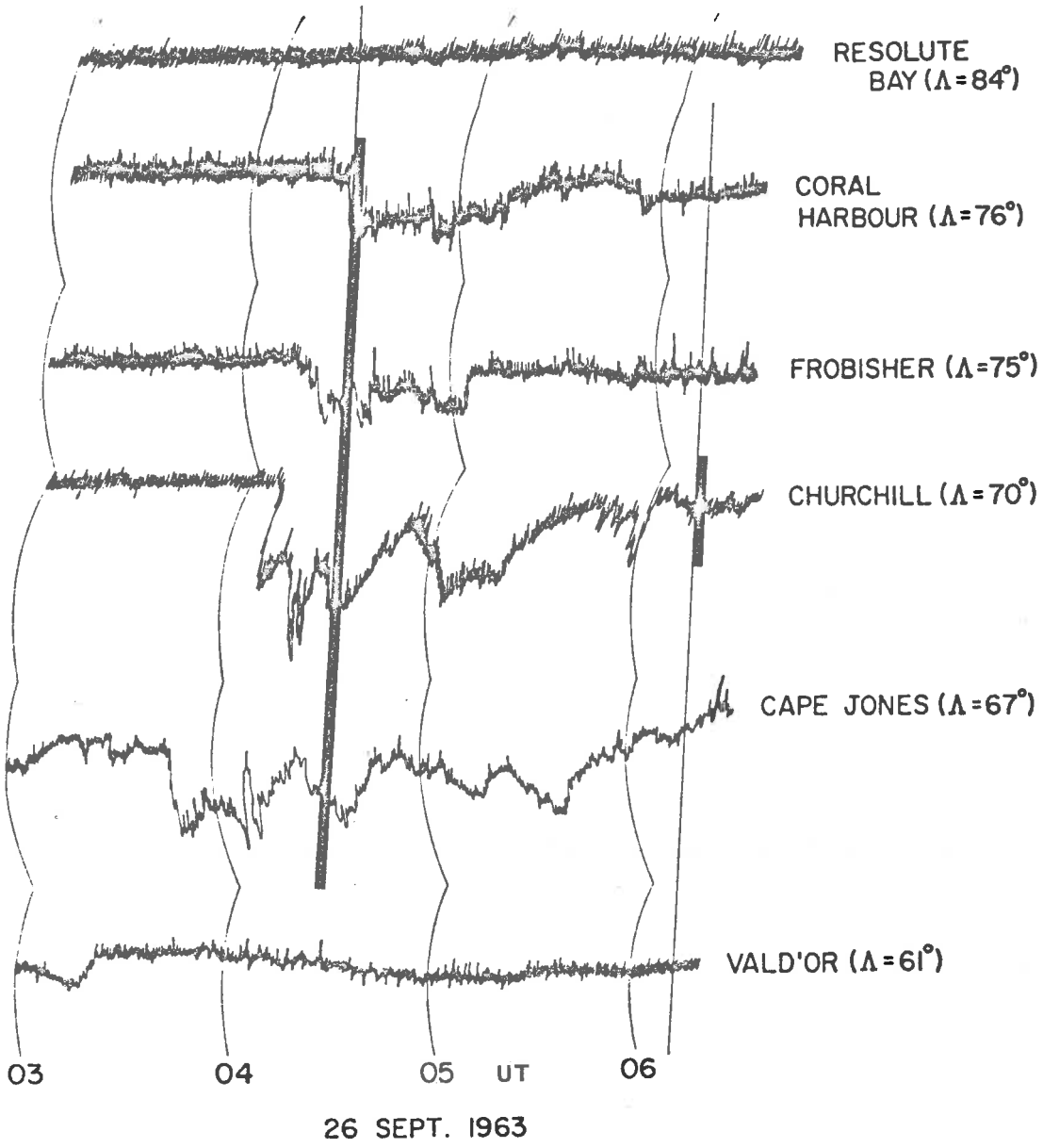

Fig. 5-2 Poleward expansion of absorption recorded by a Canadian north-south chain of riometers on 26 September 1963 (after Lin et al, 1968). L-midnight at Resolute Bay is approximately 0810 U.T.; L-midnight at the other Canadian stations ranges from 0350 to 0540 U.T.

to the X-ray burst probably occurred during the early part of a polar substorm, as it was accompanied by a rapid Pi onset, a fast decrease in magnetic H component and a strong absorption event with rapid onset.

Onset of intense absorption in the midnight sector has been found to be closely associated with the formation of auroral bulges (Jelly, 1968). An example of riometer records from a Canadian north-south chain of stations is given in Figure 5-2; these stations cover a wide range of geomagnetic L-latitude (see Appendix A). Absorption commenced at Cape Jones at about 0350 U.T.; a systematic delay in onset of absorption at higher latitudes, indicating a poleward expansion of the absorption region, can be seen.

5.2 Relation of Absorption Increases to Rapid Pi Features at Macquarie Island During the Midnight Hours

Time relationships between Pi features and absorption increases recorded at Macquarie Island during the hours 1000 to 1400 U.T. were studied to find commonly occurring patterns of polar substorm activity. As geomagnetic L-midnight at Macquarie Island is 1220 U.T., for the hours 1000 to 1400 U.T., that station is normally close to the equatorward edge of the auroral oval. It was assumed that the observation of Pi activity at Macquarie Island was a reliable indication of polar substorm activity. During periods of moderately high planetary magnetic disturbance ($Kp > 3$), absorption increases and rapid Pi features were often closely associated. During magnetically quiet periods ($Kp < 3$), Pi geomagnetic pulsations were occasionally recorded without any accompanying cosmic noise absorption.

One particular pattern of cosmic noise absorption activity commonly

recorded at Macquarie Island, during the midnight hours, was a sequence where a strong RAI was followed, within an hour, by a more slowly varying increase in absorption. Invariably, these absorption increases were features of a complex absorption event. In this pattern of activity, maximum absorption recorded during the rapid absorption increase was usually less than that recorded during the following, more slowly varying absorption increase. For every occurrence of this pattern of absorption activity, the RAI was accompanied, within the same ten-minute interval, by a rapid Pi feature.

Continuation of cosmic noise absorption was accompanied by continuation in Pi activity. This pattern of activity occurred on at least ten nights during January to March 1968.

Heacock (1967a) has distinguished two subtypes of Pi activity, namely the Pi burst, which is similar to the rapid Pi bursts discussed in Chapter 2, and Pi(c) geomagnetic pulsations characterized by a non-impulsive, continuous character. Heacock found that Pi bursts are associated with type F absorption events (c.f. Berkey and Parthasarathy, 1964). The geomagnetic pulsations recorded at Macquarie Island after rapid Pi features belong to the Pi(c) subtype.

In Table 5-1, dates where the activity described above was recorded, together with Kp values for the time intervals 0900 - 1200 U.T. and 1200 - 1500 U.T. and the maximum absorption value during the period 1000 - 1400 U.T. are given.

TABLE 5-1

Nights where a rapid absorption increase, followed by a more slowly varying increase in absorption was recorded in the time interval 1000 - 1400 U.T.

Date	Kp(0900 - 1200 U.T.)	Kp(1200 - 1500 U.T.)	Maximum Absorption (dB)
9 Feb	3 -	3 +	3.8
17 Feb	4 -	4 +	1.4
28 Feb	3o	4o	4.1
5 Mar	3 +	4 +	2.1
10 Mar	1 -	3 +	2.0
12 Mar	3 -	2 +	1.1
15 Mar	4 -	4 +	3.9
16 Mar	3 +	6 -	4.3
19 Mar	3 +	2 +	4.4
20 Mar	4o	4_o	2.9

It can be seen that of the twenty Kp values given in Table 5-1, only three values were less than 3 -.

Another pattern of activity was also recorded during the midnight hours. In this pattern, rapid Pi features were recorded without being associated in the same fifteen minute interval with strong absorption increases. In general, on the nights when this pattern was observed, if cosmic noise absorption was recorded at any time during the interval 1000 to 1400 U.T.,

absorption was weak (usually not exceeding one decibel) and slowly varying. In Table 5-2, dates, Kp values for 0900 - 1200 U.T. and 1200 - 1500 U.T. and maximum absorption values are given for nights when this type of activity was recorded. No maximum absorption value is given for the nights where detectable CNA was not recorded during the time interval 1000 - 1400 U.T.

TABLE 5-2

Nights where all rapid Pi features recorded in the time interval 1000 - 1400 U.T. could not be associated with a strong absorption increase.

Date	Kp(0900 - 1200 U.T.)	Kp(1200 - 1500 U.T.)	Maximum Absorption (dB)
18 Jan	2o	2 +	0.9
22 Jan	2 -	2 +	-
28 Jan	1 -	2o	-
30 Jan	2 +	2 +	0.4
3 Feb	2 +	1 +	0.5
8 Feb	3 -	3 +	0.2
3 Mar	3 -	2 +	0.6
17 Mar	2o	2o	-
18 Mar	3 -	2 -	0.5
21 Mar	2 -	2 -	-

It can be seen that of the twenty values of Kp given in Table 5-2, only four values exceed the value 2 +.

Although a large number of nights were not studied, this analysis

indicates that at Macquarie Island, the correlation of Pi features with strong absorption increases is dependent upon the level of planetary magnetic disturbance, with the correlation of these two phenomena improving as Kp increases from one to three.

It is suggested that on the nights tabulated in Table 5-1, which are characterized by Kp values greater than or equal to 3 -, Macquarie Island was normally inside the auroral oval during the midnight hours. On the nights tabulated in Table 5-2, which are characterized by Kp values less than 3 -, Macquarie Island was normally equatorward of the auroral oval during the midnight hours. Examples of auroral activity supporting this suggestion will be presented and discussed in the next two sections of this chapter.

5.3 Auroral Activity Inside the Auroral Oval During the Midnight Hours

The first example is from records for 9 February 1968. From the all-sky photographs (Figure 5-3), it can be seen that at 1223 U.T., a bright arc was located in the northern sky over Macquarie Island. By 1233 U.T., bright aurorae had covered the sky in a poleward expansion. There had been auroral activity before 1223 U.T., which had been accompanied by CNA, Pi activity and magnetic disturbance (see Figure 5-4).

The poleward expansion of aurorae, starting around 1225 U.T., is suggested to be due to onset of a polar substorm and was accompanied by a fast decrease in magnetic H component, a strong rapid absorption increase and a rapid enhancement in Pi activity. The strong RAI was followed by a more slowly varying increase in absorption which began at about 1240 U.T.

Fig. 5-3 All-sky photographs recorded at Macquarie Island on 9 February 1968 and 28 February 1968.

MACQUARIE ISLAND

FEB 9 1968

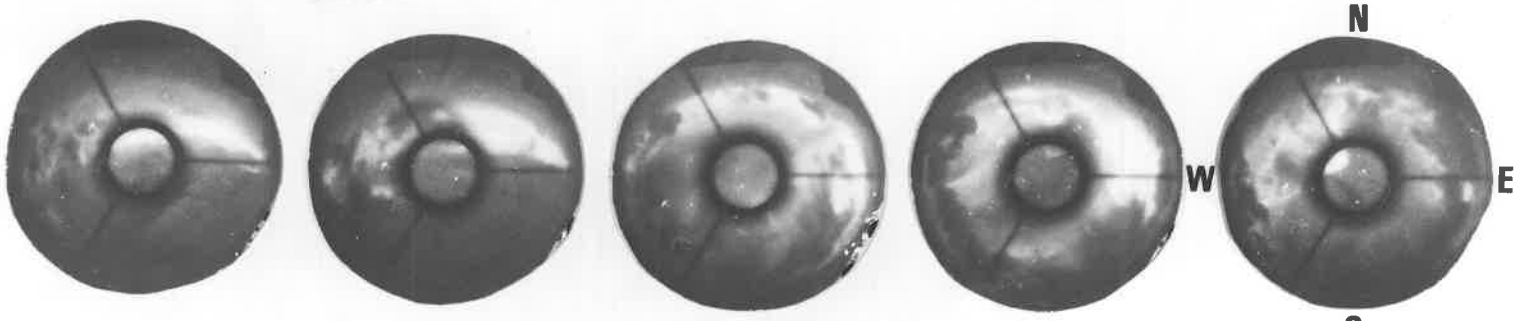

1223 UT 1228 1233 1238 1242

FEB 28 1968

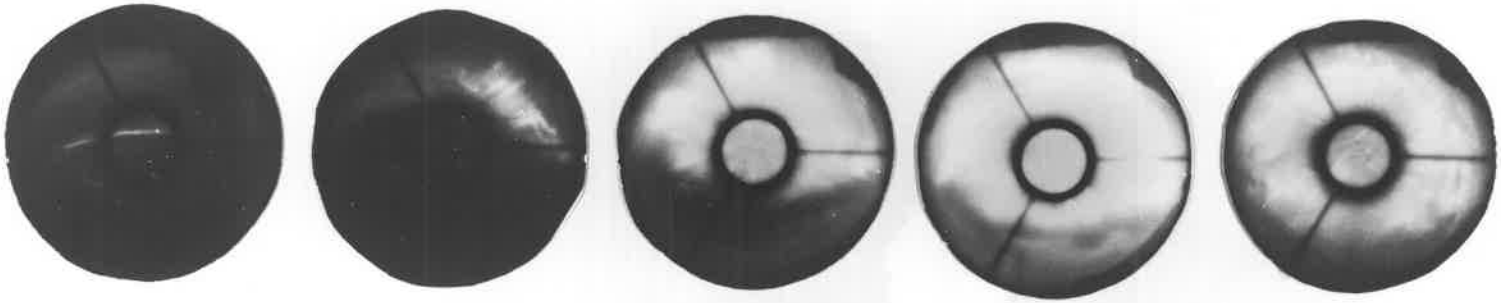

1132 1201 1203 1204 1210

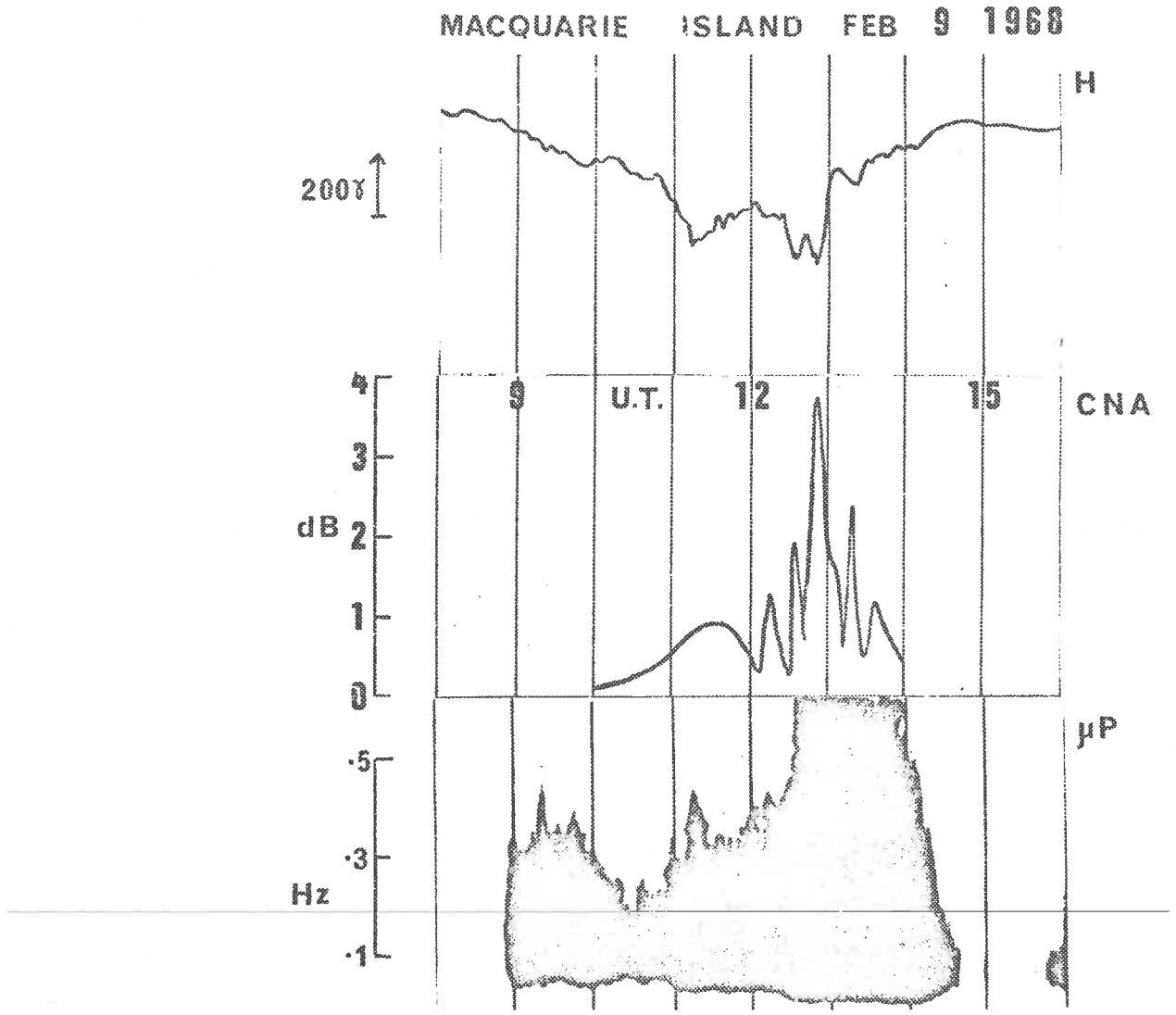

Fig. 5-4 Magnetometer, cosmic noise absorption and geomagnetic pulsations sonagraph records for Macquarie Island for the period 0800 to 1600 U.T. on 9 February 1968.

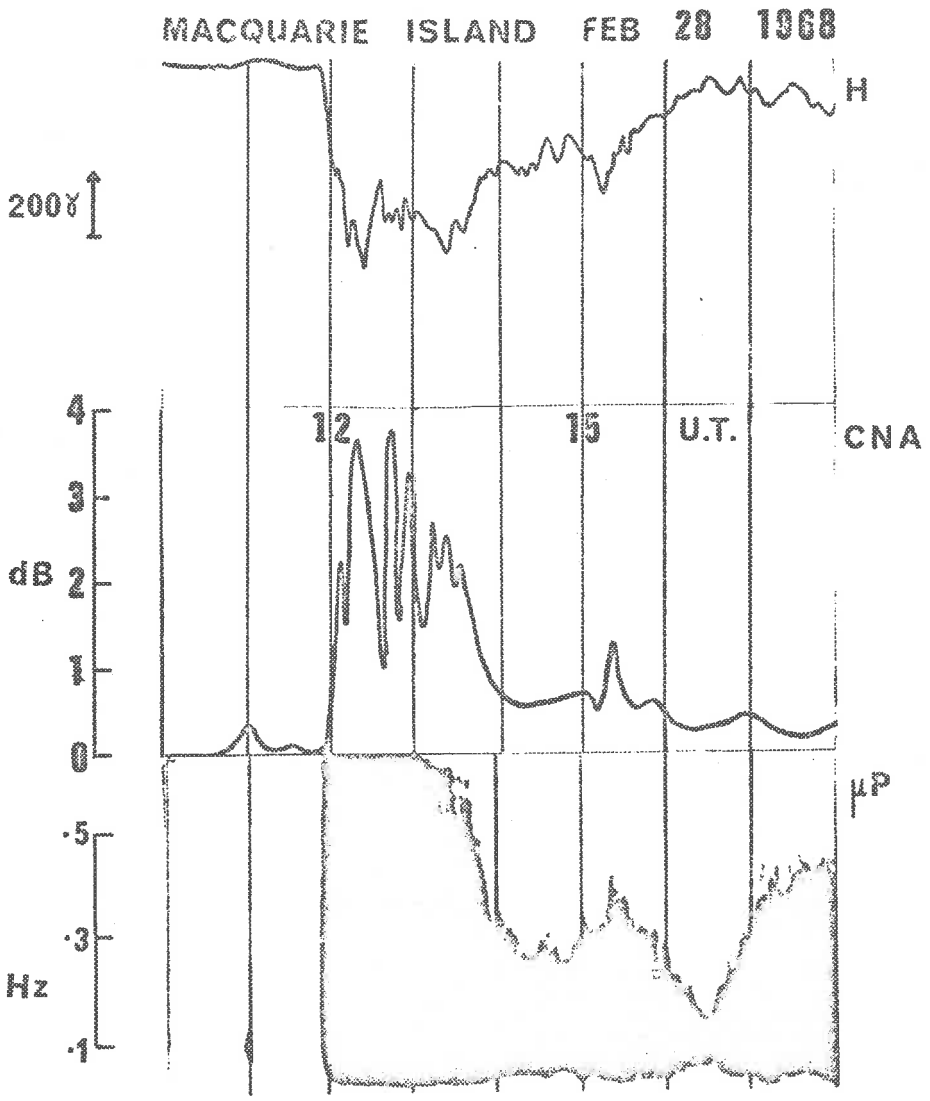

Fig. 5-5 Magnetometer, cosmic noise absorption and geomagnetic pulsations sonagraph records for Macquarie Island for the period 1000 to 1800 U.T. on 28 February 1968.

Pi(c) geomagnetic pulsations following the enhancement in Pi activity starting near 1225 U.T. was accompanied by a continuation of cosmic noise absorption having a similar duration.

The second example of a polar substorm onset is taken from records for 28 February 1968. At 1132 U.T., a thin arc was visible to the north of zenith at Macquarie Island (see Figure 5-3) and a glow was visible in the northern sky.

Around 1201 U.T., an auroral substorm commenced; aurorae to the north began an increase in brightness and moved rapidly poleward covering the sky over Macquarie Island with bright forms. The poleward expansion of aurorae was accompanied by a rapid onset in Pi activity, a sharp decrease in magnetic H component and rapid onset of a cosmic noise absorption event (see Figure 5-5). Pi(c) geomagnetic pulsations following onset of disturbance were accompanied by a continuation of cosmic noise absorption. The rapid onset to absorption was followed by a more slowly varying enhancement in absorption which began at about 1208 U.T.

5.4 Auroral Activity Equatorward of the Auroral Oval in the Midnight Hours

In the first example, taken from records for 30 January 1968, it can be seen that at 1144 U.T., a diffuse auroral glow covered the southern sky over Macquarie Island (see Figure 5-6). At 1148 U.T., a spectacular partial corona was observed. On several occasions, it was noticed that slow fluctuations in the geomagnetic field, observed on the geomagnetic pulsations channel, began a minute or so before the observation of a partial corona,

Fig. 5-6 All-sky photographs recorded at Macquarie Island on 30 January 1968 and 3 March 1968.

MACQUARIE ISLAND

JAN 30 1968

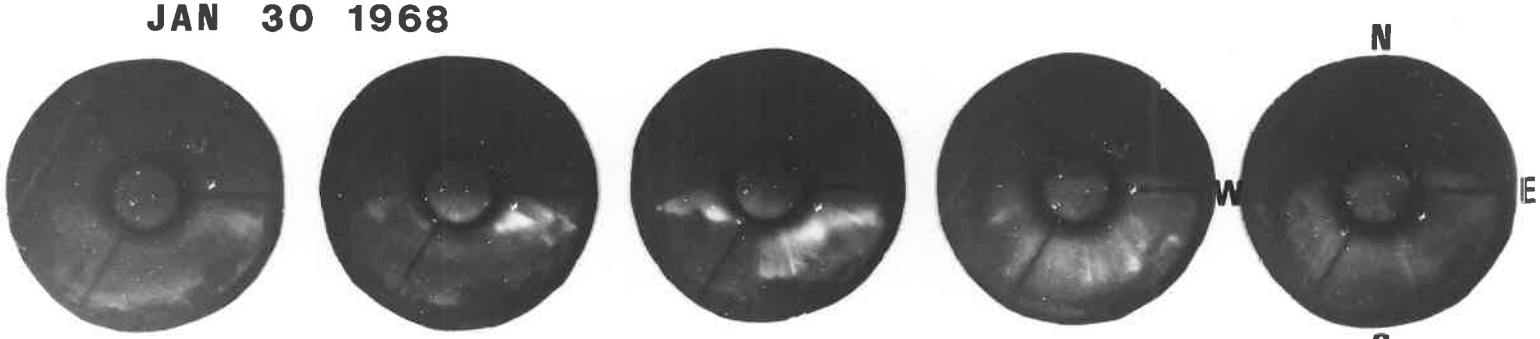

1144 UT 1148 1149 1206 1210

MAR 3 1968

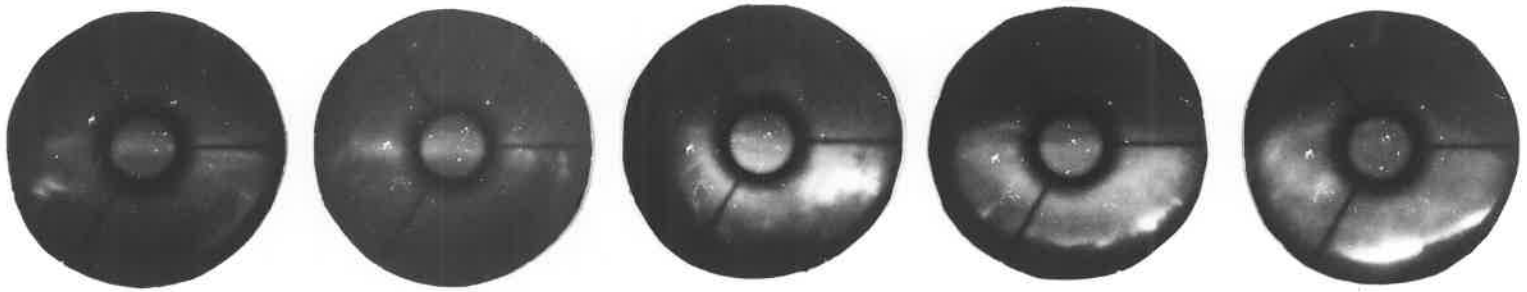

1005 1014 1026 1030 1040

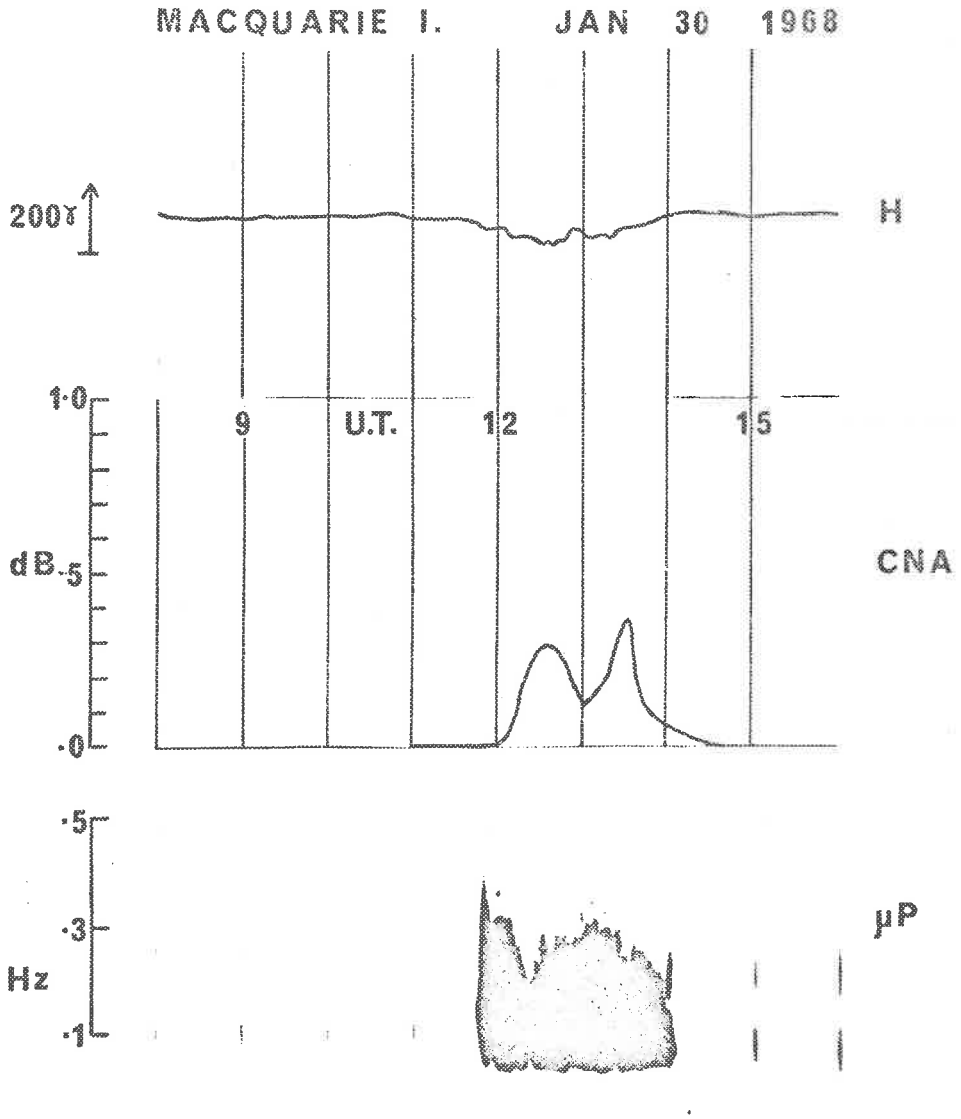

Fig. 5-7 Magnetometer, cosmic noise absorption and geomagnetic pulsations sonagraph records for Macquarie Island for the period 0800 to 1600 U.T. on 30 January 1968.

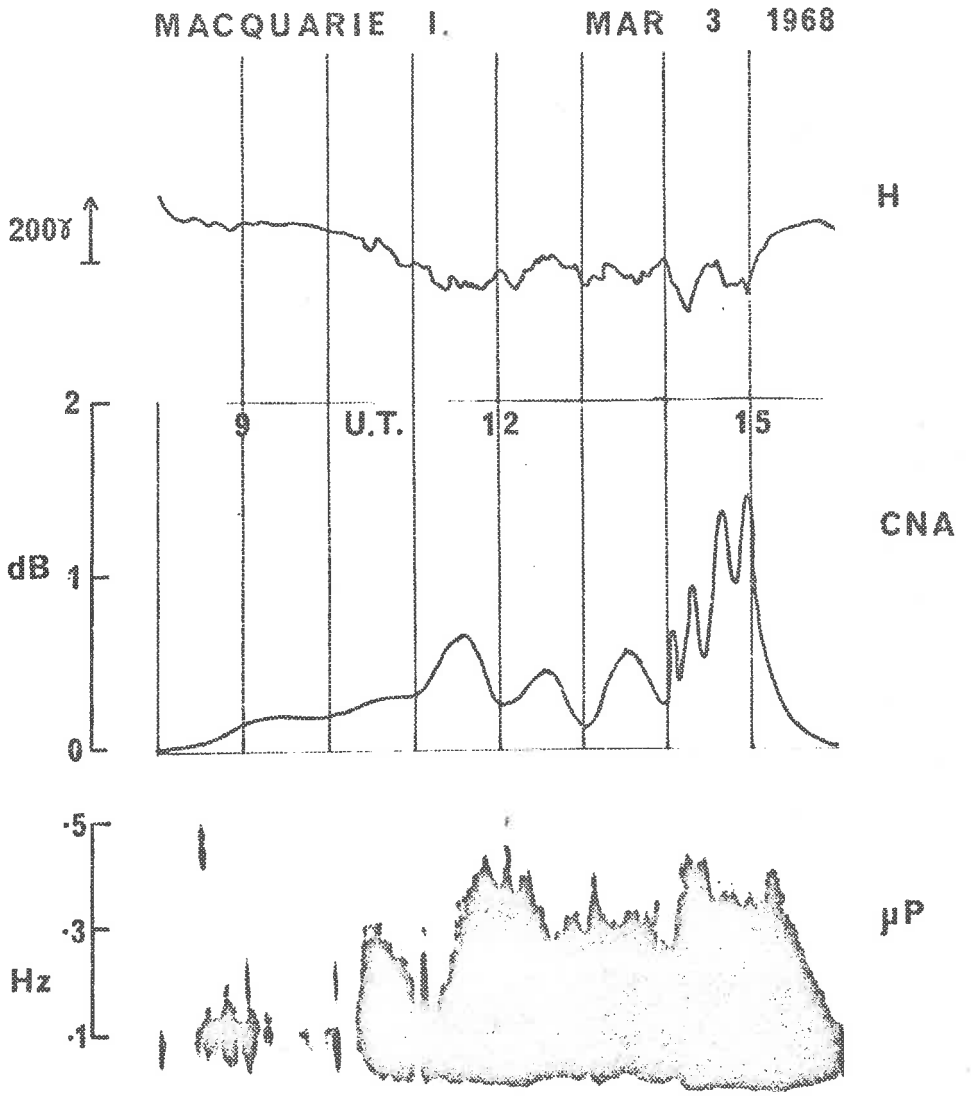

Fig. 5-8 Magnetometer, cosmic noise absorption and geomagnetic pulsations sonagraph records for Macquarie Island for the period 0800 to 1600 U.T. on 3 March 1968.

characterized by the appearance of auroral rays over most of the southern sky. The appearance of the partial corona on 30 January was accompanied by a rapid Pi burst (see Figure 5-7) but was not accompanied by strong cosmic noise absorption.

After 1148 U.T. Pi activity continued, accompanied by weak cosmic noise absorption. It is suggested that a polar substorm began at around 1148 U.T. and that at that time Macquarie Island was equatorward of the auroral oval. Observation of a partial corona in the southern sky indicates precipitation of particles in a region poleward of Macquarie Island.

The second example of activity is from records for 3 March 1968. At 1005 U.T., a bright striated band could be seen at the zenith at Macquarie Island together with some diffuse auroral glow in the southern sky. (see Figure 5-6 for the all sky camera record).

A rapid onset in Pi activity (see Figure 5-8) occurred at 1020 U.T., accompanied by brightening of aurorae to the south. By 1030 U.T. (see Figure 5-6), it can be seen that a coronal form covered the southern sky. At 1040 U.T., bright auroral forms were visible near the southern horizon.

It is suggested that around 1020 U.T., a polar substorm commenced and that activity observed at Macquarie Island i.e. onset of Pi geomagnetic pulsations, weak cosmic noise absorption and a bright partial corona in the southern sky, was due to precipitation of particles, with the most intense precipitation occurring in a region poleward of Macquarie Island.

5.5 Pi 2 Geomagnetic Pulsations Recorded at Macquarie Island

Pi 2 geomagnetic pulsations are usually observed at subauroral latitudes in the form of pulsation trains resembling damped sinusoidal oscillations (Saito and Matsushita, 1968 and Rostoker, 1967). Saito (1961) has shown that Pi 2 events are always accompanied by magnetic bays in the auroral zone; this result indicates that Pi 2 events occur during polar substorms. As very little work has been done on spectral analysis of Pi 2 geomagnetic pulsations recorded at auroral zone stations (c.f. Saito, 1969), digital sonagrams, over the frequency range .004 to 0.56 Hz, were computed for some events recorded at Macquarie Island. A discussion of these computations is given in Appendix B.

Digital sonagrams of Pi 2 geomagnetic pulsations recorded at Macquarie Island when that station was equatorward of the auroral oval (see Table 5-2) are shown in Figure 5-9. In the sonagram for 30 January 1968, pulsation at frequencies near .01 Hz is the dominant feature. This Pi 2 activity occurred during a polar substorm which commenced at about 1148 U.T. (see §5.4). Time-averaged power spectra for half-hour time intervals, between 1150 and 1320 U.T. on 30 January 1968, are shown in Figure 5-10; a peak in power, at a frequency near .01 Hz, can be seen in all of these spectra.

Pulsation at frequencies near .01 Hz is also the dominant feature of the sonagram for 8 February 1968 (see Figure 5-9). A polar substorm probably began around 1100 U.T.; at that time, magnetic disturbance at Macquarie Island began with a rapid onset to Pi activity, as observed over the frequency band 0.1 to 0.5 Hz, and a small positive excursion in magnetic H component,

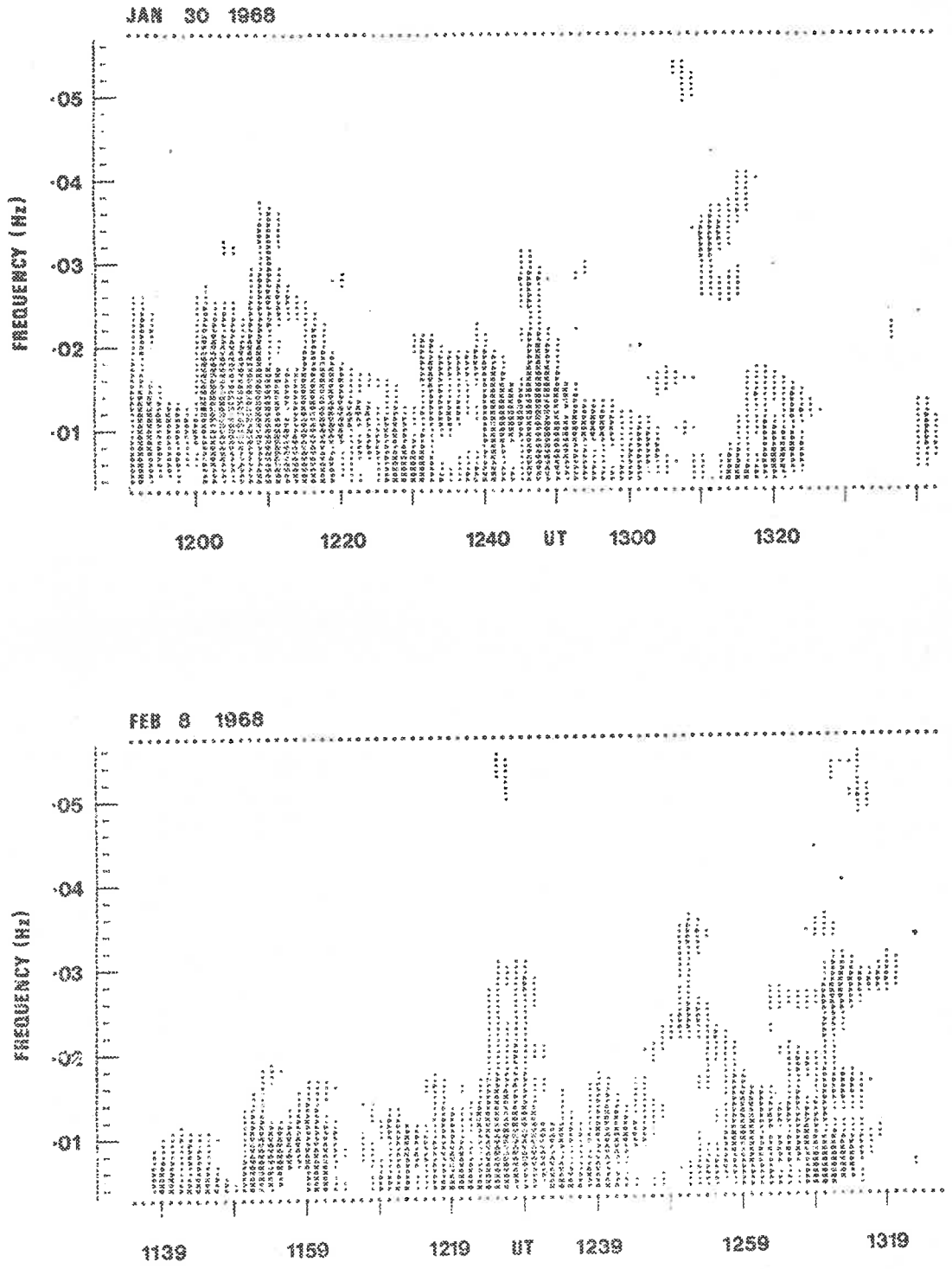

Figure 5-9. Digital sonagrams of geomagnetic pulsations recorded at Macquarie Island on 30 January 1968 and 8 February 1968.

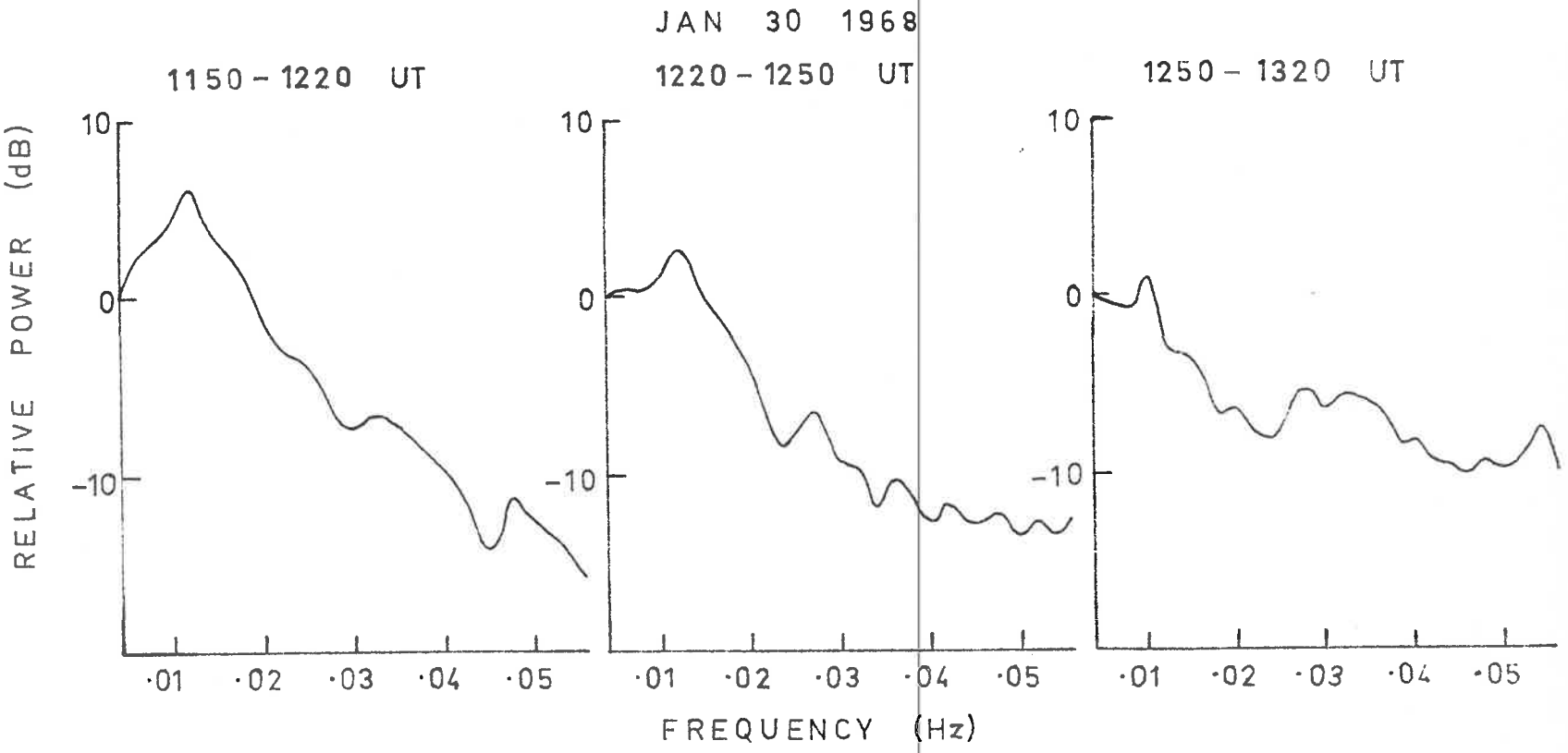

Figure 5-10. Time-averaged power spectra for geomagnetic pulsations recorded at Macquarie Island on 30 January 1968.

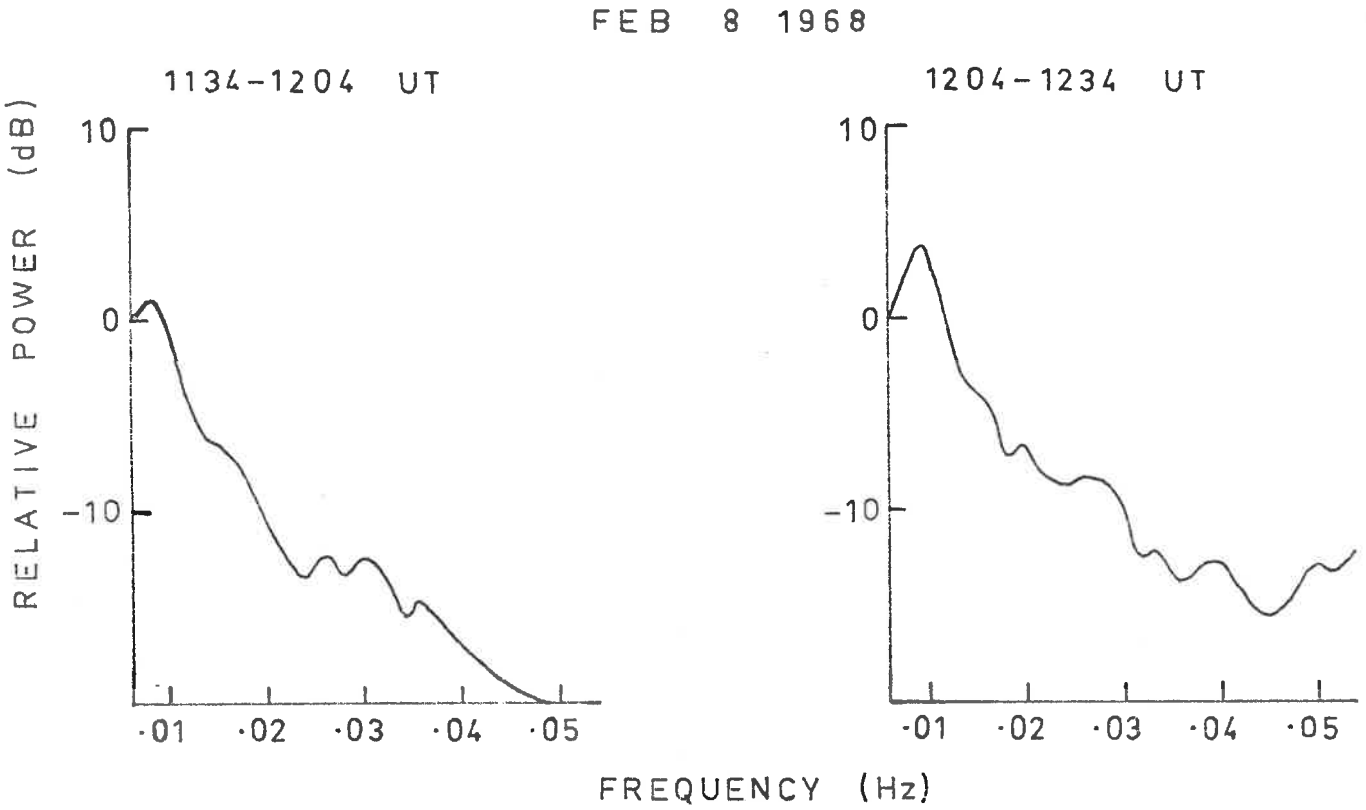

Figure 5-11. Time-averaged power spectra for geomagnetic pulsations recorded at Macquarie Island on 8 February 1968.

which preceded a prolonged negative excursion in H. Time-averaged power spectra for half-hour time intervals, between 1134 and 1234 U.T. on 8 February 1968, are shown in Figure 5-11. It can be seen that a peak in power, at a frequency near .01 Hz, occurs in each of these spectra.

Sonagrams of Pi 2 activity were also produced for two nights when Macquarie Island was inside the auroral oval. During the midnight hours on these nights, Pi 2 activity was characterized by complex frequency-time behaviour; during Pi events, a number of peaks in power were usually present in the .004 to .056 Hz frequency band. A sonagram for one of those nights, on 15 March 1968, is shown in Figure 5-12. A polar substorm began around 1225 U.T.; Pi activity began with a rapid onset at about that time (see Figure 3-5). A strong RAI was recorded at Macquarie Island at about 1230 U.T.; a negative bay commenced with a fast onset near to that time. The time-averaged power spectrum for the period 1220 to 1250 U.T. on 15 March 1968 (see Figure 5-13) shows the presence of peaks in power at frequencies of about .016, .023, .03, .04 and .048 Hz. These frequencies are approximately harmonically related, with a fundamental frequency at about .008 Hz. However, a peak at the latter frequency was not evident on the time-averaged power spectrum. Also, it was evident from the sonagram, that such a harmonic structure did not persist during the Pi event.

On 17 February 1968, Macquarie Island was inside the auroral oval during the midnight hours (see Table 5-1). A polar substorm began at about 1150 U.T. on that night; a negative bay commenced at Macquarie Island at that time. Also, at approximately the same time Pi activity commenced with a rapid onset and a strong RAI was recorded at Macquarie Island (see Figure 2-1).

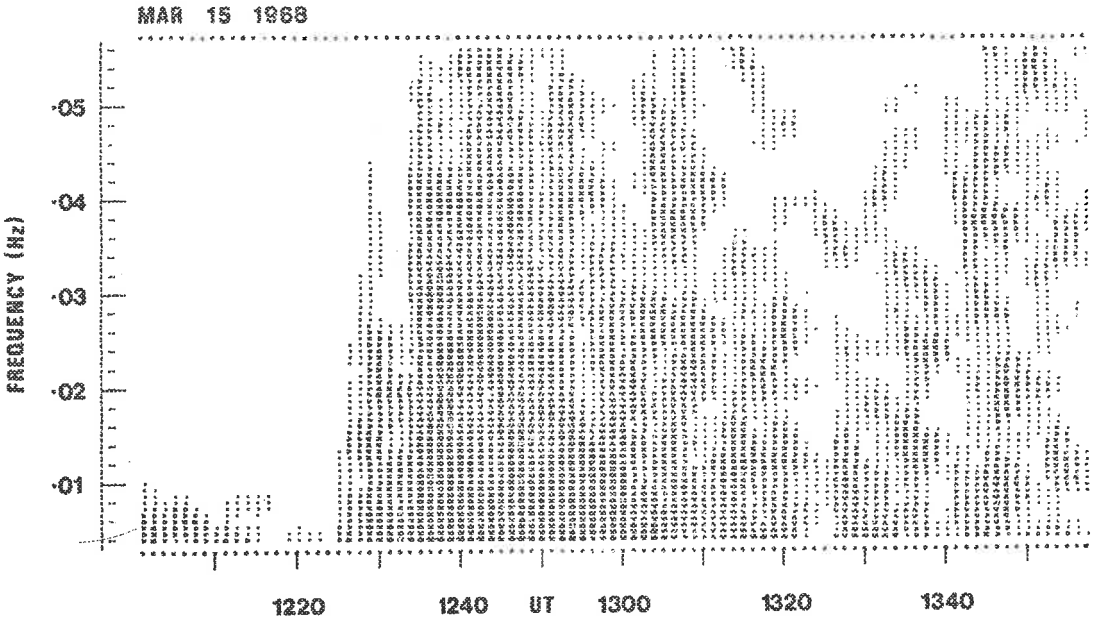

Figure 5-12. Digital sonagram of geomagnetic pulsations recorded at Macquarie Island on 15 March 1968.

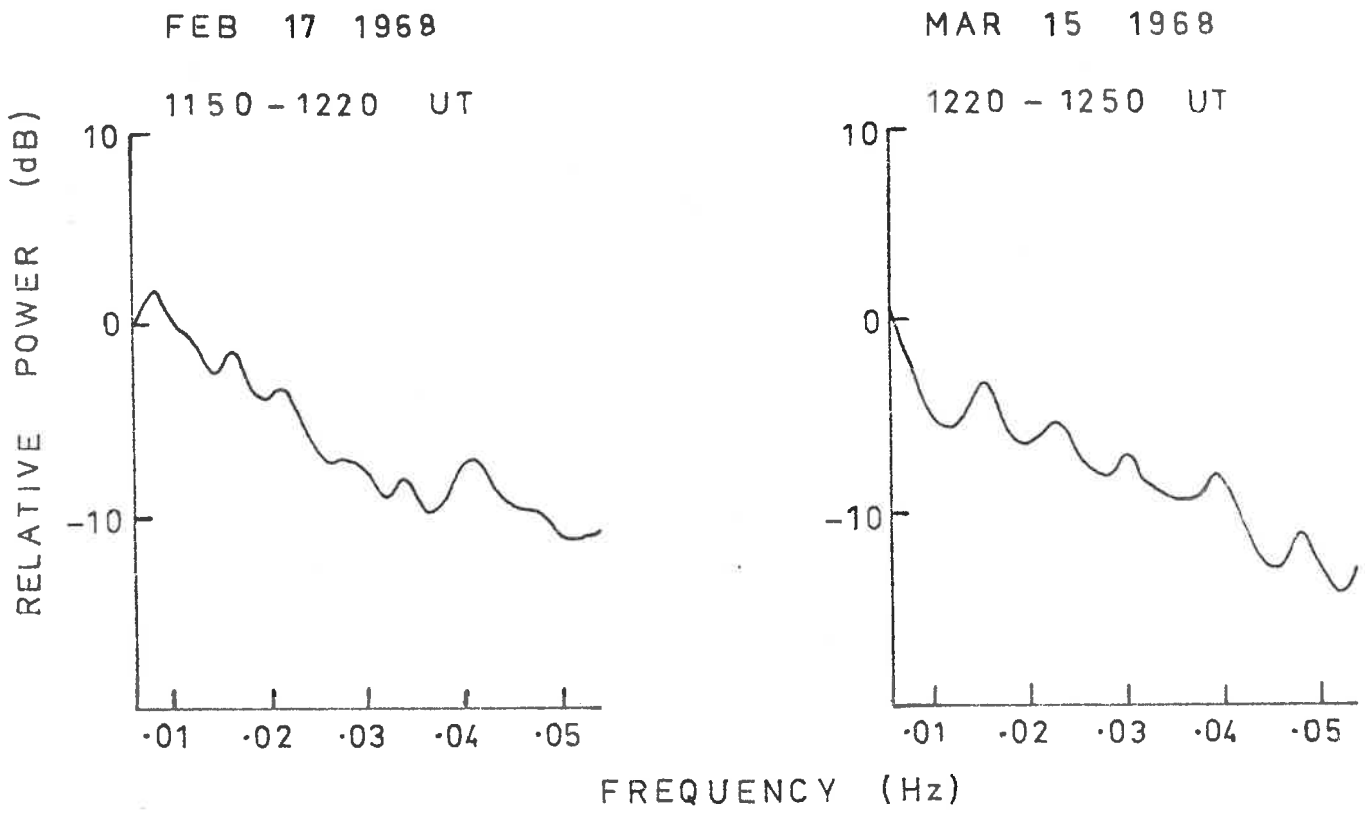

Figure 5-13. Time-averaged power spectra for geomagnetic pulsations recorded at Macquarie Island on 17 February 1968 and 15 March 1968.

A time-averaged power spectrum for the period 1150 to 1220 U.T. is given in Figure 5-13; it can be seen that peaks in power occurred at frequencies of approximately .09, .016, .022, .034 and .04 Hz.

5.6 Discussion

Jelly (1970) has recently studied the latitudinal variation of cosmic noise absorption during polar substorms, using records from a Canadian north-south chain of riometer stations. She has found a transition between the fast-onset, irregular, intense absorption at higher latitudes and the smoother, less intense absorption at lower latitudes. Jelly identifies this transition, designated as Λ_a, with the most southerly quiet arc in the auroral oval prior to substorm onset. The examples of substorm activity, discussed in this chapter, demonstrate the correctness of Jelly's identification of Λ_a with the equatorward boundary of the auroral oval; furthermore, they indicate that strong absorption will be observed at stations in the midnight sector which were inside the auroral oval prior to onset of a substorm. Thus the observed dependence of the correlation of rapid Pi features and strong absorption increases upon Kp constitutes evidence for the expansion of the auroral oval, which accompanies increase in the level of planetary magnetic disturbance (Feldstein and Starkov, 1967).

Formation of an auroral bulge in the midnight sector is accompanied by both a poleward and equatorward expansion of aurora. Most of the substorm absorption events studied by Jelly were observed to start in the vicinity of the transition Λ_a. It is suggested that the slowly varying and weak absorption observed in the midnight sector, in a region equatorward of the transition Λ_a, is associated with the equatorward expansion of aurora during a polar substorm.

At a station which was inside or polewards of the auroral oval before substorm onset, the first intense auroral activity seen consists of bright, rapidly moving bands, which are located in the front of the expanding bulge. This period of auroral substorm activity is referred to as the "break-up phase". Ansari (1964) reports that this phase lasts, typically, for only a few minutes at College, Alaska. After bright auroral forms pass over a station in the bulge region, aurora over that station become more diffuse and break up into irregular bands and patches which drift eastward. This phase of the auroral substorm, as observed at any station within the auroral bulge, is referred to as the "post breakup phase".

Ansari (1964) and Eather and Jacka (1966) find that fast onsets to absorption events are recorded during the break-up phase. From simultaneous measurements of auroral luminosity (λ 5577 Å) and cosmic noise absorption, these workers concluded that the effects recorded could be accounted for by assuming precipitation of electrons with soft energy spectra i.e. the e-folding energies were estimated to be near 10 keV. Barcus and Rosenberg (1966), who used balloon-borne x-ray detectors in the auroral zone in Alaska, also report the observation of fast-onset electron precipitation events, with soft energy spectra, which occurred around midnight during auroral breakup.

Ansari found that during the post-breakup phase of the auroral substorm, slowly varying absorption was observed. In general, absorption and auroral luminosity were not well correlated during this phase i.e. weak luminosity was observed, together with strong absorption. This type of absorption activity was referred to by Ansari as SVIA i.e. "slowly varying intense absorption". Eather and Jacka (1966) also found that at Mawson,

Antarctica, slowly varying absorption was recorded during the post-breakup phase. Ansari concluded that absorption recorded during SVIA could be explained by assuming increases in flux of precipitating electrons with energies in the range 30 to 100 keV. Eather and Jacka concluded that most SVIA could be accounted for by assuming that such activity was due to precipitation of electron fluxes with e-folding energies in the range from 7 to 40 keV. Eather and Jacka suggested that proton precipitation could be important during SVIA. This suggestion was later retracted (Eather and Burrows, 1966).

Clark and Anger (1967) have made a study of electron precipitation into a region centred on Ft. Churchill during several substorms occurring in the one night; they used balloon-borne x-ray detectors. Two substorms commenced while Ft. Churchill was in the midnight sector; during each substorm, Ft. Churchill was covered by an auroral bulge as it expanded polewards. Clark and Anger found that during the expansive phase of the substorms, the electron energy spectrum hardened. They noted that following the initial poleward expansion of aurora, x-ray fluxes were "more smoothly varying and often more intense than during the initial phase". Furthermore, this type of electron precipitation was associated with "a region of diffuse, widespread auroral glow". This type of precipitation appears to be of the same type as that associated with SVIA.

Barcus and Rosenberg (1966), who used balloon-borne x-ray detectors, report the frequent observation of a softening of the electron energy spectrum during post-breakup electron precipitation events. These events were observed primarily between midnight and dawn and were distinguished from the fast-onset night-time events, which are observed mainly in a region which was inside the

auroral oval before substorm onset. Barcus and Rosenberg carried out their observations near geomagnetic latitudes of 65°; most of these events were probably recorded in a region which was equatorward of the auroral oval before substorm onset. Thus electron precipitation in the region covered by the auroral bulge, during its equatorward expansion, may be characterized by soft energy spectra.

It is suggested that in the front of the expanding auroral bulge, there is an electron precipitation region characterized by relatively soft energy spectra i.e. e-folding energies are around 10 keV. Within a region which is inside the bulge and which was poleward of the equatorward boundary of the auroral oval before substorm onset, i.e. the "SVIA region", electron precipitation is characterized by harder energy spectra. Fast time variation in the flux of precipitating electrons is characteristic of the front of the expanding bulge; relatively slower time variation is characteristic of the SVIA region.

CHAPTER 6

THE MORNING SECTOR

6.1 Introduction

From a statistical study of optical and radio-auroral phenomena, Hartz and Brice (1967) have shown that in the auroral zone, two diurnal activity peaks, one in the midnight sector at about 22 hours geomagnetic time and one in the morning sector, at about 08 hours geomagnetic time, should be observed. The midnight peak in activity is associated with the impulsive precipitation of particles characterized by a steep energy spectrum and referred to as "splash-type" precipitation. The morning peak is associated with a continuous influx of particles, referred to as "drizzle-type" precipitation, characterized by a much flatter energy spectrum.

A demonstration of this type of diurnal pattern has already been given in Chapter 2 for cosmic noise absorption and Pi geomagnetic pulsations activity recorded at Macquarie Island, i.e. rapid absorption increases and Pi features were recorded most commonly in the midnight hours, while slowly varying absorption events, which were associated with Pi geomagnetic pulsations events, were recorded most commonly in the morning hours.

Hartz and Brice demonstrate that the "splash-type" particle precipitation is generally confined to the boundary region between open and closed field lines i.e. the auroral oval (c.f. Akasofu, 1966a, Feldstein 1966); the "drizzle-type" particle precipitation is confined to an annular region, centred on geomagnetic latitudes near 65°, which corresponds approximately to the auroral zone. An idealized representation

of the two main zones of auroral particle precipitation in the northern hemisphere is given in Figure 6-1.

The "splash-type" precipitation in the midnight sector accompanies onset of a polar substorm (see Chapter 5). Evidence has been compiled by a number of workers supporting the hypothesis that "drizzle-type" precipitation in the morning sector is directly related to "splash-type" precipitation in the midnight sector i.e. whenever a polar substorm commences, "drizzle-type" precipitation will be observed in the morning sector of the auroral zone.

Bewersdorff et al (1967a) found that SVA events recorded in the morning sector of the auroral zone could be associated with negative magnetic bays in the midnight sector and concluded that SVA events have to be regarded as being part of the polar substorm, being its typical aspect in the morning sector. A similar conclusion was arrived at by Jelley and Brice (1967) from a study of satellite and riometer records. They found that during polar substorms, significant enhancements in intensity of the Van Allen radiation and in precipitation of electrons into the auroral zone, occurred in the morning sector.

Arnoldy and Chan (1969) have studied electron flux increases recorded on the electron spectrometer on board the geostationary satellite ATS 1. They concluded that electrons in the energy range 50 - 150 Kev are produced near the midnight meridian during polar substorms and drift on closed field lines around the earth. They report that 75% of the sixty electron precipitation events studied were accompanied by an absorption event seen at the Alaskan chain of riometers, which are situated at a longitude close

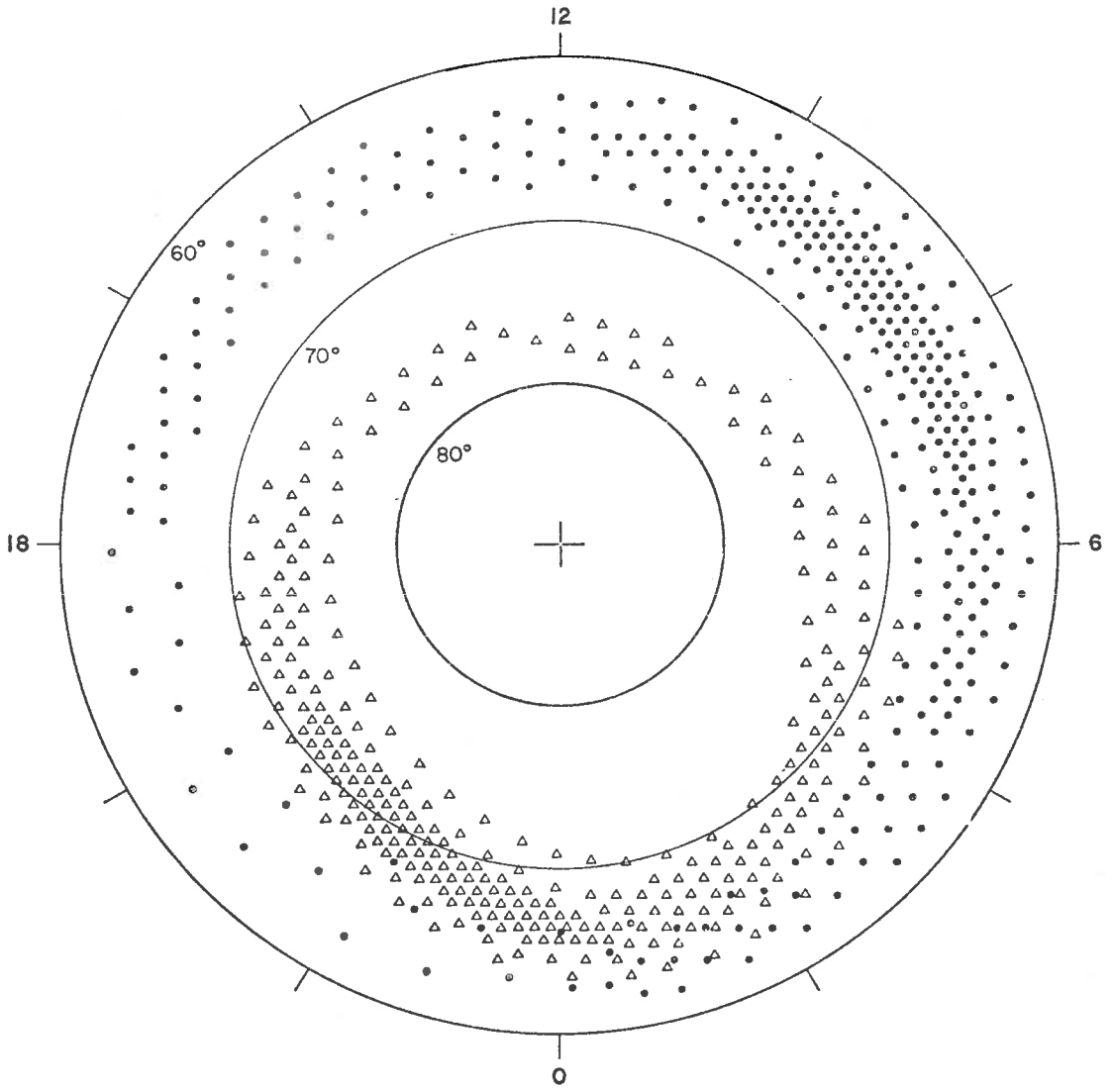

Figure 6-1. An idealised representation of the two main zones of auroral particle precipitation in the northern hemisphere, where the average intensity of the influx is indicated very approximately by the density of symbols and the coordinates are geomagnetic latitude and geomagnetic time.
The zone of splash type precipitation is indicated by the triangles; the zone of drizzle type precipitation is indicated by the dots (after Hartz and Brice, 1967).

to that of the ATS 1 satellite and which cover a range of L-values from L = 3.9 to L = 8.

6.2 Geomagnetic Pulsations and Cosmic Noise Absorption Events in the Morning Sector of the Auroral Zone

6.2.1 *Morning geomagnetic pulsations events*

Polar magnetic substorm activity was examined using magnetometer records from Barrow (Alaska), Abisko (Sweden) and Yakutsk (U.S.S.R.). Although this study was hampered by lack of magnetometer data from the Russian auroral zone stations Dixon Island and Tixie Bay, it was found that Pi events recorded at Macquarie Island always occurred during periods of polar magnetic disturbance.

Twenty Pi events were found where the Pi onset and estimated substorm onset occurred in the same half-hour time interval and where the Pi onset time occurred in the time interval 1400 - 2400 U.T. (the morning to noon hours at Macquarie Island). Any abrupt onset to a positive or negative bay disturbance at any of the stations mentioned above was taken to be the onset of a polar substorm. For fifteen of these Pi events, a riometer record was available. Fourteen were accompanied by a cosmic noise absorption event, usually a SVA event; one (on 10 February 1968) was accompanied by a rapidly varying morning absorption event. As the few RVMA events recorded at Macquarie Island, during January to March 1968, were always accompanied by intense polar magnetic activity, they were regarded as the manifestation, in the morning sector, of particularly intense polar substorms.

For Pi events which were accompanied by a CNA event, dates and onset times are given in Table 6-1. Estimated substorm onset time, CNA event onset time, together with the time of the first maximum in absorption and the absorption value at that maximum, are also given.

TABLE 6-1

Morning Pi geomagnetic pulsations events recorded at Macquarie Island during polar substorms.

Date	Substorm Onset Time (U.T.)	Pi Onset Time (U.T.)	CNA Onset Time (U.T.)	Time of first maximum (U.T.)	Absorption in dB at first maximum
5 Jan	1430	1425	1515	1550	1.33
11 Jan	2100	2100	2100	2117	0.21
12 Jan	1500	1500	1450	1545	2.04
"	1810	1810	1810	1840	1.43
17 Jan	2005	2000	2000	2100	0.33
24 Jan	1845	1910	1900	1940	1.41
30 Jan	1610	1624	1610	1702	0.79
4 Feb	1545	1540	1540	1610	0.81
8 Feb	2120	2138	2120	2213	1.62
10 Feb	1620	1620	1650	1718	4.53
11 Feb	2010	2020	2010	2050	2.05
27 Feb	1940	1940	1945	2018	1.12
2 Mar	2010	2020	1930	2055	0.89
18 Mar	1620	1610	1600	1630	0.36

It is pointed out that because of the usually gradual onset of geomagnetic pulsations and cosmic noise absorption events in the morning sector, there are uncertainties in the estimates for onset times for these

events of the order of five minutes.

From examination of onset times, it can be seen that Pi events, which are accompanied by a CNA event, can commence quite late in the morning i.e. as late as 0900 L time at Macquarie Island. It is inferred that during polar substorms, Pi geomagnetic pulsations and cosmic noise absorption should be observed over quite a wide span of longitude of the auroral zone in the morning sector. The length of this span may be variable, depending on the level of planetary magnetic disturbance. For periods of moderately high planetary magnetic disturbance (Kp > 3), Pi activity accompanied by CNA was observed to end at Macquarie Island as late as 1300 L time.

6.2.2 *Examples of morning Pi geomagnetic pulsations and cosmic noise absorption events*

An example of morning Pi geomagnetic pulsations, recorded on 12 January 1968 is given in Figure 6-2. Two events, well separated in time were recorded. A polar substorm began around 1500 U.T. At Abisko, which was in the afternoon sector, a positive bay in H began at that time. At Macquarie Island, a SVA event and a gradual Pi enhancement started at the estimated substorm onset time. The typical magnetic changes observed in the morning sector of the auroral zone during a polar substorm, i.e. a negative bay in H, with slow onset, was recorded at Macquarie Island. A negative bay was also recorded at Barrow. By 1730 U.T., polar substorm activity had virtually ceased.

Another polar substorm began at about 1810 U.T. Abisko was in the late evening sector at this time and polar magnetic substorm activity began

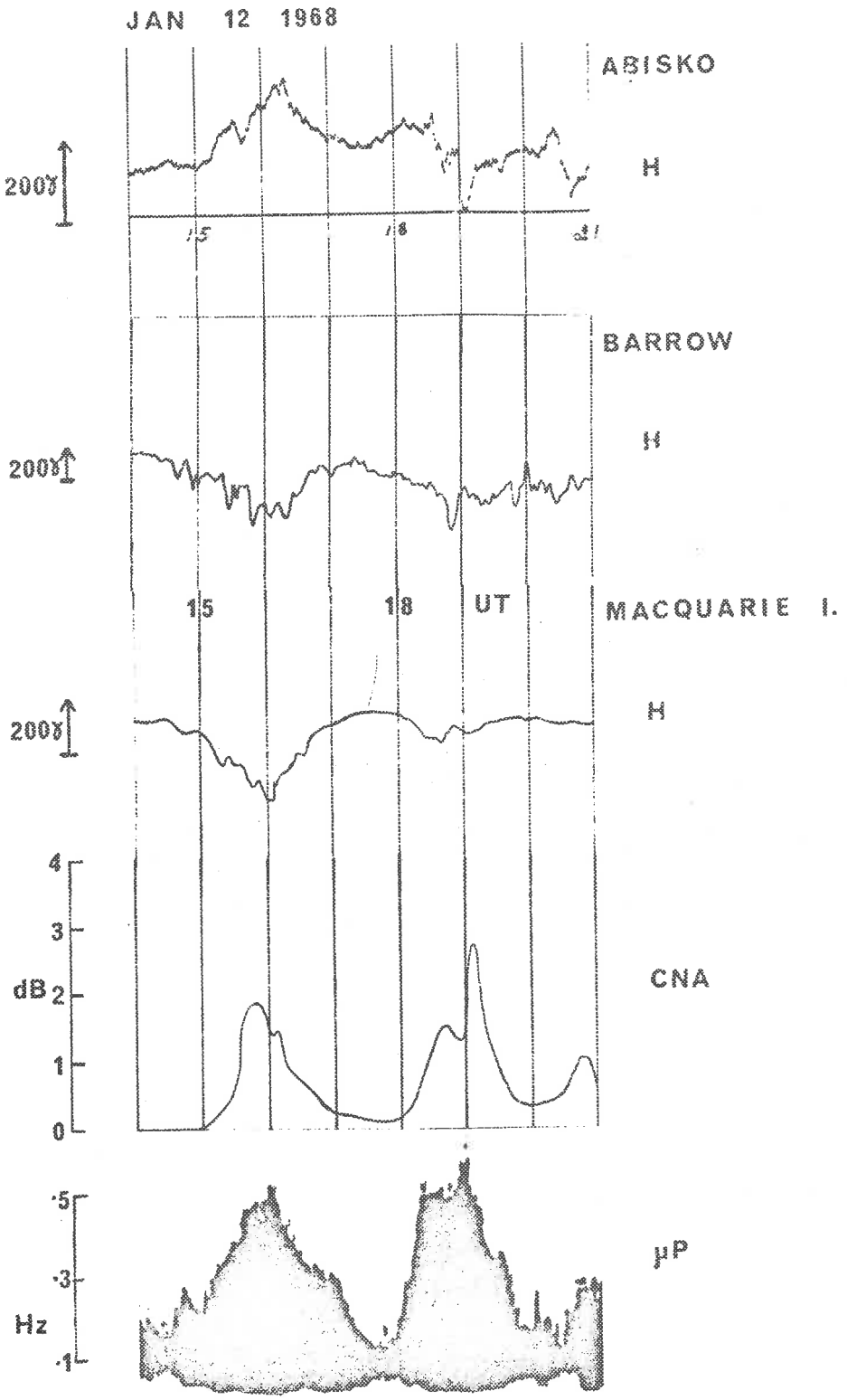

Figure 6-2. Magnetometer records for Abisko, Barrow and Macquarie Island; cosmic noise absorption and geomagnetic pulsations sonagraph records for Macquarie Island for the period 1400 to 2100 U.T. on 12 January 1968.

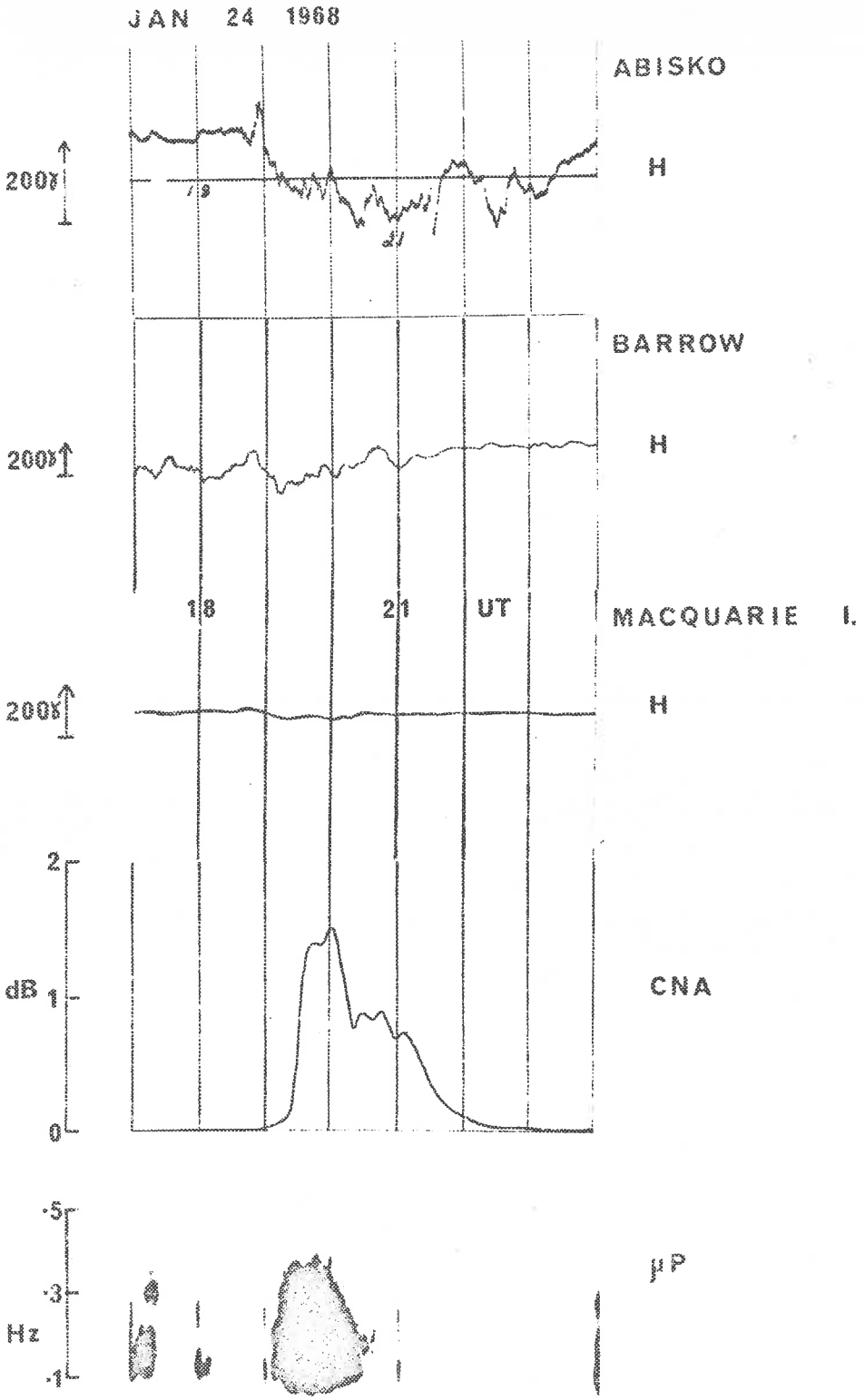

Figure 6-3. Magnetometer records for Abisko, Barrow and Macquarie Island; cosmic noise absorption and geomagnetic pulsations sonagraph records for Macquarie Island for the period 1700 to 2400 U.T. on 24 January 1968.

there with a small decrease in magnetic H component near 1810 U.T. Pi geomagnetic pulsations and an SVA event began at Macquarie Island at the estimated substorm onset time. A negative bay in H was recorded at Barrow and Macquarie Island.

A typical characteristic of negative bays recorded at Macquarie Island, during the morning hours, can be seen in Figure 6-2. The intensity of the negative bay which started late in the morning, was less than the intensity of the negative bay which started earlier. In general maximum intensity of negative bay disturbance decreases with time during the morning hours at Macquarie Island.

Another example of morning activity is illustrated in Figure 6-3. Estimated substorm onset time is 1845 U.T. Near that time, a sudden increase in magnetic H component began at Abisko; a negative bay began at Barrow and a weak negative bay began at Macquarie Island. At Macquarie Island, a slowly varying absorption event began at 1900 U.T. and a Pi event began at 1910 U.T.

6.2.3 *Character of morning geomagnetic pulsations events*

Hartz and Brice (1967) have suggested that continuous (Pc) geomagnetic pulsations, as well as slowly varying riometer absorption, should be associated with "drizzle-type" particle precipitation. Pc geomagnetic pulsations are continuous pulsations having a regular nature (Jacobs et al, 1964). However, geomagnetic pulsations recorded at Macquarie Island, during polar substorms, did not have the characteristics of the Pc-type; rather they had the characteristics of the Pi(c) subtype, proposed by Heacock (1967a), which are

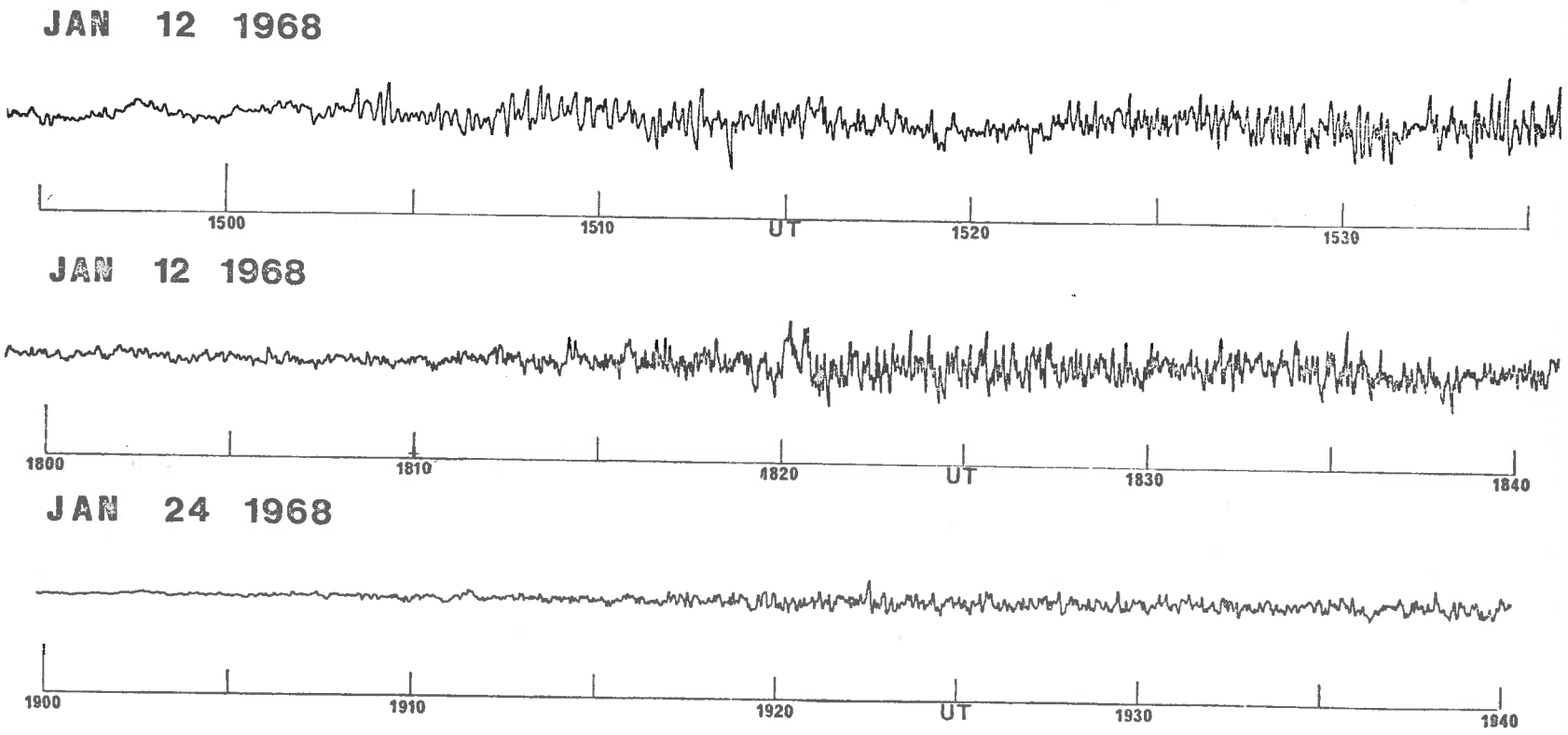

Figure 6-4. Examples of morning Pi (c) geomagnetic pulsations recorded at Macquarie Island.

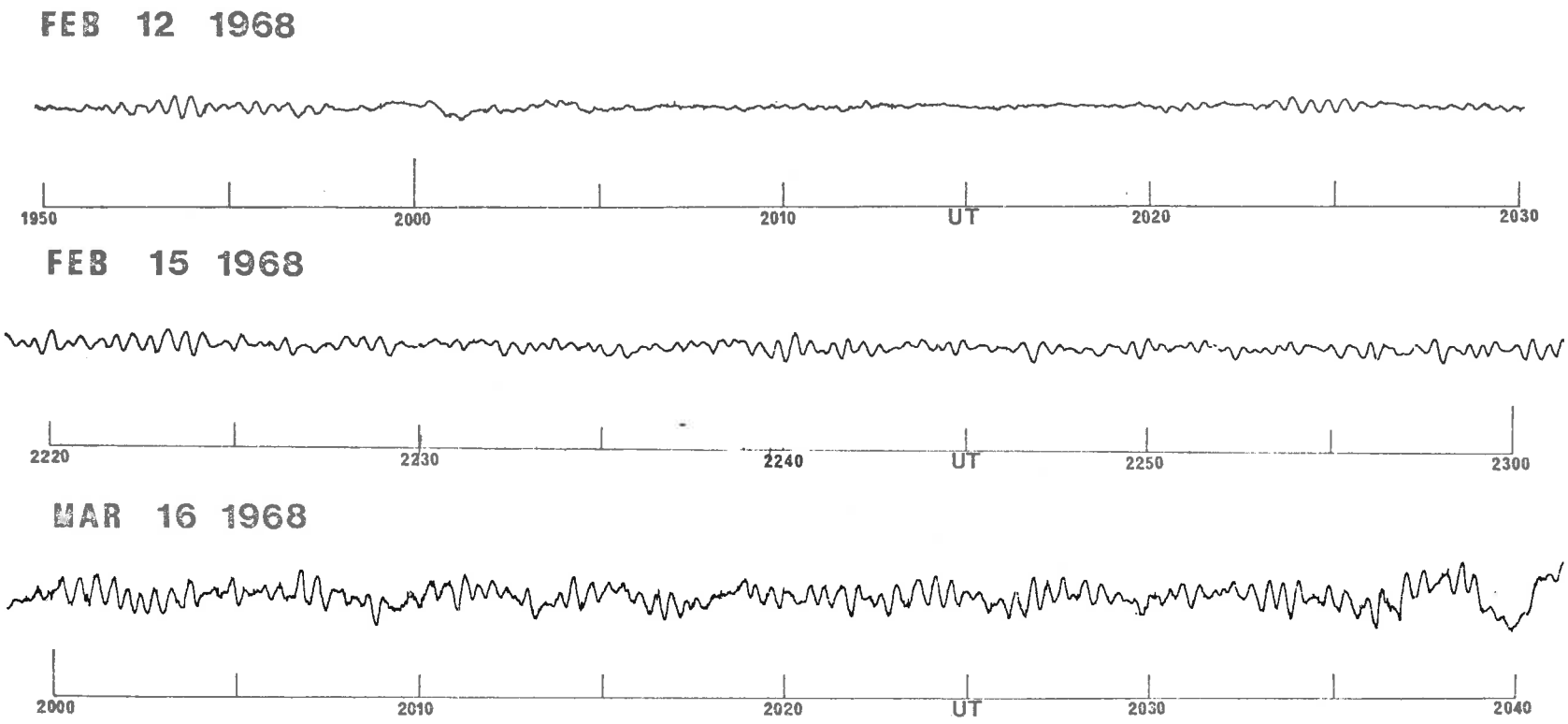

Figure 6-5. Examples of Pc 3 geomagnetic pulsations recorded at Macquarie Island.

continuous pulsations with an irregular nature.

Chart records for Pi(c) geomagnetic pulsations events discussed in the previous section are illustrated in Figure 6-4. The irregular nature and gradual changes in amplitude, the characteristics of morning geomagnetic pulsations at Macquarie Island during polar substorms, are evident in all examples given. In Figure 6-5, chart records of Pc 3 geomagnetic pulsations, recorded at Macquarie Island during January to March 1968, are reproduced to allow comparison of Pi(c) and Pc-type geomagnetic pulsations.

McPherron et al (1968) report that at Flin Flon (Canada), band-limited irregular (Pi 1) geomagnetic pulsations of 5- to 10- second period are observed during the morning hours (0200 to 1000 local time), during polar substorms. Troitskaya et al (1968) report the observation of rapid, irregular geomagnetic pulsations during the morning hours at the subauroral station, Sogra. These probably occurred during polar substorms as there was intense geomagnetic disturbance.

Fast time variations in frequency content were rarely observed in sonagrams of Pi geomagnetic pulsations recorded during the morning to noon hours at Macquarie Island (see Chapter 2). During polar substorms, Pi(c) geomagnetic pulsations and slowly varying absorption events are observed in the morning sector. It is concluded that it is the Pi(c) geomagnetic pulsations i.e. continuous, irregular pulsations in the geomagnetic field, not the Pc geomagnetic pulsations, which can be associated with "drizzle-type" particle precipitation.

6.2.4 *Pi 2 activity in the morning sector*

A study was made of spectral characteristics, over the frequency

band from .004 to .056 Hz, of geomagnetic pulsations recorded at Macquarie Island during the mornings of 24 January 1968 and 19 March 1968; a polar substorm occurred on each of these mornings. Pi 2 activity was recorded during an initial period of each substorm. A discussion of spectral analysis computations, which were carried out for this study, is given in Appendix B.

On 24 January 1968, a Pi event and a negative bay in magnetic H component, with a slow onset began at about 1500 U.T. at Macquarie Island, indicating the commencement of a polar substorm at about that time. From the College riometer record (see "High Latitude Geophysical Data", College, Alaska for the period January to March 1968), it was evident that a SVA event began at College at about 1515 U.T.; a maximum absorption of approximately 1.1 dB was recorded during this event, at 1540 U.T.

A digital sonagram for 24 January 1968 is given in Figure 6-6. Rostoker (1968) has put forward evidence suggesting that the geomagnetic bay disturbances which accompany polar substorms may have two phases of activity i.e. activity starts with a precursor or "trigger" bay, which is accompanied by a Pi 2 pulsation train; from ten to thirty minutes after onset of the trigger bay, the main bay disturbance may begin. The distinct peak in power on the sonagram in Figure 6-6, starting at about 1445 U.T., was due to a Pi 2 pulsation train with a frequency of .012 Hz. This pulsation train may have accompanied a trigger bay.

After polar substorm onset, i.e. after 1500 U.T., pulsation in the Pi 2 frequency band was a dominant feature of Pi activity. This is evident from the time-averaged power spectra for the two half-hour time intervals

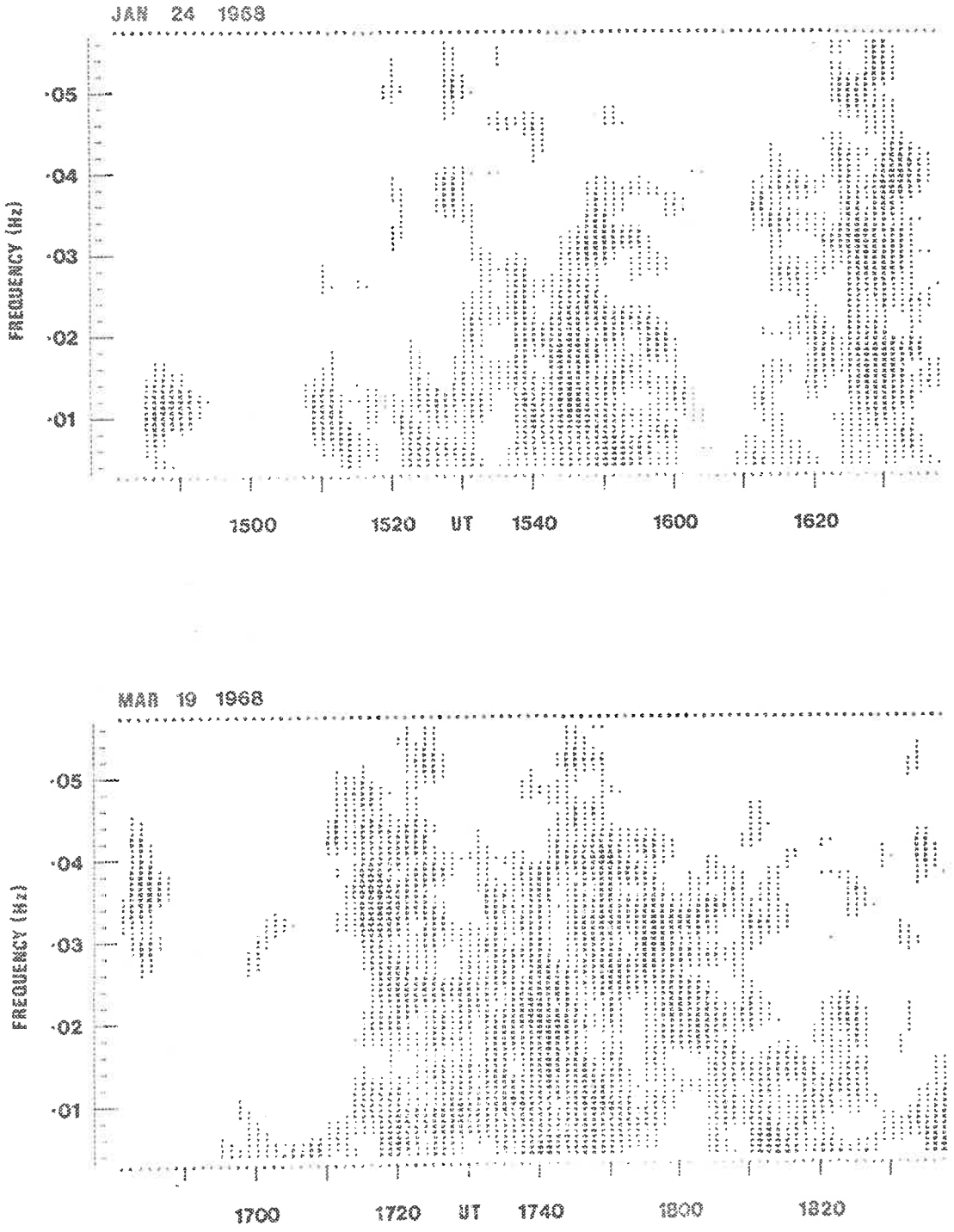

Figure 6-6. Digital sonagrams of geomagnetic pulsations recorded at Macquarie Island on 24 January 1968 and 19 March 1968.

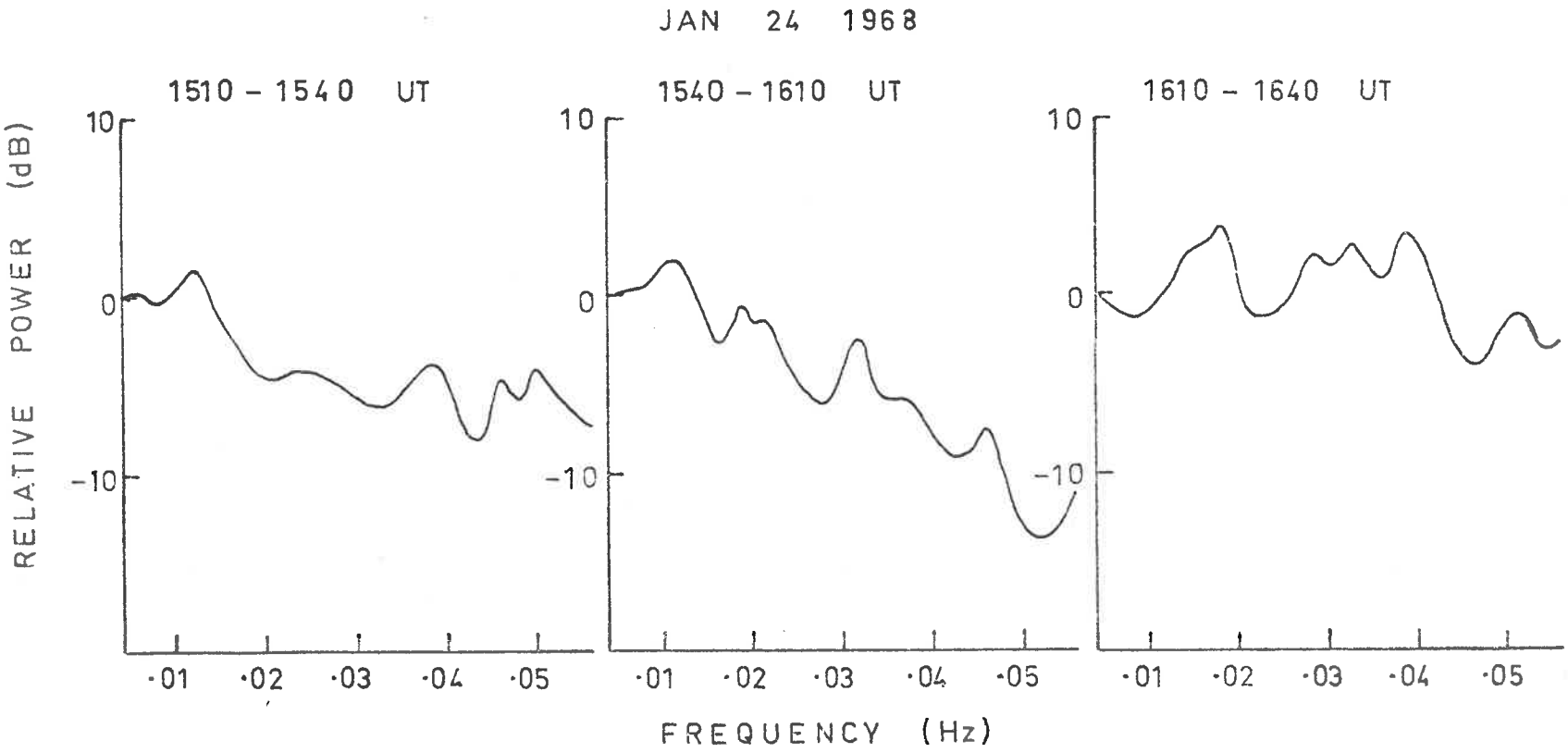

Figure 6-7. Time-averaged power spectra for geomagnetic pulsations recorded at Macquarie Island on 24 January 1968.

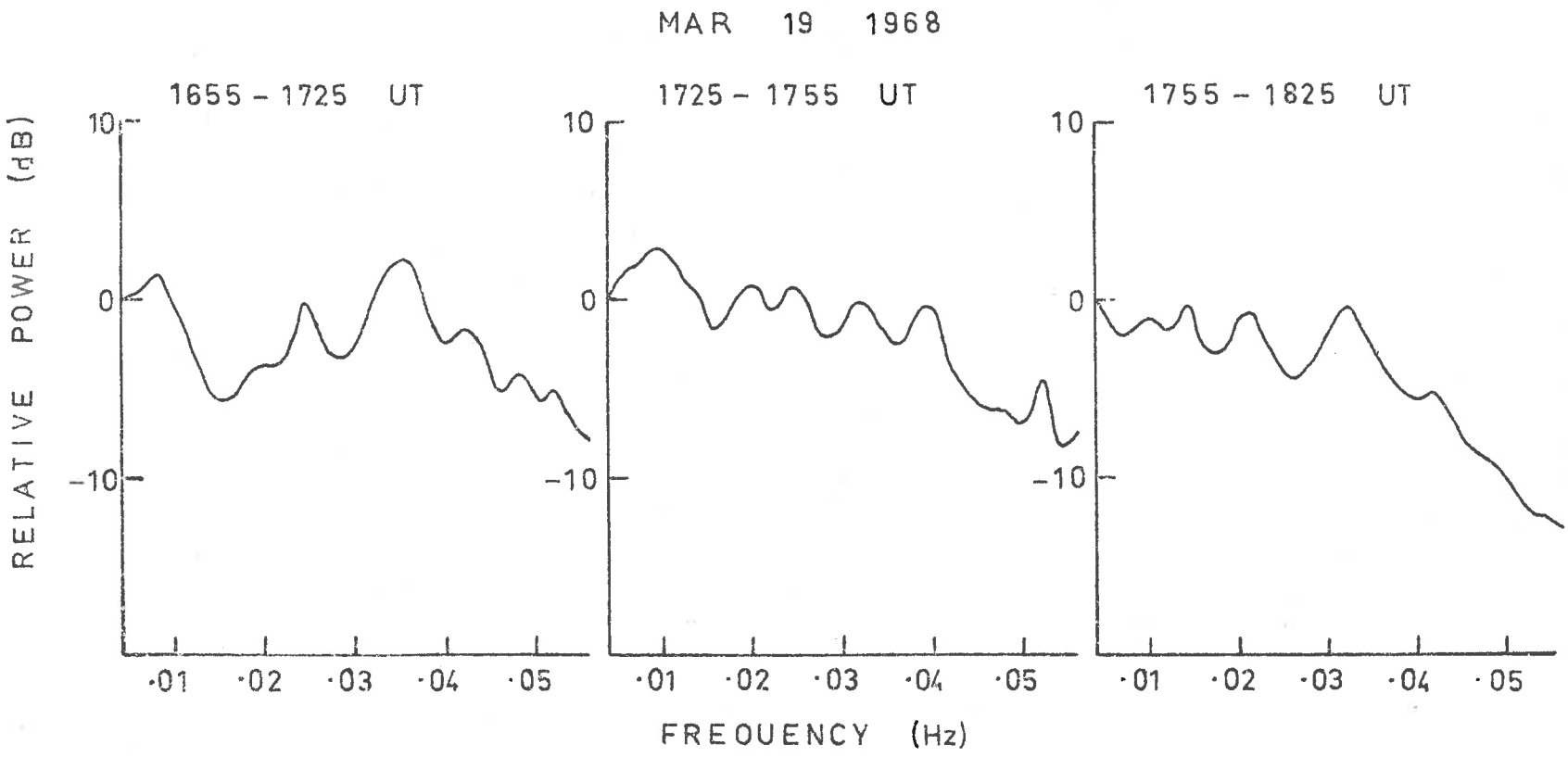

Figure 6-8. Time-averaged power spectra for geomagnetic pulsations recorded at Macquarie Island on 19 March 1968.

between 1510 and 1610 U.T. (see Figure 6-7), where a common peak at a frequency of .012 Hz can be seen. Also, pulsation at higher frequencies occurred throughout the Pi event; this is evident from the sonagram and the time-averaged power spectra for half-hour intervals between 1540 and 1640 U.T., where peaks in power near frequencies of 0.02 Hz and in the Pi 1 frequency band can be seen.

A digital sonagram of geomagnetic pulsations, recorded on the morning of 19 March 1968, is given in Figure 6-6. Around 1700 U.T., a polar substorm began; a negative bay, with slow onset, began at about that time at Macquarie Island. At approximately 1710 U.T., a Pi enhancement was recorded and a SVA event began. A maximum in absorption of approximately 1.3 dB was recorded at 1734 U.T. Geomagnetic pulsations, recorded during this morning, showed complex frequency-time behaviour; many peaks in power occurred at frequencies in the Pi 1 and Pi 2 bands. This was evident from the time-averaged power spectra for half-hour time intervals between 1655 and 1825 U.T. (see Figure 6-8). During the first hour of the substorm, pulsation in the Pi 2 frequency band was evident on the sonagram. Also, time-averaged power spectra for the two half-hour time intervals between 1655 and 1755 U.T. show a common peak in power at a frequency of approximately .009 Hz.

6.3 Auroral Luminosity Pulsations

As an auroral zone station moves from the midnight sector towards the dawn meridian, the characteristics of auroral activity, as seen from that station, gradually change. Bright and rapidly moving forms in auroral bulges which develop after onset of polar substorms are most

commonly seen in the midnight hours. Later, in the morning, glows and diffuse bands are commonly observed.

Heppner (1954) reports that at College (Alaska), homogeneous arcs are observed early in the evening, rayed arcs and bands later in the evening, breakup of aurorae into active forms near midnight and diffuse, pulsating patches or arcs are observed in the morning hours till dawn.

Pulsating aurora are most commonly observed in the morning hours. In a study of pulsations in the intensity of the λ3914 Å (N_2^+) emission at College, Campbell and Rees (1961) found that 6-10 second period pulsations occur throughout the morning hours until dawn. Campbell and Leinbach (1961) found that λ3914 Å luminosity pulsations and cosmic noise absorption amplitudes build up rapidly during the evening, reaching a broad maximum in the morning hours.

Omholt and Berger (1967) in a study of luminosity pulsations in the λ5577 Å [OI] emission at Tromso, found that almost all pulsating aurorae occurred after magnetic midnight, with a pronounced peak in activity at about 04 hours geomagnetic time.

Kvifte and Pettersen (1967), from a study conducted at Tromso, find that pulsating aurorae occur mainly near the equatorward edge of the auroral oval in the morning sector.

6.3.1 *Auroral luminosity pulsations recorded in the morning sector of the auroral zone during polar substorms*

Observations of pulsations in luminosity due to the λ4278 Å (N_2^+) emission were made at Macquarie Island during the period January to March,

1968. The photometer was directed toward geographic zenith and was operated during periods when the sky was clear in the zenith.

Enhancements in cosmic noise absorption and Pi geomagnetic pulsations, recorded during periods of photometric observation, were generally accompanied by auroral luminosity pulsations during the morning hours. Examples of auroral luminosity pulsations starting during the early stages of a polar substorm, will be discussed in this section.

The first example is for 4 February 1968. The magnetometer record for Barrow (Alaska), together with riometer record and geomagnetic pulsations sonagram for Macquarie Island, are given in Figure 6-9. At the estimated polar substorm onset time, 1545 U.T., a negative bay in magnetic H component commenced at Barrow and also at Yakutsk and Macquarie Island. A slowly varying absorption event and a Pi(c) event also began at approximately 1540 U.T. Chart records of geomagnetic and λ4278 Å luminosity pulsations recorded at Macquarie Island are given in Figure 6-10. The gradual nature of the onset of the Pi(c) event can be clearly seen.

After 1552 U.T. auroral luminosity pulsations were recorded. In general, the pulsations had a one-sided character i.e. consisting of luminosity "spikes" superimposed on a slowly varying background of luminosity. Typical spacing between luminosity spikes was ∿ 8 seconds.

During the pulsations event, a striated band formation was observed overhead. All-sky pictures are reproduced in Figure 6-11. At 1534 U.T., a glow covered most of the southern sky. Between 1540 and 1550 U.T., rapidly moving clouds obscured the photometer field of view. At 1552 U.T.,

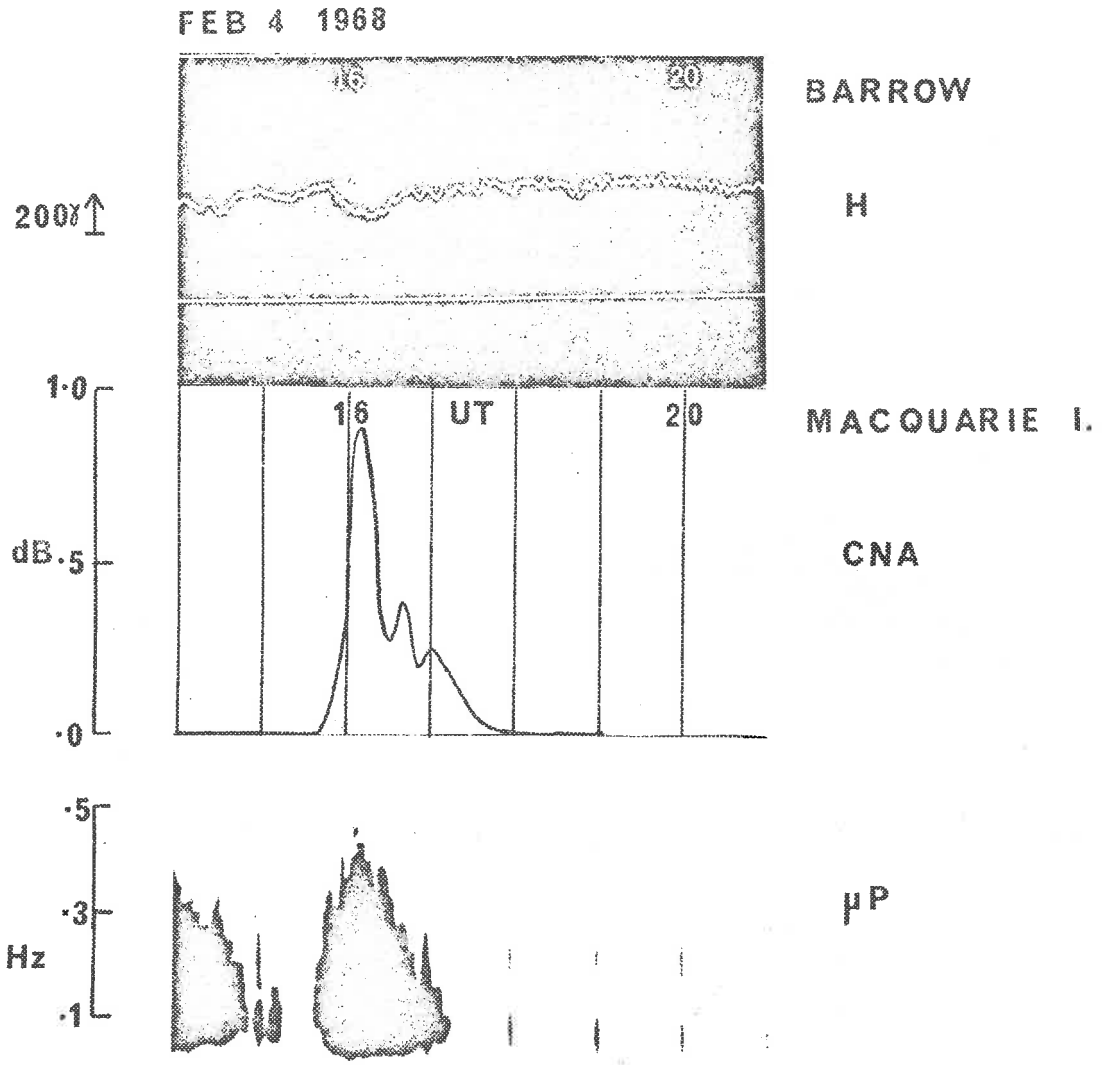

Figure 6-9. Magnetometer record for Barrow; cosmic noise absorption and geomagnetic pulsations sonagraph records for Macquarie Island for the period 1400 to 2100 U.T. on 4 February 1968.

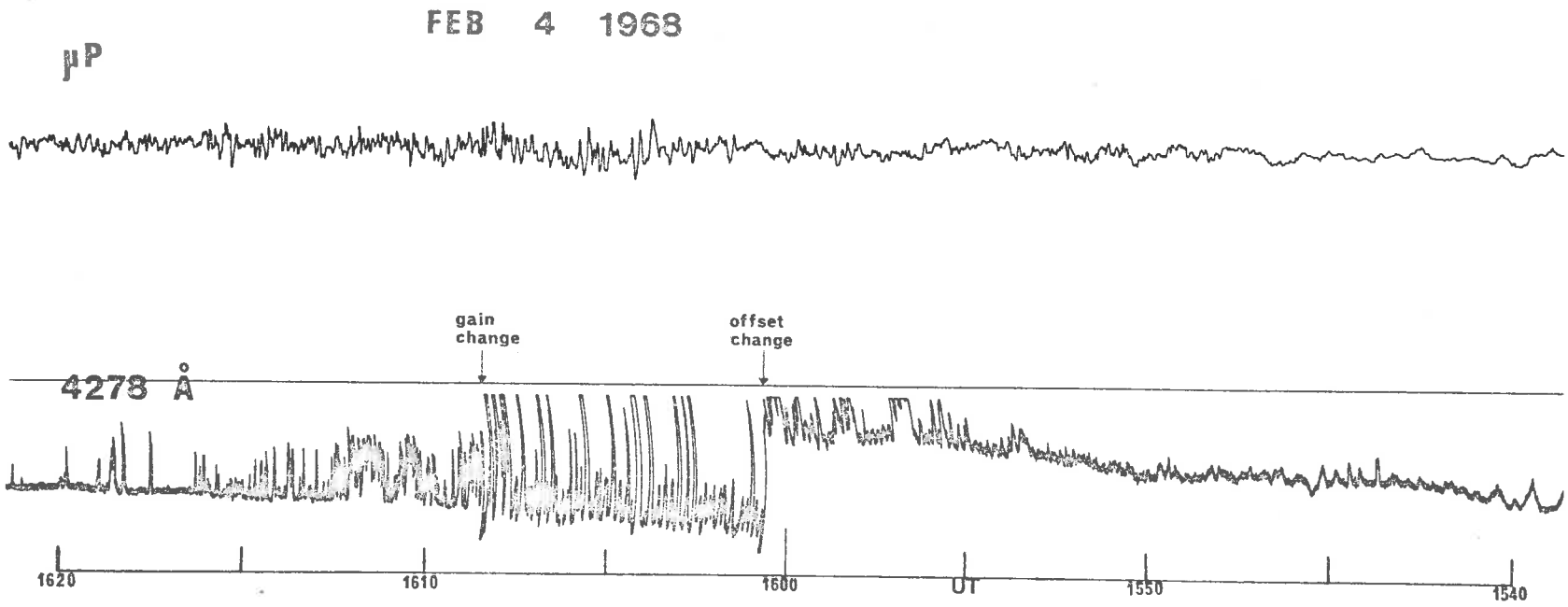

Figure 6-10. Simultaneous λ 4278 Å luminosity and geomagnetic pulsations recorded at Macquarie Island on 4 February 1968.

Fig. 6-11 All-sky photographs from Macquarie Island for 4 February 1968 and 3 March 1968.

MACQUARIE ISLAND

FEB 4 1968

1534 UT 1552 1558 1600 1604

MAR 3 1968

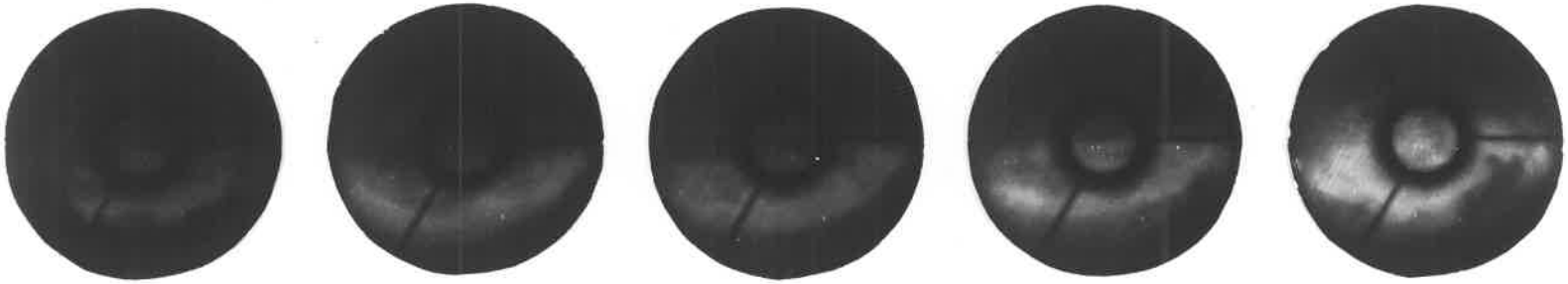

1550 1610 1613 1620 1630

the sky was clear again. By 1558 U.T., aurora over most of the southern sky had become brighter. From a visual observation, at 1558 U.T., it was noted that a striated band formation could be seen overhead.

On 3 March 1968, a polar substorm began at 1550 U.T. Magnetic H component for Barrow, together with riometer records and geomagnetic pulsations sonagram for Macquarie Island are given in Figure 6-12. At 1550 U.T., a positive bay began at Abisko, which was in the afternoon sector at the time. A negative bay began at 1550 U.T. at Barrow and Macquarie Island. Also, slowly varying absorption and an enhancement in Pi activity began at Macquarie Island at the estimated substorm onset time.

A section of the λ4278 Å luminosity pulsations record is given in Figure 6-13. After 1550 U.T., pulsations in luminosity, gradually increasing in amplitude and having a one-sided character were observed. After 1610 U.T., luminosity pulsations were particularly intense and had typical spacings near 8 seconds.

The all-sky camera record for Macquarie Island is given in Figure 6-11. At 1550 U.T., a glow was observed over most of the southern sky. Between 1610 and 1630 U.T., a broad band could be seen moving equatorward. By 1620 U.T., the northern edge of this band had reached the geographic zenith at Macquarie Island. Intense λ4278 Å luminosity pulsations were recorded at this time.

6.3.2 *Geomagnetic pulsations and cosmic noise absorption during periods of photometric observation*

Generally, when aurora was visible in the zenith at Macquarie Island,

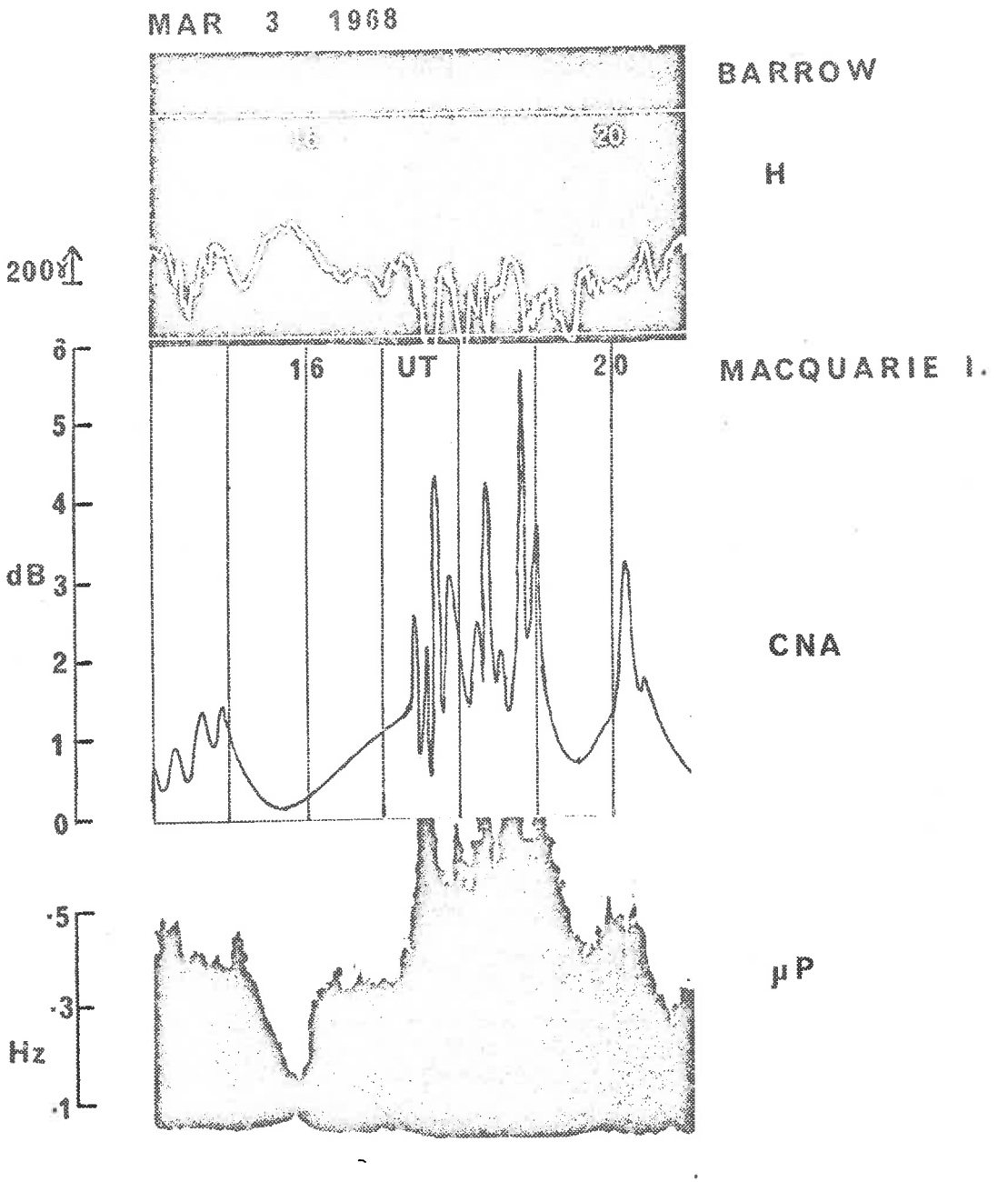

Figure 6-12. Magnetometer record for Barrow; cosmic noise absorption and geomagnetic pulsations sonagraph record for Macquarie Island for the period 1400 to 2100 U.T. on 3 March 1968.

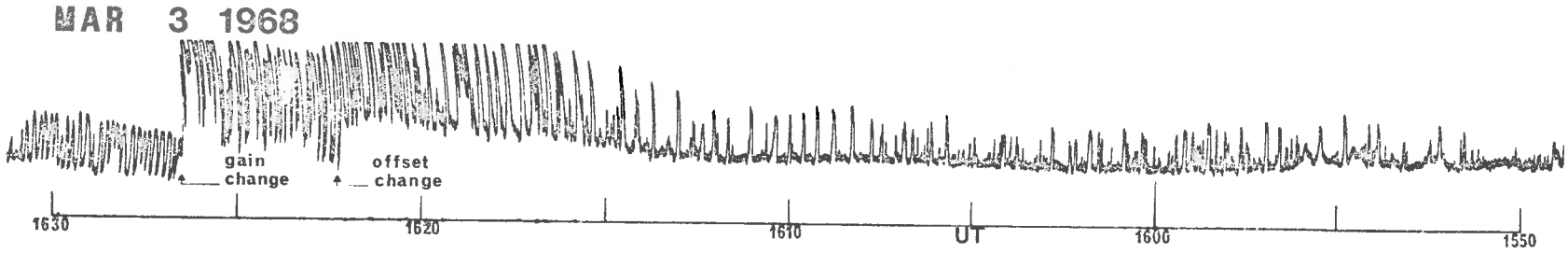

Figure 6-13. λ 4278 Å luminosity pulsations recorded at Macquarie Island on 3 March 1968.

pulsations in auroral luminosity were recorded. Usually, these pulsations were irregular; typical time intervals between luminosity peaks were between five and fifteen seconds. When the sky was clear of cloud, during magnetically quiet periods, luminosity in the λ4278 Å band usually varied slowly over time intervals with durations of the order of a few minutes.

The total number of minutes observing time for each hour (U.T.) interval is given in Figure 6-14. The total time that auroral luminosity pulsations, with period less than one minute, were recorded is also given in Figure 6-14.

Auroral Luminosity Pulsations (abbreviated A.L.P.) were normally recorded whenever Pi geomagnetic pulsations were recorded. The total time that Pi geomagnetic pulsations were recorded during periods of photometric observation for each hour (U.T.) interval is given in Figure 6-15. The total time that A.L.P. were accompanied by Pi geomagnetic pulsations is also given in Figure 6-15. Over the time interval 1400 to 1800 U.T., 91% of all A.L.P. recorded were accompanied by Pi geomagnetic pulsations.

It was also found that cosmic noise absorption events were normally accompanied by A.L.P. The total time that detectable cosmic noise absorption was recorded for each hour (U.T.) interval is given in Figure 6-16. The total time that A.L.P. were accompanied by detectable cosmic noise absorption for each hour (U.T.) time interval is also given. For the period 1400 - 1800 U.T. (early morning to mid-morning at Macquarie Island), auroral luminosity pulsations were observed for 95% of the time that detectable cosmic noise absorption was recorded during periods of photometric observation.

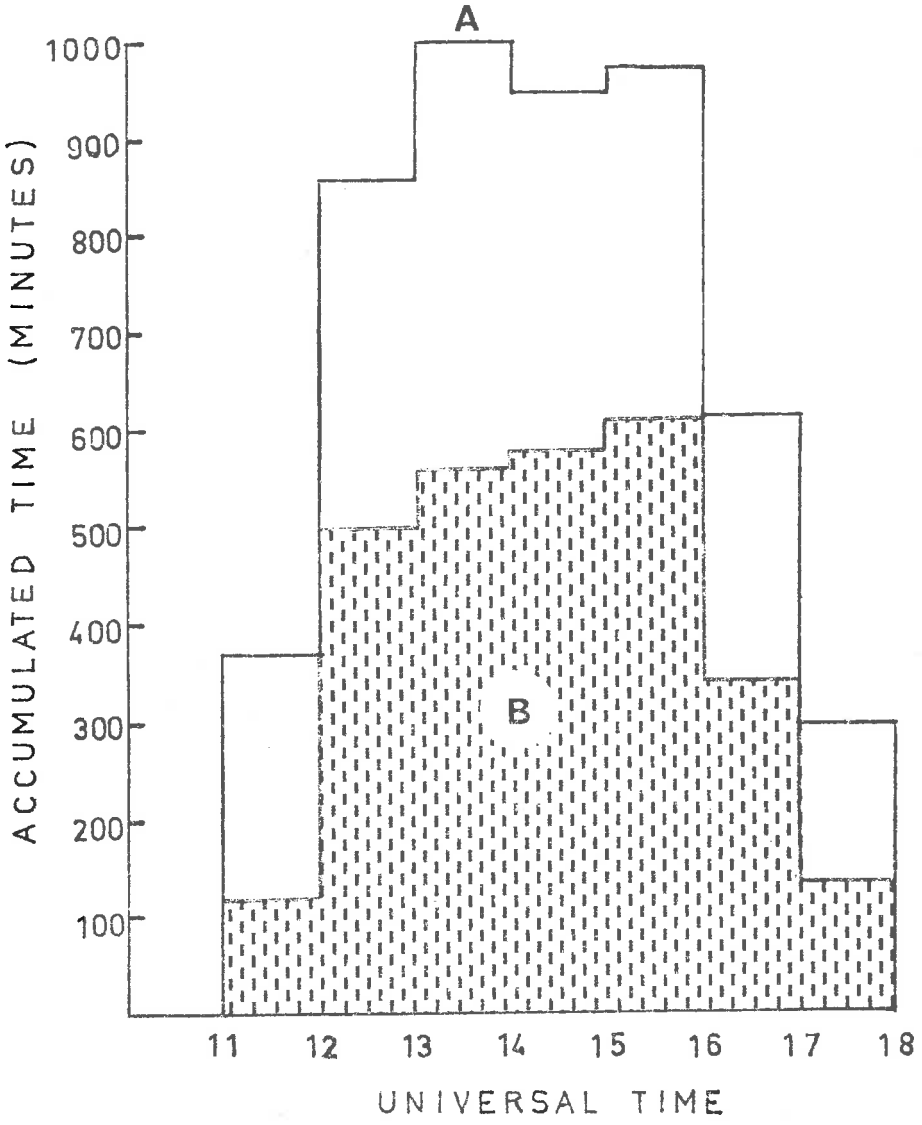

Figure 6-14. Histogram A: Total photometric observation time for January to March 1968 at Macquarie Island.
Histogram B: Total time that auroral luminosity pulsations were observed for January to March 1968 at Macquarie Island.

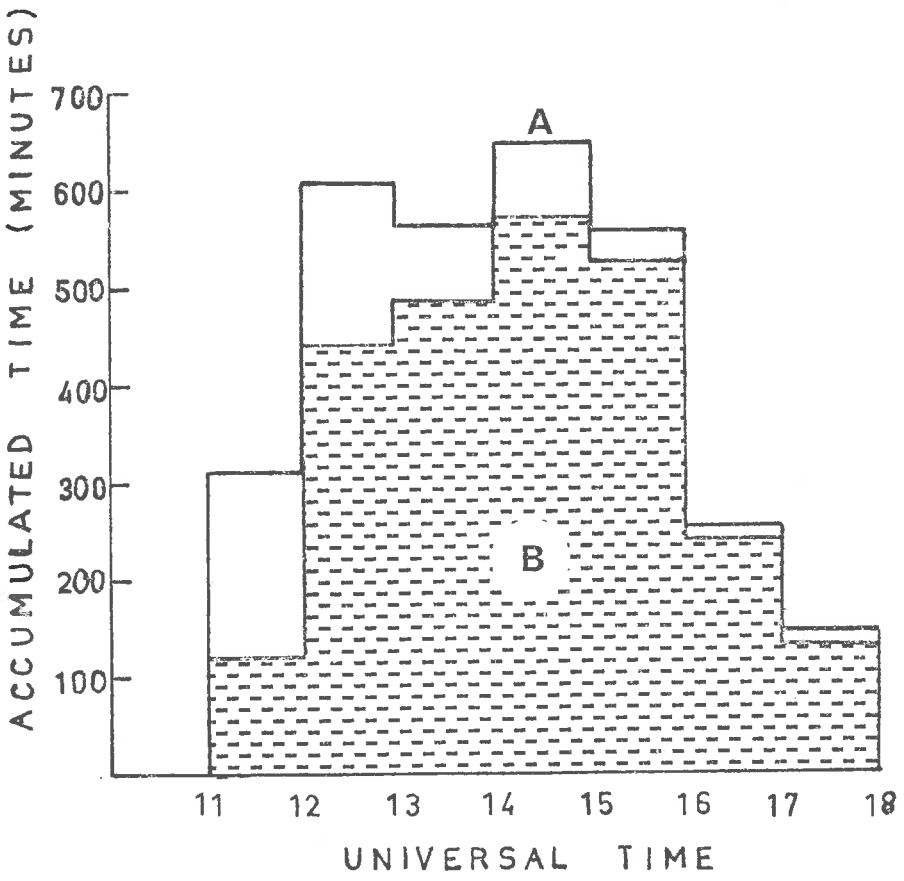

Figure 6-15. Histogram A: Total time that Pi activity was recorded during periods of photometric observation for January to March 1968 at Macquarie Island.
Histogram B: Total time that Pi activity and auroral luminosity pulsations were recorded simultaneously at Macquarie Island for January to March 1968 at Macquarie Island.

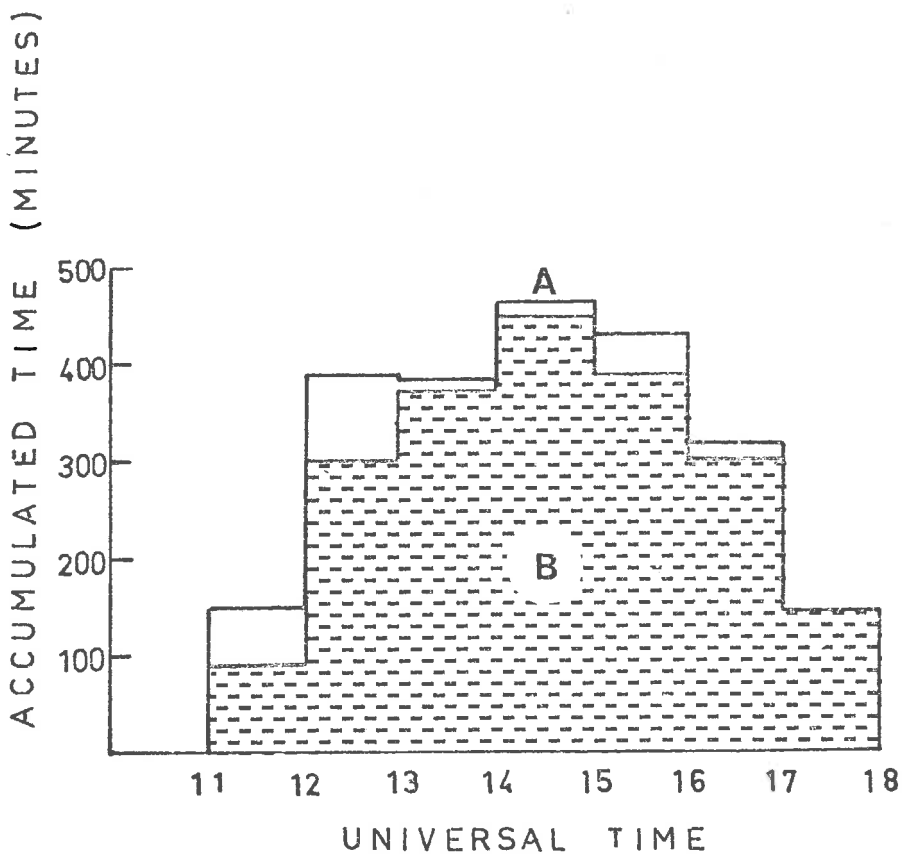

Figure 6-16. Histogram A: Total time that detectable CNA was recorded during periods of photometric observation for January to March 1968 at Macquarie Island. Histogram B: Total time that detectable CNA and auroral luminosity pulsations were recorded simultaneously at Macquarie Island for January to March 1968.

The close association between occurrence of auroral luminosity pulsations and both CNA and Pi activity recorded at Macquarie Island in the early morning hours shows that in the morning sector, pulsating aurora occur mainly during polar substorms.

Workers using balloon-borne instrumentation near geomagnetic latitudes of 65°, find that electron fluxes recorded during the morning hours often pulsate; Bewersdorff et al (1968) at Kiruna (Sweden), Barcus and Rosenberg (1966) at College (Alaska) and Brown et al (1965) at Macquarie Island, report that pulsations in the 5-15 second period range are usually observed during electron precipitation events during the morning hours.

6.4 Cosmic Noise Absorption Pulsations

Reid (1967) has reported the observation, at Macquarie Island, of CNA pulsations which were distinguished by short rise time and relatively longer decay time and which were always accompanied by Pi 2 pulsations. The example of a Pi event accompanying CNA pulsations given by Reid belongs to the Pi(c) subtype of Pi geomagnetic pulsations. CNA pulsations having a similar nature to the type described by Reid were observed during Pi(c) events during the morning hours. Examples from 15 February 1968 and 15 March 1968 are given in Figures 6-17 and 6-18.

Both sequences of CNA pulsations illustrated in Figures 6-17 and 6-18 were recorded during polar substorms. On 15 February, a strong negative bay began at Abisko at 1640 U.T., the estimated substorm onset time. Negative bays also began at Barrow and Macquarie at that time. On 15 March, negative bays began at Abisko, Barrow and Macquarie at 1820 U.T., which was

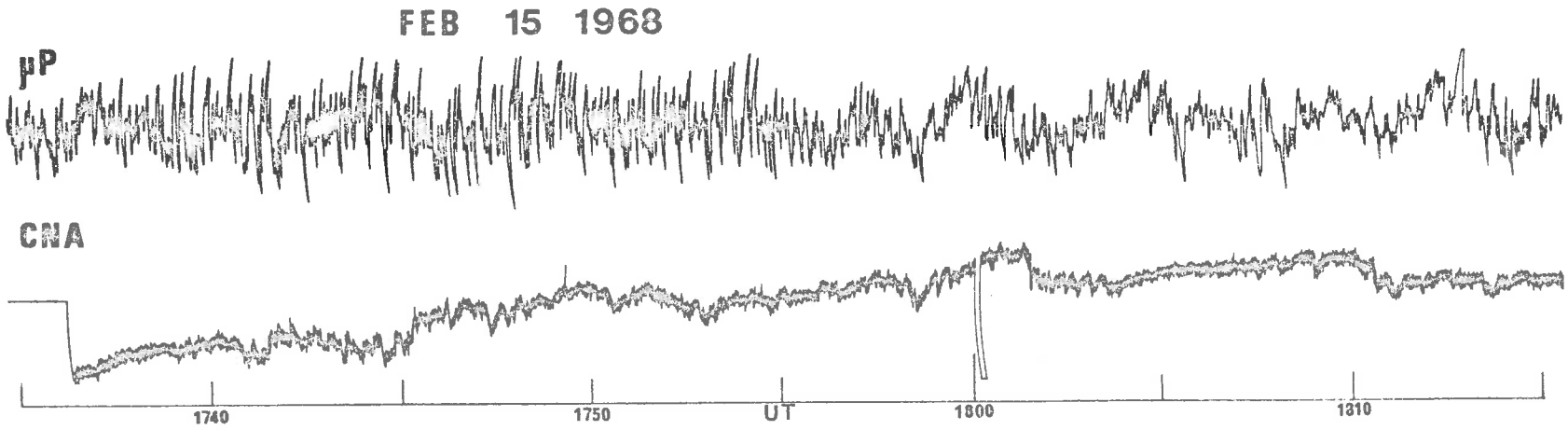

Figure 6-17. Simultaneous CNA and Pi (c) pulsations recorded at Macquarie Island on 15 February 1968.

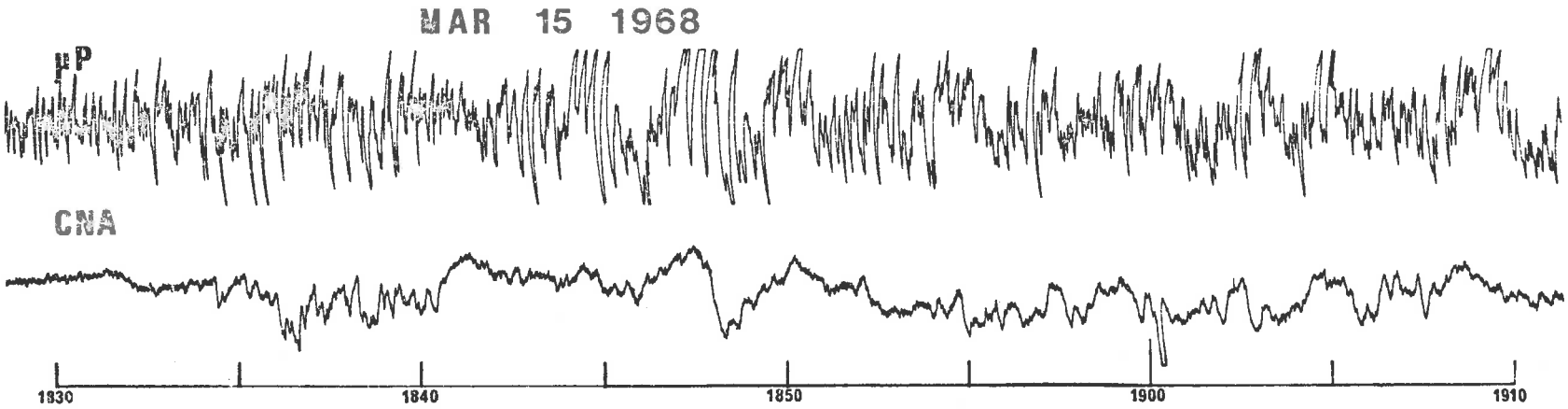

Figure 6-18. Simultaneous CNA and Pi (c) pulsations recorded at Macquarie Island on 15 March 1968.

the estimated substorm onset time.

6.5 Variation of the Absorption Region in the Morning Sector During Polar Substorms

Dubatovko et al (1968) have shown that maxima of absorption events at College show a consistent time lag relative to absorption maxima at Murmansk consistent with an injection of electrons near the midnight meridian which is followed by drift of these particles in the magnetosphere toward the noon meridian. Hargreaves (1967), using data from the riometer station pairs Great Whale River - Reykjavik and Great Whale River - College, has shown that in the morning sector of the auroral zone, cosmic noise absorption regions show an eastward movement with typical velocities of the order of 4° of longitude per minute.

Jelley and Brice (1967) have made a study of time relationships between CNA events at Kiruna and strong rapid onset absorption events at Cape Jones and Churchill. Substorm onset times were estimated from onset times of rapid onset absorption events at Cape Jones and Churchill. They found that most CNA event onset times at Kiruna followed the estimated substorm onset times; some Kiruna CNA onset times however, preceded the estimated substorm onset time.

It is pointed out that significantly erroneous estimates for substorm onset time can be obtained using the riometer record for any station if that station is not close to the midnight sector of the auroral oval. For the situation where Churchill is in the evening sector while Kiruna is in the morning sector at substorm onset time, it is quite possible for

absorption to begin at Kiruna before absorption begins at Churchill. A rapid onset absorption event will be recorded at the evening sector station, Churchill during transit of a westward travelling surge at that station (see Chapter 4). If Kiruna was closer to the midnight meridian than Churchill, absorption would often commence at Kiruna before absorption onset at Churchill after substorm onset time.

Good estimates for substorm onset times could be obtained from an east-west chain of auroral zone magnetometer stations. When onset to polar magnetic substorm activity at an auroral zone station is abrupt and thus clearly distinguishable, the onset time for the polar substorm should be obtainable with reasonable accuracy.

Hargreaves (1968) in a study of riometer records from the Antarctic stations Eights, Byrd and South Pole, found from 0400 - 1200 U.T. (midnight till mid-morning at those stations), absorption events move away from the auroral zone in both the poleward and equatorward directions. Bewersdorff et al (1968) have observed the equatorward movement of absorption in the morning sector using balloons. They found that during a typical SVA event, electron precipitation starts north of L = 6.5 and spreads southward with speeds of about 500 metres per second.

It should be remembered however, that the position of the auroral absorption zone is dependent upon Kp. When the level of planetary magnetic disturbance increases, this zone moves equatorward (Hargreaves, 1966).

6.6 Discussion

In the morning sector of the auroral zone, onset of a polar substorm

is not usually marked by abrupt enhancements of the various types of activity i.e. auroral luminosity, cosmic noise absorption and geomagnetic pulsations. After onset of a polar substorm, Pi(c) geomagnetic pulsations will be observed in the morning sector, associated with the precipitation of particles which give rise to slowly varying absorption events.

It was found that pulsations in the λ4278 Å auroral emission, with typical pulsation periods of from 5 to 15 seconds, were closely associated with geomagnatic pulsations and cosmic noise absorption during the morning hours. This indicates that precipitating electron fluxes, in the morning sector of the auroral zone, usually pulsate during polar substorms.

Berkey (1968) reports that a typical absorption event recorded at College, during the morning hours, was accompanied by pulsating and patchy aurora. Absorption to luminosity ratios for these events indicated hard electron energy spectra. Hartz and Brice (1967) have shown, using Alouette satellite data compiled by McDiarmid and Burrows (1964), that the occurrence of auroral absorption, as a function of geomagnetic latitude and time, is very similar to the occurrence of fluxes of precipitated electrons, with energies greater than 40 keV, which are in excess of 1.5×10^4 per cm^2 per sec.

Johnson et al (1966), using data from a low-altitude polar-orbiting satellite have found two distinct dayside electron precipitation zones. The electrons precipitating into the higher latitude zone were soft i.e. electron energies were mostly below 10 keV. The electrons precipitating into the lower latitude zone, most of which was located equatorward of the daytime boundary of trapping (at a geomagnetic latitude of about 75°), were found

to have a significant fraction of the energy flux above 25 keV. This lower latitude zone can be identified with the auroral absorption zone (c.f. O'Brien, 1967).

The auroral absorption zone covers several degrees in latitude and is usually centred on a geomagnetic latitude between 64° and 68° (Hargreaves, 1969). It probably coincides with the auroral oval in the midnight sector. Such a location of the auroral absorption zone is consistent with the hypothesis that electron precipitation within that zone is directly related to the longitudinal drift of particles from a source region in the midnight sector.

Energies for electrons drifting in the morning sector can be estimated from observed speeds of eastward movement of auroral absorption patterns. Hargreaves (1967) finds values ranging, typically, from 40 keV to 120 keV. Dubatovko et al (1968) estimate an average energy near 85 keV. They suggested that this average electron energy in the morning sector is evidence for the presence of an east to west directed magnetospheric electric field. Electrons drifting eastward in such a field would gain energy; they would also precipitate into the atmosphere through pitch angle scattering (the latter process will be discussed in Chapter 7). Dubatovko et al assumed that typical electron energies in the midnight sector are around 10 keV (c.f. McIlwain, 1960). It is pointed out however, that electrons with energies as high as 100 keV, could be observed in the midnight sector during SVIA (c.f. Ansari, 1964). Much more convincing evidence for the presence of an east-to-west directed magnetospheric electric field during polar substorms are the reports that the electron energy spectrum hardens during

the morning hours. Berkey (1968) finds that absorption to luminosity ratios gradually increase between 2300 and 0600 hours local time at College, implying a gradual hardening of the electron energy spectrum during that period. Barcus and Rosenberg (1966) and Bewersdorff et al (1967b), from studies of x-rays using balloons, also find that from midnight onwards, the electron energy spectrum hardens.

CHAPTER 7

THE MAGNETOSPHERIC SUBSTORM

7.1 The Magnetospheric Substorm

The polar substorm is a transient process, lasting, typically, from one to three hours. In the midnight sector, the typical explosive nature of the onset of the substorm is especially evident. Any magnetospheric substorm theory must be able to account for this particular characteristic.

Typical relationships of Pi geomagnetic pulsations and cosmic noise absorption activity to the polar substorm have been demonstrated in previous chapters. Other phenomena, also related to the polar substorm, will now be briefly discussed.

7.1.1 *The Van Allen radiation*

Shortly after its discovery (Van Allen et al, 1958), the Van Allen belt was considered as a possible storage reservoir of the particles which caused the aurora. The studies of electron precipitation carried out by O'Brien using results from satellites Injun I (O'Brien, 1962) and by Winckler et al (1962), using balloons, indicated that the Van Allen belt could supply the particles which were precipitated into the ionosphere during magnetic storms only if they were constantly replenished with fresh supplies of particles during storms. These results were confirmed by studies carried out by O'Brien (1964), using results from satellite

Injun 3; he found that during electron precipitation events, trapped electron fluxes increased.

Because of the opposing longitudinal drifts of protons and electrons, the enhanced fluxes of particles, which occur in the Van Allen belt during magnetospheric substorms, constitute the ring current. During the main phase of magnetic storms, the ring current is asymmetric (Akasofu and Chapman, 1964). Cummings (1966) suggested that this asymmetry is due to a greater concentration of low energy protons in the evening sector. This suggestion was supported by the satellite observations of Cahill (1966). Recently, Frank (1970), reported the direct detection of asymmetric increases in the ring current. He found that the strongest increases occurred in the evening to midnight quadrant; these increases occurred during polar magnetic substorms. Akasofu (1968c) has suggested that such ring current particle flux increases may give rise to the typical behaviour of proton aurora in the evening sector i.e. a brightening and a movement equatorward during an early period of substorm activity.

Eather and Carovillano (1970) have suggested that the proton aurora is produced by pitch-angle scattering of protons from the ring current through interaction with ion-cyclotron waves (c.f. Kennel and Petschek, 1966 and Cornwall 1965). It is suggested that GEA events, which are recorded in the evening sector, may be caused by pitch-angle scattering of electrons through interactions with VLF emissions (c.f. Kennel and Petschek, 1966 and Brice, 1963), during asymmetric increases in the ring current.

Pitch-angle scattering of electrons through interaction with VLF

emissions may also be an important process in the morning sector (c.f. Jelly and Brice, 1967) and in the midnight sector. Kennel and Petschek have shown that this mechanism would result in stable trapped particle flux limits for electrons and protons in the Van Allen belt. Assuming that trapped particle fluxes are being continually replenished by some acceleration mechanism, a stable flux limit would be reached when the loss by precipitation balanced the gain by acceleration. Increases in flux above the stable limit would result in increases in wave growth rate and enhanced particle precipitation, which would tend to reduce the wave growth rate till an equilibrium was restored. As intense electron precipitation occurs in the midnight sector during polar substorms, it is expected that the trapped radiation at L - values around L = 6, in the morning sector, would generally be near the stable flux limit, during geomagnetically disturbed periods (c.f. Kennel and Petschek, 1966). Electrons, injected into the midnight sector during polar substorms, would drift eastward into the morning sector and could thus be scattered into the loss cone in their interaction with VLF emissions, giving rise to SVA over a wide segment of the auroral zone. SVIA could also be produced by operation of the same pitch-angle scattering mechanism in the midnight sector.

Kennel and Petschek point out that their calculated stable flux limits are in good agreement with the largest trapped fluxes observed using satellite Explorer 14 (Frank et al, 1964). Since precipitation should occur mainly when trapped particle fluxes are near their stable limit, precipitated and trapped particle fluxes should be well correlated. Such a correlation was found by O'Brien (1964) from satellite Injun 3 results.

7.1.2 *The plasma sheet*

Within the geomagnetic tail lies the neutral sheet, which is a region of magnetic field reversal (Ness, 1967). This region is imbedded in an extensive region, populated by low energy plasma, called the plasma sheet (Bame et al, 1967). Typical average energies for the particle population in the plasma sheet are 0.1 to 10 keV for electrons and 1 - 20 keV for protons (Bame, 1968). The plasma sheet is abruptly terminated at its inner edge. This feature is illustrated in Figure 7-1, which depicts an equatorial cross-section of the magnetosphere. A meridional cross-section of the magnetosphere, depicting the plasma sheet, is given in Figure 7-2. The plasma sheet is about 6 earth radii thick near the midnight meridian at radial distances of about 17 earth radii and about 12 earth radii thick across the dawn to dusk meridian of the magnetosphere (c.f. Rothwell and Wallington, 1968).

Vasyliunas (1968) has shown that during polar substorms, the inner edge of the plasma sheet moves inwards, towards the earth. For one substorm, this movement started near the onset of a magnetic bay. It was estimated that this inward motion could have been associated with a magnetospheric east-to-west electric field of strength 2.4×10^{-4} volts/m.

During polar substorms, sudden increases in electron energy are observed in the plasma sheet. These increases, called "electron islands", were first observed on the IMP 1 satellite by Anderson (1965). Typical behaviour during these increases, is for intensity of electrons, with energies of a few tens of keV, to increase by a factor of a hundred or more;

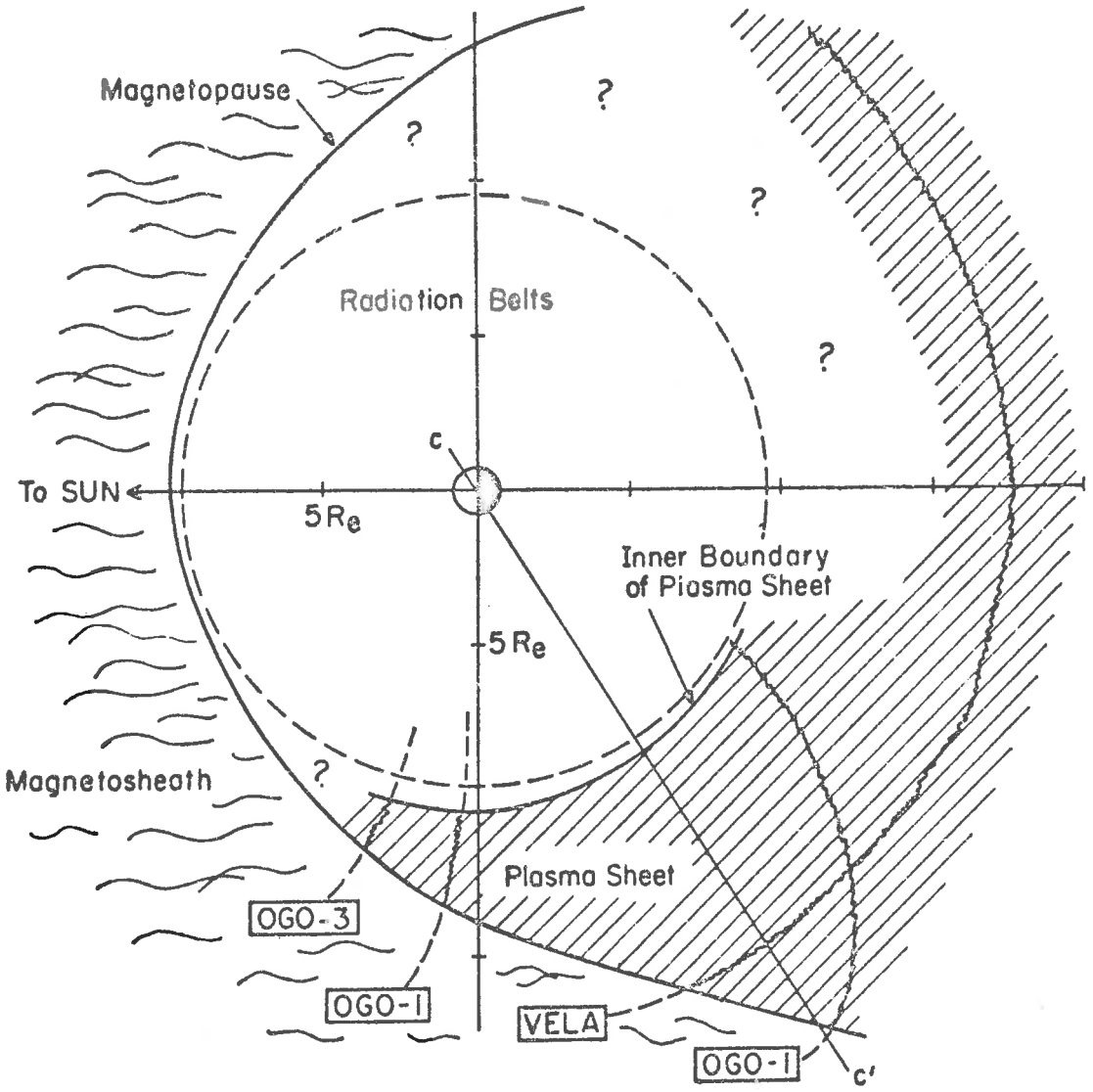

Figure 7-1. Equatorial cross-section of the magnetosphere (viewed from above the North Pole), showing schematically the principal features of the low-energy (∿ 100 - 1000 eV) electron population as established by OGO 1 and OGO 3 as well as by other satellites (after Vasyliunas, 1968).

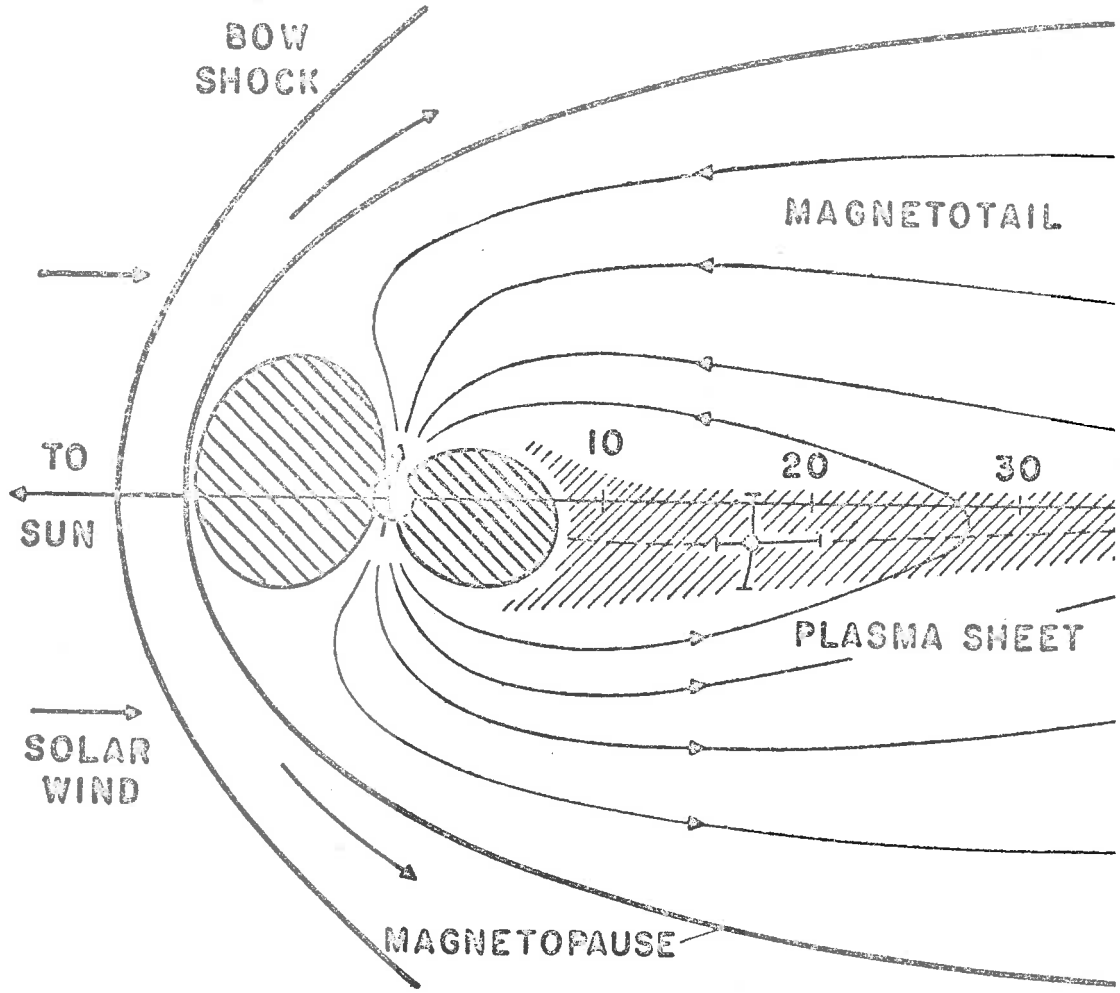

Figure 7-2. Midnight meridianal cross-section for a 12° tilt of the magnetic dipole axis. The point shows the Vela satellite determination of the plasma sheet centre at 17 R_E. The direction of the solar wind is assumed to be along the sun-earth line in this diagram (after Bame et al, 1967).

after the increase reaches maximum intensity, there is a slow intensity decrease with duration of the order of an hour.

Several groups (Rothwell and Wallington, 1968, Hones et al, 1967, Oguti and Kokubun, 1969) have observed electron islands after the onset of polar magnetic substorms. The time delay between substorm onset and detection of electron islands increases with increasing distance from the earth, implying that electron islands move outward, away from the earth. This outward flow occurs during the expansive phase of the polar substorm.

The natural deduction (c.f. Akasofu, 1968a) which follows from these observations is that the initial disturbance during a magnetospheric substorm occurs deep within the magnetosphere. This initial disturbance region is probably often near radial distances of six earth radii, near the midnight meridian of the magnetosphere, as absorption is observed to commence typically, near $L = 6$ in the midnight sector of the auroral oval during a polar substorm.

7.1.3 *Planetary magnetic disturbance*

Obayashi and Nishida (1968) distinguish two types of planetary magnetic disturbance which they term DP 1 and DP 2. The DP 1 disturbance is associated with the magnetospheric substorm; DP 2 disturbance is associated with a magnetospheric convection system driven by the solar wind.

7.1.3.1 *The DP 1 current system*

There is at present no general agreement on the form of the DP 1 current system. Figure 7-3 illustrates the classical two-vortex system (Silsbee and Vestine, 1942, Nagata and Fukushima, 1952), the single vortex

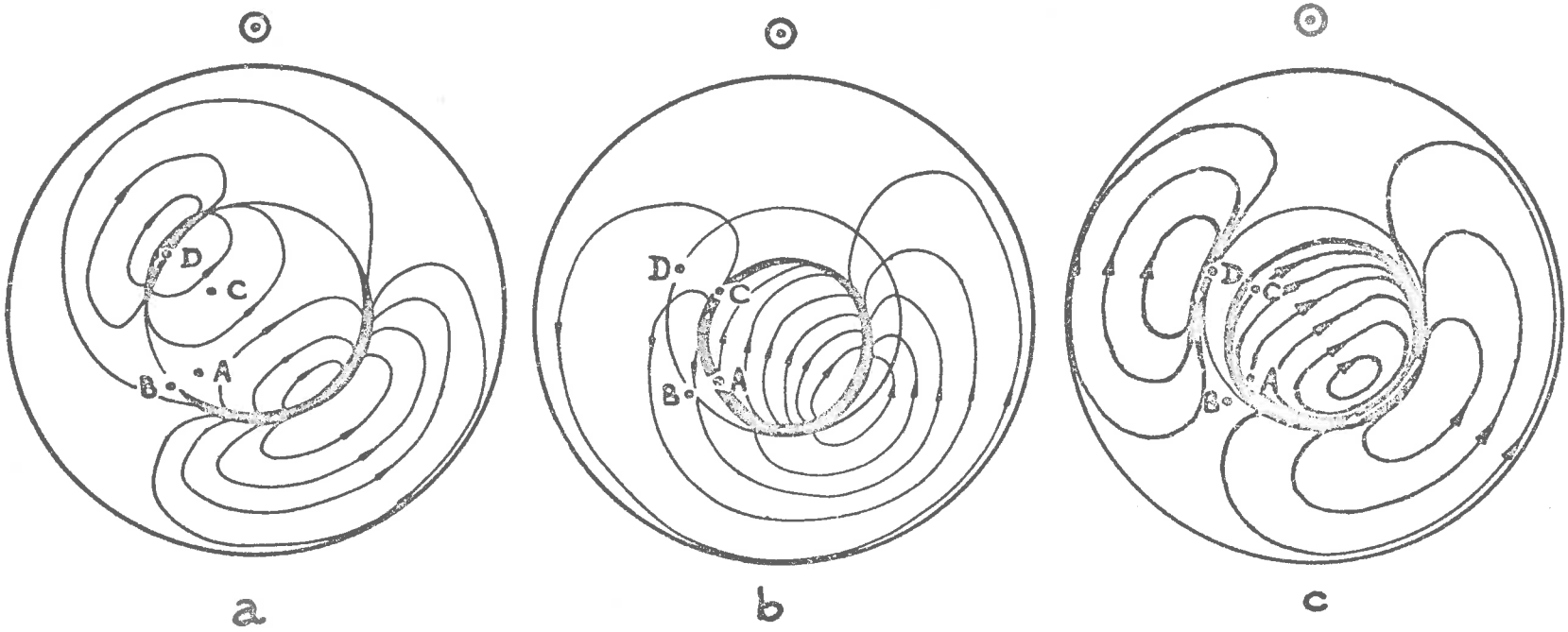

Figure 7-3. Schematic representation of the current system of a DP 1 disturbance in the Northern Hemisphere (a) classical current system; (b) single-vortex system with westward electrojet along the auroral oval; (c) double-vortex system with westward electrojet along auroral oval. The solar direction is upward (after Feldstein, 1969).

current system proposed by Akasofu et al (1965a) and the two-vortex current system proposed by Feldstein and Zaitsev (1965), with a westward electrojet flowing in the auroral oval and an eastward electrojet in the afternoon sector centred on geomagnetic latitudes near 65°. At a geomagnetic latitude of 65°, all of the above current systems are similar; in the evening sector, positive bays should be observed; in the midnight and morning sectors, negative bays should be observed.

Akasofu and Meng (1968) point out that the latitudinal distributions of magnetic changes, which occur during polar substorms at low latitude stations, cannot be accounted for by using the classical two-vortex current system. They demonstrate that these changes can be accounted for by using a model where the high latitude changes are due mainly to growth of the auroral electrojet, while magnetic changes at middle and low latitudes are due to the combined magnetic effects of return currents from the auroral electrojet and the magnetic effect of an asymmetric ring current.

The true DP 1 current system probably includes field-aligned currents (Bostrom, 1964). However, both Bostrom (1964) and Fukushima (1968) suggest magnetic effects observed at the ground, during DP 1 disturbances, are due mainly to ionospheric Hall currents. Akasofu and Meng (1969) have put forward three-dimensional current system (see Figure 7-4), in which currents flow along field lines into the auroral ionosphere in the morning sector, along the auroral oval towards the dusk meridian, outward along field lines in the evening and afternoon sectors, with completion of the circuit with an eastward flow in the asymmetric ring current, on the day sector of the equatorial plane. This model, similar to one proposed by Kirkpatrick (1952),

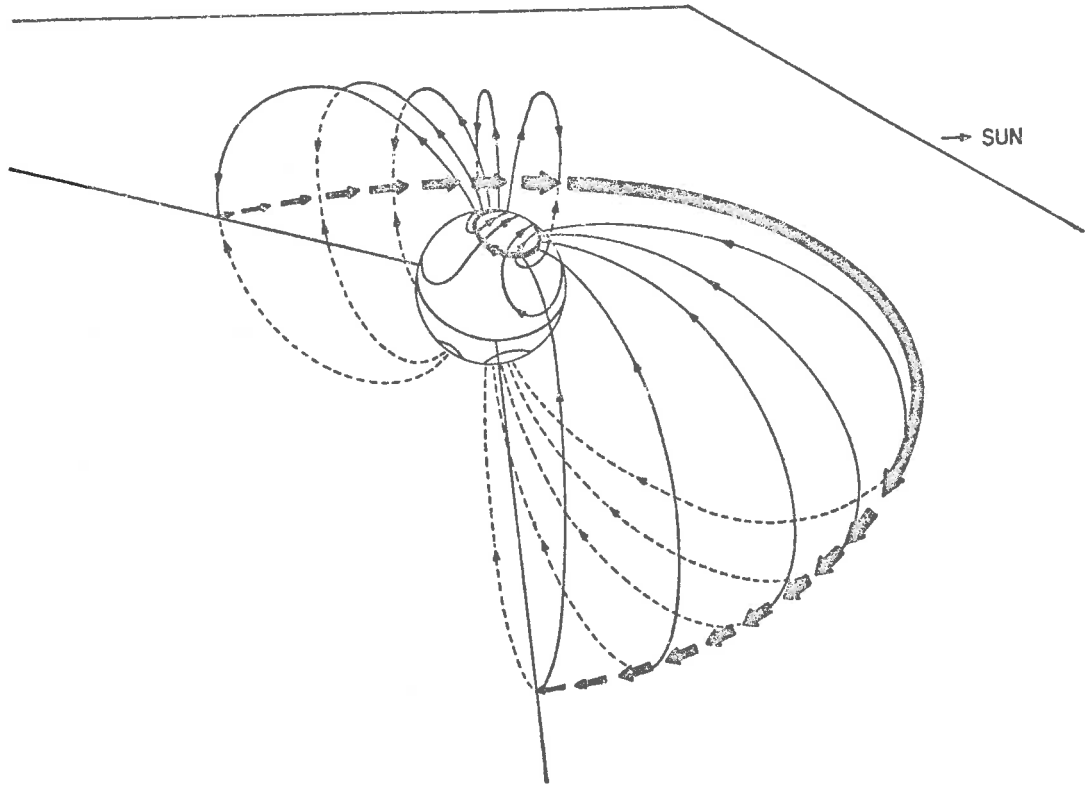

Figure 7-4. Magnetospheric electric current system associated with the polar substorm (after Akasofu and Meng, 1969).

can account for magnetic disturbances observed at geomagnetic latitudes below 55° during polar substorms.

The DP 1 current system is characterized by a relatively rapid growth phase i.e. a typical time for the current system to develop from a quiet condition to a maximum intensity is about half an hour. This period corresponds to the expansive phase of the polar substorm. The most intense magnetic changes which occur during DP 1 disturbances occur at auroral region stations.

7.1.3.2 *The DP 2 current system*

In the DP 2 current system, a two-vortex system (see Figure 7-5), the ratio of current intensity at the auroral zone to that at the pole is not as high as in the case of the DP 1 disturbance. Also, the current flow at low latitude stations is directly connected to current flow in the polar cap (Nishida, 1968a).

In Figure 7-6, examples of simultaneous DP 1 and DP 2 fluctuations are shown. DP 1 fluctuations are clearly observable at College and Macquarie Island. DP 2 fluctuations are clearly observable at Thule (North Pole), Bangui (Equator) and Vostok (South Pole). DP 2 fluctuations appear coherently over the globe and a typical fluctuation period is one hour (Nishida, 1968a).

By using the simplifying assumptions that the DP 2 current system is essentially due to Hall currents and that geomagnetic field lines are equipotentials, then it can be shown that the DP 2 current system is the result of the interaction between the ionosphere and a magnetospheric

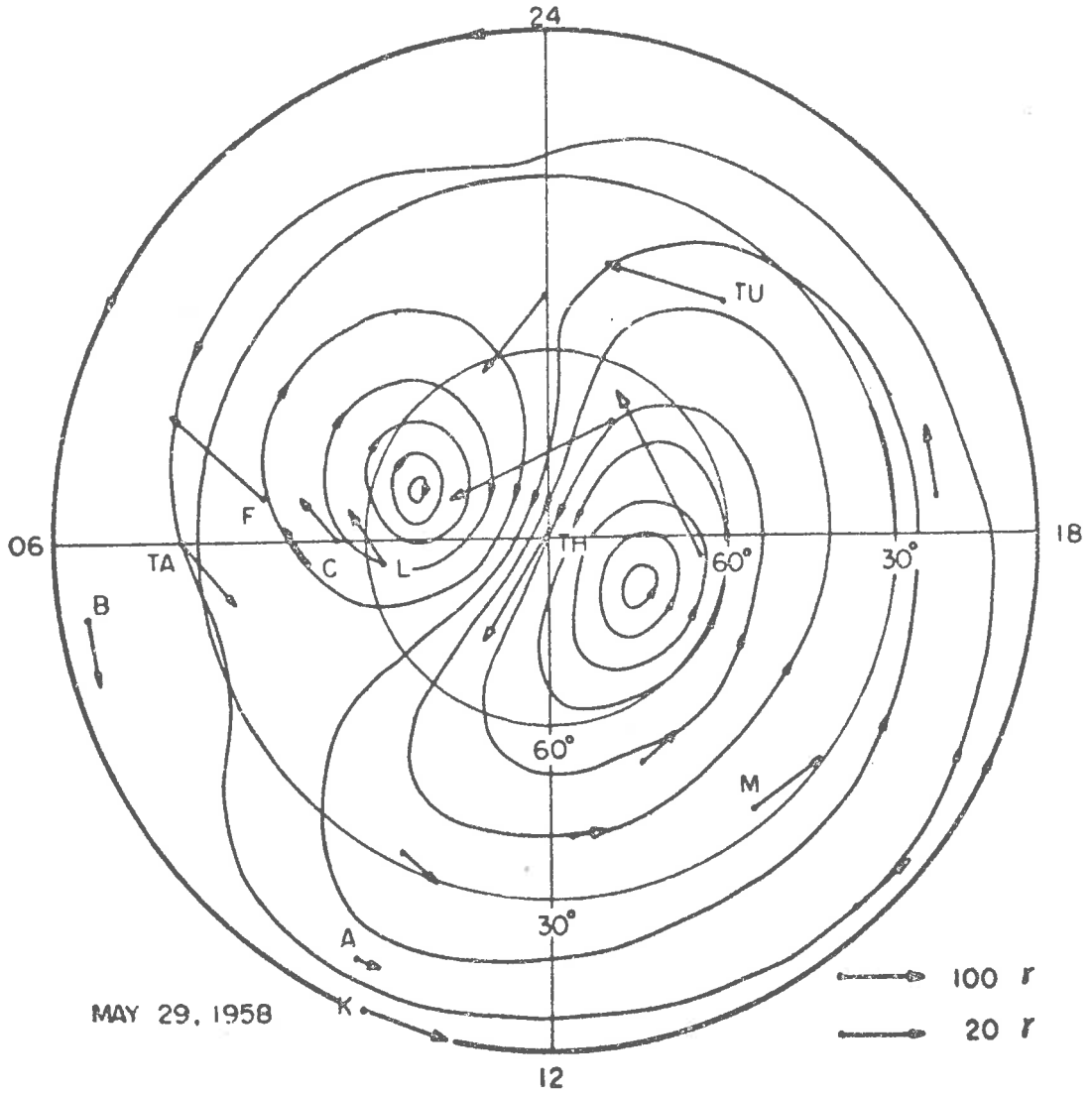

Figure 7-5. Equivalent ionospheric current system of a DP 2 fluctuation that occurred between 0525 and 0640 U.T., May 29, 1958. Current between adjacent streamlines is 5×10^4 amps (after Nishida, 1968a).

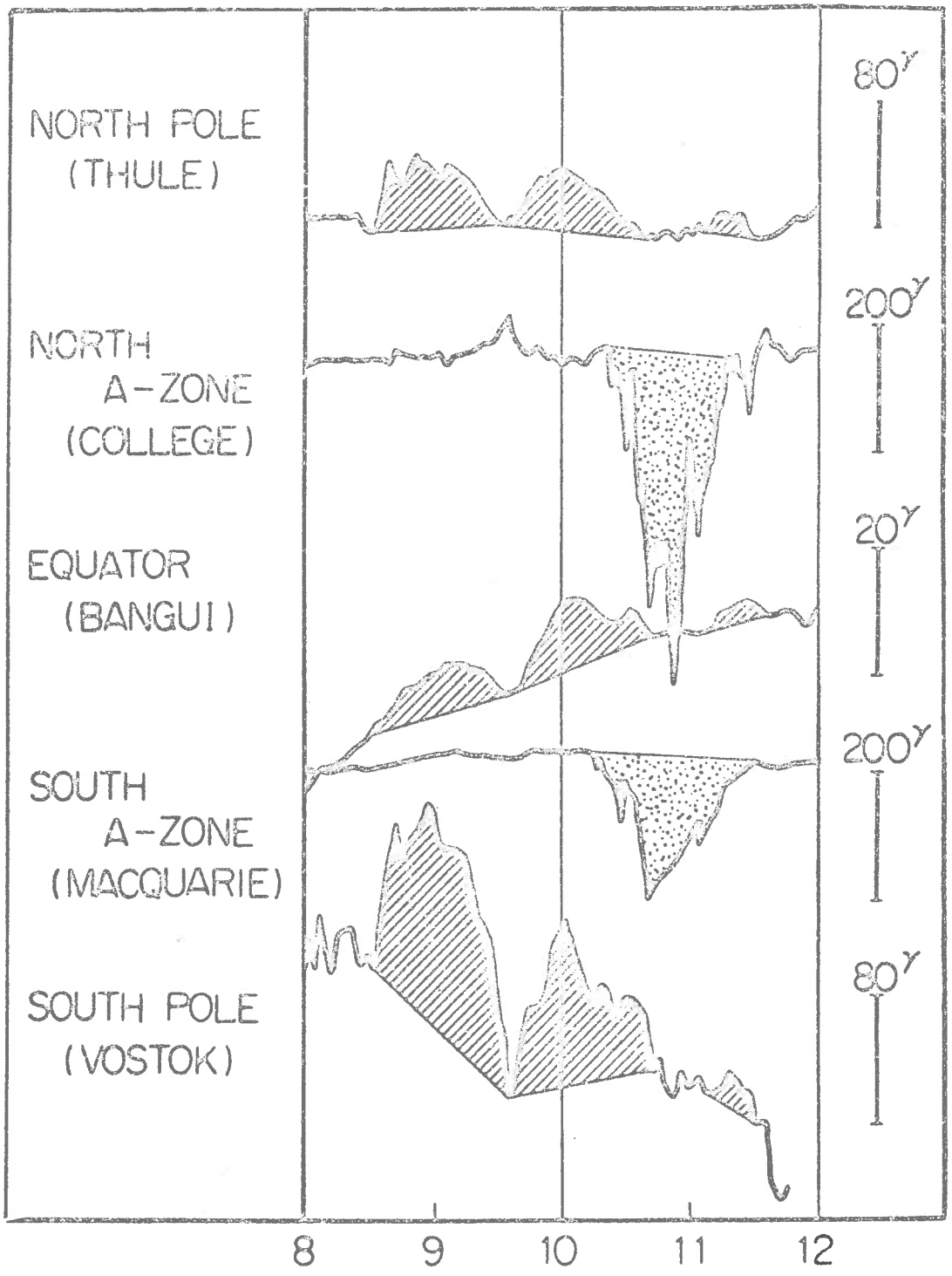

Figure 7-6. Examples of simultaneous DP 1 (College, Macquarie Island) and DP 2 (Thule, Bangui, Vostok) geomagnetic variations (after Nishida, 1968a).

convection system (c.f. Axford, 1969) similar to the one proposed by Axford and Hines (1961).

Figure 7-7 shows an equatorial cross-section of the magnetosphere depicting the plasma flow discussed by Axford and Hines. They suggest that a "viscous-like interaction", between the outer magnetospheric material and the solar wind, drives this convection.

Axford and Hines base their convection system on a "closed" magnetosphere model i.e. geomagnetic field lines are not connected to interplanetary field lines. Dungey (1961) has proposed an "open" model, in which southward directed interplanetary field lines, frozen into an earthward moving solar plasma, connect with geomagnetic field lines at a subsolar point. After this connection, the geomagnetic field lines follow the flow of solar plasma and are pulled into the tail. This movement of geomagnetic field lines is accompanied by a movement of field lines from within the magnetosphere, towards the sun. Thus a magnetospheric plasma flow, similar to that suggested by Axford and Hines, results.

Nishida (1968b) has found that DP 2 fluctuations are coherent with fluctuations in the north-south component of the interplanetary magnetic field (B_z). This coherence was observed to be independent of the direction of B_z, contrary to expectation for Dungey's open magnetosphere model. In this model, the geomagnetic field is connected to the interplanetary magnetic field only if the latter field has a southward component. Thus coherency between DP 2 and B_z would be expected only for southward-directed B_z in Dungey's model.

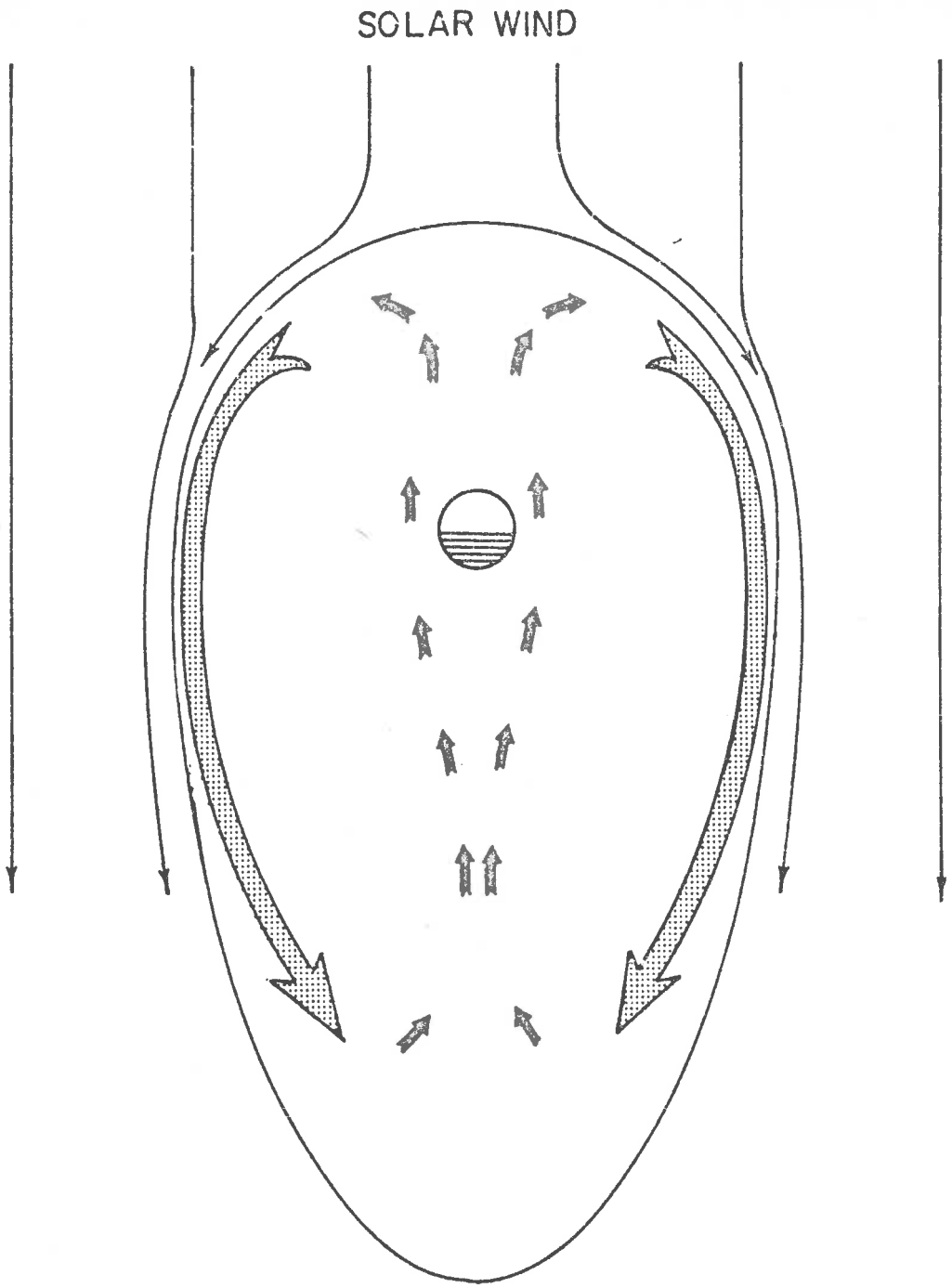

Figure 7-7. Equatorial section of the magnetosphere showing convection system due to viscous-like interaction with the solar wind. The interaction causes tubes of force which lie near the surface of the magnetosphere to be pulled around into the geomagnetic tail, as indicated by large arrows. A return flow (indicated by small arrows) takes place in the interior of the magnetosphere (after Axford and Hines, 1961).

Nishida (1968b) has suggested that the association between B_z and DP 2 fluctuations may be accounted for by assuming a partially shielded model of the magnetosphere. In Nishida's model (see Figure 7-8), the front of the magnetopause, indicated by the thick, solid curve, is assumed to be equipotential, while a potential difference exists along the flanks of the magnetosphere (indicated by the dashed curve). The field which penetrates into the magnetosphere is associated with the flow of solar plasma and is a v x B field, where v is the bulk velocity for the solar plasma. This field would thus drive the DP 2 current system (c.f. Brice, 1967).

7.1.4 *The relationship between interplanetary magnetic field fluctuations and magnetospheric substorms*

Fairfield and Cahill (1966), using data from the satellite Explorer 12, have found that intensity of planetary magnetic disturbance is strongly correlated with the z-component (north-south) in the interplanetary magnetic field B_z. Their results were supported by a study, using IMP 1 satellite data, made by Rostoker and Falthammar (1967). It was found that polar magnetic substorms usually occurred while the interplanetary magnetic field had a southward component. Quiet periods were associated with a northward component to the interplanetary magnetic field. Polar substorms tended to start soon after a change in B_z from north to south. DP 1 disturbance often ended soon after a change in B_z from south to north. However, changes in B_z from north to south were not always followed by onset of a polar substorm, indicating that there are other factors which cause substorms.

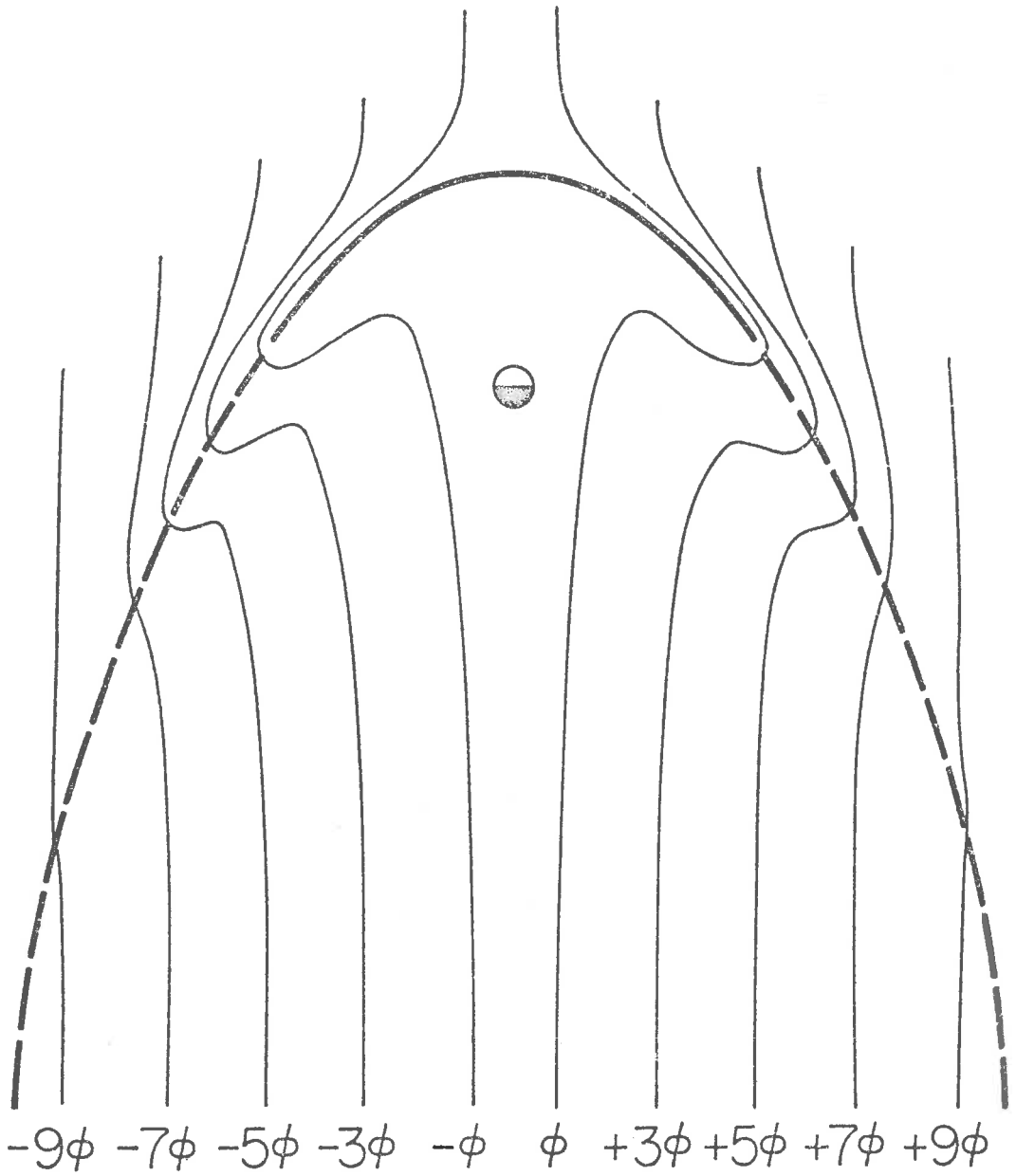

Figure 7-8. Equatorial section of the partially shielded magnetosphere model. The magnetopause is electrically equipotential in parts drawn by solid curve, and is not so in parts drawn by dashed curve. Potential ϕ is positive when B_z is directed southward and negative when B_z is directed northward. Magnitude of ϕ is about 20 kV (after Nishida, 1968b).

Pudovkin and Shumilov (1969) point out that even in the situation where magnetic field lines, frozen into the solar wind plasma, do not penetrate into the magnetospheric cavity, it is possible for interplanetary electric fields to penetrate into the magnetosphere. By considering a simple model, roughly approximating the actual situation, they show that during steady-state solar plasma flow, an electric polarisation field is set up, neutralizing the interplanetary electric field which is impressed into the magnetospheric cavity. However, in the case of a changing solar plasma flow, a penetration of interplanetary electric field into the magnetosphere should occur. An increase in a southward directed B_z would set up a magnetospheric electric field directed from east to west. Pudovkin and Shumilov suggest that such a field could persist for approximately 1.5 hours. They suggest that E x B drift of plasma would result from such a field; thus plasma blobs would drift in from the tail, towards the earth, causing a polar substorm.

Although the discussion of Pudovkin and Shumilov, concerning the possible penetration of an interplanetary electric field into the magnetospheric cavity, is not criticized, their discussion of the possible cause of the polar substorm can be criticized on several points. Pudovkin and Shumilov propose that the polar substorm is due to drift of plasma blobs or "islands" from the tail, toward the earth. They were referring to the electron islands discovered by Anderson (1965). However, electron islands are observed after onset of polar substorms and it has been found that they move away from the earth, not towards the earth, as suggested by Pudovkin and Shumilov. Furthermore, these authors do not show that the onset of

the polar substorm, as observed using magnetometers or riometers, will be sudden, especially in the midnight sector. Also, the change in solar plasma flow Pudovkin and Shumilov assume, in order to calculate a typical strength for the impressed magnetospheric field, is an extreme change. In their calculation, the bulk velocity of solar plasma flow increases from zero to 5×10^7 cm/sec.

Obayashi and Nishida (1968) suggest that DP 1 disturbance may be caused by penetration of the interplanetary field mainly in the tail region. Thus a build up of plasma, on the night side of the magnetosphere and near to the earth, would result, through an inward flow of plasma from the tail. Such a build up of plasma could then lead to magnetospheric instability i.e. the magnetospheric substorm. There is evidence that such a plasma flow does occur before substorms. Carpenter and Stone (1967), from whistler studies, find that inward plasma motions occur in the night side magnetosphere before polar substorms. For one substorm, they found that the inward motion began half an hour before the onset of a polar substorm and continued during the substorm.

7.2 Magnetospheric Substorm Models

In this section, two magnetospheric substorm models will be discussed. At present, there is insufficient experimental data to allow discrimination between these models.

7.2.1 *Fast magnetic field line merging*

Axford (1967) and Atkinson (1966) have suggested that the polar substorm may be due to rapid reconnection of magnetic field lines in the

tail region. Energy is stored in the tail region by an increase in tail magnetic flux as geomagnetic field lines are swept into the tail region by the solar wind. They suggest that the substorm begins when a rapid reconnection of tail field lines occurs deep in the magnetosphere. A schematic diagram illustrating a possible behaviour of tail field lines, during a magnetospheric substorm, is given in Figure 7-9. The top diagram represents a possible situation before onset of the substorm. The shaded region, which will be referred to as the cusp, is inflated. Axford (1969) suggests that plasma pressure in the cusp region controls the rate of tail field-line reconnection. At the start of the substorm, field lines near the outer boundary of the cusp region rapidly reconnect. Magnetic field energy is transferred to particles which precipitate into the auroral ionosphere. As inflated magnetic flux tubes collapse into the cusp region, further reconnection of tail field lines proceeds and the disturbance thus propagates outwards into the tail region as indicated in the bottom two diagrams of Figure 7-9. Thus an auroral bulge is formed, expanding poleward as flux tubes are added into the night side region of closed geomagnetic field lines.

As particles move in towards the earth, they would gain energy through betatron acceleration. Thus an increase in B by a factor x 10 at the equatorial crossing point would be associated with increase in energy of 1 KeV protons to 10 keV. In addition, due to grad B drift, protons would drift westward, giving rise to a partial ring current, due to their concentration in the afternoon sector.

A two-vortex Hall current system, with one vortex centred east of

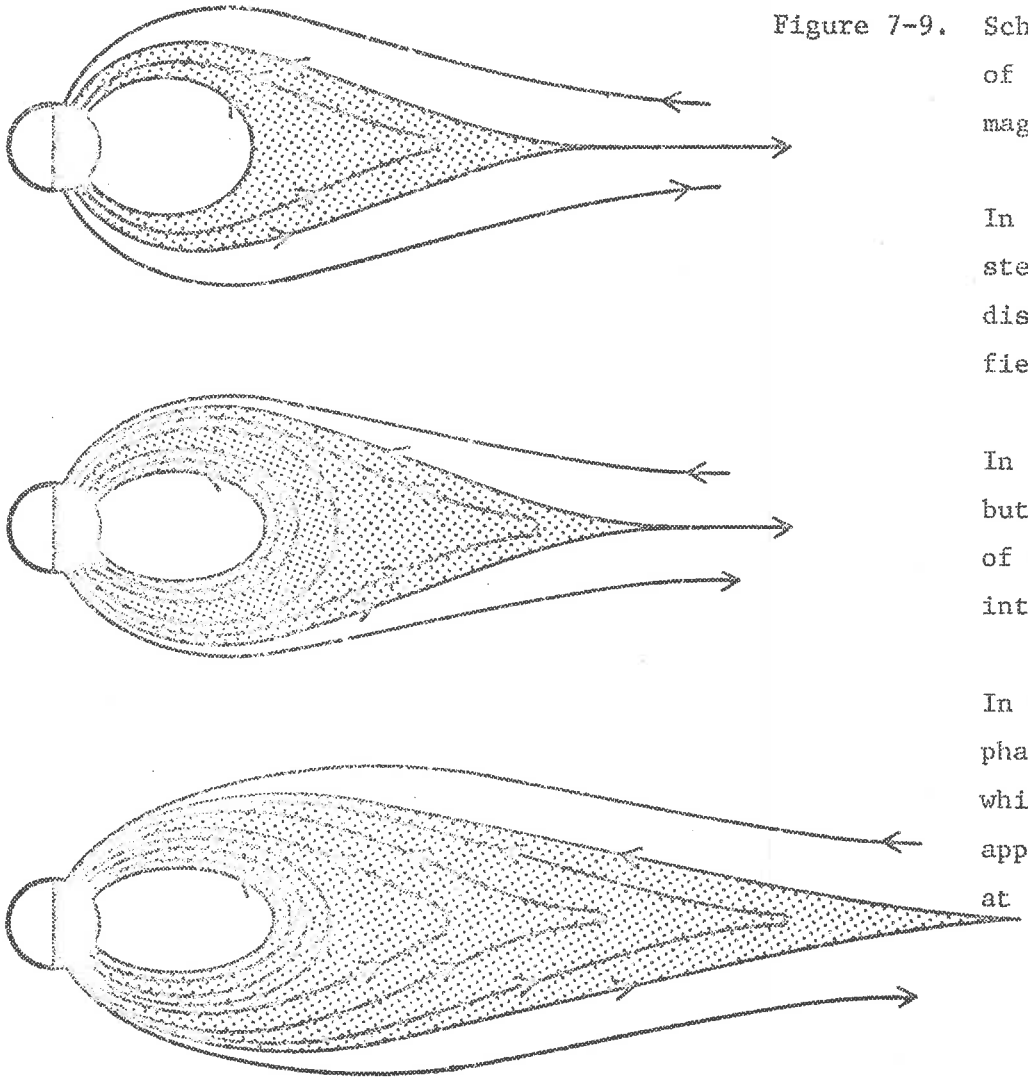

Figure 7-9. Schematic representation of a possible sequence of events involving the cusp plasma during a magnetospheric substorm, following Axford (1969).

In the top diagram, convection is more or less steady. Plasma pressure in the cusp, which distends the cusp magnetic field, keeps the tail field lines from reconnecting too rapidly.

In the middle diagram, the convection continues, but its nature is changed because of a collapse of the cusp on its inner side, associated with intense precipitation into the atmosphere.

In the lower diagram (corresponding to the later phases of the substorm), field line reconnection, which has taken place rapidly, leads to the appearance of the cusp and its associated plasma at larger distances down the tail.

the midnight meridian and the other centred to the west, would be formed by flow of plasma from the tail (c.f. Atkinson 1967). In addition, a Cowling current flows in regions of enhanced ionization, particularly in the front of the expanding bulge, giving rise to the intense negative bays observed in the bulge region. By using an analogue model to simulate the flow of plasma during formation of the bulge, Atkinson has accounted for the magnetic variations observed in the vicinity of the bulge.

In this model of the substorm, the front of the rapidly expanding bulge, where soft electron energy spectra should be observed, corresponds to the region of rapid field-line reconnection. The region inside the auroral bulge, where SVIA precipitation is observed, corresponds to the magnetospheric region where newly connected magnetic field lines are collapsing. Particles moving with these flux tubes will be undergoing betatron and Fermi acceleration.

A major difficulty in the formulation of this model of the magnetospheric substorm has been in finding a mechanism enabling a sudden and rapid reconnection of tail field lines across the neutral sheet, giving rise to the observed explosive character of the onset of a polar substorm. Mechanisms put forward by Sweet (1958) and Petschek (1964) are steady-state mechanisms (c.f. Atkinson, 1966). Axford (1967) points out that over-all magnetospheric stability conditions should be considered in discussion of a mechanism which would cause magnetospheric substorms.

7.2.2 *Instability of a magnetospheric electric current system*

Akasofu (1969) has suggested that the magnetospheric substorm may

result from an instability in the three-dimensional current system described in §7.1.3.1 (see Figure 7-4). In this current system, field-aligned currents flow into and out of the auroral ionosphere in two current sheets, with one in the afternoon to evening sector and one in the morning sector.

Jacobsen and Carlqvist (1964) and Alfvén and Carlqvist (1967) have pointed out that a low pressure discharge may become unstable if the current intensity reaches a critical value. If gradients in plasma density are set up along the flux tubes in which current flows, the plasma tends to readjust so that there is uniformity of current density in these flux tubes. If the current density exceeds the critical value, which is dependent upon plasma density and temperature, plasma tends to move towards regions of higher plasma density, creating a gap in plasma distribution and a disruption of the current circuit. Magnetic energy of the discharge circuit is dissipated exposively by energization of particles, which are accelerated to energies corresponding to the voltage generated across the gap.

Akasofu estimates, assuming that a current of 2×10^6 A flows in the magnetospheric circuit, that the instability could occur if the north-south thickness of either of the two ionospheric current sheets was of the order of 1.2 Km or less. This distance roughly corresponds to the north-south extent of aurora prior to break-up. As a result of the instability, electrons are accelerated downward and protons upward in the evening sector current sheet; electrons are accelerated upward and protons downward in the morning sector current sheet. Akasofu estimate that a typical energy gained by these particles is 50 keV. Thus electrons are readily precipitated in the evening sector. However, the typical energy quoted by Akasofu is

probably too large by a factor of 10. Akasofu however, mentions that his estimates for various typical parameters could lead to errors of this magnitude.

Akasofu suggests that in the equatorial plane, the energy density of particles resulting from the acceleration process could be much greater than the local magnetic energy density. Thus an outward motion of plasma would result, giving rise to outward flow of plasma in the tail and the poleward expansion of aurora which are observed during substorms.

Due to precipitation of energetic electrons into the auroral ionosphere in the midnight sector, a great enhancement in ionisation would result. Thus an intense Cowling current would flow in the region of enhanced ionization due to a north-south polarization field associated with the flow of Hall current in the north-south direction across the highly ionized region (c.f. Bostrom, 1968). This Hall current is due to the electric field associated with the partial ring current. Such an electric field would also give rise to the inward (ExB) motion of the plasma sheet which has been observed by Vasyliunas (1968) during magnetospheric substorms.

In this model, the magnetospheric substorm is the result of asymmetry in the ring current belt, whereas in the model involving tail-field line merging, the asymmetric ring current is a by-product of the substorm.

7.3 Pi Geomagnetic Pulsations

It is clear that Pi geomagnetic pulsations are characteristic of polar substorms. From study of geomagnetic pulsations recorded at Macquarie Island, it is suggested that the typical Pi activity observed during polar

substorms, at geomagnetic latitudes near 65° is as follows:

In the evening sector, Pi activity begins soon after substorm onset. The westward travelling surge is associated with rapid Pi features.

In the midnight sector, the onset of the polar substorm is usually accompanied by a rapid onset or enhancement in Pi activity. Pi (c) geomagnetic pulsations are associated with SVIA.

In the morning sector Pi (c) events, which are characterised by absence of rapid Pi features, are associated with SVA events.

Pi 2, with a dominant pulsation frequency near .01 Hz, were observed on two nights at Macquarie Island during polar substorms, while that station was in the midnight sector and equatorward of the auroral oval i.e. while that station was inside the closed geomagnetic field-line region. This type of Pi activity was also observed during the morning hours, when Macquarie Island is normally equatorward of the boundary of the closed geomagnetic field-line region. It is suggested that Pi activity occurring during polar substorms, at auroral zone stations which are inside the closed geomagnetic field region on the night side of the earth, may be characterised by the presence of a dominant frequency component in the Pi 2 band.

On the basis of the limited data available, it appears that inside the auroral oval, in the midnight sector, Pi 2 activity is characterised by more complex frequency-time behaviour during substorms.

In a recent review, Saito (1969) suggested that Pi geomagnetic pulsations may generally be composed of

Pi 2 + IPDP before midnight,

Pi 1 + Pi 2 near midnight and

Pi 2 + Pi (c) after midnight.

Assuming that the period of time " near midnight" corresponds to the auroral breakup period i.e. an early period of polar substorm activity, then Saito's suggestions for the typical Pi activity in the midnight and morning hours are consistent with the results obtained at Macquarie Island. However, it is pointed out that Pi 1 are also observed before midnight; these pulsations are a dominant component of Pi activity accompanying westward travelling surges (see §4.6).

7.3.1 *Pi generation mechanisms*

Pi 1 pulsations are associated with the intense fluxes of particles which occur in the magnetosphere during polar substorms; at auroral zone stations, Pi 1 events are closely associated with cosmic noise absorption events. As they are commonly observed over a wide range of geomagnetic latitudes (c.f. Saito, 1969), Pi 2 pulsations are considered to be large-scale oscillations of magnetospheric field lines.

Campbell (1964) has suggested that Pi geomagnetic pulsations could be due to fluctuations in ionospheric conductivity caused by particle precipitation, which would give rise to auroral electrojet fluctuations. If the driving electric field is slowly varying relative to the gyrofrequency and collision frequency, then for j_y the eastward component of current density and n_e the electron density

$$\frac{dj_y}{j_y} \propto \frac{dn_e}{n_e}$$

(c.f. Campbell, 1964). The north-south component in the magnetic field strength will be proportional to j_y. Campbell demonstrates that fluctuations of the order of one percent in electron density would be sufficient to account for observed pulsation amplitudes.

It is noted that rapid Pi features are observed in the vicinity of the front of the expanding auroral bulge. This observation is consistent with Campbell's mechanism. In the evening sector, the westward travelling surge is the front of a region of intense, predominantly westward ionospheric current. For a station close to the path of the westward travelling surge, rapid Pi features would be observed as surges moved through the longitude of such a station. In the midnight sector, rapid Pi features are observed at a station if an auroral bulge covers that station during its poleward expansion; intense ionospheric currents localised within the bulge would give rise to these rapid Pi features.

Heacock (1967a) suggests that Pi (c) pulsations are due to fluctuations in auroral electrojet intensity; he finds that the amplitude of Pi (c), observed at College, show consistently high correlation with negative bays in magnetic H component.

Nishida (1964) suggests that rapid Pi features may be due to growth of a hydromagnetic instability resulting from interaction between a beam of precipitating electrons and the ambient plasma. In this instability, energy from the precipitating electrons is transferred to growing hydromagnetic waves. For the simple case of a beam of 10 keV electrons, with density of $1/cm^3$ at the top of the ionosphere and an ambient plasma density of $10/cm^3$, Nishida obtains a frequency range for growing hydromagnetic waves in good

agreement with observation.

Pi 2 pulsations are considered to be due to oscillation of the field lines of the night side inner magnetosphere. At present, there is uncertainty about the type of oscillatory motion that produces Pi 2. Many authors report that periods of Pi 2 events do not vary with latitude (c.f. Saito and Matsushite, 1968 and Troitskaya, 1967); these observations indicate that Pi 2 are due to an oscillation similar to the poloidal type (c.f. Dungey, 1954). On the other hand, Obayashi (1958) has demonstrated a latitudinal dependence for periods of Pi 2 events, observed over a range of geomagnetic latitudes from 40 to 67 degrees, suggesting that Pi 2 are due to torsional oscillations of geomagnetic field lines.

Saito and Matsushita (1968) have suggested that Pi 2 may be a quasi-poloidal oscillation, excited by impulsive reconnection of field lines in the geomagnetic tail region. On the other hand, Rostoker (1967) has compiled evidence indicating that often more than one Pi 2 event may occur during a polar substorm; he found that the frequency spectrum of Pi 2 during substorms often contained more than one frequency peak. Rostoker suggested that the polar substorm is caused by rapid reconnection of tail field-lines and that as these field-lines reconnect, they may oscillate independently i.e. in a mode similar to the torsional oscillation mode. During reconnection, the boundary of the closed field-line region would move poleward; any regeneration of Pi 2 activity would thus give rise to oscillations with frequencies lower than those at the start of the substorm. Rostoker however, did not compute time-varying power spectra and did not demonstrate systematic decreases in period for Pi 2 events recorded during substorms.

It is not surprising that differences are observed in Pi 2 activity inside and equatorward of the auroral oval. Field lines with feet lying in the auroral oval are usually drawn out into the geomagnetic tail, while those with feet lying equatorward of the auroral oval are inside the trapping region. During polar substorms, field lines in the two regions may oscillate differently. For instance, field lines in the first region may undergo torsional oscillations, while those in the trapping region may undergo a poloidal oscillation. Also, the multiple peak structure evident in the power spectra of Pi 2 in the auroral oval may be due to higher order components of oscillation. The approximate harmonic relationship between the frequencies of the peaks suggests analogy with a non-uniform stretched string.

7.4 Cosmic Noise Absorption During Polar Substorms

During polar substorms, cosmic noise absorption is observed over a wide span of longitude in the auroral zone, i.e. typically from the dusk meridian to the noon meridian. Akasofu (1968a) has suggested a pattern of development of the absorption region during a polar substorm; this is illustrated in Figure 7-10, which shows, during the early part of the substorm, an equatorward and poleward expansion in the midnight sector, with speeds of the order of 1 Km/sec. Such a rapid equatorward movement of the absorption region has not been demonstrated.

In Figure 7-11, an alternative scheme is illustrated, essentially a modification of Akasofu's, showing regions of soft and hard electron precipitation, both of which give rise to cosmic noise absorption. In this

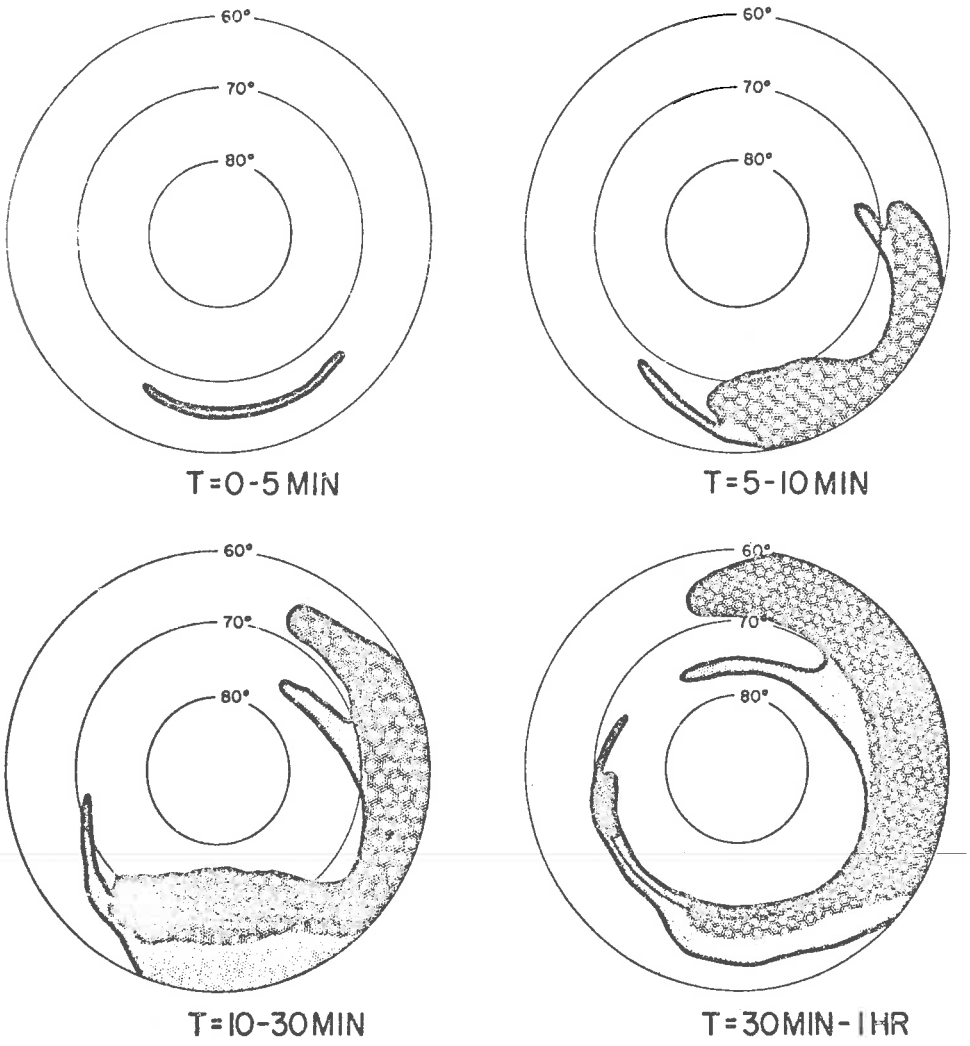

Figure 7-10. Development of absorption region during a polar substorm (after Akasofu, 1968a).

context, "soft" implies typical energies in the region of 5 keV; "hard" implies energies of the order of tens of keV. This scheme is consistent with the discussions of Chapters 4, 5 and 6.

In this scheme, there is an equatorward expansion of the absorption region in the midnight sector. However, this expansion is much slower than the poleward expansion. Parts of the auroral regions where little is known concerning the variation of the absorption region are marked with question marks.

At the start of the substorm (T = 0), absorption is recorded in the region where arcs in the auroral oval begin an intensification in brightness prior to formation of the auroral bulge.

After substorm onset, an absorption region, characterized by soft electron energy spectra and associated with the westward travelling surge, moves westward along the auroral oval in the evening sector. Soft electron energy spectra are also observed in a region at the front of the expanding bulge. Inside the bulge region, hard electron energy spectra are observed.

In the morning sector of the auroral zone, the absorption region expands rapidly eastward along the auroral zone. Typical speeds for this equatorward movement are 4° of longitude per minute (Hargreaves, 1967). Absorption begins first near L = 7 (c.f. Hargreaves, 1968) and expands both poleward and equatorward.

It is suggested that the SVIA and SVA regions are contiguous. Both regions are characterized by hard electron spectra and slow time variation in absorption.

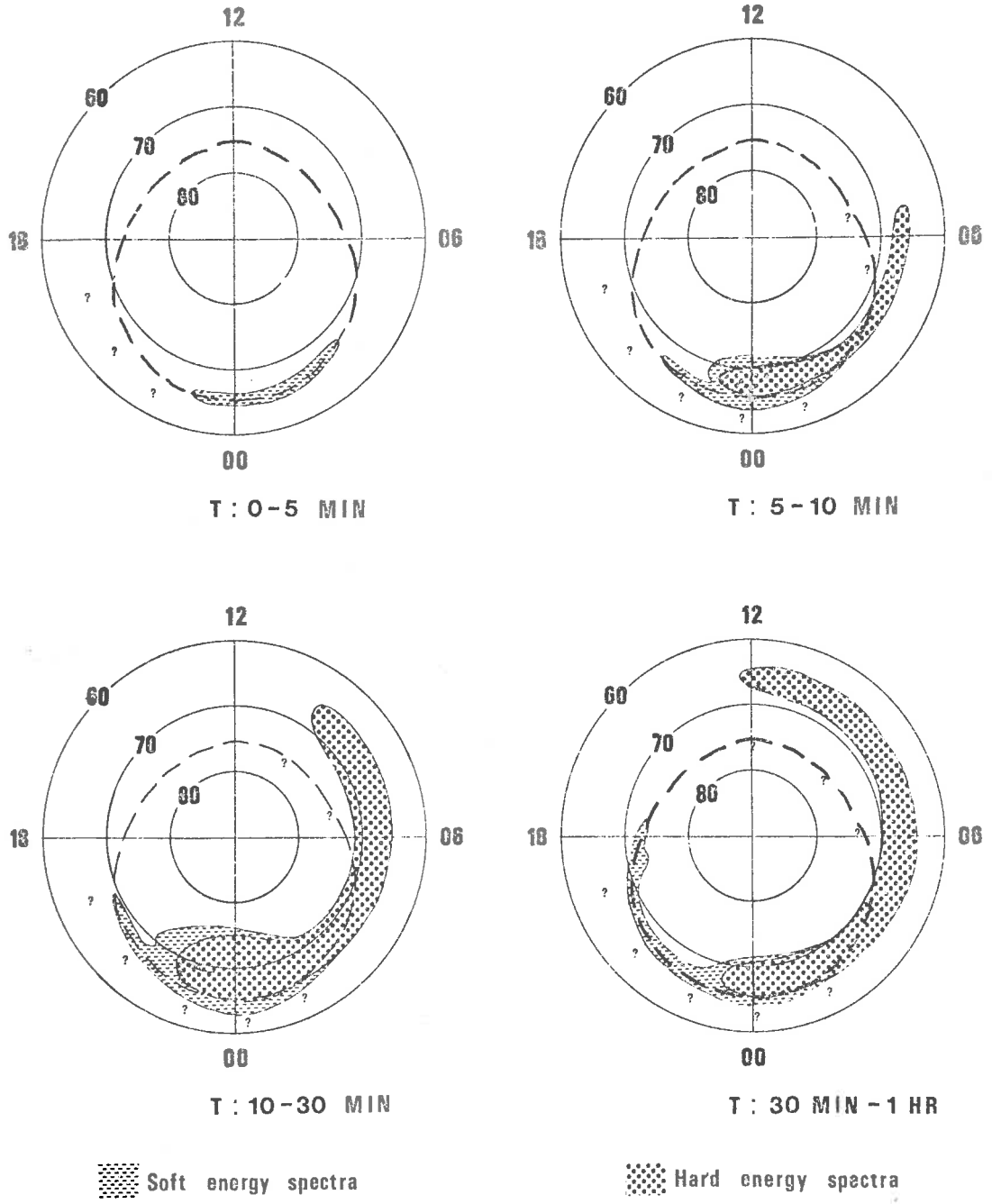

Figure 7-11. A suggested development of absorption during a polar substorm. The dashed curve indicates the equatorward edge of the auroral oval.

7.4.1 *The average time-latitude distribution of auroral absorption*

The typical pattern of development of the absorption region during substorms should be consistent with the average time-latitude distribution of auroral absorption. A geomagnetic latitude-time plot of the latter distribution, determined by Driatskiy (1966) using the Soviet arctic riometer network, is given in Figure 7-12. This distribution is similar to analogous distributions determined in Scandinavia and Canada (c.f. Hartz et al., 1963).

The morning maximum and the afternoon minimum in absorption are evident in Figure 7-12. Also, it is evident that strong absorption was recorded mainly inside a zone, centred on a geomagnetic latitude of approximately 68°, and coinciding approximately with the auroral zone. Primarily because of this zonal character of auroral absorption, particularly in the segment of the auroral zone covering the midnight, morning and early afternoon hours, it was suggested that the SVIA and SVA regions were contiguous. The SVIA region corresponds to a region on the distribution in Figure 7-12, centred around the secondary maximum in absorption around geomagnetic midnight.

Absorption in the early afternoon hours (see Figure 7-12) appears to be an extension of the absorption region in the morning sector. This characteristic of early afternoon absorption is consistent with Akasofu's suggestion that some afternoon absorption events are due to an eastward drift of electrons from the midnight and morning sectors (Akasofu, 1968a).

Driatskiy's average latitude-time distribution of auroral absorption

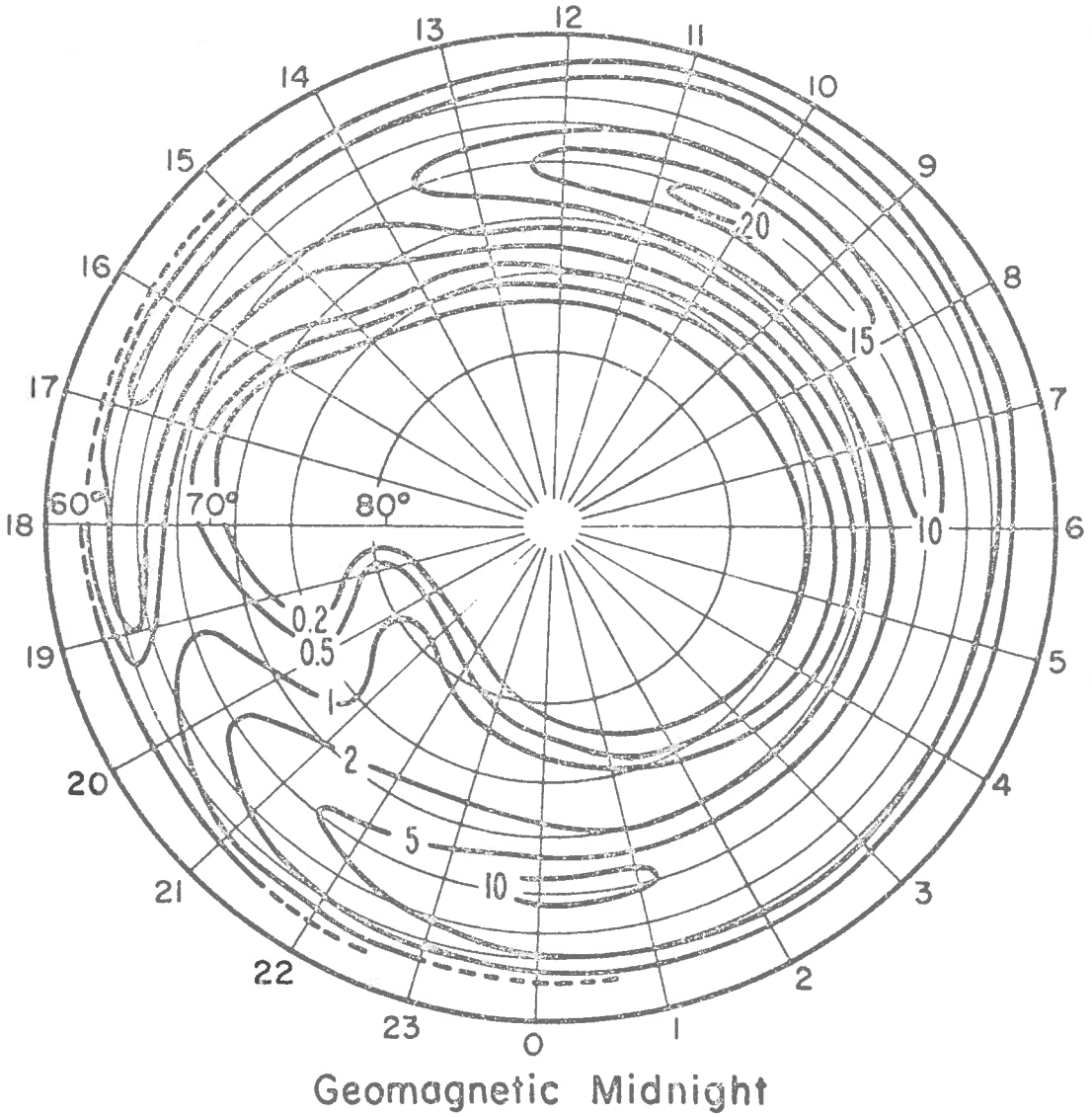

Figure 7-12. Average geomagnetic latitude-time distribution of auroral absorption (after Driatskiy, 1966). This diagram shows the percentage of time that absorption exceeds 1.0 dB.

shows a bifurcation of the absorption region in the early evening hours, around 20 hours geomagnetic time. This result is in agreement with the proposal (see Chapter 4), that there are two types of evening absorption events i.e. REA and GEA events. In Driatskiy's average distribution, there is an absorption region which follows the auroral oval in the evening sector; auroral absorption is observed at a geomagnetic latitude around 80° at about 19 hours geomagnetic time. This region corresponds to the region where REA events, associated with the westward travelling surge, are observed. Also, there is an absorption region in the evening sector of the auroral zone; it is suggested that this corresponds to the region where GEA events are observed. This GEA region is not contiguous with the absorption in the early afternoon hours (see Figure 7-12); instead, it appears to be an extension of the absorption region in the midnight sector. It is thus evident that GEA events are not due to the eastward drift of electrons from the morning and midnight sectors.

GEA events commence in the evening sector of the auroral zone during an early phase of substorm activity e.g. often within the first ten minutes of substorm activity (see §4.3). Furthermore, two examples have been given of evening absorption events recorded at two stations on the same geomagnetic meridian, College and Ft. Yukon; onset of the GEA event recorded at the lower latitude station, College, preceded onset of absorption associated with transit of a westward travelling surge over the higher latitude station by more than twenty minutes in each case (see §4.7). From this evidence, it is suggested that the development of the GEA region, which may cover an extended segment of the auroral zone in the evening

sector, is much more rapid than that of the absorption region associated with the westward travelling surge.

APPENDIX A

GEOMAGNETIC L COORDINATES FOR STATIONS REFERRED TO IN THIS THESIS

The geomagnetic coordinate system used throughout this work is the one proposed by Kilfoyle and Jacka (1968), in which the invariant latitude λ, defined by $L \cos^2 \lambda = 1$, is used. L is the parameter introduced by McIlwain (1961). If the location at which a meridian of this coordinate system, i.e. a L meridian, cuts the equator is labelled as P, then the mean L time at all points on this meridian is defined as being equal to the mean solar time at P and the L longitude is equal to the geographic longitude at P.

Values for geomagnetic L latitude and longitude, L midnight (U.T.) and geographic coordinates for various stations are given in Table A-1. The geomagnetic L coordinate values given are those of Schaeffer (1970), who used the GSFC 12/66 magnetic field model.

At any particular instant of time, the auroras tend to be distributed in a belt which is not concentric with the auroral zone (c.f. Khorosheva, 1961). Akasofu et al (1965a) have proposed that this belt should be termed the auroral oval (or auroral belt). Typical locations of the auroral oval at various universal times, as given by Akasofu (1968a), are shown in Figure A-1.

The auroral zone is the locus of the midnight sector of the auroral

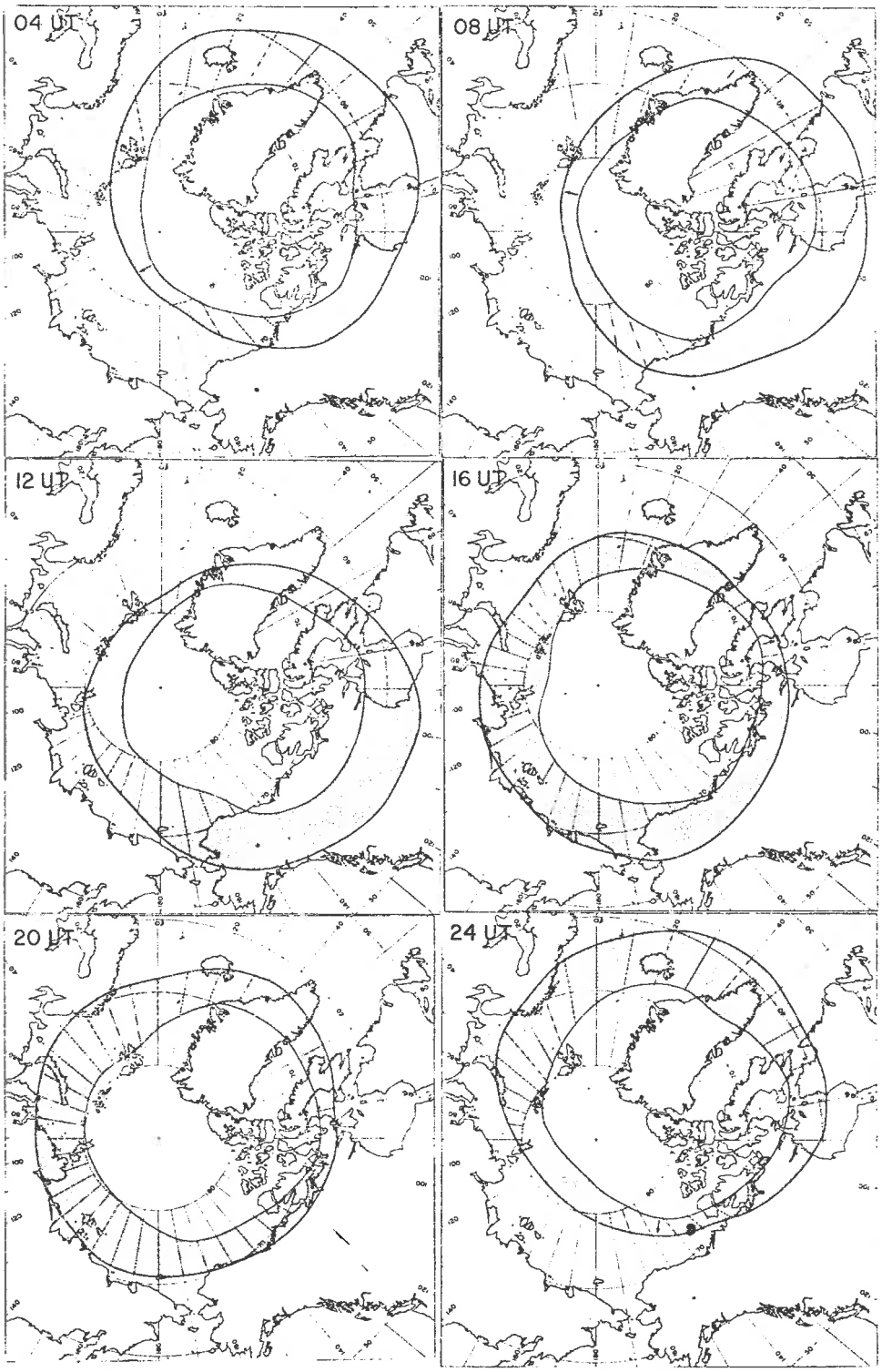

Figure A-1. Typical locations of the auroral oval in the northern hemisphere (after Akasofu, 1968a).

TABLE A-1

Geographic and geomagnetic L coordinates

for various world stations

Station	GEOMAGNETIC			GEOGRAPHIC	
	Latitude (degrees)	Longitude (degrees E)	L-Midnight (U.T.)	Latitude o '	Longitude o '
Abisko	65.3	33.8	2150	68-21N	18-49E
Barrow	69.5	176.7	1210	71-18N	156-45W
Bettles	66.0	185.1	1140	66-53N	151-51W
Byrd	68.0	282.9	0510	80-00S	119-30W
Cape Chelyuskin	71.0	104.4	1720	77-43N	104-17E
Cape Jones	66.9	282.8	0510	54-35N	79-05W
Churchill	70.0	258.0	0650	58-48N	94-06W
College	64.8	190.1	1120	64-52N	147-50W
Coral Harbour	75.7	275.9	0540	64-10N	83-15W
Dixon Island	67.6	85.7	1820	73-33N	80-34E
Eagle	66.0	195.7	1140	64-46N	141-20W
Eights	59.7	294.9	0420	75-14S	77-10W
Flin Flon	64.9	247.8	0730	54-47N	101-51W
Frobisher Bay	74.7	302.7	0350	63-45N	68-30W
Ft. Yukon	67.0	190.6	1120	66-34N	145-18W
Grt. Whale River	67.5	285.0	0500	55-16N	77-47W
Kerguelen	58.6	51.2	2040	49-21S	70-12E

TABLE A-1 continued

Station	GEOMAGNETIC Latitude (degrees)	GEOMAGNETIC Longitude (degrees E)	GEOMAGNETIC L-Midnight (U.T.)	GEOGRAPHIC Latitude o '	GEOGRAPHIC Longitude o '
Kiruna	64.5	34.6	2140	67-50N	20-25E
Kotzebue	64.1	177.1	1210	66-53N	162-36W
Macquarie I.	64.2	175.9	1220	54-30S	158-57E
Mawson	70.4	18.8	2250	67-36S	62-53E
Meanook	62.4	232.6	0830	54-37N	113-20W
Murmansk	64.2	44.6	2100	68-15N	33-05E
Resolute Bay	84.1	238.7	0810	74-42N	94-54W
Reykjavik	66.4	358.7	0010	64-09N	21-58W
Saskatoon	61.3	242.2	0750	52-10N	106-40W
Sogra	58.2	52.4	2030	62-47N	46-16E
South Pole	73.8	306.7	0330	89-57S	13-19W
Syowa	66.3	359.6	0000	69-00S	39-35E
Tixie Bay	65.0	125.2	1540	71-35N	129-00E
Tromso	66.5	35.2	2140	69-40N	18-57E
Val D'Or	60.7	284.3	0500	48-07N	77-47W
Wrangel I.	66.0	160.5	1320	71-00N	178-36W
Yakutsk	55.1	128.7	1530	62-01N	129-43E

oval. This zone was mapped using the data of Akasofu (1968a); it was found to lie in a region bounded by geomagnetic latitudes of approximately 65° and 75° (see Figure A-2). Locations of some auroral region stations, often referred to in this work, are also indicated in Figure A-2.

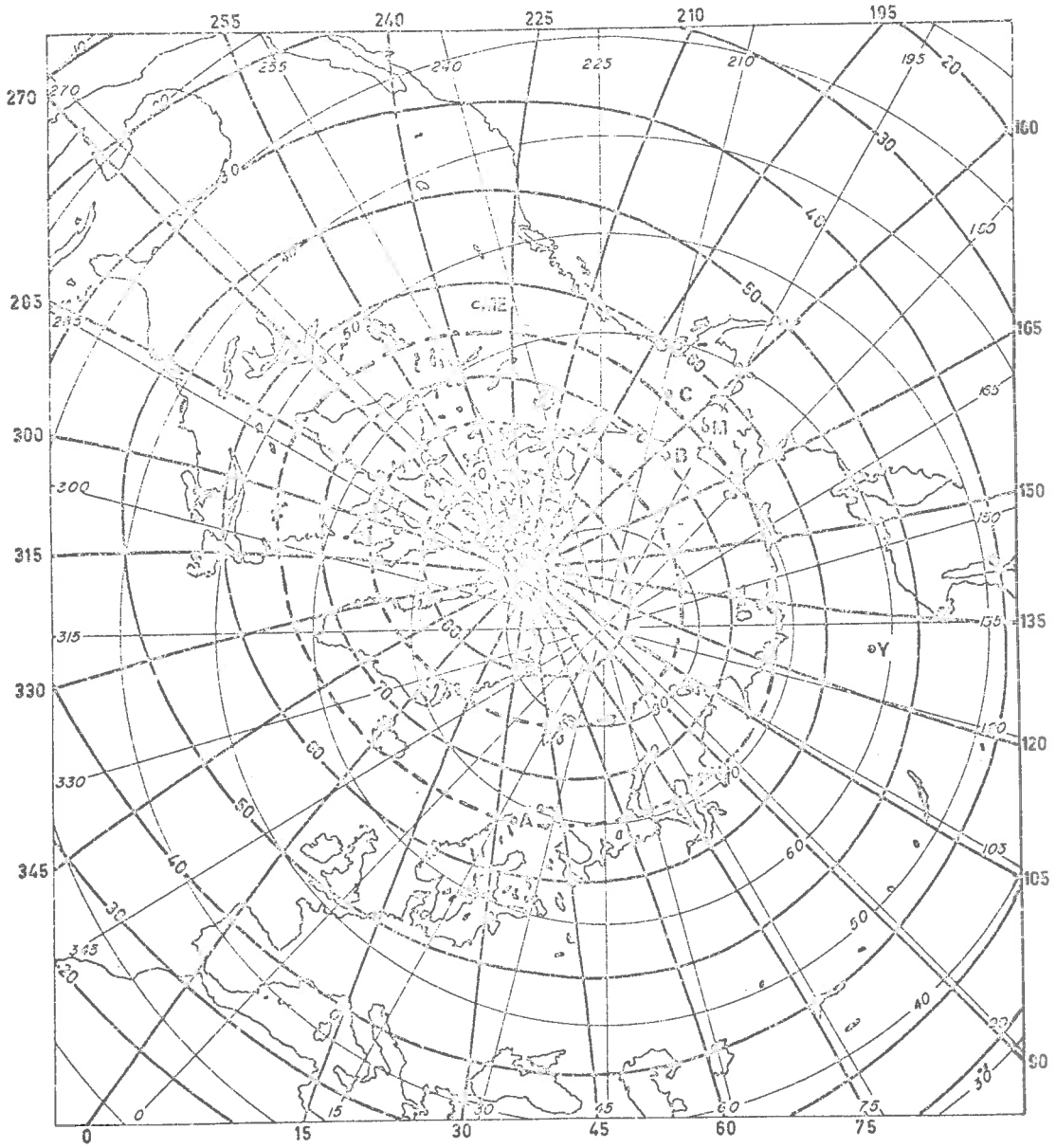

Figure A-2. Polar equidistant geographic projection (light) of the northern hemisphere with L coordinates (heavy) superimposed (after Schaeffer, 1970).
The dashed lines of constant L latitude enclose the auroral zone.

KEY TO STATION LOCATIONS:

A = Abisko
B = Barrow
C = College
M = Macquarie Island conjugate
ME = Meanook
Y = Yakutsk

APPENDIX B

SPECTRAL ANALYSIS OF Pi 2 GEOMAGNETIC PULSATIONS

Time-varying power spectra of geomagnetic pulsations over the frequency band .004 to .056 Hz, which includes the Pi 2 frequency band, were computed using the procedures outlined in Chapter 3. Prior to spectral analysis of a data section, the zero-frequency component was removed by subtracting the mean data value for that section. Also, the raw data were smoothed and re-sampled prior to spectral analysis; a 61-point moving average was used for this data smoothing. The power transfer function for this data smoothing is given in Figure B-1.

Time-averaged power spectra were calculated using the instantaneous power function $P'(\omega, nT)$ (see equation (19) of Chapter 3); time-averaged power spectra $P_{AV}(\omega)$, over a time interval $t = i\,T$ to $t = j\,T$, were estimated using the formula

$$P_{AV}(\omega) = Ko \sum_{r=i}^{r=j-1} P'(\omega, rT)$$

Ko is the normalisation constant, chosen so that $P_{AV}(\omega_o) = 1$, for ω_o the lowest centre-frequency in the array of band-pass filters used to compute the time-varying power spectrum. The above formula differs slightly from that given in Chapter 3, i.e. equation (21). However, there are no significant differences in results obtained using the two formulae when

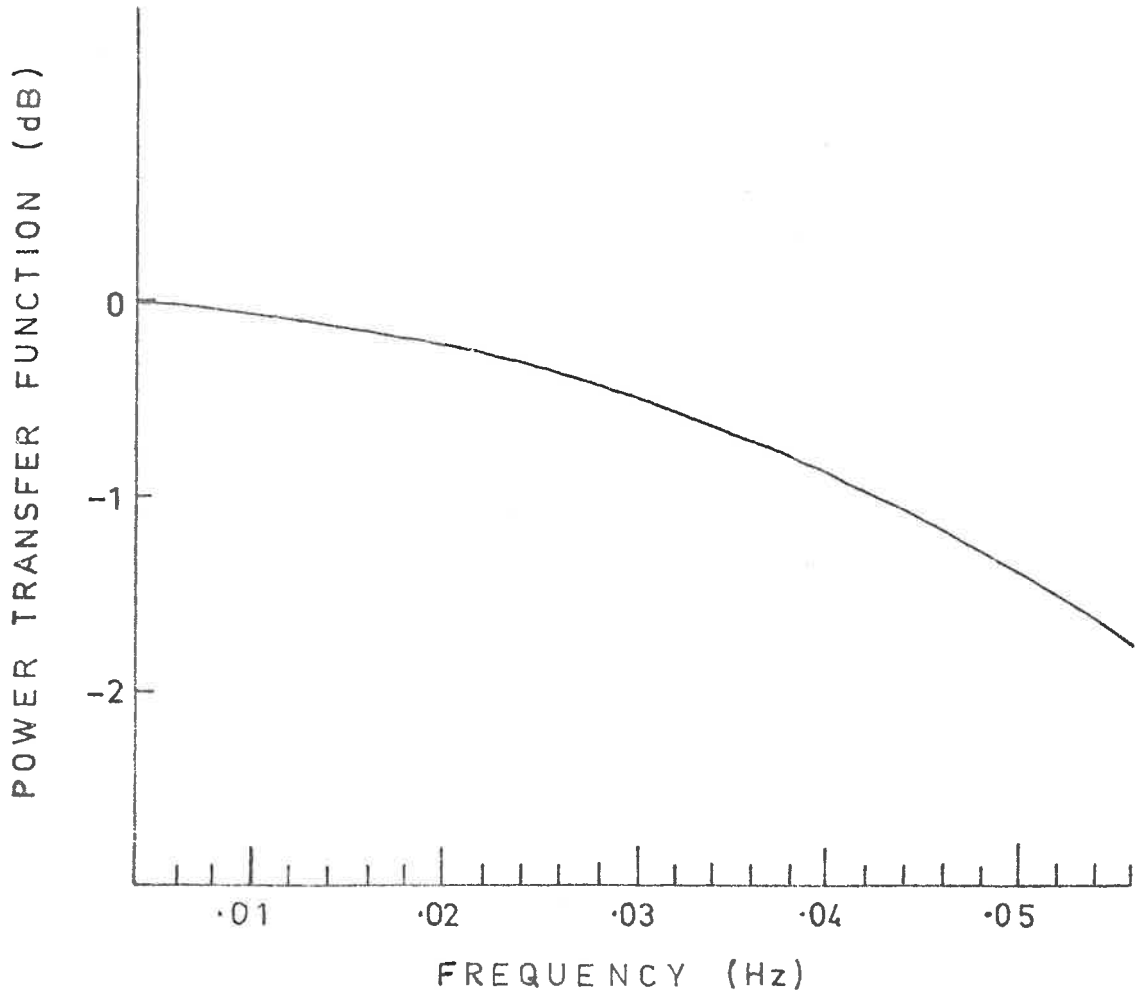

Figure B-1. Power transfer function for smoothing performed by using a 61-point moving average. Sampling interval for raw data was 0.1 seconds.

time-averaged power spectra are computed by averaging over a large number of data points i.e. of the order of 1000.

APPENDIX C

Yuan, F. F. F., & Jacka, F. (1969). Simultaneous geomagnetic and cosmic noise absorption pulsations near geomagnetic noon. *Nature, 222*(5194), 653-654.

BIBLIOGRAPHY

Akasofu S.-I. (1964)

The development of the auroral substorm.

Planetary and Space Science Vol. 12, 273 - 282.

Akasofu S.-I. (1966a)

The auroral oval, the auroral substorm and their relation with the internal structure of the magnetosphere.

Planetary and Space Science Vol. 14, 587 - 595.

Akasofu S.-I. (1966b)

Electrodynamics of the magnetosphere: geomagnetic storms.

Space Science Reviews Vol. 6, 21 - 143.

Akasofu S.-I. (1968a)

Polar and magnetic substorms.

Astrophysics and Space Science Library Vol. 11.

Akasofu S.-I. (1968b)

Auroral observations by the constant local time flight.

Planetary and Space Science Vol. 16, 1365 - 1370.

Akasofu S.-I. (1968c)

The growth of the storm-time radiation belt and the magnetospheric substorm.

Geophysical Journal Vol. 15, 7 - 21.

Akasofu S.-I. (1969)

Magnetospheric substorm as a discharge process.

Nature Vol. 221, 1020 - 1022.

Akasofu S.-I. and Chapman S. (1964)

On the asymmetric development of the main phase of magnetic storms.

Planetary and Space Science Vol. 12, 607 - 626.

Akasofu S.-I. and Meng C.-I. (1967a)

Polar magnetic substorm in the evening sector.

Journal of Atmospheric and Terrestrial Physics Vol. 29, 1127 - 1135.

Akasofu S.-I. and Meng C.-I. (1967b)

The abnormally early appearance of active auroras.

Journal of Atmospheric and Terrestrial Physics Vol. 29, 601 - 602.

Akasofu S.-I. and Meng C.-I. (1968)

Low latitude negative bays.

Journal of Atmospheric and Terrestrial Physics Vol. 30, 227 - 241.

Akasofu S.-I. and Meng C.-I. (1969)

A study of polar magnetic substorms.

Journal of Geophysical Research Vol. 74, 293 - 313.

Akasofu S.-I., Chapman S., and Meng C.-I. (1965a)

The polar electrojet.

Journal of Atmospheric and Terrestrial Physics Vol. 27, 1275 - 1305.

Akasofu S.-I., Kimball D.S. and Meng C.-I. (1965b)

Dynamics of the aurora-III. Westward drifting loops.

Journal of Atmospheric and Terrestrial Physics Vol. 27, 189 - 196.

Akasofu S.-I. Meng C.-I. and Kimball D.S. (1965c)

Dynamics of the aurora-II. Westward travelling surges.

Journal of Atmospheric and Terrestrial Physics Vol. 27, 173 - 187.

Akasofu S.-I., Kimball D.S. and Meng C.-I. (1966a)

Dynamics of the aurora-V. Poleward motions.

Journal of Atmospheric and Terrestrial Physics Vol. 28, 497 - 503.

Akasofu S.-I., Meng C.-I. and Kimball D.S. (1966b)

Dynamics of the aurora-VI. Formation of patches and their eastward motion.

Journal of Atmospheric and Terrestrial Physics Vol. 28, 505 - 511.

Akasofu S.-I., Kimball D.S. and Meng C.-I. (1969)

Dynamics of the aurora and associated phenomena.

Annals of the I.G.Y. Vol. 45, Pt. 1.

Alfvén H. and Carlqvist P. (1967)

Currents in the solar atmosphere and a theory of solar flares.

Solar Physics Vol. 1, 220 - 228.

Anderson K.A. (1965)

Energetic electron fluxes in the tail of the geomagnetic field.

Journal of Geophysical Research Vol. 70, 4741 - 4763.

Ansari Z.A. (1963)

The spatial and temporal vibrations in high latitude cosmic noise absorption and their relation to luminous aurora.

Geophysical Institute Scientific Report UAG-R138, University of Alaska.

Ansari Z.A. (1964)

The aurorally associated absorption of cosmic noise at College, Alaska.

Journal of Geophysical Research Vol. 69, 4493 - 4513.

Ansari Z.A. (1965)

A peculiar type of daytime absorption in the auroral zone.

Journal of Geophysical Research Vol. 70, 3117 - 3122.

Arnoldy R.L. and Chan K.W. (1969)

Particle substorms observed at the geostationary orbit.

Journal of Geophysical Research Vol. 74, 5019 - 5028.

Atkinson G. (1966)

A theory of polar substorms.

Journal of Geophysical Research Vol. 71, 5157 - 5164.

Atkinson G. (1967)

The current system of geomagnetic bays.

Journal of Geophysical Research Vol. 72, 6063 - 6067.

Axford W.I. (1967)

The interaction between the solar wind and the magnetosphere.

Aurora and Airglow edited by B.M. McCormac, pp. 499 - 509,

Reinhold Publishing Corporation.

Axford W.I. (1969)

Magnetospheric convection.

Reviews of Geophysics Vol. 7, 421 - 459.

Axford W.I. and Hines C.O. (1961)

A unifying theory of high-latitude geophysical phenomena and geomagnetic storms.

Canadian Journal of Physics Vol. 39, 1433 - 1464.

Bame J.S. (1968)

Plasma sheet and adjacent regions.

Earth's Particles and Fields edited by B.M. McCormac, pp. 373 - 383, Reinhold Book Corporation.

Bame J.S., Ashbridge H.E., Felthauser H.E., Hones E.W. and Strong I.B. (1967)

Characteristics of the plasma sheet in the earth's magnetotail.

Journal of Geophysical Research Vol. 72, 113 - 129.

Barcus J.R. and Rosenberg T.J. (1966)

Energy spectrum for auroral zone x-rays 1. Diurnal and type effects.

Journal of Geophysical Research Vol. 71, 803 - 823.

Basler R.P. (1963)

Radio wave absorption in the auroral ionosphere.

Journal of Geophysical Research Vol. 68, 4665 - 4681.

Belon A.E., Maggs T.E., Davis T.N., Mather K.B., Glass N.W. and Hughes G.F. (1969)

Conjugacy of visual auroras during magnetically quiet periods.

Journal of Geophysical Research Vol. 74, 1 - 26.

Berkey F.T. (1968)

Coordinated measurements of auroral luminosity using the narrow beam technique.

Journal of Geophysical Research Vol. 73, 319 - 337.

Berkey F.T. and Parthasarathy R. (1964)

An investigation of selected types of radiowave absorption events in the auroral zone.

Geophysical Institute Scientific Report UAG-R151, University of Alaska.

Bewersdorff A., Kremser G., Riedler W. and Legrand J.P. (1967a)

Some properties of the slowly varying ionospheric absorption events in the auroral zone.

Arkiv für Geofysik Vol. 5, 115 - 127.

Bewersdorff A., Dion J., Legrand J.P., Keppler E., Kremser G. and Riedler W. (1967b)

Energy variation of auroral electrons according to balloon measurements.

Space Research Vol. 7, 645 - 653.

Bewersdorff A., Kremser G., Stadsnes J., Trefall H. and Ullaland S. (1968)

Simultaneous balloon measurements of auroral x-rays during slowly varying ionospheric absorption events.

Journal of Atmospheric and Terrestrial Physics Vol. 30, 591 - 607.

Bingham C., Godfrey M.D. and Tukey J.W. (1967)

Modern techniques of power spectrum estimation.

IEEE Transactions on Audio and Electroacoustics Vol. AU-15, 56 - 66.

Blackman R.B. and Tukey J.W. (1958)

The measurement of power spectra.

Dover publications, New York.

Bostrom R. (1964)

A model of the auroral electrojet.

Journal of Geophysical Research Vol. 69, 4983 - 5000.

Bostrom R. (1968)

Currents in the ionosphere and magnetosphere.

Annales de Géophysique Vol. 24, 681 - 694.

Bozorth R.M. and Chapin D.M. (1942)

Demagnetising factors of rods.

Journal of Applied Physics Vol. 13, 320 - 326.

Brice N.M. (1963)

An explanation of triggered very-low-frequency emissions.

Journal of Geophysical Research Vol. 68, 4626 - 4628.

Brice N.M. (1967)

Bulk motion of the magnetosphere.

Journal of Geophysical Research Vol. 72, 5193 - 5211.

Brown R.R. (1964)

A study of slowly varying and pulsating ionospheric absorption events in the auroral zone.

Journal of Geophysical Research Vol. 69, 2315 - 2321.

Brown R.R., Barcus J.R. and Parsons N.R. (1965)

Balloon observations of auroral zone x-rays in conjugate regions. 2. Microbursts and pulsations.

Journal of Geophysical Research Vol. 70, 2599 - 2612.

Cahill L.J. (1966)

Inflation of the inner magnetosphere during a magnetic storm.

Journal of Geophysical Research Vol. 71, 4505 - 4519.

Campbell W.H. (1964)

A study of geomagnetic effects associated with auroral zone electron precipitation observed by balloons.

Journal of Geomagnetism and Geoelectricity Vol. 16, 41 - 61.

Campbell W.H. and Leinbach H. (1961)

Ionospheric absorption at times of auroral and magnetic pulsations.

Journal of Geophysical Research Vol. 66, 25 - 34.

Campbell W.H. and Matsushita S. (1962)

Auroral zone geomagnetic micropulsations with periods 5 to 30 seconds.

Journal of Geophysical Research Vol. 67, 555 - 573.

Campbell W.H. and Rees M.H. (1961)

A study of auroral coruscations.

Journal of Geophysical Research Vol. 66, 41 - 55.

Carpenter D.L. and Stone K. (1967)

Direct detection by a whistler method of the magnetospheric electric field associated with a polar substorm.

Planetary and Space Science Vol. 15, 395 - 397.

Clark T.A. and Anger C.D. (1967)

Morphology of electron precipitation during auroral substorms.

Planetary and Space Science Vol. 15, 1287 - 1301.

Cornwall J.M. (1965)

Cyclotron instabilities and electromagnetic emission in the ultra low frequency and very low frequency ranges.

Journal of Geophysical Research Vol. 70, 61 - 69.

Cummings W.D. (1966)

Asymmetric ring currents and the low latitude disturbance daily variation.

Journal of Geophysical Research Vol. 71, 4493 - 4503.

Dalgarno A. (1964)

Corpuscular radiation in the upper atmosphere.

Annales de Géophysique Vol. 20, 65 - 74.

Davies F.T. (1950)

Visual auroral observations in Canada, 1943-7.

Transactions of the Oslo Meeting of the I.U.G.G., 1948. pp. 255 - 264.

Driatskiy V.M. (1966)

Study of the space and time distribution of auroral absorption according to observations of the riometer network in the Arctic.

Geomagnetism and Aeronomy Vol. 6, 828 - 834.

Dubatovko O.YE., Pudovkin M.I. and Shumilov O.I. (1968)

Some problems concerning auroral absorption.

Geomagnetism and Aeronomy Vol. 8, 240 - 243.

Dungey J.W. (1954)

Electrodynamics of the outer atmosphere.

Pennsylvania State University Scientific Report No. 69.

Dungey J.W. (1961)

Interplanetary magnetic field and the auroral zones.

Physical Review Letters Vol. 6, 47 - 48.

Eather R.H. and Burrows K.M. (1966)

Corrigendum to "Excitation and ionization by auroral protons."

Australian Journal of Physics Vol. 19, 717.

Eather R.H. and Carovillano R.L. (1970)

The ring current as the source region for proton auroras.

Private communication.

Eather R.H. and Jacka F. (1966)

Auroral absorption of cosmic radio noise.

Australian Journal of Physics Vol. 19, 215 - 239.

Fairfield D.H. and Cahill L.J., Jr. (1966)

Transition region magnetic field and polar magnetic disturbances.

Journal of Geophysical Research Vol. 71, 155 - 169.

Feldstein Y.I. (1966)

Peculiarities in the aurora distribution caused by the asymmetrical form of the magnetosphere.

Planetary and Space Science Vol. 14, 121 - 130.

Feldstein Y.I. (1969)

Polar auroras, polar substorms and their relation with the dynamics of the magnetosphere.

Reviews of Geophysics Vol. 7, 179 - 218.

Feldstein Y.I. and Starkov G.V. (1967)

Dynamics of auroral belt and polar geomagnetic disturbances.

Planetary and Space Science Vol. 15, 209 - 230.

Feldstein Y.I. and Zaitzev A.N. (1965)

Current system of S_D variations at high latitudes in winter during the I.G.Y.

Geomagnetism and Aeronomy Vol. 5, 884 - 885.

Frank L.A. (1970)

Direct detection of asymmetric increases of extraterrestrial "ring current" proton intensities in the outer radiation zone.

Journal of Geophysical Research Vol. 70, 1263 - 1268.

Frank L.A., Van Allen J.A. and Hills H.K. (1964)

An experimental study of charged particles in the outer radiation zone.

Journal of Geophysical Research Vol. 69, 2171 - 2191.

Fukunishi H. (1969)

Occurrence of sweepers in the evening sector following the onset of magnetospheric substorms.

Report of Ionosphere and Space Research (Japan) Vol. 23, 21 - 34.

Fukushima N. (1968)

Three dimensional electric current and toroidal magnetic field in the ionosphere.

Report of Ionosphere and Space Research (Japan) Vol. 22, 173 - 195.

Gendrin R. and Lacourly S. (1968)

Irregular micropulsations and their relations with the far magnetospheric perturbations.

Annales de Géophysique Vol. 24, 267 - 273.

Golden R.M. and Kaiser J.F. (1964)

Design of wideband sampled-data filters.

Bell System Technical Journal Vol. 43, 1533 - 1546.

Hargreaves J.K. (1966)

On the variation of auroral radio absorption with geomagnetic activity.

Planetary and Space Science Vol. 14, 991 - 1006.

Hargreaves J.K. (1967)

Auroral motions observed with riometers: movements between stations widely separated in longitude.

Journal of Atmospheric and Terrestrial Physics Vol. 29, 1159 - 1164.

Hargreaves J.K. (1968)

Auroral motions observed with riometers: latitudinal movements and a median global pattern.

Journal of Atmospheric and Terrestrial Physics Vol. 30, 1461 - 1470.

Hargreaves J.K. (1969)

Auroral absorption of HF radio waves in the ionosphere: A review of results from the first decade of riometry.

Proceedings of the I.E.E.E. Vol. 57, 1348 - 1373.

Hartz T.R. and Brice N.M. (1967)

The general pattern of auroral particle precipitation.

Planetary and Space Science Vol. 15, 301 - 329.

Hartz T.R., Montbriand L.F. and Vogan E.L. (1963)

A study of auroral absorption at 30 Mc/S.

Canadian Journal of Physics Vol. 41, 581 - 595.

Heacock R.R. (1967a)

Two subtypes of Pi micropulsations.

Journal of Geophysical Research Vol. 72, 3905 - 3917.

Heacock R.R. (1967b)

Evening micropulsations events with a rising midfrequency characteristic.

Journal of Geophysical Research Vol. 72, 399 - 408.

Heppner J.P. (1954)

A study of the relationships between the aurora borealis and the geomagnetic disturbances caused by electric currents in the ionosphere.

Thesis, California Institute of Technology.

Holt O., Landmark B. and Lied F. (1961)

Analysis of riometer observations obtained during polar radio blackouts.

Journal of Atmospheric and Terrestrial Physics Vol. 23, 229 - 243.

Hones E.W., Jr., Asbridge J.R., Bame S.J. and Strong I.B. (1967)

Outward flow of plasma in the magnetotail following geomagnetic bays.

Journal of Geophysical Research Vol. 72, 5879 - 5892.

Jacobs J.A. and Sinno K. (1960)

World-wide characteristics of geomagnetic micropulsations.

Geophysical Journal Vol. 3, 333 - 353.

Jacobs J.A., Kato Y., Matsushita S. and Troitskaya V.A. (1964)

Classification of geomagnetic micropulsations.

Journal of Geophysical Research Vol. 69, 180 - 181.

Jacobsen C. and Carlqvist P. (1964)

Solar flares caused by circuit interruptions.

Icarus Vol. 3, 270 - 272.

Jánossy L. (1950)

Cosmic Rays.

Oxford University Press.

Jelley D.H. (1968)

Apparent poleward motion of onsets of auroral absorption events.

Canadian Journal of Physics Vol. 46, 33 - 37.

Jelly D.H. (1970)

On the morphology of auroral absorption during substorms.

Canadian Journal of Physics Vol. 48, 335 - 345.

Jelly D.H. and Brice N.M. (1967)

Changes in Van Allen radiation associated with polar substorms.

Journal of Geophysical Research Vol. 72, 5919 - 5931.

Johansen O.E. (1965)

Variations in energy spectrum of auroral electrons detected by simultaneous observation with photometer and riometer.

Planetary and Space Science Vol. 13, 225 - 235.

Johnson R.G., Sharp R.D., Shea M.F. and Snook G.B. (1966)

Satellite observations of two distinct dayside zones of auroral electron precipitation.

Transactions of the American Geophysical Union (Abstract) Vol. 47, 64.

Kelly R.D., Enochson L.D. and Rondinelli L.A.

Techniques and errors in measuring cross-correlation and spectral density functions.

NASA Contract Report, CR-74505.

Kennel C.F. and Petschek H.E. (1966)

Limit on stably trapped particle fluxes.

Journal of Geophysical Research Vol. 71, 1 - 28.

Khorosheva O.V. (1961)

The space and time-distribution of auroras and their relationship with high-latitude geomagnetic disturbances.

Geomagnetism and Aeronomy Vol. 1, 615 - 621.

Kilfoyle B.P. and Jacka F. (1968)

Geomagnetic L coordinates.

Nature Vol. 220, 773 - 775.

Kirkpatrick C.B. (1952)

On current systems proposed for S_D in the theory of magnetic storms.

Journal of Geophysical Research Vol. 57, 511 - 526.

Knaflich H.B. and Kenney J.F. (1967)

IPDF events and their generation in the magnetosphere.

Earth and Planetary Science Letters Vol. 2, 453 - 459.

Kvifte G.J. and Pettersen H. (1969)

Morphology of the pulsating aurora.

Planetary and Space Science Vol. 17, 1599 - 1607.

Leinbach H. and Basler R.P. (1963)

Ionospheric absorption of cosmic radio noise at magnetically conjugate auroral zone stations.

Journal of Geophysical Research Vol. 68, 3375 - 3382.

Lin W.C., McDiarmid I.B. and Burrows J.R. (1968)

Electron fluxes at 1000 Km altitude associated with auroral substorms.

Canadian Journal of Physics Vol. 46, 80 - 83.

Little C.G. (1954)

High latitude ionospheric absorption using extra-terrestrial radio waves.

Proceedings of the I.R.E. Vol. 42, 1700 - 1701.

McDiarmid I.B. and Burrows J.R. (1964)

Diurnal Intensity variations in the outer radiation zone at 1000 Km.

Canadian Journal of Physics Vol. 42, 1135 - 1148.

McIlwain C.E. (1960)

Direct measurement of charged particles associated with auroral zone radio-wave absorption.

Journal of Geophysical Research Vol. 65, 2727 - 2747.

McIlwain C.E. (1961)

Coordinates for mapping the distribution of magnetically trapped particles.

Journal of Geophysical Research Vol. 66, 3681 - 3691.

McPherron (1968)

A digital technique for obtaining dynamic spectra (digital sonagram).

Space Sciences Laboratory Report, University of California.

McPherron R.L., Parks G.K., Coroniti F.V. and Ward S.H. (1968)

Studies of the magnetospheric substorm. 2. Correlated magnetic micropulsations and electron precipitation occurring during auroral substorms.

Journal of Geophysical Research Vol. 73, 1697 - 1713.

Nagata T. and Fukushima N. (1952)

Constitution of polar magnetic substorms.

Report of Ionosphere and Space Research (Japan) Vol. 6, 85 - 96.

Ness N.F. (1967)

Observations of the interaction of the solar wind with the geomagnetic field during quiet conditions.

Solar Terrestrial Physics edited by J.W. King and W.S. Newman, pp. 57 - 89, Academic Press.

Nishida A. (1964)

Theory of irregular magnetic micropulsations associated with a magnetic bay.

Journal of Geophysical Research Vol. 69, 947 - 954.

Nishida A. (1968a)

Geomagnetic DP 2 fluctuations and associated magnetospheric phenomena.

Journal of Geophysical Research Vol. 73, 1795 - 1803.

Nishida A. (1968b)

Coherence of geomagnetic DP 2 fluctuations with interplanetary magnetic field variations.

Journal of Geophysical Research Vol. 73, 5549 - 5559.

Obayashi T. (1958)

Geomagnetic storms and the earth's outer atmosphere.

Report on Ionosphere and Space Research (Japan) Vol. 12, 301 - 335.

Obayashi T. and Nishida A. (1968)

Large-scale electric fields in the magnetosphere.

Space Science Reviews Vol. 8, 3 - 31.

O'Brien B.J. (1962)

Lifetimes of outer-zone electrons and their precipitation into the atmosphere.

Journal of Geophysical Research Vol. 67, 3687 - 3706.

O'Brien B.J. (1964)

High-latitude geophysical studies with satellite Injun 3, 3.

Precipitation of electrons into the atmosphere.

Journal of Geophysical Research Vol. 69, 13 - 43.

O'Brien B.J. (1967)

Satellite observations of particle fluxes and atmospheric emissions.

Aurora & Airglow edited by B.M. McCormac, pp. 623 - 642, Reinhold Publishing Corporation.

Oguti T. and Kokubun S. (1969)

Polar magnetic disturbances and associated increase in flux of energetic electrons in the magnetosphere.

Report of Ionosphere and Space Research (Japan) Vol. 23, 151 - 161.

Omholt A. and Berger S. (1967)

The occurrence of auroral pulsations in the frequency range 0.01 - 0.10 c/s over Tromso.

Planetary and Space Science Vol. 15, 1075 - 1080.

Ortner J. and Riedler W. (1964)

A smooth type of cosmic noise absorption.

Nature Vol. 204, 1181 - 1182.

Petschek H.E. (1964)

Magnetic field annihilation.

AAS-NASA Symposium on Physics of Solar Flares. NASA SP-50.

Edited by W.N. Hess, pp. 425 - 439.

Pudovkin M.I. and Shumilov O.I. (1969)

On the theory of polar substorms.

Annales de Géophysique Vol. 25, 125 - 134.

Rader C.M. and Gold B. (1967)

Digital filter design techniques in the frequency domain.

Proceedings of the I.E.E.E. Vol. 55, 149 - 171.

Reid J. (1967)

Auroral zone cosmic noise absorption pulsations.

Nature Vol. 214, 1321 - 1322.

Romañá A. and Cardús J.O. (1962)

Geomagnetic rapid variations during IGY and IGC.

Journal of the Physical Society of Japan Vol. 17, Supplement A-II,

47 - 55.

Rostoker G. (1967)

The frequency spectrum of Pi 2 micropulsation activity and its

relation to planetary magnetic activity.

Journal of Geophysical Research Vol. 72, 2032 - 2039.

Rostoker G. (1968)

Macrostructure of geomagnetic bays.

Journal of Geophysical Research Vol. 73, 4217 - 4229.

Rostoker G. and Fälthammar C.G. (1967)

Relationship between changes in the interplanetary magnetic field and variations in the magnetic field at the earth's surface.

Journal of Geophysical Research Vol. 72, 5853 - 5862.

Rothwell P. and Wallington V. (1968)

The polar substorm and electron "islands" in the earth's magnetic tail.

Planetary and Space Science Vol. 16, 1441 - 1451.

Saito T. (1961)

Oscillation of the geomagnetic field with progress of Pt - type pulsation.

Scientific Report, Tohuku University, Series 5, Geophysics, 13, 53 - 61.

Saito T. (1969)

Geomagnetic pulsations.

Space Science Reviews 10, 319 - 412.

Saito T. and Matsushita S. (1968)

Solar cycle effects on geomagnetic Pi 2 pulsations.

Journal of Geophysical Research Vol. 73, 267 - 286.

Schaeffer R.C. (1970)

Computation of geomagnetic L coordinates.

Australian Journal of Physics - in the press.

Shain C.A. (1951)

Galactic radiation at 18.3 Mc/s.

Australian Journal of Scientific Research, Series A, Vol. 4, 258 - 267.

Silsbee H.C. and Vestine E.H. (1942)

Geomagnetic bays, their frequency and current systems.

Terrestrial Magnetism and Atmospheric Electricity Vol. 47, 195 - 208.

Snyder C.W., Neugebauer M. and Rao U.R. (1963)

The solar wind velocity and its correlation with cosmic ray variations and with solar and geomagnetic activity.

Journal of Geophysical Research Vol. 68, 6361 - 6370.

Storer J.E. (1957)

Passive network synthesis.

McGraw-Hill.

Sweet P.A. (1958)

The neutral point theory of solar flares.

I.A.U. Symposium No. 6: Electromagnetic Phenomena in Cosmical Physics edited by B. Lehnert, pp. 123 - 140, Cambridge University Press.

Troitskaya V.A. (1961)

Pulsations of the earth's electromagnetic field with periods of 1 to 15 seconds and their connection with phenomenae in the high atmosphere.

Journal of Geophysical Research Vol. 65, 5 - 18.

Troitskaya V.A. (1967)

Micropulsations and the state of the magnetosphere.

Solar-Terrestrial Physics edited by J.W. King and W.S. Newman, pp. 213 - 274, Academic Press.

Troitskaya V.A., Kleymenova N.G., Raspopov O.M., Geller L.A., Roldugin V.K., Vigneron J., Karachevskiy Z.H. and Loran J. (1968)

Relationship between irregular geomagnetic field pulsations and the pulsations of auroras and of VLF emission.

Geomagnetism and Aeronomy Vol. 8, 872 - 874.

Van Allen J.A., Ludwig G.H., Ray E.C. and McIlwain C.E. (1958)

Observations of high intensity radiation by satellites 1958 Alpha and Gamma.

Jet Propulsion Vol. 28, 588 - 592.

Vasyliunas V.M. (1968)

A survey of low-energy electrons in the evening sector of the magnetosphere with OGO 1 and OGO 3.

Journal of Geophysical Research 73, 2839 - 2884.

Vernov S.N., Gorchakov E.V., Kuznetsov S.N., Logachev Yu.I., Sosnovets E.N. and Stolpovsky V.S. (1969)

Particle fluxes in the outer geomagnetic field.

Reviews of Geophysics Vol. 7, 257 - 280.

Victor L.J. (1965)

Correlated auroral and geomagnetic micropulsations in the period range 5 to 40 seconds.

Journal of Geophysical Research 70, 3123 - 3130.

Wescott E.M. and Mather K.B. (1965)

Magnetic conjugacy from L = 6 to L = 1.4. 1. Auroral zone, conjugate area, seasonal variations and magnetic coherence.

Journal of Geophysical Research Vol. 70, 29 - 42.

Winckler J.R., Bhavsar P.D. and Anderson K.A. (1962)

A study of the precipitation of energetic electrons from the geomagnetic field during magnetic storms.

Journal of Geophysical Research Vol. 67, 3717 - 3736.